

DISSERTATION

PROGRESS TOWARDS THE TOTAL SYNTHESIS OF THE
WELWITINDOLINONE ALKALOIDS AND THE DISCOVERY OF A
NOVEL TANDEM O-H INSERTION CONIA-ENE CYCLIZATION

Submitted by

David Blandy Freeman

Department of Chemistry

In partial fulfillment of the requirements

For the Degree of Doctor of Philosophy

Colorado State University

Fort Collins, Colorado

Spring 2011

Doctoral Committee:

Advisor: John L. Wood

Alan J. Kennan

Eric M. Ferreira

Matthew P. Shores

Michael R. McNeil

Copyright by David Blandy Freeman 2011

All Rights Reserved

ABSTRACT

PROGRESS TOWARDS THE TOTAL SYNTHESIS OF THE
WELWITINDOLINONE ALKALOIDS AND THE DISCOVERY OF A
NOVEL TANDEM O–H INSERTION CONIA-ENE CYCLIZATION

The broth of blue-green algae *Hapalosiphon wewitschii* and *Westiella intricata* was shown to possess interesting biological activity, including insecticidal and P-glycoprotein inhibiting capabilities. Upon further investigation, the welwitindolinone alkaloids were isolated from the lipophilic extracts and shown to be responsible for the observed biological activity. Herein are described efforts towards the total synthesis of the welwitindolinone alkaloids and novel chemistry developed in the process.

In efforts towards *N*-methylwelwitindolinone C isothiocyanate, we employed a sequential O–H insertion Claisen rearrangement to provide compounds capable of undergoing a [3+2] dipolar cycloaddition to access the bicyclo[4.3.1] core. Attempts to install the requisite quaternary center of *N*-methylwelwitindolinone C isothiocyanate during the [3+2] dipolar cycloaddition event were unsuccessful. Ultimately, a chloronium-ion semi-Pinacol rearrangement was utilized to install the key quaternary center.

Due to complications encountered during the synthesis of *N*-methylwelwitindolinone C isothiocyanate we shifted our focus to *N*-methylwelwitindolinone D

isonitrile. Investigation into the construction of the bridged ether embedded within *N*-methylwelwitindolinone D isonitrile led to the discovery of a novel tandem O–H insertion Conia-ene cyclization.

To My Family and Friends

“To strive, to seek, to find, and not to yield.”
—Alfred Lord Tennyson, Ulysses

Acknowledgements

Engraved on a stone bench at Colorado State University is a quote from Isaac Newton that reads, “If I have seen a little further it is by standing on the shoulders of Giants.” My tenure on the welwitindolinone project has made me realize that no truer words were spoken. Above all others, I would like to first thank Professor John Wood for his support and encouragement throughout my graduate career and for believing in me. John’s dedication to organic chemistry is only matched by his desire and ability to inspire and train new scientists. John’s patience and realism made the struggles of organic synthesis bearable and solvable problems. Whenever I was stuck, John was always there for advice. On a personal note, one of my favorite things about John is that we share similar personal views. Over the past five and a half years, those views sparked conversations and comments that I will cherish always. In hindsight, I wish I wrote them all down for ammunition at a reunion.

I would like to thank all past and present Wood group members who worked or are working on the welwitindolinones: Alexandra Holubec, Matthew Weiss, Julie Dixon, Akio Kakefuda, Masami Ohtsuka, Munenori Inoue, Rishi Vaswani, Hidenori Ohki, Brian Doan, Sarah Reisman, Brian Stoltz, Joshua Day, and John Enquist. Although I haven’t met some of you, your ideas and notes laid the foundation for my contributions to the project. Truly, you are all Giants. To my undergrads, Nancy Tao and Noah Deitrich, thank you for your hard work and the material. I know the both of you will be successful in whatever you set your minds to.

During my graduate career, I have had the honor and privilege of working with some of the finest chemists collectively known as W6. To the past and present members Barry, Elnaz, Josh, Medeiros, Brett, Sarah, Ping, Rishi, Graham, Jen, Genessa (aka “G–Unit”), Aaron, Travis, Sam, Ke, Haley, Chris, Enquist, Bilal, and Eesh, thank you for the personal and professional support. Your ideas and daily enthusiasm made my experience in the Wood lab unforgettable. I will never forget the laughs we all shared. I especially would like to thank Rishi Vaswani. Through your work ethic and personal attention to developing my skills as a chemist, I am indebted. You always made me strive to be better than I am and I thank you for it. To my lab-partner-in-crime, Josh, I do miss our lunches.

I cherish the time we spent working side by side and couldn't have asked for a better coworker and friend. To the rest of W6, there are too many memories to list, but know that each of you has contributed to my life.

I would like to thank all of the chemistry laboratories at CSU for their cooperation and collaboration. The ability to use any of their instruments, resources, and chemicals facilitated the advancement of my project. I would especially like to thank the Rovic group, the Williams group, the Kennan group, the Shi group, the Ferreira group, and McNaughton group for their chemical insight and friendships. I would like to thank my roommate and member of the Rovic group Claire Filloux. You helped me rediscover the English language and kept me company throughout my final year. To my graduate committee including Matt Shores, Alan Kennan, Tom Rovic, Michio Kurosu, and recently, Eric Ferreira and Mike McNeil, thank you for always having your doors open and for your willingness to help with whatever I needed. I especially would like to thank Alan Kennan. Your friendship and support for both personal and chemistry problems has gotten me through graduate school. I will miss our Thursday nights at Vincent's.

Outside of lab I have developed many lasting friendships over the past six years. To my softball team, the Banana Hammocks, thank you for much needed R&R. Especially to Joe and Shannon for organizing the team and entertaining Lan while I was busy at work. A special thanks goes to BPP and my cycling buddies Timmy, Nicole, Ross, Austin, Brent, Claire and Lewandowski. You guys helped me discover a passion that took me all over Colorado and kept me in shape. Your friendships have given me countless hours of laughs and I hope more still remain on rides yet ridden.

Finally, I'd like to thank my family. My dog Lan's continual excitement always brightened my day even when I was in a bad mood. To Jason, thanks for always keeping me company on the way home from work. To my brother Phil, we are true nerds and everyday I'm glad that you are my brother. To my parents Dennis and Barbie, there are no words for your love and commitment to me over the years. It is because of you both I am who I am today. Thank you.

Table of Contents

Abstract.....	iii
Dedication.....	v
Acknowledgement	vi
Table of Contents	viii
List of Figures and Schemes.....	xiii
List of Abbreviations.....	xxii

CHAPTER ONE

1.1 Background and Introduction.....	1
1.1.1 Isolation and Biological Activity.....	1
1.1.2 Microtubule Structure and Function	4
1.1.3 MDR and P-glycoprotein	5
1.2 Biosynthesis	9
1.2.1 Biogenesis of the Welwitindolinone Alkaloids and Their Relationship to the Fisherindoles and Hapalindoles	9
1.3 Synthetic Efforts Towards the Welwitindolinone Alkaloids.....	12
1.3.1 Welwitindolinone C Attempts	13
1.3.1.1 Wood’s “Application of Reactive Enols in Synthesis: A Versatile, Efficient, and Stereoselective Construction of the Welwitindolinone Carbon Skeleton.”.....	13
1.3.1.2 Konopelski’s “Stereoselective Conjugate Addition Directed by an Enantiomerically Pure Ketal. Preparation of the Cyclohexanone Fragment of N-Methylwelwitindolinone C Isothiocyanate.”	17
1.3.1.3 Konopelski’s “Aryllead(IV) Reagents in Synthesis: Formation of the C11 Quaternary Center of N-Methylwelwitindolinone C Isothiocyanate.”	18

1.3.1.4	Avendaño's "Controlled Generation of Three Contiguous Stereocentres in the Michael Addition of 1-Pyrrolidinocyclohexene to (E)-(1-Methyl-2-oxoindolin-3-ylidene)acetophenone."	19
1.3.1.5	Jung's "Rhodium-Catalyzed Decomposition of Indole-Substituted α -Diazo- β -Keto Esters: Three Different Reactions Based on Indole Oxidation State."	20
1.3.1.6	Rawal's "Rapid Synthesis of the N-methylwelwitindolinone Skeleton."	21
1.3.1.7	Simpkins' "Rapid Access to the Welwitindolinone Alkaloid Skeleton by Cyclization of Indolecarboxaldehyde Substituted Cyclohexanones."	22
1.3.1.8	Funk's "An Approach to the Total Synthesis of Welwistatin."	23
1.3.1.9	Shea's "A Synthesis of the Welwistatin Core."	25
1.3.1.10	Shea's "Synthesis of the Bicyclic Welwitindolinone Core via an Alkylation/Cyclization Cascade Reaction."	26
1.3.1.11	Trost's "Access to a Welwitindolinone Core Using Sequential Cycloadditions."	28
1.3.1.12	Garg's "Concise Synthesis of the Bicyclic Scaffold of N-Methylwelwitindolinone C Isothiocyanate via an Indolyne Cyclization."	29
1.3.1.13	Martin's "Approaches to N-Methylwelwitindolinone C Isothiocyanate: Facile Synthesis of the Tetracyclic Core."	31
1.3.2	Welwitindolinone A Isonitrile Syntheses	32
1.3.2.1	Baran's "Enantioselective Total Synthesis of Welwitindolinone A and Fischerindoles I and G."	32
1.3.2.2	Wood's "Total Synthesis of (\pm)-Welwitindolinone A Isonitrile."	34
1.4	Notes and References	37

CHAPTER TWO

2.1 Initial Considerations.....	45
2.2 First Generation [3+2] Dipolar Cycloaddition Approach.....	46
2.2.1 Retrosynthetic Analysis.....	46
2.2.2 Aryl C–H Insertion and Construction of Diazoketone 52	47
2.2.3 O–H Insertion Sequential Claisen Rearrangement and [3+2] Dipolar cycloaddition Model	49
2.2.4 Construction of the Welwitindolinone C Core via [3+2] Dipolar Cycloaddition.....	51
2.2.5 Unexpected Result from Alternative Allylic Alcohol.....	53
2.3 Second Generation [3+2] Dipolar Cycloaddition.....	55
2.3.1 Revised Retrosynthetic Analysis	55
2.3.2 Model System: Attempted Installation of Quaternary Center via Nitron Cycloaddition and Epoxide-opening	56
2.3.3 Model System: Installation of Quaternary Center via Nitron Cycloaddition and Chloronium-ion-mediated Elimination	58
2.3.4 Attempted Installation of Quaternary Center via Nitron Cycloaddition	60
2.4 Chloronium-ion Semi-Pinacol	62
2.4.1 Revised Retrosynthetic Analysis	62
2.4.2 Construction of the Requisite Tertiary Alcohol.....	64
2.4.3 Attempted Alternate Route to Tertiary Alcohol	65
2.4.4 Installation of Quaternary Center via Chloronium-ion Semi-Pinacol	68
2.4.4.1 Relative Stereochemical Rationale of Chloronium-ion semi- Pinacol Rearrangement	69
2.5 Michael Addition Approach.....	70
2.5.1 Retrosynthetic Analysis.....	70
2.5.2 Indium-Mediated Reductive Amination.....	71
2.5.3 Attempted Formation of an Isonitrile from 242	73
2.5.4 Trisubstituted Olefin Formation: Cross-Metathesis.....	75

2.5.5	Formation of Requisite γ -Hydroxy Enal 257	77
2.5.6	Attempted Michael Additions.....	78
2.6	Conclusion.....	79
2.7	Experimental Section.....	80
2.7.1	Material and Methods.....	80
2.7.2	Preparative Procedures.....	81
2.8	Notes and References.....	111
APPENDIX ONE: SPECTRA RELEVANT TO CHAPTER TWO.....		119
CHAPTER THREE		
3.1	Initial Considerations.....	176
3.2	Carbonyl-ylide Approach.....	177
3.2.1	Retrosynthetic Analysis.....	177
3.2.2	Carbonyl-ylide Model System.....	178
3.2.3	A Redesigned Coupling Partner Leads to New Reaction Sequence.....	180
3.3	O–H Insertion and Conia-ene Cyclization Background.....	183
3.3.1	O–H Insertion Claisen Rearrangement.....	183
3.3.2	Conia-ene Cyclization.....	186
3.3.3	Recent Advances in the Conia-ene Cyclization.....	187
3.4	<i>N</i> -Methylwelwitindolinone D isonitrile and a Tandem O–H Insertion Conia-ene Cyclization.....	190
3.4.1	Retrosynthetic Analysis.....	190
3.4.2	Model System.....	191
3.4.2.1	Exploration of Reaction Conditions.....	194
3.4.2.2	Mechanistic Rationale.....	198
3.4.3	Attempted O–H Insertion Conia-ene Cyclization of a Complex Alcohol: Inspiration from Fukuyama.....	199
3.5	Conclusion.....	203
3.6	Experimental Section.....	205

3.6.1	Material and Methods.....	205
3.6.2	Preparative Procedures.....	206
3.7	Notes and References.....	223
APPENDIX TWO: SPECTRA RELEVANT TO CHAPTER THREE.....		230
APPENDIX THREE: X-RAY CRYSTALLOGRAPHY REPORTS RELEVANT TO CHAPTER THREE.....		263
APPENDIX FOUR: NOTEBOOK CROSS-REFERENCES.....		280
Bibliography.....		284
About the Author.....		298

List of Figures and Schemes

CHAPTER ONE

Figure 1.1.1	Compounds Isolated with the Welwitindolinones.....	2
Figure 1.1.2	The Welwitindolinones	3
Figure 1.1.3	Anti-Microtubule Drugs.....	6
Figure 1.1.4	MDR-Inhibitors	7

CHAPTER TWO

Figure 2.2.1	<i>N</i> -Methylwelwitindolinone C Isothiocyanate.....	46
--------------	--	----

APPENDIX ONE

Figure A.1.1	¹ H NMR (300 MHz, CDCl ₃) of compound 203	120
Figure A.1.2	Infrared Spectrum (thin film/NaCl) of compound 203	121
Figure A.1.3	¹³ C NMR (75 MHz, CDCl ₃) of compound 203	121
Figure A.1.4	¹ H NMR (400 MHz, CDCl ₃) of compound 204	122
Figure A.1.5	Infrared Spectrum (thin film/NaCl) of compound 204	123
Figure A.1.6	¹³ C NMR (100 MHz, CDCl ₃) of compound 204	123
Figure A.1.7	¹ H NMR (400 MHz, CDCl ₃) of compound 208	124
Figure A.1.8	Infrared Spectrum (thin film/NaCl) of compound 208	125
Figure A.1.9	¹³ C NMR (100 MHz, CDCl ₃) of compound 208	125
Figure A.1.10	¹ H NMR (400 MHz, CDCl ₃) of compound 344	126
Figure A.1.11	Infrared Spectrum (thin film/NaCl) of compound 344	127
Figure A.1.12	¹³ C NMR (100 MHz, CDCl ₃) of compound 344	127
Figure A.1.13	¹ H NMR (400 MHz, CDCl ₃) of compound 210 and 345	128
Figure A.1.14	Infrared Spectrum (thin film/NaCl) of compound 210 and 345 ...	129
Figure A.1.15	¹³ C NMR (100 MHz, CDCl ₃) of compound 210 and 345	129
Figure A.1.16	¹ H NMR (400 MHz, CDCl ₃) of compound 212	130
Figure A.1.17	Infrared Spectrum (thin film/NaCl) of compound 212	131

Figure A.1.18	^{13}C NMR (100 MHz, CDCl_3) of compound 212	131
Figure A.1.19	^1H NMR (400 MHz, CDCl_3) of compound 213	132
Figure A.1.20	Infrared Spectrum (thin film/ NaCl) of compound 213	133
Figure A.1.21	^{13}C NMR (100 MHz, CDCl_3) of compound 213	133
Figure A.1.22	^1H NMR (400 MHz, CDCl_3) of compound 214	134
Figure A.1.23	Infrared Spectrum (thin film/ NaCl) of compound 214	135
Figure A.1.24	^{13}C NMR (100 MHz, CDCl_3) of compound 214	135
Figure A.1.25	^1H NMR (400 MHz, CDCl_3) of compound 216	136
Figure A.1.26	Infrared Spectrum (thin film/ NaCl) of compound 216	137
Figure A.1.27	^{13}C NMR (100 MHz, CDCl_3) of compound 216	137
Figure A.1.28	^1H NMR (400 MHz, CDCl_3) of compound 223	138
Figure A.1.29	Infrared Spectrum (thin film/ NaCl) of compound 223	139
Figure A.1.30	^{13}C NMR (100 MHz, CDCl_3) of compound 223	139
Figure A.1.31	^1H NMR (400 MHz, CDCl_3) of compound 218	140
Figure A.1.32	^{13}C NMR (100 MHz, CDCl_3) of compound 218	141
Figure A.1.33	^1H NMR (300 MHz, CDCl_3) of compound 226	142
Figure A.1.34	Infrared Spectrum (thin film/ NaCl) of compound 226	143
Figure A.1.35	^{13}C NMR (75 MHz, CDCl_3) of compound 226	143
Figure A.1.36	^1H NMR (400 MHz, CDCl_3) of compound 227	144
Figure A.1.37	Infrared Spectrum (thin film/ NaCl) of compound 227	145
Figure A.1.38	^{13}C NMR (100 MHz, CDCl_3) of compound 227	145
Figure A.1.39	^1H NMR (400 MHz, CDCl_3) of compound 229	146
Figure A.1.40	^{13}C NMR (100 MHz, CDCl_3) of compound 229	147
Figure A.1.41	^1H NMR (300 MHz, CDCl_3) of compound 240a	148
Figure A.1.42	Infrared Spectrum (thin film/ NaCl) of compound 240a	149
Figure A.1.43	^{13}C NMR (75 MHz, CDCl_3) of compound 240a	149
Figure A.1.44	^1H NMR (400 MHz, CDCl_3) of compound 240b	150
Figure A.1.45	Infrared Spectrum (thin film/ NaCl) of compound 240b	151
Figure A.1.46	^{13}C NMR (100 MHz, CDCl_3) of compound 240b	151
Figure A.1.47	^1H NMR (400 MHz, CDCl_3) of compound 241	152
Figure A.1.48	Infrared Spectrum (thin film/ NaCl) of compound 241	153

Figure A.1.49	^{13}C NMR (400 MHz, CDCl_3) of compound 241	153
Figure A.1.50	^1H NMR (300 MHz, CDCl_3) of compound 242	154
Figure A.1.51	Infrared Spectrum (thin film/ NaCl) of compound 242	155
Figure A.1.52	^{13}C NMR (75 MHz, CDCl_3) of compound 242	155
Figure A.1.53	^1H NMR (400 MHz, CDCl_3) of compound 247	156
Figure A.1.54	Infrared Spectrum (thin film/ NaCl) of compound 247	157
Figure A.1.55	^{13}C NMR (100 MHz, CDCl_3) of compound 247	157
Figure A.1.56	^1H NMR (400 MHz, CDCl_3) of compound 251	158
Figure A.1.57	Infrared Spectrum (thin film/ NaCl) of compound 251	159
Figure A.1.58	^{13}C NMR (100 MHz, CDCl_3) of compound 251	159
Figure A.1.59	^1H NMR (400 MHz, CDCl_3) of compound 252	160
Figure A.1.60	Infrared Spectrum (thin film/ NaCl) of compound 252	161
Figure A.1.61	^{13}C NMR (100 MHz, CDCl_3) of compound 252	161
Figure A.1.62	^1H NMR (300 MHz, CD_3CN) of compound 253	162
Figure A.1.63	Infrared Spectrum (thin film/ NaCl) of compound 253	163
Figure A.1.64	^{13}C NMR (100 MHz, CDCl_3) of compound 253	163
Figure A.1.65	^1H NMR (300 MHz, CD_3CN) of compound 254	164
Figure A.1.66	Infrared Spectrum (thin film/ NaCl) of compound 254	165
Figure A.1.67	^{13}C NMR (100 MHz, CDCl_3) of compound 254	165
Figure A.1.68	^1H NMR (400 MHz, CDCl_3) of compound 255a	166
Figure A.1.69	Infrared Spectrum (thin film/ NaCl) of compound 255a	167
Figure A.1.70	^{13}C NMR (100 MHz, CDCl_3) of compound 255a	167
Figure A.1.71	^1H NMR (400 MHz, CDCl_3) of compound 255b	168
Figure A.1.72	Infrared Spectrum (thin film/ NaCl) of compound 255b	169
Figure A.1.73	^{13}C NMR (100 MHz, CDCl_3) of compound 255b	169
Figure A.1.74	^1H NMR (400 MHz, CDCl_3) of compound 256a	170
Figure A.1.75	Infrared Spectrum (thin film/ NaCl) of compound 256a	171
Figure A.1.76	^{13}C NMR (100 MHz, CDCl_3) of compound 256a	171
Figure A.1.77	^1H NMR (400 MHz, CD_2Cl_2) of compound 256b	172
Figure A.1.78	Infrared Spectrum (thin film/ NaCl) of compound 256b	173
Figure A.1.79	^{13}C NMR (100 MHz, CD_2Cl_2) of compound 256b	173

Figure A.1.80	^1H NMR (400 MHz, CDCl_3) of compound 259	174
Figure A.1.81	Infrared Spectrum (thin film/ NaCl) of compound 259	175
Figure A.1.82	^{13}C NMR (100 MHz, CDCl_3) of compound 259	175

CHAPTER THREE

Figure 3.1.1	Comparison Between Welwitindolinone C and D	177
Figure 3.2.1	X-Ray Crystal Structure of compound 283	183
Figure 3.3.1	Mechanistic Pathways of Metal-Mediated Conia-ene Cyclizations	189

APPENDIX TWO

Figure A.2.1	^1H NMR (300 MHz, DMSO-d_6) of compound 269	231
Figure A.2.2	Infrared Spectrum (KBR pellet) of compound 269	232
Figure A.2.3	^{13}C NMR (75 MHz, DMSO-d_6) of compound 269	232
Figure A.2.4	^1H NMR (400 MHz, DMSO-d_6) of compound 270	233
Figure A.2.5	Infrared Spectrum (thin film/ NaCl) of compound 270	234
Figure A.2.6	^{13}C NMR (100 MHz, DMSO-d_6) of compound 270	234
Figure A.2.7	^1H NMR (400 MHz, CDCl_3) of compound 271	235
Figure A.2.8	Infrared Spectrum (thin film/ NaCl) of compound 271	236
Figure A.2.9	^{13}C NMR (100 MHz, CDCl_3) of compound 271	236
Figure A.2.10	^1H NMR (400 MHz, CDCl_3) of compound 283	237
Figure A.2.11	Infrared Spectrum (thin film/ NaCl) of compound 283	238
Figure A.2.12	^{13}C NMR (100 MHz, CDCl_3) of compound 283	238
Figure A.2.13	^1H NMR (400 MHz, CDCl_3) of compound 323	239
Figure A.2.14	Infrared Spectrum (thin film/ NaCl) of compound 323	240
Figure A.2.15	^{13}C NMR (75 MHz, CDCl_3) of compound 323	240
Figure A.2.16	^1H NMR (400 MHz, CDCl_3) of compound 317	241
Figure A.2.17	Infrared Spectrum (thin film/ NaCl) of compound 317	242
Figure A.2.18	^{13}C NMR (100 MHz, CDCl_3) of compound 317	242
Figure A.2.19	^1H NMR (400 MHz, CDCl_3) of compound 324	243

Figure A.2.20	Infrared Spectrum (thin film/NaCl) of compound 324	244
Figure A.2.21	¹³ C NMR (100 MHz, CDCl ₃) of compound 324	244
Figure A.2.22	¹ H NMR (400 MHz, CDCl ₃) of compound 318	245
Figure A.2.23	Infrared Spectrum (thin film/NaCl) of compound 318	246
Figure A.2.24	¹³ C NMR (100 MHz, CDCl ₃) of compound 318	246
Figure A.2.25	¹ H NMR (400 MHz, CDCl ₃) of compound 319	247
Figure A.2.26	Infrared Spectrum (thin film/NaCl) of compound 319	248
Figure A.2.27	¹³ C NMR (100 MHz, CDCl ₃) of compound 319	248
Figure A.2.28	¹ H NMR (400 MHz, CDCl ₃) of compound 328	249
Figure A.2.29	Infrared Spectrum (thin film/NaCl) of compound 328	250
Figure A.2.30	¹³ C NMR (100 MHz, CDCl ₃) of compound 328	250
Figure A.2.31	¹ H NMR (400 MHz, CDCl ₃) of compound 329	251
Figure A.2.32	Infrared Spectrum (thin film/NaCl) of compound 329	252
Figure A.2.33	¹³ C NMR (100 MHz, CDCl ₃) of compound 329	252
Figure A.2.34	¹ H NMR (400 MHz, CDCl ₃) of compound 330	253
Figure A.2.35	Infrared Spectrum (thin film/NaCl) of compound 330	254
Figure A.2.36	¹³ C NMR (100 MHz, CDCl ₃) of compound 330	254
Figure A.2.37	¹ H NMR (400 MHz, CDCl ₃) of compound 334	255
Figure A.2.38	Infrared Spectrum (thin film/NaCl) of compound 334	256
Figure A.2.39	¹³ C NMR (100 MHz, CDCl ₃) of compound 334	256
Figure A.2.40	¹ H NMR (400 MHz, CDCl ₃) of compound 335	257
Figure A.2.41	Infrared Spectrum (thin film/NaCl) of compound 335	258
Figure A.2.42	¹³ C NMR (100 MHz, CDCl ₃) of compound 335	258
Figure A.2.43	¹ H NMR (400 MHz, CDCl ₃) of compound 354	259
Figure A.2.44	Infrared Spectrum (thin film/NaCl) of compound 354	260
Figure A.2.45	¹³ C NMR (100 MHz, CDCl ₃) of compound 354	260
Figure A.2.46	¹ H NMR (400 MHz, CDCl ₃) of compound 342	261
Figure A.2.47	Infrared Spectrum (thin film/NaCl) of compound 342	262
Figure A.2.48	¹³ C NMR (100 MHz, CDCl ₃) of compound 342	262

APPENDIX THREE

CHAPTER ONE

Scheme 1.2.1	Proposed biosynthesis of welwitindolinones A–C	11
Scheme 1.2.2	Proposed biosynthesis of welwitindolinone D analogs	12
Scheme 1.3.1	Wood’s Formation of α -Diazo Ketone 44	14
Scheme 1.3.2	Wood’s Formation of Aryl C–H Insertion Product 50	15
Scheme 1.3.3	Substituent Effects of O–H Insertion Claisen Rearrangement	16
Scheme 1.3.4	Formation of the Welwitindolinone C Core	17
Scheme 1.3.5	Konopelski’s Synthesis of Enantiomerically Pure Ketal 67	18
Scheme 1.3.6	Konopelski’s Formation C4–C11 Bond of Welwitindolinone C ..	19
Scheme 1.3.7	Avendaño’s Attempt at the Welwitindolinone C Core	20
Scheme 1.3.8	Jung’s Aryl C–H Insertion Attempt	21
Scheme 1.3.9	Rawal’s Synthesis of the Welwitindolinone C Core	22
Scheme 1.3.10	Simpkins’ Formation of Welwitindolinone C Core 99	23
Scheme 1.3.11	Funk’s Approach to Welwistatin	24
Scheme 1.3.12	Shea’s Synthesis of the Welwistatin Core	26
Scheme 1.3.13	Shea’s Alkylation/Cyclization Cascade Reaction Approach	27
Scheme 1.3.14	Trost’s Access to a Welwitindolinone Core	29
Scheme 1.3.15	Garg’s Indolyne Cyclization Approach	30
Scheme 1.3.16	Martin’s Approach to the Tetracyclic Core of 16	32
Scheme 1.3.17	Baran’s Synthesis of Welwitindolinone A Isonitrile	34
Scheme 1.3.18	Wood’s Synthesis of Urethane 170	35
Scheme 1.3.19	Quaternary Center Installation of 10	36
Scheme 1.3.20	Wood’s Synthesis of Welwitindolinone A Isonitrile	37

CHAPTER TWO

Scheme 2.2.1	[3+2] Dipolar Cycloaddition Retrosynthetic Analysis I	47
Scheme 2.2.2	Construction of α -Diazo ketone 52	48
Scheme 2.2.3	Production of 183 via O–H Insertion Claisen Rearrangement	49
Scheme 2.2.4	Dipolar Cycloaddition Model System I	50

Scheme 2.2.5	Dipolar Cycloaddition Model System II	51
Scheme 2.2.6	Projected Construction of the Welwitindolinone Core via [3+2] Dipolar Cycloaddition	52
Scheme 2.2.7	Construction of the Welwitindolinone Core via [3+2] Dipolar Cycloaddition	53
Scheme 2.2.8	Installation of a Quaternary Center via [3+2] Dipolar Cycloaddition	54
Scheme 2.3.1	[3+2] Dipolar Cycloaddition Retrosynthetic Analysis II	56
Scheme 2.3.2	Model System: Attempted Installation of Quaternary Center	57
Scheme 2.3.3	Model System: Attempted Formation of 207	58
Scheme 2.3.4	Chloronium-Ion Model System	59
Scheme 2.3.5	Attempted Allylic Chloride [3+2] Dipolar Cycloaddition	60
Scheme 2.3.6	Formation of Vinyl Epoxide 214	61
Scheme 2.3.7	Attempted [3+2] Dipolar Cycloaddition of Diene 216	62
Scheme 2.4.1	Welwitindolinone A Chloronium-Ion Semi-Pinacol Rearrangement	63
Scheme 2.4.2	Revised Retrosynthetic Analysis: Chloronium-Ion Semi-Pinacol Rearrangement	64
Scheme 2.4.3	Construction of Homo Allylic Alcohol 218	65
Scheme 2.4.4	Projected Alternate Route to Tertiary Alcohol 218	66
Scheme 2.4.5	Allylic Transposition of Alcohol 226 to 224	67
Scheme 2.4.6	Attempted Formation of Isoxazolidine 225	67
Scheme 2.4.7	Chloronium-Ion Semi-Pinacol Rearrangement of 218	68
Scheme 2.4.8	Chloronium-Ion Semi-Pinacol Rearrangement: Stereochemical Rationale	70
Scheme 2.5.1	Michael Addition Retrosynthetic Analysis	71
Scheme 2.5.2	Attempted Benzylic Imine Formation of 183	72
Scheme 2.5.3	Indium-Mediated Reductive Amination	73
Scheme 2.5.3	Projected Isonitrile Formation from 243	74
Scheme 2.5.5	Attempted Formation of an Isonitrile from 242	74
Scheme 2.5.6	Oxazole 247 Formation Rational	75

Scheme 2.5.7	Formation of Trisubstituted Olefin 251	76
Scheme 2.5.8	Desilation of Trisubstituted Olefin 251	76
Scheme 2.5.9	Formation of Requisite γ -Hydroxy Enal 257	77
Scheme 2.5.10	Attempted Michael Addition of γ -Hydroxy Enal 257	78
Scheme 2.5.11	Attempted Protection of γ -Hydroxy Enal 257	79

CHAPTER THREE

Scheme 3.2.1	Welwitindolinone D Carbonyl-Ylide Retrosynthetic Analysis	178
Scheme 3.2.2	Carbonyl-Ylide Model System	179
Scheme 3.2.3	Formation of Diazoisatin 271	179
Scheme 3.2.4	Attempted Carbonyl-Ylide 1,4-Addition	180
Scheme 3.2.5	Failed Carbonyl-Ylide 1,4-Addition Rationale	181
Scheme 3.2.6	Projected O–H Insertion π -Lewis Acid-Mediated Ring Closure ..	181
Scheme 3.2.7	Formation of Homo Allylic Alcohol 281	182
Scheme 3.2.8	O–H Insertion Conia-ene Cyclization	182
Scheme 3.2.9	Structure Confirmation of Spiro-cycle 283	183
Scheme 3.3.1	Assembly of β -Hydroxy Esters via O–H Insertion Claisen Rearrangement	183
Scheme 3.3.2	Scope of O–H Insertion Claisen Rearrangement	185
Scheme 3.3.3	[3,3] vs. [2,3] Rearrangement of Propargylic Alcohols	186
Scheme 3.3.4	Generic Conia-ene Cyclization	186
Scheme 3.3.5	Toste's Gold(I)-Catalyzed Conia-ene Reaction	187
Scheme 3.3.6	Kerr's Zn(NTf ₂) ₂ Catalyzed Tandem Nucleophilic Cyclopropane Ring-Opening/Conia-ene cyclization	188
Scheme 3.4.1	Welwitindolinone D O–H Insertion Conia-ene Retrosynthetic Analysis	191
Scheme 3.4.2	O–H Insertion Conia-ene Cyclization Model System	192
Scheme 3.4.3	Formation of Homo Allylic Alcohol 323	192
Scheme 3.4.4	O–H Insertion Conia-ene Cyclization of Alcohol 323	193
Scheme 3.4.5	Implementation of O–H Insertion Conia-ene Model System	194
Scheme 3.4.6	Investigation of O–H Insertion Conia-ene Reaction Conditions ...	195

Scheme 3.4.7	Investigation of Alcohol Substrate 327	196
Scheme 3.4.8	Investigation of Diazo Compound 284	197
Scheme 3.4.9	Influence of Rhodium(II) in Conia-ene Cyclization of 334	197
Scheme 3.4.10	Proposed Mechanistic Rationale of Reaction Outcome.....	199
Scheme 3.4.11	Outline of Fukuyama's Synthesis of (-)-Hapalindole G	200
Scheme 3.4.12	Proposed Rubottom Oxidation of 340	200
Scheme 3.4.13	Synthesis of Fukuyama's Ketone (340).....	202
Scheme 3.4.14	Rubottom Oxidation of Fukuyama's Ketone 340	203
Scheme 3.4.15	Attempted O–H Insertion Conia-ene Cyclization of 342	203

List of Abbreviations

9-BBN (BBN)	9-borabicyclo[3.3.1]nonane
Ac	acetyl
acac	acetylacetonyl
AIBN	<i>a,a'</i> -azoisobutyronitrile
Ar	aryl
aq	aqueous
BAIB (PIDA)	bis(acetoxy) iodobenzene
BHT	butylated hydroxytoluene
BINAL-H	2,2'-dihydroxy-1,1'-binaphthyl lithium aluminum hydride
BINAP	2,2'- <i>bis</i> (diphenylphosphino)-1,1'-binaphthyl
BINOL	1,1'-bi-2,2'-naphthol
Bn	benzyl
Boc	<i>tert</i> -butoxycarbonyl
bp	boiling point
BQ	benzoquinone
BRSM (b.r.s.m.)	based on recovered starting material
BSA	<i>N,O</i> -bis(trimethylsilyl)acetamide
Bu	butyl
Bz	benzoyl
CAN	cerium(IV) ammonium nitrate
CB	catechol borane
Cbz	benzyloxycarbonyl
CDMT	2-Chloro-4,6-dimethoxy-1,3,5-triazine
COD	1,5-cyclooctadiene
cp	cyclopentadienyl
CSA	camphorsulfonic acid
cy	cyclohexyl
d.e. (de)	diastereomeric excess
d.r. (dr)	diastereomeric ratio

DABCO	1,4-diazabicyclo[2.2.2]-octane
dba	dibenzylidene acetone
DBU	1,8-diazabicyclo[5.4.0]undec-7ene
DCE	1,2-dichloroethane
DCM	dichloromethane
DDQ	2,3-dichloro-5,6-dicyano benzoquinone
DEAD	diethyl azodicarboxylate
DET	diethyl tartrate
DIBAL	diisobutylaluminum hydride
DIPA	diisopropylamine
DIPEA	diisopropylethylamine
DMAP	4-(dimethylamino)pyridine
DMDO	dimethyldioxirane
DME	dimethoxyethane, glyme
DMF	<i>N,N</i> -dimethylformamide
DMI	1,3-dimethylimidazolidin-2-one
DMP	Dess-Martin periodinane
DMPU	<i>N,N</i> -dimethyl propylene urea
DMS	dimethylsulfide
DMSO	dimethylsulfoxide
DNA	deoxyribonucleic acid
DPPA	diphenylphosphoryl azide
dppf	diphenylphosphinoferrocene
DTBP	2,6- <i>tert</i> -butylpyridine
e.e. (ee)	enantiomeric excess
e.r. (er)	enantiomeric ratio
EDA	ethyl diazoacetate
Et	ethyl
hfacac	hexafluoroacetylacetyl
hv	irradiation with light
HMDS	1,1,1,3,3,3-hexamethyldisilazane

HMPA	hexamethylphosphoramide
IBX	<i>o</i> -iodoxybenzoic acid
imid	imidazole
IR	infrared spectroscopy
KHMDS	potassium bis(trimethylsilyl)amide
LAH	lithium aluminum hydride
LDA	lithium diisopropylamine
LiHMDS (LHMDS)	lithium hexamethyldisilazide
L-selectride	lithium tri- <i>sec</i> -butylhydroborate
M.S.	mass spectrometry
<i>m</i> -CPBA	<i>m</i> -chloroperbenzoic acid
Me	methyl
Mes	mesityl
Ms	methanesulfonyl
MS	molecular sieves
MTBE	methyl- <i>tert</i> -butylether
MVK	methyl vinyl ketone
mw (μ w)	microwave
NaHMDS	sodium bis(trimethylsilyl)amide
NBS	<i>N</i> -bromosuccinimide
NCS	<i>N</i> -chlorosuccinimide
NIS	<i>N</i> -iodosuccinimide
NMM	<i>N</i> -methylmorpholine
NMO	<i>N</i> -methylmorpholine oxide
NMP (MPD)	<i>N</i> -methyl-2-pyrrolidinone
PCC	pyridinium chlorochromate
PDC	pyridinium dichromate
Ph	phenyl
PIFA	phenyliodonium <i>bis</i> (trifluoroacetate)
piv	pivaloyl
PMB	<i>p</i> -methoxybenzyl

PPTS	pyridinium toluenesulfonate
Pr	propyl
PTSA (<i>p</i> -TSA, TsOH)	<i>p</i> -toluenesulfonic acid
R _f	retention factor
r.t. (rt)	room temperature
TADDOL	2,2-dimethyl- $\alpha,\alpha,\alpha^1,\alpha^1$ -tetraaryl-1,3-dioxolane-4,5-dimethanol
TBAF	tetra- <i>n</i> -butylammonium fluoride
TBAOH	tetrabutylammonium hydroxide
TBDPS	<i>tert</i> -butyl-diphenyl silyl
TBHP	<i>tert</i> -butyl hydroperoxide
TBS (TBDMS)	<i>tert</i> -butyl-dimethyl silyl
TEA	triethylamine
TEMPO	2,2,6,6-tetramethyl-1-piperidinyloxy free radical
Tf	trifluoromethanesulfonyl
TFA	trifluoroacetic acid
TFa	trifluoroacetamide
TFAA	trifluoroacetic anhydride
Th	2-thienyl
THF	tetrahydrofuran
TIPS	triisopropyl silyl
TMEDA	<i>N,N,N',N'</i> -tetramethylethylenediamine
TMS	trimethyl silyl
TMU	tetramethylurea
TPAP	tetra- <i>n</i> -propylammonium perruthenate
Tr	trityl
Ts	<i>p</i> -toluenesulfonyl

Chapter 1

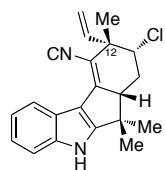
The Welwitindolinone Alkaloids: Complex Natural Products from Cyanobacteria with Promising Biological Activity

1.1 Background and Introduction.

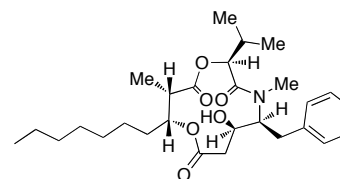
1.1.1 Isoation and Biological Activity.

In 1994 Moore and coworkers found that “the lipophilic extracts of the blue-green algae (cyanobacteria) *Hapalosiphon wewitschii* W. & G.S. West (UH strain IC-52-3, Stigonemataceae) is antifungal and inhibits P-glycoprotein-mediated multidrug resistance (MDR) in a vinblastine resistant subline (SK-VLB) of a human ovarian adenocarcinoma line (SK-OV-3) and the lipophilic extracts of *Westiella intricate* Borzi (UH strain HT-29-1, Stigonemataceae) shows insecticidal activity against blowfly larva.”¹ Intrigued by the biological activity demonstrated by the extracts Moore sought to isolate the compounds responsible. As a result, he discovered fischerindoles **1** → **4**, hapalosin (**5**), hapalindoles **6** → **9** (Figure 1.1.1), and a new class of alkaloids termed the welwitindolinones (**10** → **16**) (Figure 1.1.2). Five years later Moore isolated oxidized welwitindolinones **17** → **20** from the epilithic algae *Fischerella muscicola* (Thuret) Gomont (HG-39-5) and *Fischerella major* Gomont (HX-7-4).² Unfortunately, no biological assays have been conducted on welwitindolinones **17** → **20** and therefore they remain of unknown biological relevance.

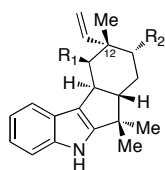
Figure 1.1.1



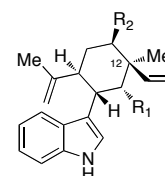
12-*epi*-fisherindole I isonitrile (1)



hapalosin (5)



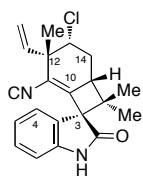
R₁ = NC, R₂ = Cl: 12-*epi*-fisherindole G isonitrile (2)
 R₁ = NC, R₂ = H: 12-*epi*-fisherindole U isonitrile (3)
 R₁ = NCS, R₂ = H: 12-*epi*-fisherindole U isothiocyanate (4)



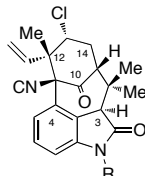
R₁ = NC, R₂ = Cl: 12-*epi*-hapalindole E isonitrile (6)
 R₁ = NC, R₂ = H: 12-*epi*-hapalindole C isonitrile (7)
 R₁ = NCS, R₂ = Cl: 12-*epi*-hapalindole F isothiocyanate (8)
 R₁ = NCS, R₂ = H: 12-*epi*-hapalindole D isothiocyanate (9)

Moore's investigation of the isolated compounds found that *N*-methylwelwitindolinone C isothiocyanate (**16**) and hapalosin (**5**) were responsible for the MDR-reversing-activity associated with the extracts.^{3,4} Studies with hapalosin (**5**) displayed a chemosensitization of P-glycoprotein-overexpressing breast carcinoma (MCF-7/ADR) cell lines with doses as low as 2.5 μ M.³ Close inspection of the welwitindolinone **10** \rightarrow **16** congeners found that *N*-methylwelwitindolinone C isothiocyanate (**16**) and its demethylated analogue, welwitindolinone C isothiocyanate (**14**, welwistatin), possessed the most relevant biological activity of the entire family. A report in 1995 by Smith and coworkers showed that *N*-methylwelwitindolinone C isothiocyanate (**16**) potentiates vinblastine (**21**) and actinomycin (**25**) accumulations in the MCF-7/ADR cell lines with chemosensitization doses as low as 1 μ M.⁴

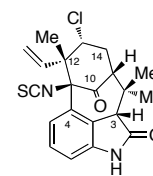
Figure 1.1.2



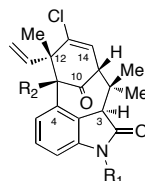
welwitindolinone A isonitrile (**10**)



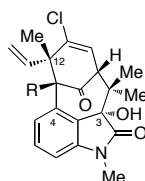
R = H: welwitindolinone B isonitrile (**11**)
R = Me: *N*-methylwelwitindolinone B isonitrile (**12**)



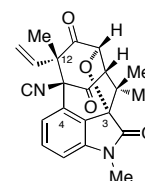
3-*epi*-welwitindolinone B isothiocyanate (**13**)



R₁ = H, R₂ = NCS: welwitindolinone C isothiocyanate (welwistatin) (**14**)
R₁ = Me, R₂ = NC: *N*-methylwelwitindolinone C isonitrile (**15**)
R₁ = Me, R₂ = NCS: *N*-methylwelwitindolinone C isothiocyanate (**16**)



R = NC: 3-hydroxy-*N*-methylwelwitindolinone C isonitrile (**17**)
R = NCS: 3-hydroxy-*N*-methylwelwitindolinone C isothiocyanate (**18**)
R = NHCHO: 3-hydroxy-*N*-methylwelwitindolinone C formamide (**19**)



N-methylwelwitindolinone D isonitrile (**20**)

This study also found that welwistatin (**14**) possessed significant cytotoxicity towards MCF-7 cell lines with an IC₅₀ value of approximately 0.12 μM. Additional assays discovered that welwistatin (**14**) inhibited cell proliferation of SK-OV-3 and A-10 cells with IC₅₀ values of 72 nM and 900 nM, respectively.⁵ These results prompted investigation into welwistatin's mode of action that revealed **14** to be a microtubule inhibitor.

1.1.2 Microtubule Structure and Function

Microtubules are responsible for a variety of functions in eukaryotic cells including structure, motility, and transport.⁶⁻⁹ Microtubules are composed of α - and β -tubulin (each with about 450 amino acid residues) arranged in an alternating pattern that constitute protofilaments. These protofilaments are arranged in a spiral pattern (usually about 13 units) to form a hollow tube with a diameter of about 25 nm. Microtubules are polar by nature and stretch outward from their nucleating centers (negative), where γ -tubulin and γ -tubulin ring complex (γ -TuRC) are located, to the outer ends (positive) where there is a constant flux of elongation and contraction. Microtubules undergo a process of *dynamic instability* as a result of their constant polymerization and depolymerization. Each β -tubulin is bound to GDP except for the β -tubulin located at the very end of the microtubule. This β -tubulin is bound to GTP, which along with magnesium ions assists in microtubule elongation via hydrolysis.⁷

The microtubule cytoskeletal structure interacts with a large number of proteins including MAPs (microtubule associated proteins), +TIPs (plus-end tracking proteins), and motor proteins that support cellular function. The motor proteins kinesin and dynein help cell division and interphase when coupled with microtubules. Disruption of the microtubule polymerization and depolymerization equilibrium inhibits transport of kinesin and dynein motor proteins and the cell cannot function properly.⁹

There are several drugs that affect the polymerization and depolymerization of microtubules and thus affect mitosis (Figure 1.1.3). Drugs that depolymerize microtubules tend to bind to tubulin at the colchicine binding site (named after the natural

product colchicine) and inhibit mitotic progression. Some of these drugs include synthetic indanocine (**22**) and the natural product vinblastine (**21**) (a vinca alkaloid). Drugs that bind β -tubulin, such as paclitaxel (**21**), increase the stability of the microtubule lattice by promoting nucleation and thus increase polymerization. This process, in turn, locks a cell in prometaphase.^{6,9}

According to Smith and Zhang, welwistatin (**14**) binds similarly to colchicine and the vinca alkaloids. Treatment of aortic smooth muscle (A-10) cells with welwistatin (**14**) (monitored by indirect immunofluorescence) displayed a disruption and eventual loss of microtubules. Tubulin was then detected via staining, providing evidence of welwistatin's ability to depolymerize microtubules. To further support this conclusion A-10 cells were pretreated with varying doses of paclitaxel (**21**), which prevented microtubules from depolymerizing when welwistatin was added. However, when welwistatin pretreated cells were exposed to paclitaxel (**21**) the restoration of microtubules was seen.⁵

1.1.3 MDR and P-glycoprotein

Multidrug resistance (MDR) is the ability of a cell to resist treatment with cytotoxic drugs. Some current methods for cancer therapy involve the treatment of cancerous cells with multiple, structurally unrelated drugs in order to avoid creating mutant MDR cells. However, studies have shown an alarming rate of resistance suggesting a commonality for MDR development.¹⁰⁻¹⁷

In 1950 Burchenal and coworkers reported the first account of drug resistance while studying the effects of 4-amino-N₁₀-methyl-pteroylglutamic acid on mouse leukemia cells. Approximately 20 years later Chinese hamster ovarian cells, chosen for their resistance to colchicines (**23** for example), were found to be resistant to daunomycin (**27**) and puromycin (**26**) (Figure 1.1.3).¹⁵ Around the same time Dano and coworkers discovered that Ehrlich ascites tumor cells transported daunorubicin (**28**) outward to the extracellular space via active transport. They proposed a carrier-mediated efflux as an MDR mechanism. Efforts were then made to understand the cause of MDR and eventually lead to the discovery of a 170 kDa plasma membrane glycoprotein or P-gp (mistakenly named for its affect on membrane permeability).¹⁵

Figure 1.1.3

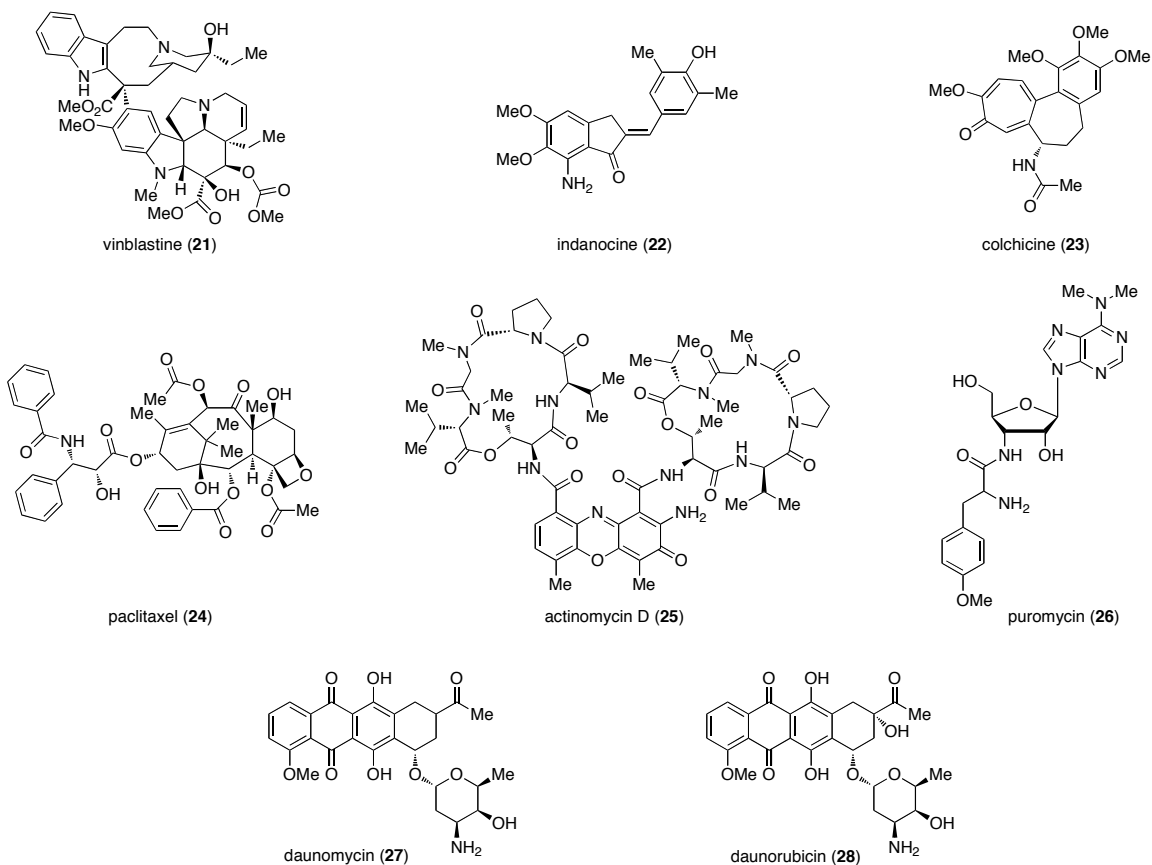
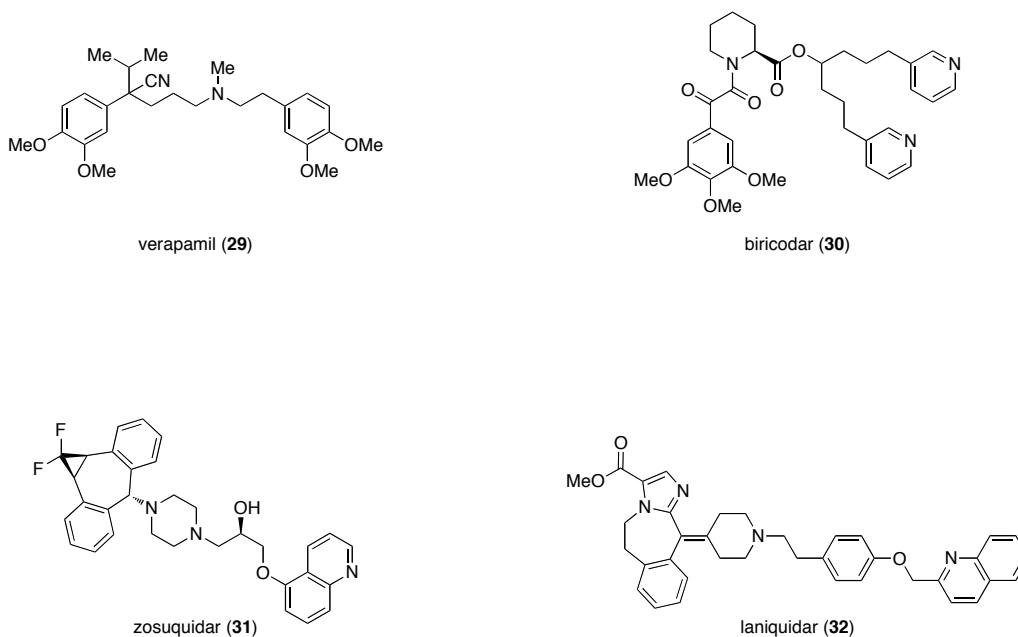


Figure 1.1.4



P-gp is an ATP-binding cassette (ABC) transporter that contains about 1280 amino acid residues and is encoded by the MDR1 (ABCB1) gene located on chromosome seven in humans. It is believed that human P-gp is a single polypeptide chain that consists of two transmembrane domains that each contain six transmembrane α -helices connected by extracellular or cytosolic linkers. A cytosolic domain containing two nucleotide-binding domains (in this case ATP-binding domains) comprises the core of the protein. It is believed that within this domain two asynchronous ATP hydrolysis actions promote drug efflux.¹⁶ P-gp expression was not only found in cancerous cells, but also in normal tissue cells such as the blood-brain barrier, the placenta, and intestinal epithelial cells. This suggests that P-gp acts as a defense against uptake of toxins from the digestive track or blood stream into sensitive organs.¹³

There are currently three models of P-gp mechanism of action: classical pump, vacuum cleaner, and flippase.¹⁴ The classical pump model suggests that toxins (i.e. drugs) in the cytoplasm interact with the cytosolic region of the two transmembrane domains. This interaction creates a flexible drug-binding pocket within P-gp. Hydrolysis of ATP initiates a conformational change that expels the toxins from the cell and a second ATP hydrolysis returns the protein to its original position. The vacuum cleaner model uses a similar mechanism, however this model proposes a removal of hydrophobic toxins from the lipid bilayer as well as the cytoplasm. The last model to be proposed is the flippase model. It suggests that P-gp interacts with toxins in the inner leaflet of the lipid bilayer and “flips” them to the outer leaflet, thus eliminating toxins via diffusion to the extracellular medium. All three models are experimentally supported, however significant evidence suggests the classical pump method is the most likely.¹⁴

Since its discovery, significant effort has been made to overcome P-gp’s mechanism of action through MDR-inhibitors (Figure 1.1.4).^{11,12,17} P-gp was found to interact with a variety of compounds that can be grouped into two main categories: 1) hydrophobic, positively charged or neutral compounds and 2) modulators (P-gp interacting compounds that are not transported). P-gp interacts with a wide range of compounds and serves as a defense mechanism for healthy cells, therefore exclusive inhibition of P-gp without cytotoxic effects makes drug development extremely difficult. As a consequence, there is a constant need to screen and create new transport modulators.

In 1995 Smith and coworkers screened the extracts of approximately 1500 strains of cyanobacteria in an effort to find MDR-reversing compounds. During this study they found that the hydrophobic extracts of *Hapalosiphon welwitschii* chemosensitized SK-

VLB-1 cells to daunomycin (**27**) and actinomycin D (**25**) and increased [³H]-vinblastine (**21**) accumulation. Upon further investigation, Smith discovered that *N*-methylwelwitindolinone C isothiocyanate (**16**) potentiates vinblastine (**21**) and actinomycin (**25**) accumulations in the MCF-7/ADR cell lines with chemosensitization as low as 1 μM and an IC₅₀ value of 2.88 μM.⁵ These results beckon further investigation into analogues of this class of natural product.

1.2 Biosynthesis.

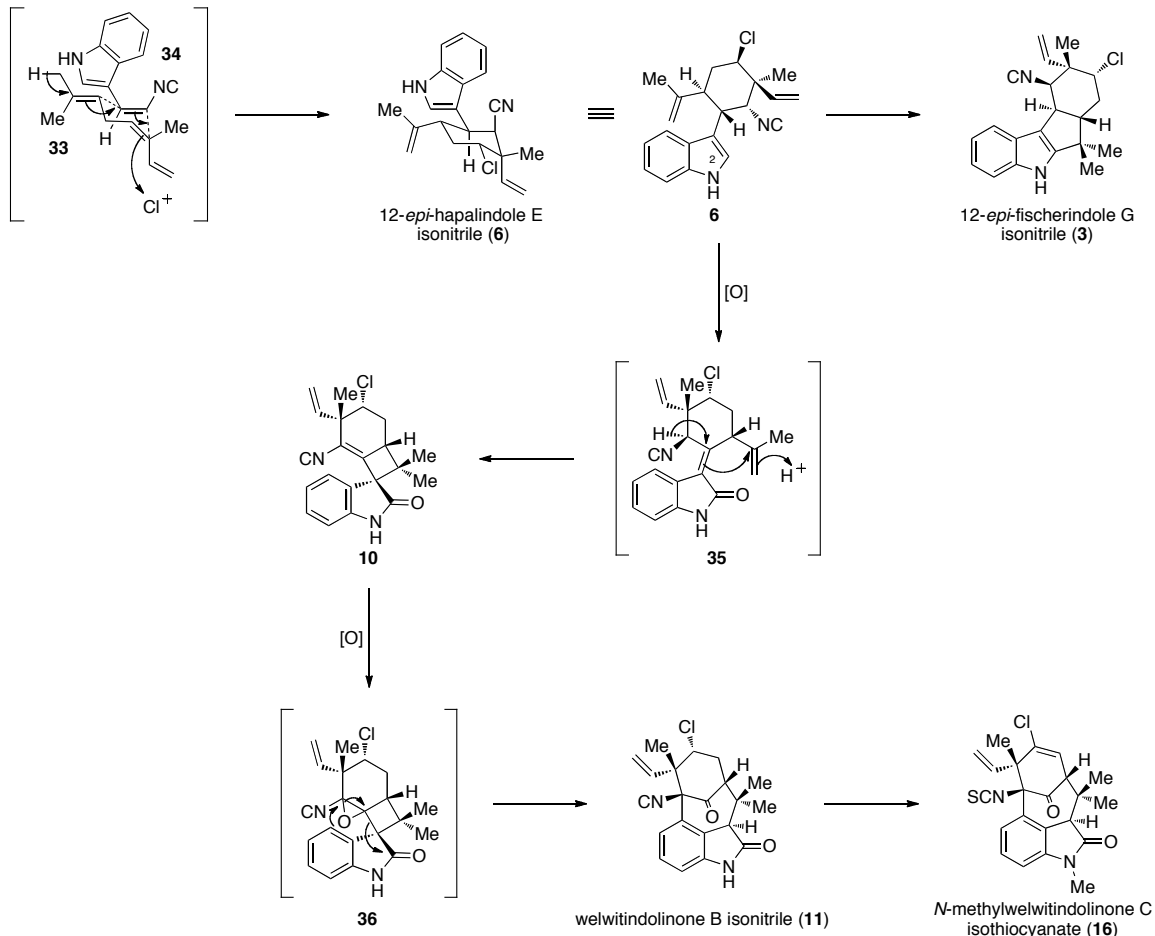
1.2.1 Biogenesis of the Welwitindolinone Alkaloids and Their Relationship to the Fisherindoles and Hapalindoles.

Moore and coworkers identified the hapalindoles as biosynthetic precursors for the fisherindoles and the welwitindolinones (Scheme 1.2.1). They proposed that 12-*epi*-hapalindole E isonitrile (**6**) could be constructed from a chloronium ion-induced cyclization of dehydrated geraniol adduct **33** and tryptamine derivative **34**. Alternatively, the dechlorinated hapalindoles could arise via a protonation/tertiary allylic carbocation cyclization mechanism with the aforementioned starting materials (not shown). An enzyme-controlled protonation/cyclization of the isopropenyl group onto the C2 position on the indole ring of **6** followed by loss of a proton could give access to 12-*epi*-fisherindole G isonitrile (**3**).

Moore suggested that further elaboration of **6** through oxidation would provide oxindole intermediate **35** where another enzyme-controlled protonation/cyclization of the

isopropenyl group could forge the cyclobutane moiety found within welwitindolinone A isonitrile (**10**). In contrast to Moore's proposed biosynthesis, Baran's construction of welwitindolinone A isonitrile (**10**) proceeded through an oxidative ring contraction of 12-*epi*-fischerindole G isonitrile (**3**) (Baran's synthesis of welwitindolinone A isonitrile is discussed in more detail in Section 1.3.2.1).^{34,35} His synthesis casts doubt on the details of Moore's hypothesized biosynthesis, yet reinforces the biogenesis of the welwitindolinones from the fischerindoles. An enzyme-controlled oxidation of the vinyl isonitrile to the isocyano epoxide **36** could eventually provide welwitindolinone B isonitrile (**11**) following rearrangement. Subsequent methylation, oxidation, and isothiocyanate formation could then furnish **16**.

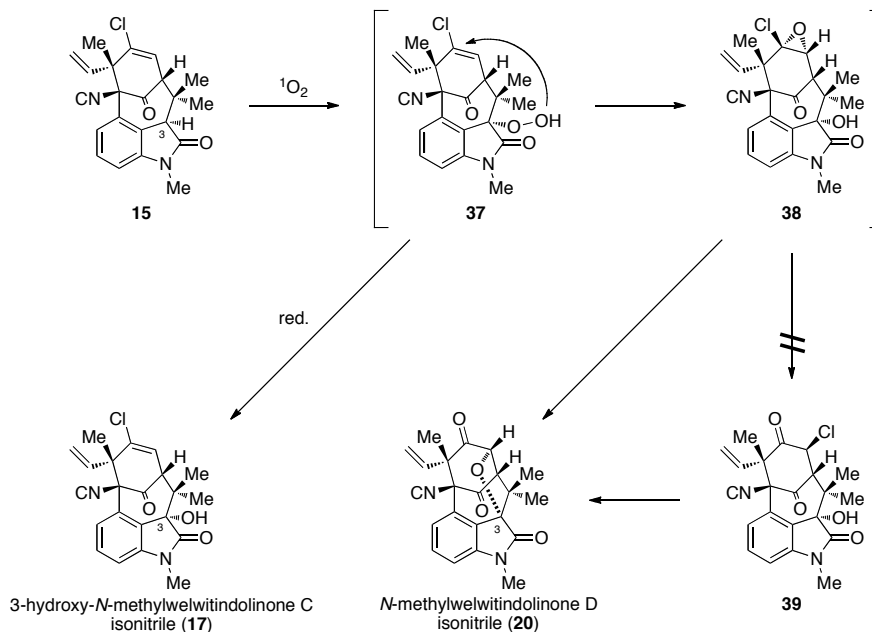
Scheme 1.2.1



After isolating the C3 oxidized welwitindolinones (17 → 20), Moore proposed that singlet oxygen was responsible.² Oxidation of the C3 carbon of *N*-methylwelwitindolinone C isonitrile (15) could result in peroxide 37. Reduction of the peroxide from an external source could then give 3-hydroxy-*N*-methylwelwitindolinone C isonitrile (17). However, an intramolecular oxidation of the vinyl chloride could lead to chloroepoxide 38. Examples from the literature have shown chloroepoxides capable of rearrangement to α -chloroketones. However, these reactions require elevated temperatures and thus the mechanistic pathway from 38 to 39 is discredited. Instead,

direct opening of the chloroepoxide by the C3-hydroxyl group to a chlorohydrin, followed by immediate expulsion of the chloride could give *N*-methylwelwitindolinone D isonitrile (**20**).

Scheme 1.2.2



1.3 Synthetic Efforts Toward the Welwitindolinone Alkaloids

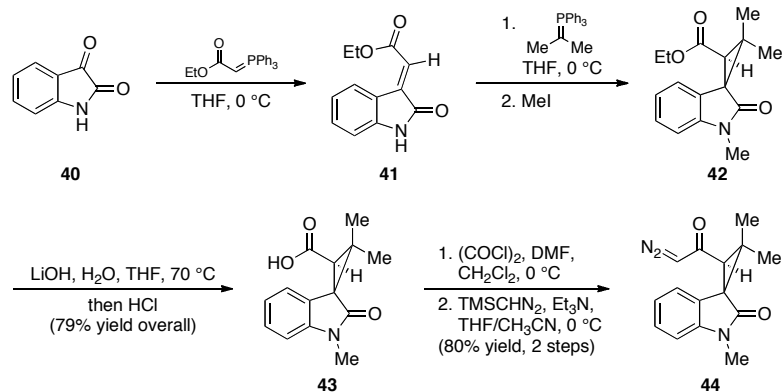
Since the welwitindolinones were discovered, there has been significant effort from the synthetic community to devise an elegant and concise route to these structurally complex molecules. There are currently 21 published synthetic works on the welwitindolinone family by 12 separate groups spanning the globe.¹⁸⁻³⁹ Within this body of work are only two completed total syntheses of welwitindolinone A isonitrile (**10**) by Baran³⁴⁻³⁶ and Wood.^{38, 39}

1.3.1 Welwitindolinone C Synthetic Efforts

1.3.1.1 Wood's "Application of Reactive Enols in Synthesis: A Versatile, Efficient, and Stereoselective Construction of the Welwitindolinone Carbon Skeleton."

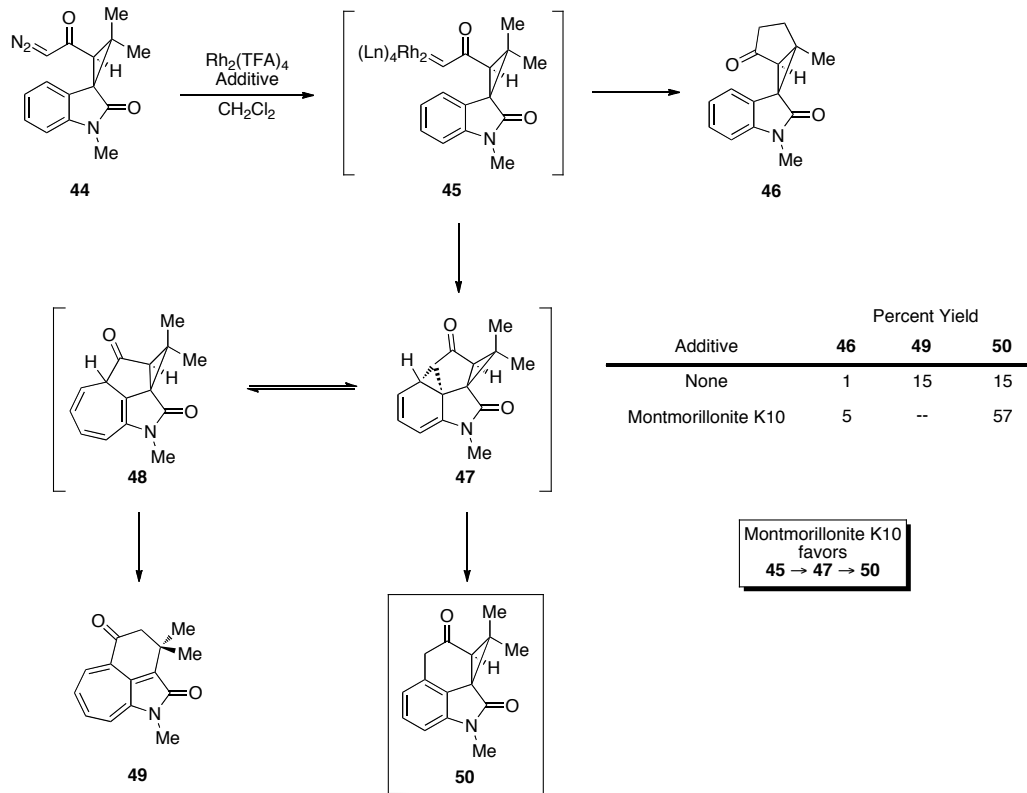
In 1999 our group published preliminary efforts toward the synthesis of *N*-methylwelwitindolinone C isothiocyanate (**16**).²⁰ This strategy was designed to incorporate a sequential O–H insertion Claisen rearrangement, methodology that was developed in our laboratory to access the bicyclo[4.3.1] backbone of welwitindolinone C. To that end, the synthesis began with construction of two key α -diazoketones (**44** and **52**, Scheme 1.3.1, 1.3.2, and 1.3.3). The first α -diazoketone **44** was synthesized starting from commercially available isatin (**40**) (Scheme 1.3.1). In the forward sense, a Wittig homologation with ethyl triphenylphosphoranylidene acetate provided enoate **41**. Subsequent exposure to isopropyl triphenylphosphorane and MeI gave clean conversion to the cyclopropyl adduct **42**. Saponification of the ethyl ester delivered acid **43**. Treatment of acid **43** with oxalyl chloride and DMF produced the intermediate acid chloride (not shown), which was immediately displaced by trimethylsilyldiazomethane to produce the first key α -diazoketone **44** in good overall yield.

Scheme 1.3.1



With α -diazoketone **44** in hand, our attention shifted to implementing an intramolecular aryl C–H insertion reaction that would access an intermediate en route to the second desired α -diazoketone **52** (see Scheme 1.3.3). Studies conducted in our laboratory have shown that the use of $\text{Rh}_2(\text{TFA})_4$ produced trace amounts of spirocycle **46**, in addition to equal molar amounts of the undesired cycloheptatriene **49** and the desired tetracycle **50**. Both products **49** and **50** presumably arose via the interconversion of norcaradiene **47** and cycloheptatriene **48**. After considerable screening efforts, it was found that a mildly Lewis acidic clay, Montmorillonite K10, led to formation of the aryl C–H insertion product in notably higher yield.

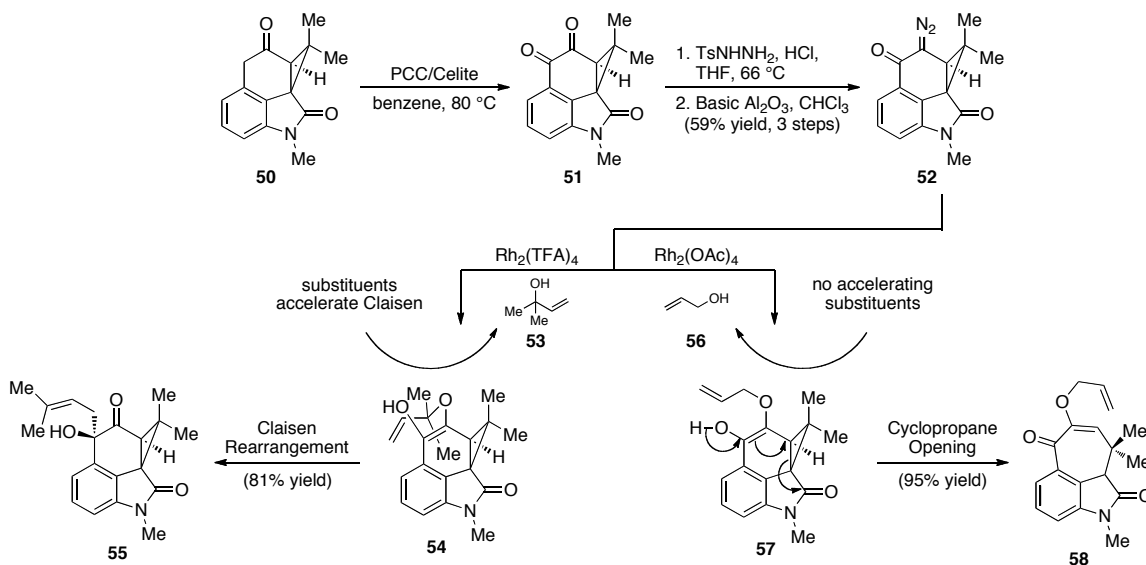
Scheme 1.3.2



Having established a facile route to aryl C–H insertion product **50**, we next implemented our strategy to access α -diazoketone **52** (Scheme 1.3.3). To that end, benzylic oxidation of **50** using PCC/Celite forged diketone **51**, which was followed by a regioselective diazotization to complete the synthesis of the second, key α -diazoketone (**52**). The stage was set to employ our sequential O–H insertion Claisen rearrangement chemistry. Our previous studies on the sequential O–H insertion/Claisen rearrangement, revealed that the substitution on the allylic alcohol influenced the rate of the Claisen rearrangement after the initial O–H insertion reaction. As illustrated in Scheme 1.3.3, when α -diazoketone **52** was exposed to allyl alcohol (**56**) in the presence of a rhodium(II) catalyst the resulting allyl vinyl ether did not undergo a Claisen rearrangement, but rather

proceeded to open the cyclopropane ring and produce cycloheptenone **58** in excellent yield. In contrast, when α -diazoketone **52** was exposed to allylic alcohol **53**, containing accelerating functionality, in the presence of a rhodium(II) catalyst, the resulting vinyl enol ether (**54**) rapidly underwent a Claisen rearrangement to afford alcohol **55**. Attempts were made to use the more functionalized Claisen product **55** to build the welwitindolinone core, but our efforts ultimately proved futile. Attention was then redirected to cycloheptenone **58** for the completion of *N*-methylwelwitindolinone C isothiocyanate.

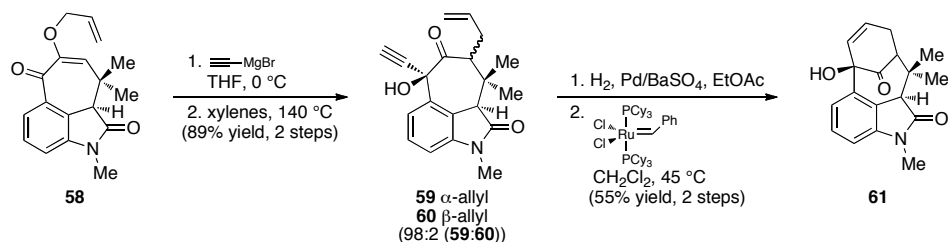
Scheme 1.3.3



As illustrated in Scheme 1.3.4, exposure of ketone **58** to ethynyl magnesium bromide and subsequent heating yielded ene-yne diastereomers **59** and **60** as a 98:2 mixture, respectively. Fortunately, the major diastereomer **59** had the allyl group positioned on the same face as the alkyne group, thus making ring-closing metathesis an

appealing strategy to construct the last ring of welwitindolinone C (**16**). Reduction of the alkyne using Lindlar's catalyst followed by treatment of the resulting diene with Grubbs first generation catalyst afforded the welwitindolinone core **61**. Attempts were made to convert the bridgehead hydroxyl group to the amine using Ritter chemistry, but unfortunately were unsuccessful. This synthetic strategy was the first to access the core of welwitindolinone C and was conducted in an efficient and stereoselective manner (15 steps).²⁰

Scheme 1.3.4

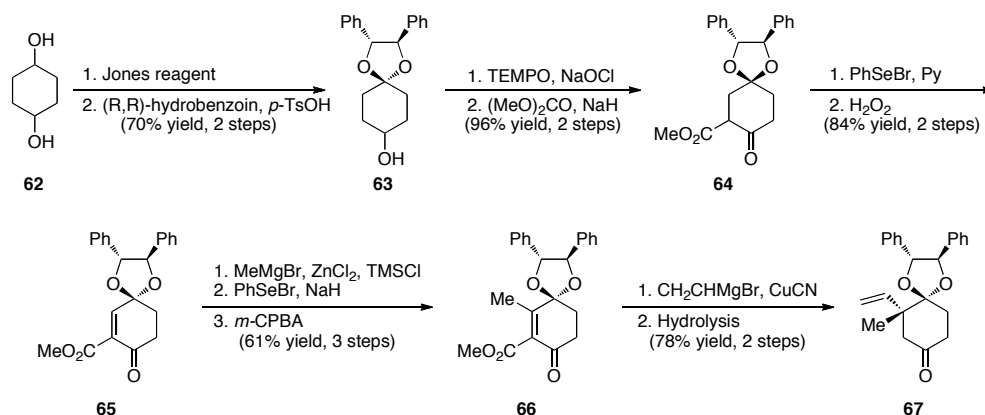


1.3.1.2 Konopelski's "Stereoselective Conjugate Addition Directed by an Enantiomerically Pure Ketal. Preparation of the Cyclohexanone Fragment of *N*-Methylwelwitindolinone C Isothiocyanate."

Konopelski's strategy towards the synthesis of *N*-methylwelwitindolinone C isothiocyanate utilized a convergent approach that initially focused on the six-membered ring embedded within the bridged polycyclic alkaloid.²¹ In 1998 he reported a concise, stereoselective synthesis of a functionalized cyclohexane ring system (Scheme 1.3.5). In the event diol **62** was subjected to mono-oxidation with Jones reagent followed by protection of the resultant ketone with (*R,R*)-hydrobenzoin to provide acetal **63** in 70%

yield over the two steps. A TEMPO oxidation and acylation gave the corresponding β -keto ester **64**. The key enone **66** was obtained following a five-step procedure involving enone installation, methyl magnesium bromide conjugate addition, and enone re-installation. The enantiomerically pure acetal then dictated the diastereoselectivity of the subsequent copper-mediated vinyl Grignard addition (81:19, 78% yield). Hydrolysis and decarboxylation then afforded the functionalized cyclohexane **67**.

Scheme 1.3.5

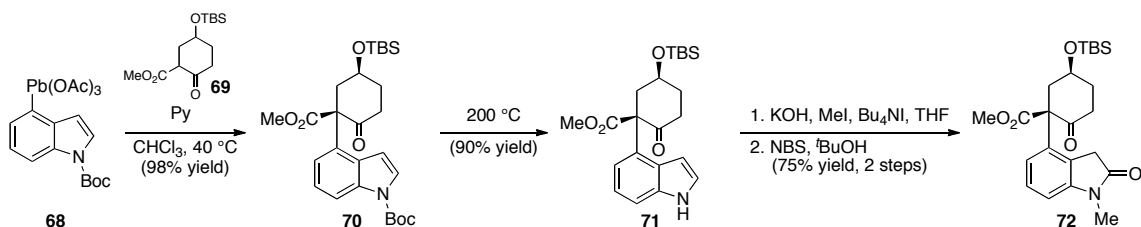


1.3.1.3 Konopelski's "Aryllead(IV) Reagents in Synthesis: Formation of the C11 Quaternary Center of *N*-Methylwelwitindolinone C Isothiocyanate."

Konopelski's approach began with a coupling of aryllead indole **68** with cyclohexanone **69** to forge the requisite carbon–carbon bond between C4 and C11 in high yield (Scheme 1.3.6).²² Subsequent heating of the Boc-protected indole **70** at 200 °C furnished free indole **71**. A two-step sequence involving methylation and oxidation then delivered compound **72** with the desired oxindole motif present in *N*-

methylwelwitindolinone C isothiocyanate (**16**). Konopelski suggested that advancement of oxindole **72** was difficult, yet they are still attempting to build the welwitindolinone core via this process. In 2007, Konopelski reported an exploration of the aryllead(IV) couplings with substituted cyclohexanone ring systems as a welwistatin support study. He found that increasing substitution on the cyclohexanone ring system resulted in markedly decreased yields.

Scheme 1.3.6

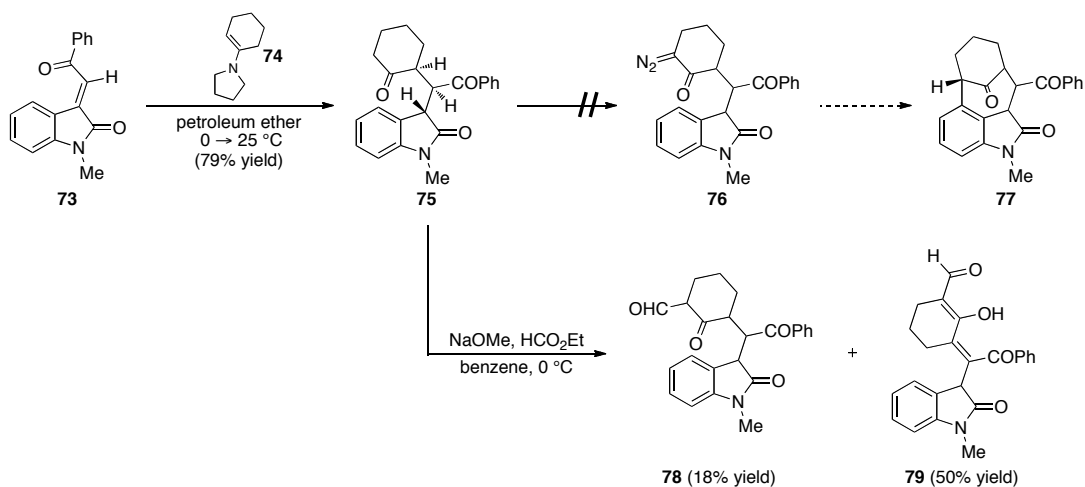


1.3.1.4 Avendaño's "Controlled Generation of Three Contiguous Stereocentres in the Michael Addition of 1-Pyrrolidinocyclohexene to (*E*)-(1-Methyl-2-oxoindolin-3-ylidene)acetophenone."

Avendaño designed a synthesis that relied on the aryl C–H insertion of **76** to deliver the core of **16** (Scheme 1.3.7).²³ In the process of constructing their desired α -diazoketone for the planned aryl C–H insertion, they explored the stereochemical outcome of the Michael addition of 1-pyrrolidinocyclohexene (**74**) onto (*E*)-(1-methyl-2-oxoindolin-3-ylidene)acetophenone (**73**). Avendaño found that by changing the reaction temperature and time, the reaction could be tuned to deliver **75** in good yield.

Unfortunately, their attempts to produce the targeted α -diazoketone (**76**) via deacylative or debenzoylative diazotransfer ultimately failed and they abandoned this route.

Scheme 1.3.7

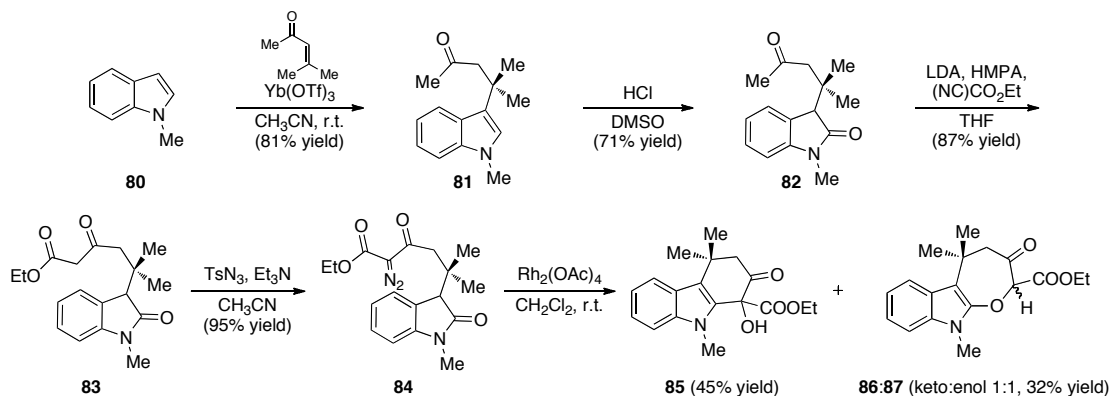


1.3.1.5 Jung's "Rhodium-Catalyzed Decomposition of Indole-Substituted α -Diazo- β -Keto Esters: Three Different Reactions Based on Indole Oxidation State."

Jung reports an exploration of rhodium-catalyzed aryl C–H insertions of oxindole- or indole-tethered diazo compounds to construct the seven-membered bridged ring system found within *N*-methylwelwitindolinone C isothiocyanate (**16**).²⁴ Unfortunately, after considerable experimentation, he was unable to effect this plan and instead reports his findings of varying reactivities of different indolyl substrates. A representative example is highlighted in Scheme 1.3.8. In the case of oxindole **84**, intermediate carbonyl ylide formation out-competed the desired aryl C–H insertion reaction and generated

compounds **85**, **86**, and **87** through proton transfers or intermediate epoxide formations, respectively.

Scheme 1.3.8

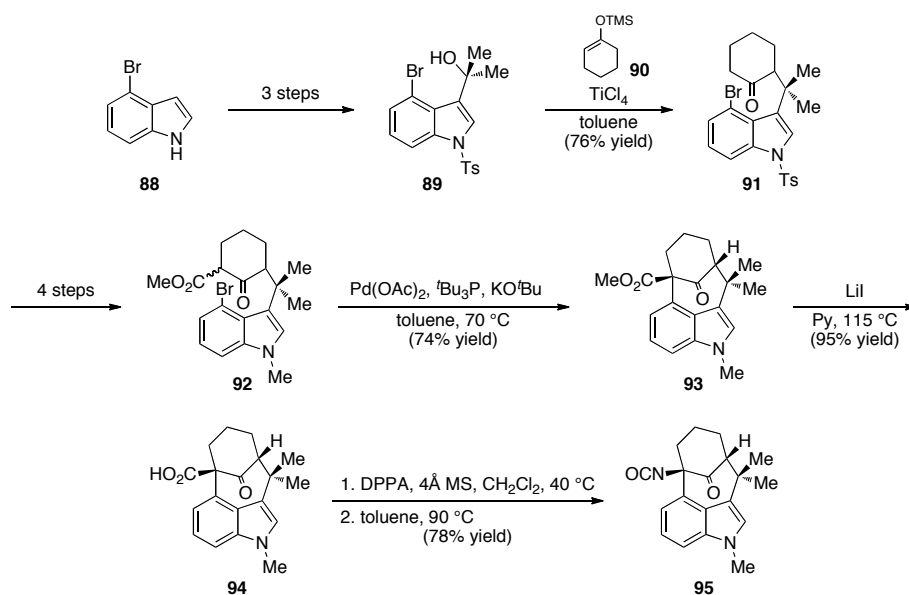


1.3.1.6 Rawal's "Rapid Synthesis of the N-methylwelwitindolinone Skeleton."

Reported in 2005, Rawal's approach to the *N*-methylwelwitindolinone skeleton highlights the utility of a Lewis acid-mediated alkylative coupling to assemble the carbon framework, a Pd-catalyzed intramolecular enolate arylation reaction to forge the [4.3.1] bicyclic backbone, and a Curtius rearrangement to install the bridgehead isocyanate (Scheme 1.3.9).²⁵ Starting from commercially available 4-bromoindole (**88**), a three-step process (not shown) gave access to tertiary alcohol **89**. Using modified Natsume's conditions silyl enol ether **90** and tertiary alcohol **89** were coupled in the presence of TiCl₄ in good yield providing adduct **91**. After four additional steps, Rawal arrived at key β-ketoester **92**, a substrate poised for implementation of a Pd-catalyzed intramolecular enolate arylation reaction. Fortunately, exposing **92** to Pd(OAc)₂, ^tBu₃P, and KO^tBu generated intermediate **93** possessing the bicyclo[4.3.1] backbone of *N*-

methylwelwitindolinone C isothiocyanate (**16**). Saponification of methylester **93** failed, but dealkylative conditions provided carboxylic acid **94** without formation of side-products resulting from decarboxylation. Exposure of acid **94** to diphenylphosphoryl azide led to a Curtius rearrangement, which gave isocyanate **95** in the absence of an external alcohol nucleophile.

Scheme 1.3.9

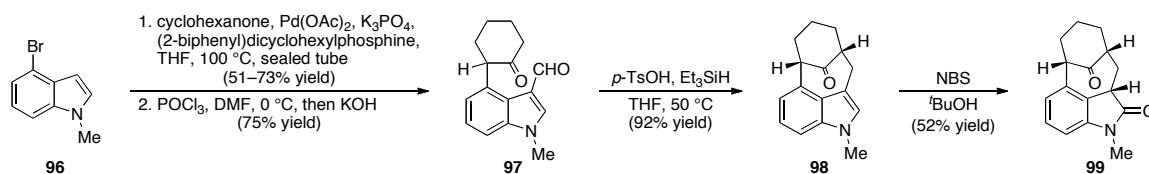


1.3.1.7 Simpkins' "Rapid Access to the Welwitindolinone Alkaloid Skeleton by Cyclization of Indolecarboxaldehyde Substituted Cyclohexanones."

Simpkins was the first to highlight the utility of an enolate arylation reaction as a means to forge the bicyclo[4.3.1] backbone of *N*-methylwelwitindolinone C isothiocyanate (**16**) in his 2005 report (Scheme 1.3.10).^{26,27} Starting from readily available 4-bromo-*N*-methylindole (**96**), an arylation reaction with cyclohexanone was

performed using conditions pioneered by Buchwald. Subsequent Vilsmeier-Hack formylation gave cyclohexyl adduct **97** in variable yield. Exposure of **97** to *p*-toluene sulfonic acid induced an intramolecular aldol reaction that was sequentially treated with Et₃SiH to reduce the intermediate extended iminium ion to produce core structure **98**. Oxidation to the oxindole (**99**) proceeded via treatment of **98** with NBS in ^tBuOH, and thus completed the welwitindolinone core.

Scheme 1.3.10

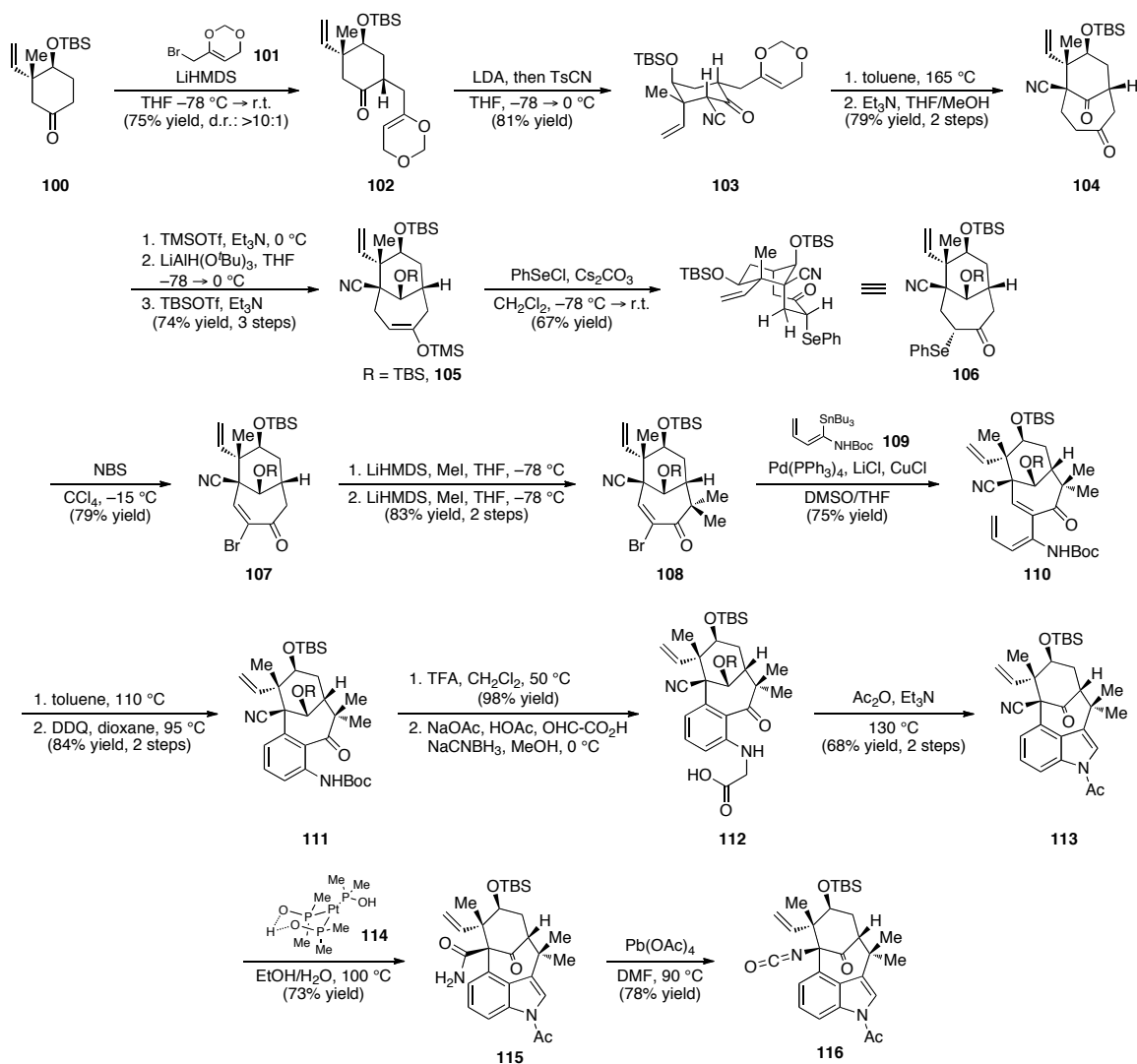


1.3.1.8 Funk’s “An Approach to the Total Synthesis of Welwistatin.”

Funk’s approach to the total synthesis of welwistatin (**14**) was designed to incorporate several methods developed within his lab (Scheme 1.3.11). His synthesis highlighted the utility of a masked bromomethyl vinyl ketone (**101**) to forge a bicyclo[4.3.1] system and an annulation sequence to construct indoles.²⁸ He began his synthesis from easily accessible cyclohexanone **100** where formation of the kinetic enolate and alkylation from the α -face with allylic bromide **101** resulted in compound **102** with good diastereoselectivity. The relative stereochemistry was assigned after a regioselective cyanation provided α -ketonitrile **103**. Heating **103** in toluene in a sealed tube at 165 °C initiated a retro-cycloaddition that extruded formaldehyde and generated an intermediate enone (not shown) whereupon subsequent treatment with triethylamine

forged bicyclo[4.3.1] **104** via an intramolecular Michael addition. A three-step process involving silyl enol ether formation, reduction of the bridgehead carbonyl, and protection of the resulting alcohol yielded **105** in good overall yield. Formation of vinyl bromide **107** proceeded through an α -selenylation (**106**), and a one-pot α -bromination, selenium oxidation, and selenoxide elimination sequence.

Scheme 1.3.11



Tandem alkylations with LiHMDS and MeI generated the requisite *gem*-dimethyl moiety (**108**) present within welwistatin (**14**). A Stille coupling with α -stannyl enecarbamate **109** and vinyl bromide **108** provided triene **110**, a compound set for Funk's annulation sequence. Heating triene **110** initiated a 6π -electrocyclization to generate the intermediate cyclohexadiene moiety (not shown) where subsequent treatment with DDQ aromatized the ring to construct aniline derivative **111**. Removal of the Boc-protecting group with TFA provided the free aniline that underwent reductive amination forming glyoxylic acid **112**. Treatment of acid **112** with acetic anhydride and triethylamine at 130 °C delivered acylated indole **113**. A two-step process involving hydrolysis of the nitrile using Parkins' catalyst (**114**) to amide **115** and a modified Hofmann rearrangement delivered isocyanate **116**.

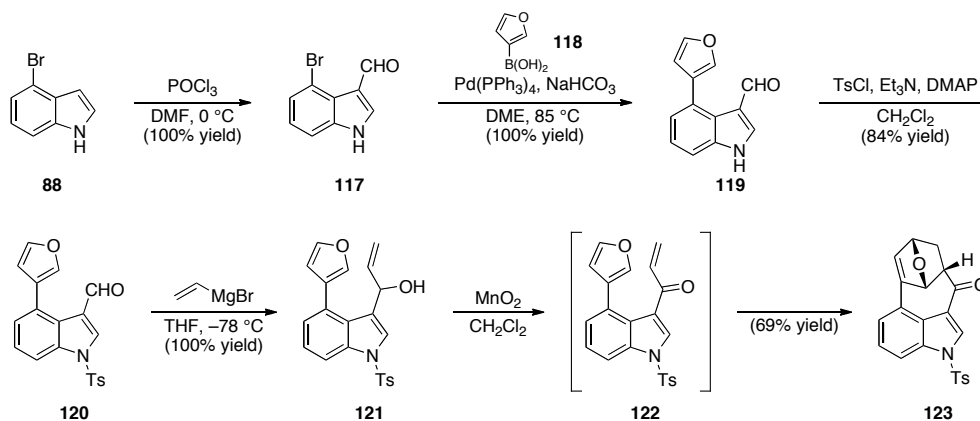
Funk's approach to welwistatin (**15**) is an elegant, precisely designed synthesis that sets itself apart from other attempts. To date, there have only been two reported routes that have generated the welwitindolinone C core containing a quaternary center at C12 (Funk and Wood). Funk's synthetic effort is unique in that it generates the correct vicinal fully substituted centers, a feat that no one had accomplished previously.

1.3.1.9 Shea's "A Synthesis of the Welwistatin Core."

Shea's 2006 report of their synthetic efforts toward the synthesis of the welwistatin core exploited a type 2 intramolecular Diels–Alder reaction to build the bicyclo[4.3.1] core and bridged indole present within welwistatin (Scheme 1.3.12).²⁹ To that end, they started from 4-bromoindole (**88**) and in a three-step sequence converted it

to allylic alcohol **121**. Exposure of allylic alcohol **121** to activated MnO_2 in methylene chloride at room temperature oxidized the allylic alcohol to the intermediate enone **122** that spontaneously underwent a type 2 intramolecular Diels–Alder reaction to give the welwitindolinone backbone (**123**) in a single operation.

Scheme 1.3.12

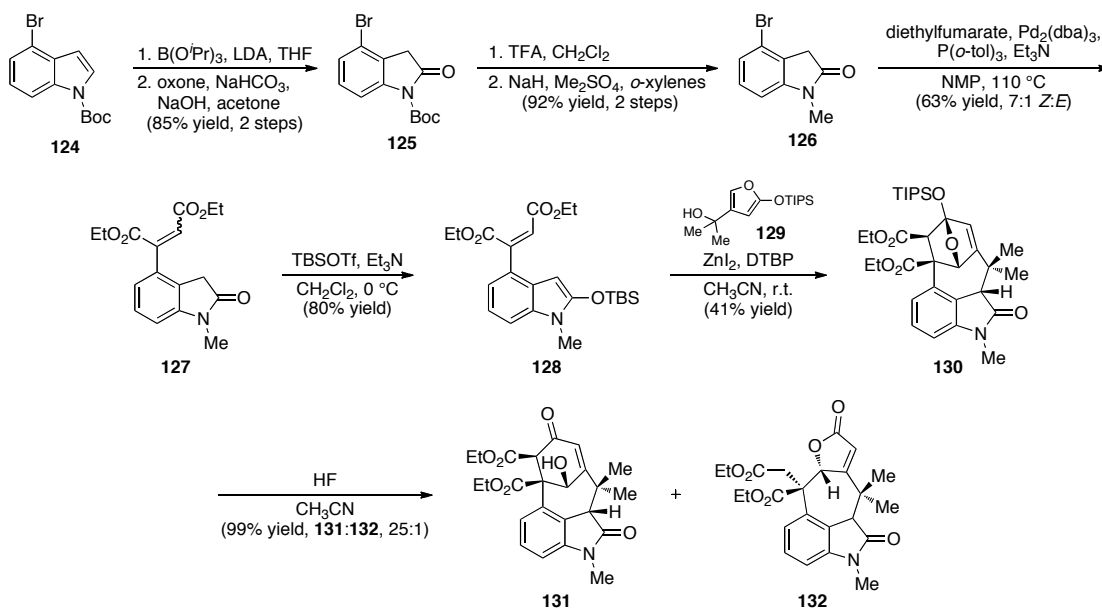


1.3.1.10 Shea's "Synthesis of the Bicyclic Welwitindolinone Core via an Alkylation/Cyclization Cascade Reaction."

Shea's synthesis of the bicyclic welwitindolinone core builds on his previous report highlighting an intramolecular Diels–Alder reaction. In an impressive and facile eight-step sequence, he was able to construct a functionalized welwitindolinone core (Scheme 1.3.13).³⁰ Beginning with 4-bromoindole **124**, oxidation of an intermediate 2-indolyl boronic ester delivered oxindole **125** in good overall yield. An acid induced Boc-removal and subsequent methylation provided *N*-methyloxindole **126**. A vinylation reaction with diethylfumarate under Heck coupling conditions afforded diester **127** as a

7:1 (*Z:E*) mixture of olefin isomers in 63% yield. In the course of installing the silyl enol ether moiety present in oxindole **128**, Shea discovered that the olefin isomers of **127** were equilibrated exclusively to the corresponding *Z*-isomer. Exposure of **128** to ZnI₂ and tertiary alcohol **129** promoted the intermediacy of an alkylated product (not shown) that immediately underwent an intramolecular Diels-Alder reaction to forge the bicyclo[4.3.1] core of welwitindolinones B, C, and D. Removal of the TIPS protecting group proceeded in the presence of HF to produce a 25:1 mixture of enone **131** and lactone **132**. Compound **131** was found to slowly rearrange to lactone **132** under basic or Lewis-acidic conditions.

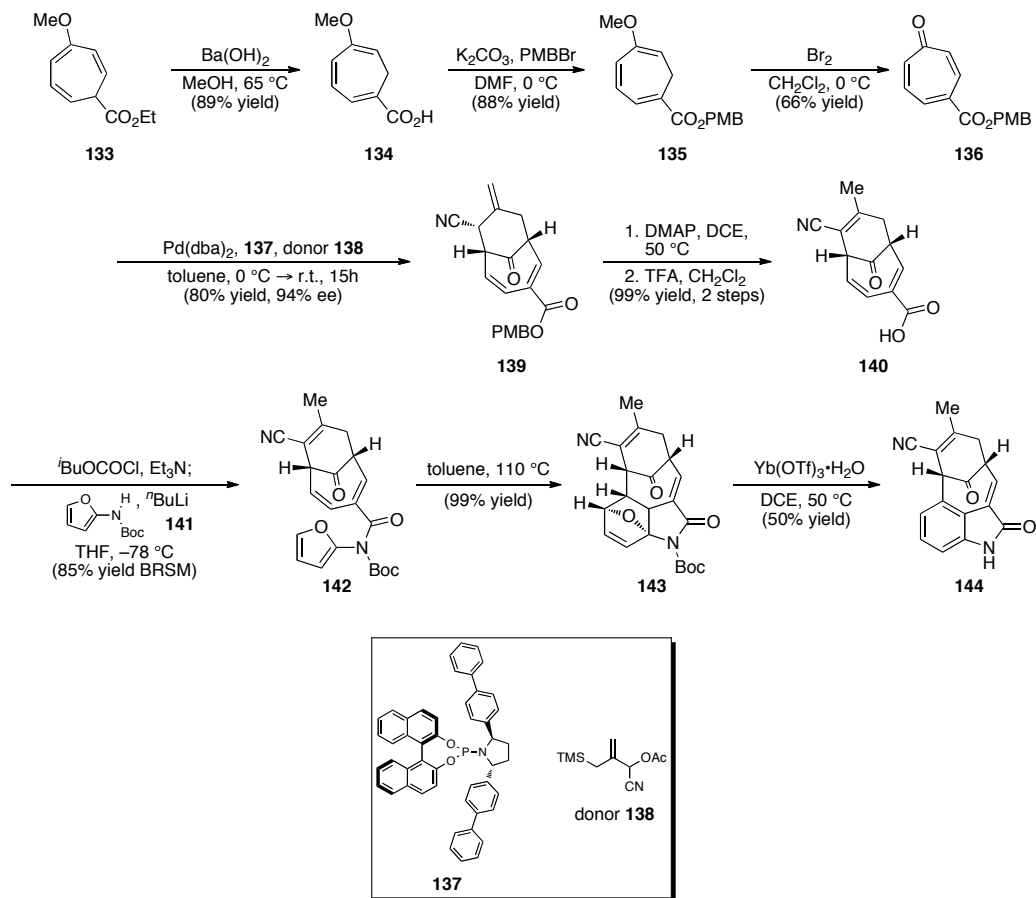
Scheme 1.3.13



1.3.1.11 Trost's "Access to a Welwitindolinone Core Using Sequential Cycloadditions."

Trost formulated a strategy toward the welwitindolinone core using previous work performed in his lab on an asymmetric palladium-catalyzed trimethylenemethane (Pd-TMM) [6+3] cycloaddition reaction (**136** → **139**) (Scheme 1.3.14).³¹ Starting from known ethyl ester **133**, three steps were conducted including saponification to acid **134**, subsequent protection as the PMB ester (**135**), and demethylation of the methyl enol ether that provided tropone **136**. Exposure of tropone **136** to Pd(dba)₂ in the presence of phosphoramidite ligand **137** and the cyano TMM donor **138** induced a key [6+3] cycloaddition to forge cycloadduct **139** in 80% yield and 94% *ee*. Having established the desired functionalized bicyclo[4.3.1] motif, they next needed to build the oxindole moiety of the welwitindolinones. An isomerization of the exo-methylene of **139** was necessary to avoid [3,3] rearrangement side-products. Treatment of **139** with DMAP at 50 °C in DCE followed by removal of the PMB group delivered acid **140** in excellent yield. Creation of the intermediate mixed anhydride and subsequent displacement with *N*-Boc-amidofuran **141** afforded the [4+2] cycloaddition precursor **142**. Upon heating **142**, a Diels-Alder reaction produced oxabicyclo **143** as a single diastereomer in near-quantitative yield. Use of Yb(OTf)₃•H₂O then converted **143** to oxindole **144** in moderate yield.

Scheme 1.3.14

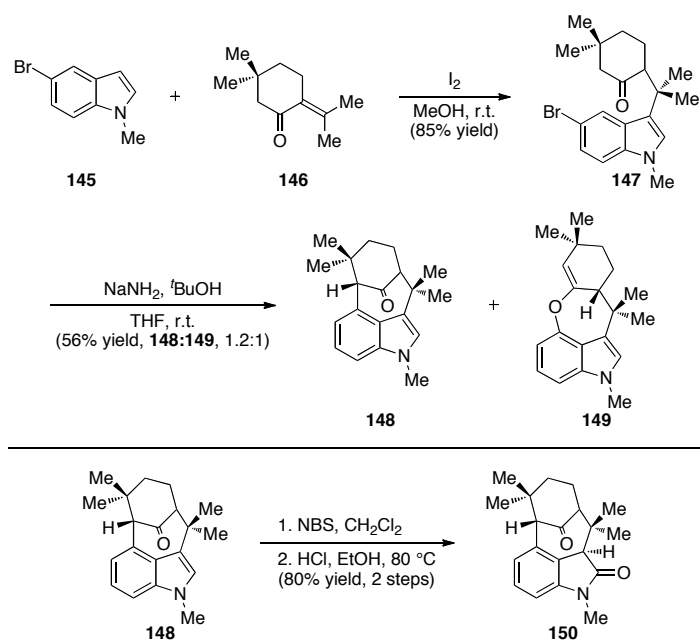


1.3.1.12 Garg's "Concise Synthesis of the Bicyclic Scaffold of N-Methylwelwitindolinone C Isothiocyanate via an Indolyne Cyclization."

Garg presents a concise synthesis of the bicyclo[4.3.1] backbone of N-methylwelwitindolinone C isothiocyanate highlighting the utility of an iodine Lewis acid-mediated conjugate addition and indolyne cyclization (Scheme 1.3.15).³² His strategy began with an iodine Lewis acid-mediated conjugate addition of 5-bromo-N-methylindole (**145**) onto enone **146** to construct indole **147**. Exposure of **147** to NaNH_2 and $t\text{BuOH}$ induced an in situ indolyne formation and subsequent trapping with the

pendant enolate. The products were the result of both *C*-arylation (**148**) and *O*-arylation (**149**) in a 1.2:1 ratio, respectively, and in a combined moderate yield (approx. 31% yield for **148** and 25% yield for **149**). Garg also investigated the oxidation of indole **148** to the corresponding oxindole **150**. He found after extensive experimentation that a two-step process involving NBS bromination and HCl-promoted hydrolysis afforded oxindole **150** cleanly and with the correct relative stereochemistry.

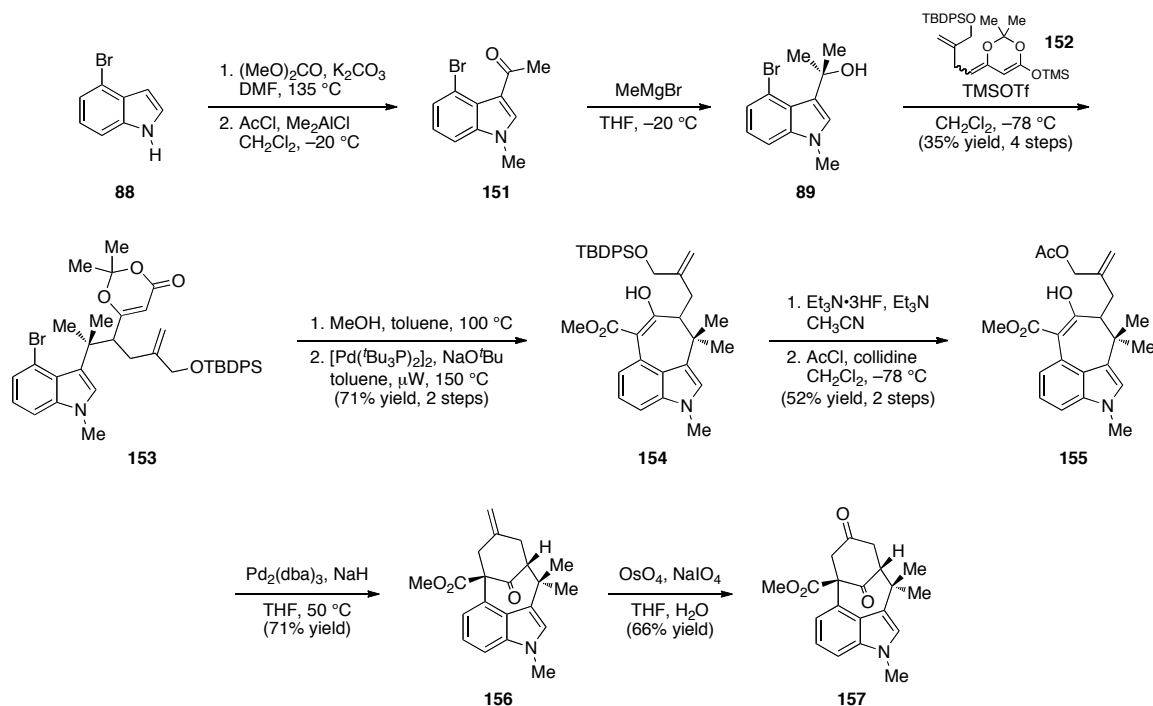
Scheme 1.3.15



1.3.1.13 Martin's "Approaches to *N*-Methylwelwitindolinone C Isothiocyanate: Facile Synthesis of the Tetracyclic Core."

In 2010 Martin published their group's effort towards *N*-methylwelwitindolinone C isothiocyanate (**16**) (Scheme 1.3.16).³³ In this report, Martin highlighted the utility of an enolate arylation reaction and an allylic alkylation to forge the core of the target natural product. Starting from 4-bromoindole (**88**), a *N*-methylation and acetylation provided **151**. Subsequent exposure of **151** to methylmagnesium bromide gave the unstable tertiary alcohol **89** that was immediately treated with **152** in the presence of TMSOTf to afford acetal **153** in 35% yield over 4 steps. Heating acetal **153** in methanol and toluene at 100 °C resulted in the opening of the acetal to the methyl ester (not shown). Treatment resulting methyl ester with [Pd(^tBu₃P)₂]₂ at 150 °C in a microwave initiated an enolate arylation producing **154** in good yield. Desilylation of **154** and sequential acylation delivered allylic acetate **155**. Palladium catalyzed allylic alkylation then converted **155** to the core of *N*-methylwelwitindolinone C isothiocyanate (**156**). Oxidative cleavage of the 1,1-disubstituted olefin within **156** provided the corresponding ketone (**157**), leaving functionality for later conversion to the natural product.

Scheme 1.3.16



1.3.2 Welwitindolinone A Isonitrile Syntheses.

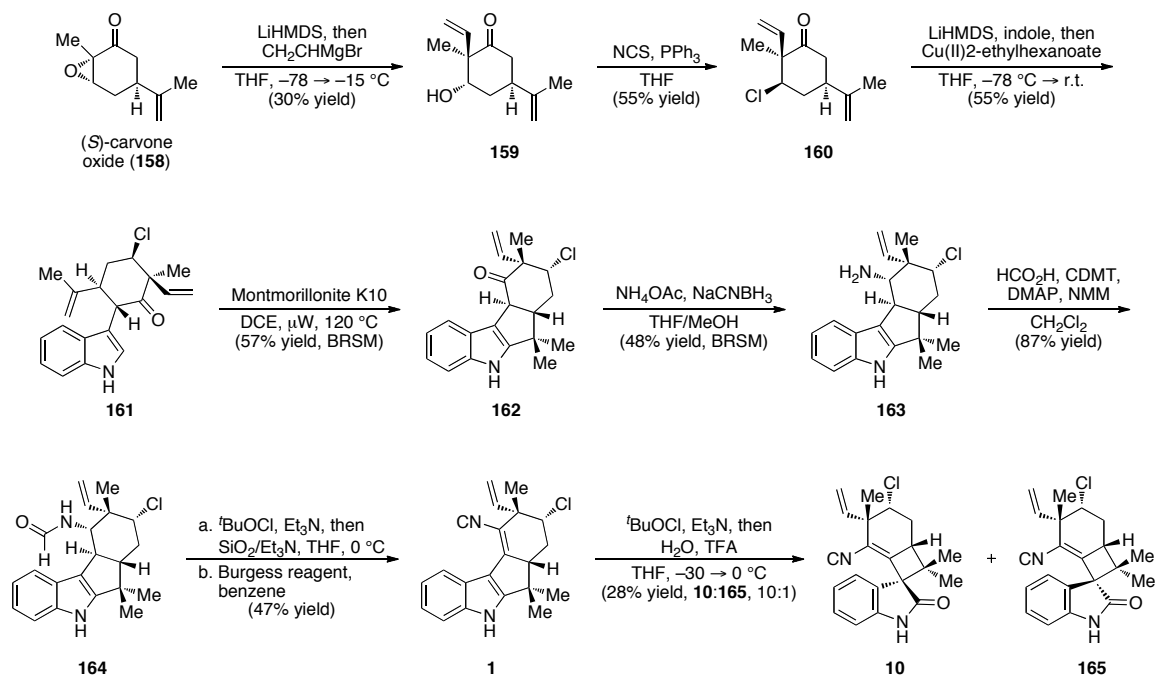
1.3.2.1 Baran's "Enantioselective Total Synthesis of Welwitindolinone A and Fischerindoles I and G."

The design of Baran's enantioselective synthesis of welwitindolinone A and fischerindoles I and G focuses on a strategy that utilized novel chemical reactions to avoid the use of protecting groups. The result was a concise synthesis of the target compounds (Scheme 1.3.17).³⁴⁻³⁶ Starting from commercially available (*S*)-carvone oxide (**158**), an in situ protection of the carbonyl as the enolate followed by vinylmagnesium bromide addition provided alcohol **159** diastereoselectively and with the desired

quaternary center installed in a single operation. Alcohol **159** was converted to alkyl chloride **160** using NCS and PPh₃. Subsequent treatment of ketone **160** with LiHMDS followed by addition of indole and copper(II)-2-ethylhexanoate forged **161** in moderate yield. Microwave irradiation of **161** in the presence of Montmorillonite K10 clay furnished Friedel–Crafts cyclization product **162**, thus completing the core of the fischerindoles.

Conversion of the carbonyl of **162** to the vinyl isonitrile of fischerindole I proved more difficult than Baran had anticipated. Ultimately they discovered that a reductive amination (**162** → **163**), formylation (**163** → **164**), and oxidation/dehydration sequence (**164** → **1**) delivered (–)-12-*epi*-fischerindole I (**1**). Exposure of **1** to ^tBuOCl under basic conditions followed by addition of an acidic solution successfully induced a ring contraction to give (+)-welwitindolinone A (**10**) and (+)-3-*epi*-welwitindolinone A (**165**) as a 10:1 mixture, respectively.

Scheme 1.3.17

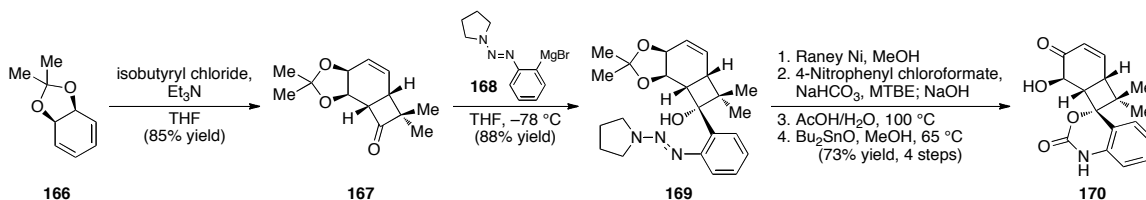


1.3.2.2 Wood's "Total Synthesis of (±)-Welwitindolinone A Isonitrile."

Intrigued by the structural complexity of welwitindolinone A isonitrile, our group initiated a strategy towards its synthesis in 2002. Four years later we reported the efficient total synthesis of welwitindolinone A isonitrile (2.5% yield overall with an average yield of 81%).³⁷⁻³⁹ Its construction began with a stereo- and regioselective [2+2] cycloaddition of cyclohexadiene acetonide **166** and dimethyl ketene (derived from isobutyryl chloride) to deliver bicyclo[4.2.0] **167** in excellent yield (Scheme 1.3.18). Addition to the carbonyl of **167** with aryl magnesium bromide **168** from the convex face of the fused bicycle gave alcohol **169** as a single diastereomer. A four-step sequence composed of a chemoselective reduction of the triazene moiety, protection of the

resultant aniline as the urethane, deprotection of the acetonide, and selective oxidation of the allylic alcohol provided enone **170** in good overall yield.³⁷

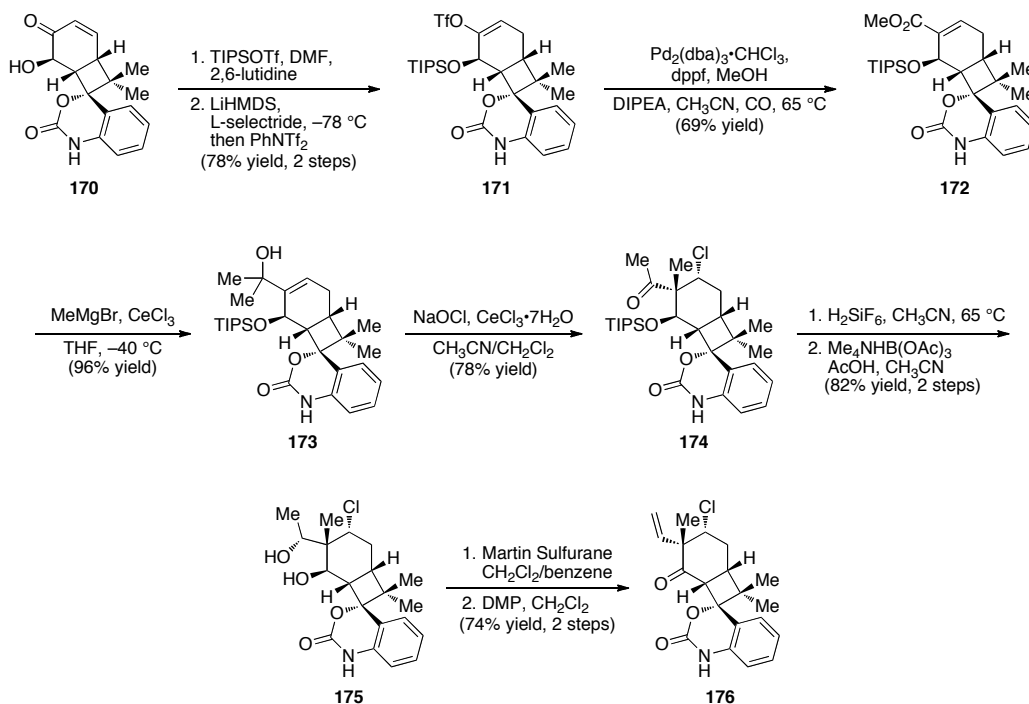
Scheme 1.3.18



Having built the welwitindolinone A core, attention then turned to incorporating the necessary functionality in the cyclohexane portion (Scheme 1.3.19).^{38,39} The two-step sequence began with initial protection of alcohol **170** as the TIPS silyl ether. The intermediate TIPS-protected **170** was then treated with LiHMDS to protect the urethane in situ as the lithium anion before reduction of the enone with L-selectride and trapping of the enolate as the vinyl triflate could occur to produce **171**. A palladium catalyzed carbonylation reaction converted the vinyl triflate of **171** to enoate **172** that when exposed to excess methylmagnesium bromide provided tertiary allylic alcohol **173**. Treatment of **173** with NaOCl and CeCl₃•7H₂O initiated a chloronium-ion induced semi-pinacol rearrangement that delivered the all-carbon quaternary center and requisite secondary chloride in a single operation and with the correct relative stereochemistry to deliver **174**. Based upon the relative stereochemistry of **174**, the chloronium ion approached from the more hindered concave face of the molecule. Our group postulated that the TIPS-protected alcohol forced the incoming chloronium ion to approach from the concave face of the olefin, thus giving the desired relative stereochemistry. Completion

of the cyclohexane portion to give **175** proceeded through desilylation of the protected hydroxyl group and reduction of the ketone. Using Martin's sulfurane the less hindered secondary alcohol was selectively converted to the monosubstituted alkene and oxidation of the more hindered alcohol created **176**.

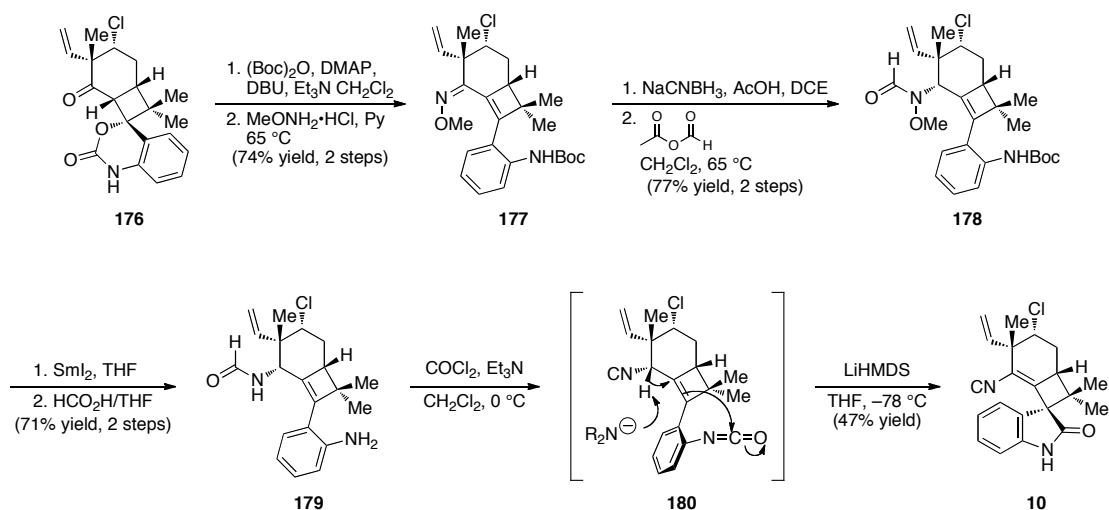
Scheme 1.3.19



We next turned to the assembly of the spiro-oxindole functionality. Previous studies in our lab set precedence for a SmI₂-mediated reductive cyclization onto aryl isocyanates to form spiro-oxindoles. Opening of urethane **176** was accomplished via a one-pot Boc-protection/CO₂ extrusion sequence to give the protected aniline moiety that was directly followed by condensation of *O*-methylhydroxylamine to form oxime ether **177**. Reduction of the oxime ether and formylation of the generated methoxyamine provided **178**, a compound now susceptible to N–O bond cleavage. The N–O bond was

successfully cleaved in the presence of SmI_2 and the aniline was unmasked under acidic conditions to deliver **179** in good yield. A two-step one pot process involving initial isonitrile formation with phosgene and subsequent treatment of the crude mixture with LiHMDS at $-78\text{ }^\circ\text{C}$ successfully completed the total synthesis of **10** as a single diastereomer.

Scheme 1.3.20



1.4 Notes and References

- (1) Stratmann, K.; Moore, R. E.; Bonjouklian, R.; Deeter, J. B.; Patterson, G. M. L.; Shaffer, S.; Smith, C. D.; Smitka, T. A. "Welwitindolinones, Unusual Alkaloids from the Blue-Green Algae *Hapalosiphon welwitschii* and *Westiella intricata*. Relationship to Fischerindoles and Hapalindoles" *J. Am. Chem. Soc.* **1994**, *116*, 9935–9942.

- (2) Jimenez, J. I.; Huber, U.; Moore, R. E.; Patterson, G. M. L. "Oxidized Welwitindolinones from Terrestrial *Fischerella* spp." *J. Nat. Prod.* **1999**, *62*, 569–572.
- (3) Stratmann, K.; Burgoyne, D. L.; Moore, R. E.; Patterson, G. M. L. "Hapalosin, a Cyanobacteria Cyclic Depsipeptide with Multidrug-Resistance Reversing Activity" *J. Org. Chem.* **1994**, *59*, 7219–7226.
- (4) Smith, C. D.; Zilfou, J. T.; Stratmann, K.; Patterson, G. M. L.; Moore, R. E. "Welwitindolinone Analogues that Reverse P-Glycoprotein-Mediated Multiple Drug Resistance" *Mol. Pharmacol.* **1995**, *47*, 241–247.
- (5) Zhang, X. Q.; Smith, C. D. "Microtubule Effects of Welsistatin, a Cyanobacterial Indolinone that Circumvents Multiple Drug Resistance" *Mol. Pharmacol.* **1996**, *49*, 288–294.
- (6) Checchi, P. M.; Nettles, J. H.; Zhou, J.; Snyder, J. P.; Joshi, H. C. "Microtubule-Interacting Drugs for Cancer Treatment" *Trends Pharmacol. Sci.* **2003**, *24*, 361–365.
- (7) Mandelkow, E.; Mandelkow, E.-M. "Microtubule Structure" *Curr. Opin. Struct. Biol.* **1994**, *4*, 171–179.

- (8) Aldaz, H.; Rice, L. M.; Stearns, T.; Agard, D. A. “Insight into Microtubule Nucleation from the Crystal Structure of Human γ -Tubulin” *Nature* **2005**, *435*, 523–527.
- (9) Wade, R. H. “On and Around Microtubules: An Overview” *Mol. Biotechnol.* **2009**, *43*, 177–191.
- (10) Bellamy, W. T. “P-glycoproteins and Multidrug Resistance” *Annu. Rev. Pharmacol. Toxicol.* **1996**, *36*, 161–183.
- (11) Avendaño, C.; Menéndez, J. C. “Inhibitors of Multidrug Resistance to Antitumor Agents (MDR)” *Curr. Med. Chem.* **2002**, *9*, 159–193.
- (12) Zamora, J. M.; Pearce, H. L.; Beck, W. T. “Physical-Chemical Properties Shared by Compounds that Modulate Multidrug Resistance in Human Leukemic Cells” *Mol. Pharmacol.* **1988**, *33*, 454–462.
- (13) Ambudkar, S. V.; Dey, S.; Hrycyna, C. A.; Ramachandra, M.; Pastan, I.; Gottesman, M. M. “Biochemical, Cellular, and Pharmacological Aspects of the Multidrug Transporter” *Annu. Rev. Pharmacol. Toxicol.* **1999**, *39*, 361–398.

- (14) Sheps, J.; Ling, V. "Introduction: What is Multidrug Resistance?" In *ABC Transporters and Multidrug Resistance*; Boumendjel, A.; Boutonnat, J.; Robert, J.; John Wiley and Sons, Inc.: Hoboken, **2009**; 1–13.
- (15) Grandjean-Forestier, F.; Stenger, C.; Robert, J.; Verdier, M.; Ratinaud, M.-H. "The P-glycoprotein 170: Just a Multidrug Resistance Protein of a Protean Molecule?" In *ABC Transporters and Multidrug Resistance*; Boumendjel, A.; Boutonnat, J.; Robert, J.; John Wiley and Sons, Inc.: Hoboken, **2009**; 17–46.
- (16) Morjani, H.; Madoulet, C. "Reversal Agents for P-glycoprotein-Mediated Multidrug Resistance" In *ABC Transporters and Multidrug Resistance*; Boumendjel, A.; Boutonnat, J.; Robert, J.; John Wiley and Sons, Inc.: Hoboken, **2009**; 241–259.
- (17) Pérez-Tomás, R. "Multidrug Resistance: Retrospect and Prospects in Anti-Cancer Drug Treatment" *Curr. Med. Chem.* **2006**, *13*, 1859–1876.
- (18) Avendaño, C.; Menéndez, J. C. "Synthetic Studies on *N*-Methylwelwitindolinone C Isothiocyanate (Welwistatin) and Related Substructures" *Curr. Org. Synth.* **2004**, *1*, 65–82.
- (19) Menéndez, J. C. "Chemistry of the Welwitindolinones" *Top. Heterocycl. Chem.* **2007**, *11*, 63–101.

- (20) Wood, J. L.; Holubec, A. A.; Stoltz, B. M.; Weiss, M. M.; Dixon, J. A.; Doan, B. D.; Shamji, M. F.; Chen, J. M.; Heffron, T. P. "Application of Reactive Enols in Synthesis: A Versatile, Efficient, and Stereoselective Construction of the Welwitindolinone Carbon Skeleton" *J. Am. Chem. Soc.* **1999**, *121*, 6326–6327.
- (21) Konopelski, J. P.; Deng, H.; Schiemann, K.; Keane, J. M.; Olmstead, M. M. "Stereoselective Conjugate Addition Directed by an Enantiomerically Pure Ketal. Preparation of the Cyclohexanone Fragment of *N*-Methylwelwitindolinone C Isothiocyanate." *Synlett*, **1998**, 1105–1107.
- (22) Deng, H.; Konopelski, J. P. "Aryllead(II) Reagents in Synthesis: Formation of the C11 Quaternary Center of *N*-Methylwelwitindolinone C Isothiocyanate" *Org. Lett.* **2001**, *3*, 3001–3004.
- (23) López-Alvarado, P.; García-Granda, S.; Álvarez-Rúa, C.; Avendaño, C. "Controlled Generation of Three Contiguous Stereocentres in the Michael Addition of 1-Pyrrolidinocyclohexene to (*E*)-(1-Methyl-2-oxoindolin-3-ylidene)acetophenone" *Eur. J. Org. Chem.* **2002**, 1702–1707.
- (24) Jung, M. E.; Slowinski, F. "Rhodium-Catalyzed Decomposition of Indole-Substituted α -Diazo- β -keto Esters: Three Different Reactions Based on Indole Oxidation State" *Tetrahedron Lett.* **2001**, *42*, 6835–6838.

- (25) MacKay, J. A.; Bishop, R. L.; Rawal, V. H. "Rapid Synthesis of the *N*-Methylwelwitindolinone Skeleton" *Org. Lett.* **2005**, *7*, 3421–3424.
- (26) Baudoux, J.; Blake, A. J.; Simpkins, N. S. "Rapid Access to the Welwitindolinone Alkaloid Skeleton by Cyclization of Indolcarboxaldehyde Substituted Cyclohexanones" *Org. Lett.* **2005**, *7*, 4087–4089.
- (27) Boissel, V.; Simpkins, N. S.; Bhalay, G. "Singlet oxygen conversion of indoles into α,β -unsaturated oxindoles in model compounds related to the welwitindolinone alkaloids" *Tetrahedron Lett.* **2009**, *50*, 3283–3286.
- (28) Greshock, T. J.; Funk, R. L. "An Approach to the Total Synthesis of Welwistatin" *Org. Lett.* **2006**, *8*, 2643–2645.
- (29) Lauchli, R.; Shea, K. J. "A Synthesis of the Welwistatin Core" *Org. Lett.* **2006**, *8*, 5287–5289.
- (30) Brailsford, J. A.; Lauchli, R.; Shea, K. J. "Synthesis of the Bicyclic Welwitindolinone Core via an Alkylation/Cyclization Cascade Reaction" *Org. Lett.* **2009**, *11*, 5330–5333.

- (31) Trost, B. M.; McDougall, P. J. "Access to a Welwitindolinone Core Using Sequential Cycloadditions" *Org. Lett.* **2009**, *11*, 3782–3785.
- (32) Tian, X.; Hutters, A. D.; Douglas, C. J.; Garg, N. K. "Concise Synthesis of the Bicyclic Scaffold of *N*-methylwelwitindolinone C Isothiocyanate via an Indolyne Cyclization" *Org. Lett.* **2009**, *11*, 2349–2351.
- (33) Heidebrecht, R. W.; Gullledge, B.; Martin, S. F. "Approaches to *N*-Methylwelwitindolinone C Isothiocyanate: Facile Synthesis of the Tetracyclic Core" *Org. Lett.* **2010**, *12*, 2492–2495.
- (34) Baran, P.S.; Maimone, T.J.; Richter, J.M. "Total synthesis of marine natural products without using protecting groups" *Nature* **2007**, *446*, 404–408.
- (35) Baran, P. S.; Richter, J. M. "Enantioselective Total Syntheses of Welwitindolinone A and Fischerindoles I and G" *J. Am. Chem. Soc.* **2005**, *127*, 15394–15396.
- (36) Richter, J. M.; Ishihara, Y.; Masuda, T.; Whitefield, B. W.; Llamas, T.; Pohjakallio, A.; Baran, P. S. "Enantiospecific Total Synthesis of the Hapalindoles, Fischerindoles, and Welwitindolinones *via* a Redox Economic Approach" *J. Am. Chem. Soc.* **2008**, *130*, 17938–17954.

- (37) Ready, J. M.; Reisman, S. E.; Hirata, M.; Weiss, M. M.; Tamaki, K.; Ovaska, T. V.; Wood, J. L. "A Mild and Efficient Synthesis of Oxindoles: Progress Towards the Synthesis of Welwitindolinone A Isonitrile" *Angew. Chem., Int. Ed.* **2004**, *43*, 1270–1272.
- (38) Reisman, S. E.; Ready, J. M.; Hasuoka, A.; Smith, C. J.; Wood, J. L. "Total Synthesis of (±)-Welwitindolinone A Isonitrile" *J. Am. Chem. Soc.* **2006**, *128*, 1448–1449.
- (39) Reisman, S. E.; Ready, J. M.; Weiss, M. M.; Hasuoka, A.; Hirata, M.; Tamaki, K.; Ovaska, T. V.; Smith, C. J.; Wood, J. L. "Evolution of a Synthetic Strategy: Total Synthesis of (±)-Welwitindolinone A Isonitrile" *J. Am. Chem. Soc.* **2008**, *130*, 2087–2100.

Chapter 2

Construction of the Welwitindolinone C Core:

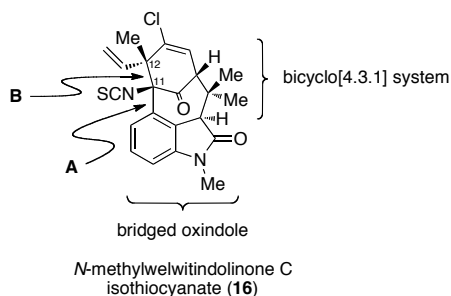
[3+2] Dipolar Cycloaddition and Michael Addition

2.1 Initial Considerations.

To date, our efforts towards the synthesis of *N*-methylwelwitindolinone C isothiocyanate have encompassed the works of six graduate students¹ and seven postdoctoral researchers² over twelve years. Each has contributed significant ideas to the project, and the synthetic work outlined in this chapter builds upon their contributions.

Although our first-generation synthesis of the core of *N*-methylwelwitindolinone C isothiocyanate was concise (see Chapter 1, Section 1.3.1.1), it provided a skeletal system lacking much of the functionality required for subsequent elaboration to the natural product.³ Based upon this assessment, we decided to develop an alternate route. We began by focusing on the construction of bonds A and B depicted in Figure 2.1.1. Upon close inspection of the two vicinal, fully-substituted carbon centers (i.e. C11 and C12), we realized that a [3+2] dipolar cycloaddition would not only forge bond B, completing the bicyclo[4.3.1] system but would also establish the desired *cis*-relationship between the methyl at stereogenic C12 and the isothiocyanate functionality at C11.⁴⁻⁹ To test this hypothesis, we needed to construct a bridged oxindole capable of undergoing a [3+2] dipolar cycloaddition. Fortunately, chemistry already developed in our first-generation efforts could be applied to create bond A via aryl C–H insertion.

Figure 2.1.1



2.2 First Generation [3+2] Dipolar Cycloaddition Approach.

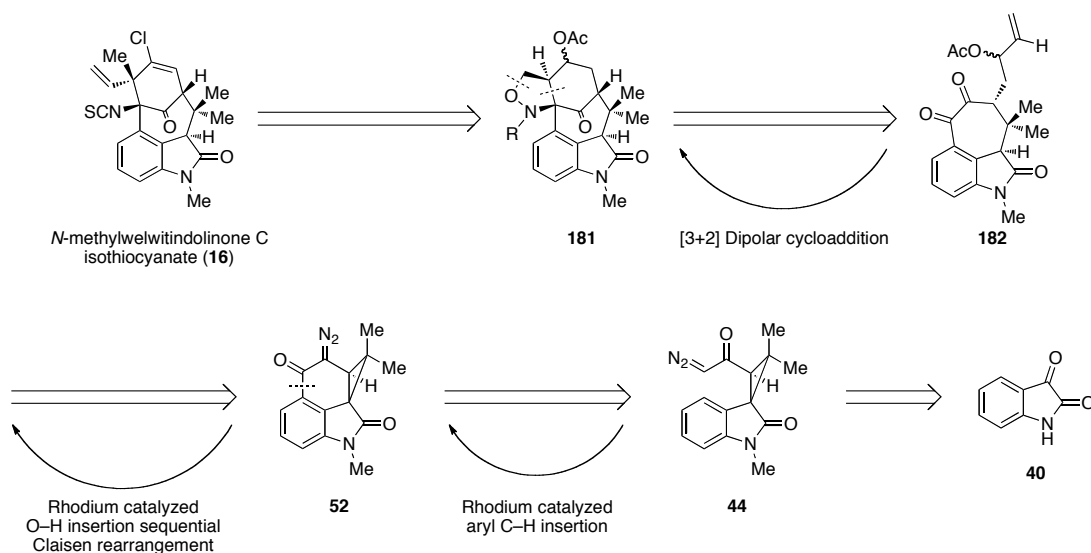
2.2.1 Retrosynthetic Analysis.

Implementation of our nitron-mediated dipolar cycloaddition strategy necessitated the development of a concise retrosynthetic blueprint (Scheme 2.2.1). To that end, we planned late stage installation of the potentially labile isothiocyanate moiety as well as formation of the vinyl chloride. In order to gain access to functional groups capable of being converted to the desired substituents, N–O bond cleavage of isoxazolidine **181** followed by deacylation and oxidation of the resultant alcohol to the ketone would be required. The quaternary center would then be installed via alkylative processes.

Key isoxazolidine **181** would be constructed by our planned [3+2] dipolar cycloaddition of the pendant olefin of **182** onto an in situ-generated nitron at the benzylic carbonyl position. The allylic acetate side-chain of **182** would be created using

rhodium(II)-catalyzed O–H insertion sequential Claisen rearrangement chemistry of an appropriate allylic alcohol and α -diazoketone **52**. Finally, α -diazoketone **52** would arise via aryl C–H insertion of α -diazoketone **44**, a compound previously proven to be accessible from commercially available isatin (**40**).

Scheme 2.2.1



2.2.2 Aryl C–H Insertion and Construction of Diazoketone **52**.

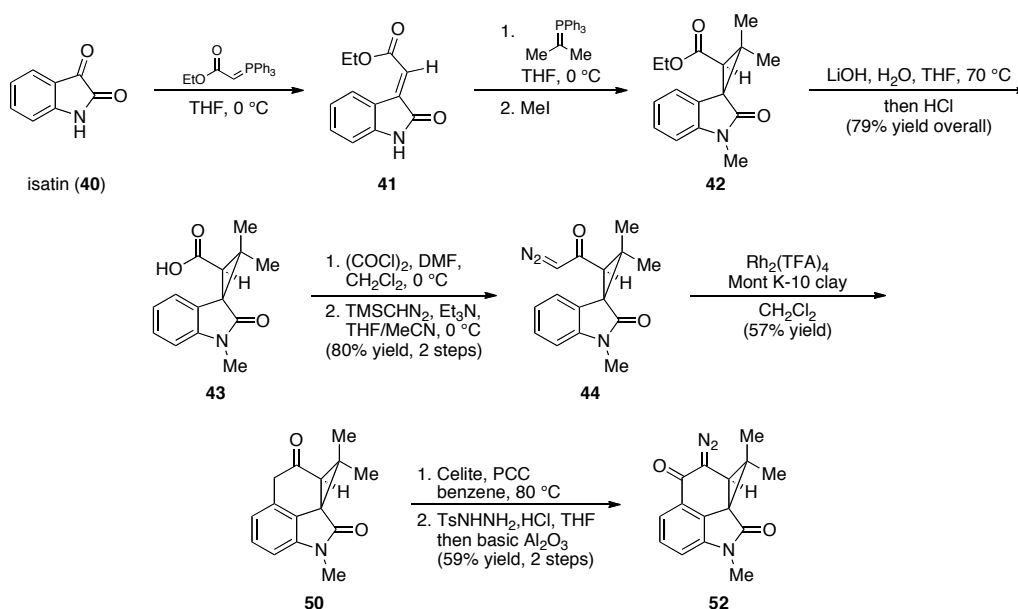
According to our proposed retrosynthetic approach, we began our synthesis by utilizing chemistry previously developed in our lab.^{10,11} As reported in our first synthetic attempt towards *N*-methylwelwitindolinone C isothiocyanate (**16**), we developed methods to access key α -diazoketones **44** and **52**. Their syntheses are outlined in Scheme 2.2.2.

Starting from commercially available and inexpensive isatin (**40**), a Wittig-olefination afforded enoate **41**. Subsequent Michael addition of isopropyl

triphenylphosphorane and treatment with MeI provided spiro-cyclopropane adduct **42**. Saponification of the ethyl ester then delivered carboxylic acid **43**. The four-step, two-pot sequence was conducted without purification prior to a final recrystallization from methanol to give **43** in a 79% overall yield. Conversion of the carboxylic acid to the intermediate acid chloride using oxalyl chloride was followed directly by displacement with TMSCHN₂ to forge key α -diazoketone **44**.

Having built α -diazoketone **44**, efforts were then directed towards the construction of α -diazoketone **52**. After exhaustive catalyst and additive screening, our group discovered that we could generate tetracyclic ketone **50** from an intramolecular aryl C–H insertion of diazoketone **44** in good yield using rhodium(II) trifluoroacetate dimer in the presence of Montmorillonite K10 clay (a mild Lewis-acid source). Benzylic oxidation and a regio- and chemoselective diazotization successfully created the second desired α -diazoketone **52**.

Scheme 2.2.2



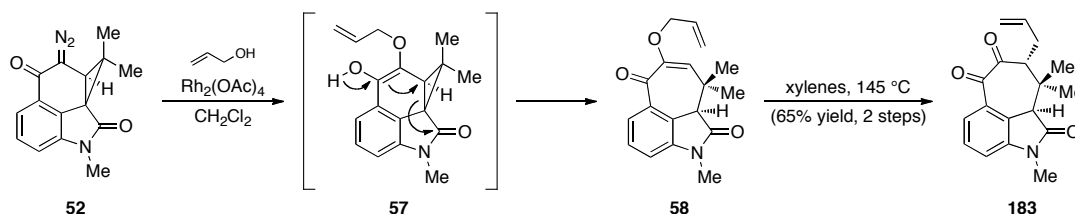
2.2.3 O–H Insertion Sequential Claisen Rearrangement and [3+2]

Dipolarcycloaddition Model.

Having established an effective route to requisite diazoketone **52**, we were poised to test our projected [3+2] dipolar cycloaddition reaction that would construct the core of *N*-methylwelwitindolinone C isothiocyanate. To that end, we decided to focus on an easily accessible model system that would challenge the viability of our strategy. We began by targeting a substrate with a pendant olefin capable of cyclizing onto a benzylic nitrene (Scheme 2.2.3). For this purpose, **183** was chosen.

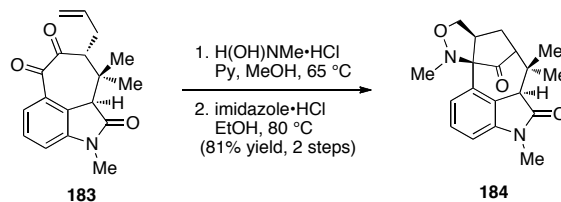
Starting from our diazoketone **52** and allyl alcohol, we initiated an O–H insertion by exposing the reaction mixture to rhodium(II) acetate dimer. The resultant O–H insertion product immediately enolized to intermediate **57** and subsequently underwent a ring-opening event to give allyl vinyl ether **58**. Heating this compound in xylenes at reflux induced a Claisen rearrangement that delivered terminal olefin adduct **183** in good yield.

Scheme 2.2.3



With our targeted mono-substituted olefin (**183**) in hand, we hoped to condense a hydroxylamine to form a nitron on the inherently more reactive benzylic carbonyl. Fortunately, upon exposure of diketone **183** to *N*-methylhydroxylamine in methanol at reflux, we were able to form and isolate the corresponding *N*-methylnitron (not shown). Further optimization of the reaction conditions led to the establishment of a one-pot, two-step sequence wherein the intermediate *N*-methylnitron was concentrated, diluted in ethanol and heated in the presence of imidazole hydrochloride to produce isoxazolidine **184** (Scheme 2.2.4).

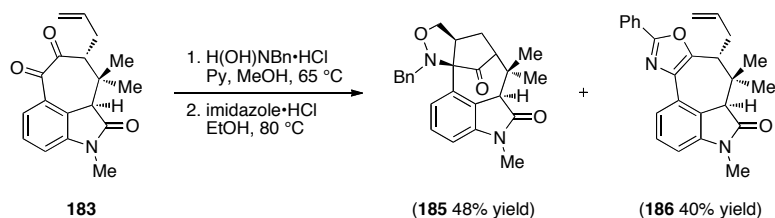
Scheme 2.2.4



Although we were pleased with this operationally simple strategy for the installation of the welwitindolinone backbone, we recognized that N–O bond cleavage of an *N*-methylisoxazolidine was potentially problematic; thus, we decided to pursue alternative *N*-substituted-hydroxylamines within our model system. As a representative example we exposed diketone **183** to the dipolar cycloaddition conditions developed to construct isoxazolidine **184**, except *N*-methyl hydroxylamine was substituted with *N*-benzyl hydroxylamine (Scheme 2.2.5).⁴ From this reaction, our desired isoxazolidine **185** was isolated in almost equal amounts with oxazole side-product **186**. Unfortunately, no further manipulation of reaction conditions could curb formation of oxazole side-product

186.^{12,13} Because the use of other *N*-substituted-hydroxylamines led to formation of undesired side-products, we decided to advance our synthesis with *N*-methylhydroxylamine and to address the issue of ring size.¹⁴

Scheme 2.2.5

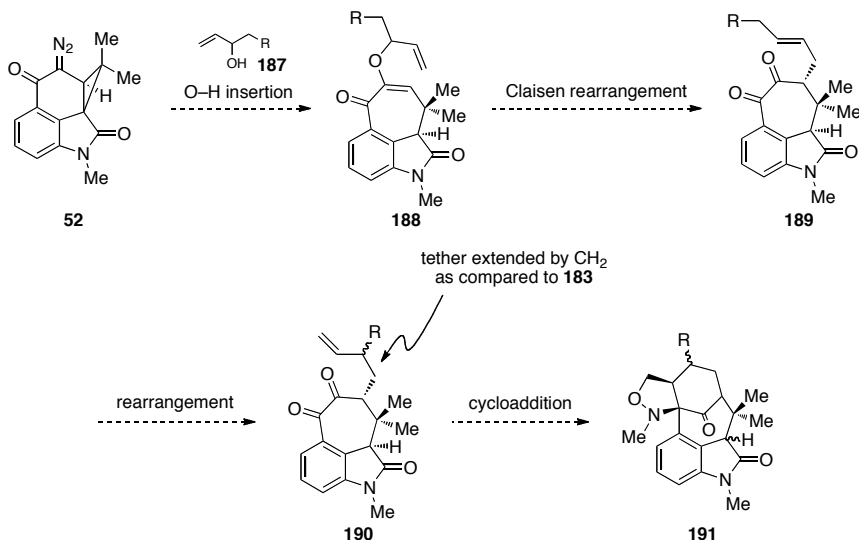


2.2.4 Construction of the Welwitindolinone C Core via [3+2] Dipolar Cycloaddition.

The success of a [3+2] dipolar cycloaddition in our model system prompted the design of a synthetic strategy to reach the core of *N*-methylwelwitindolinone C isothiocyanate (**16**). We realized that in order to use the same method to arrive at our goal, we needed to extend the dipolarophile tether by a single methylene unit as depicted by the curved arrow above compound **190** in Scheme 2.2.6 (see compound **183** in Scheme 2.2.4 for comparison). In light of the results obtained with our model system, compound **190** was expected to undergo a [3+2] dipolar cycloaddition to produce **191**. However, in contrast to olefin **183**, homologated olefin **190** could not arise from our established O-H insertion/Claisen directly. Rather than deviating from our plan, we devised a strategy that would start from an O-H insertion of functionalized allylic alcohol **187** with diazoketone **52** to give allyl vinyl ether **188**. Claisen rearrangement would

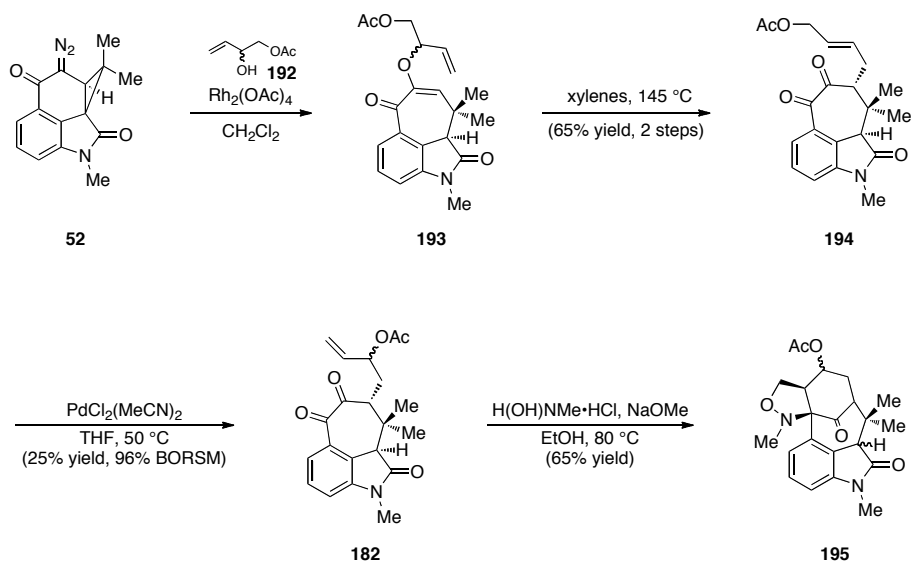
provide disubstituted olefin **189** in which the functionality represented by R would be transposable. Transposition of the R-group would thus deliver desired compound **190**.

Scheme 2.2.6



In accordance with our strategy, O-H insertion of known allylic alcohol **192** with diazoketone **52** afforded allyl vinyl ether **193**, which was subsequently heated at reflux in xylenes to produce allylic acetate **194** in good yield (Scheme 2.2.7).¹⁵ Palladium-catalyzed allylic transposition of **194** gave the contra-thermodynamic allylic acetate **182** in poor yield; however, recycling the recovered starting material provided ample material to press forward.¹⁶ Heating terminal olefin **182** in ethanol in the presence of free-based *N*-methylhydroxylamine gratifyingly forged the welwitindolinone C core structure **195**.¹⁷⁻¹⁹

Scheme 2.2.7



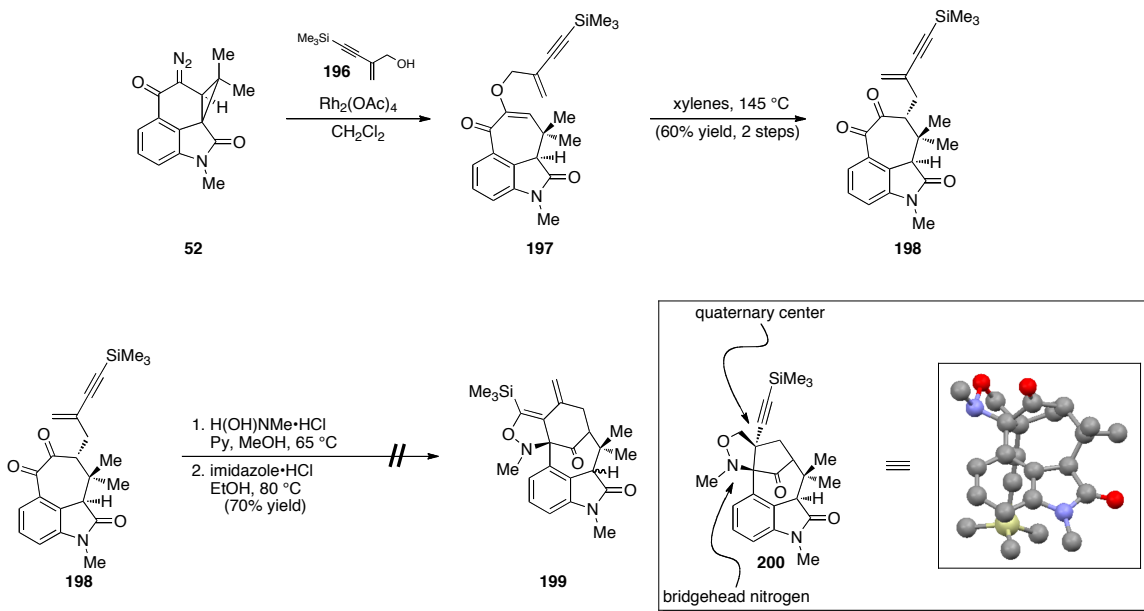
2.2.5 Unexpected Result from Alternative Allylic Alcohol.

Concurrent to the studies that led to the construction of the core of *N*-methylwelwitindolinone C isothiocyanate (**16**) we briefly pursued the use of alternative allylic alcohols in hopes of installing alternative functionalities. In the course of our screen, the use of allylic alcohol **196** resulted in an unexpected but fortuitous formation of **200** (Scheme 2.2.8).²⁰⁻²²

Rhodium(II)-mediated O–H insertion of allylic alcohol **196** with diazoketone **52** gave allyl vinyl ether **197**, whereupon subsequent heating induced a Claisen rearrangement to produce ene-yne **198**. Because the tether of compound **198** contains two functional groups capable of undergoing a [3+2] dipolar cycloaddition, multiple product

outcomes are possible. We predicted that exposure of compound **198** to our standard [3+2] dipolar cycloaddition conditions would provide bicyclo[4.3.1] **199**. However, in the event, we isolated isoxazolidine **200**, the structure of which was confirmed by X-ray crystallography.^{4,23} Attempts to modify the chemoselectivity of the cycloaddition by removal of the trimethylsilyl group or by olefin functionalization were unsuccessful. Although the selectivity observed in the cycloaddition of **200** was undesired, we were encouraged by our ability to stereoselectively forge the fully-substituted quaternary carbon adjacent to the bridgehead nitrogen of **16**. Indeed, this observation motivated the pursuit of an alternate strategy wherein the requisite bicyclo[4.3.1] backbone and C12 quaternary center would be produced in a single step.

Scheme 2.2.8



2.3 Second Generation [3+2] Dipolar Cycloaddition.

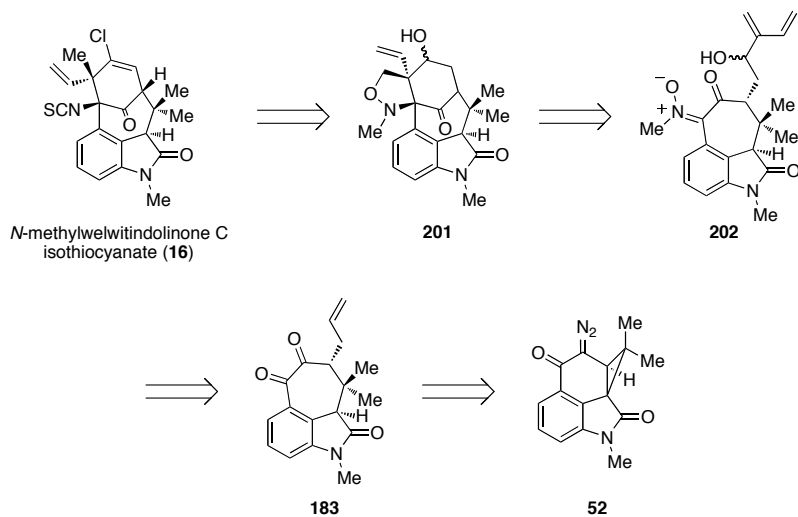
2.3.1 Revised Retrosynthetic Analysis.

With the discovery that we could introduce a quaternary center of the welwitindolinone core via a [3+2] dipolar cycloaddition (Scheme 2.2.8), we decided to revise our retrosynthetic strategy to take advantage of this method. Incorporation of a 1,1-disubstituted olefin within a dipolarophile tether would thus enable quaternary center formation. This single reaction would install the core components of **16** including the bicyclo[4.3.1] system, the vicinal, fully-substituted carbon centers, the correct substitution at the quaternary center, and the bridgehead nitrogen.

As shown in Scheme 2.3.1, *N*-methylwelwitindolinone C isothiocyanate (**16**) would arise from cleavage of the N–O bond within isoxazolidine **201**. Deoxygenation of the resultant primary hydroxyl group, isothiocyanate formation from the free amine, and conversion of the secondary hydroxyl group to the vinyl chloride moiety would complete the synthesis of **16**. In order to achieve these late stage manipulations, a [3+2] dipolar cycloaddition between the 1,1-disubstituted olefin and the nitron of compound **202** would need to be successful to produce isoxazolidine **201**. Synthesis of diene **202** would commence from an O–H insertion of diazoketone **52** and allyl alcohol where a subsequent Claisen rearrangement would give known olefin **183**. The olefin within **183**

would serve as a functional handle for conversion to the diene moiety within substrate **202**.

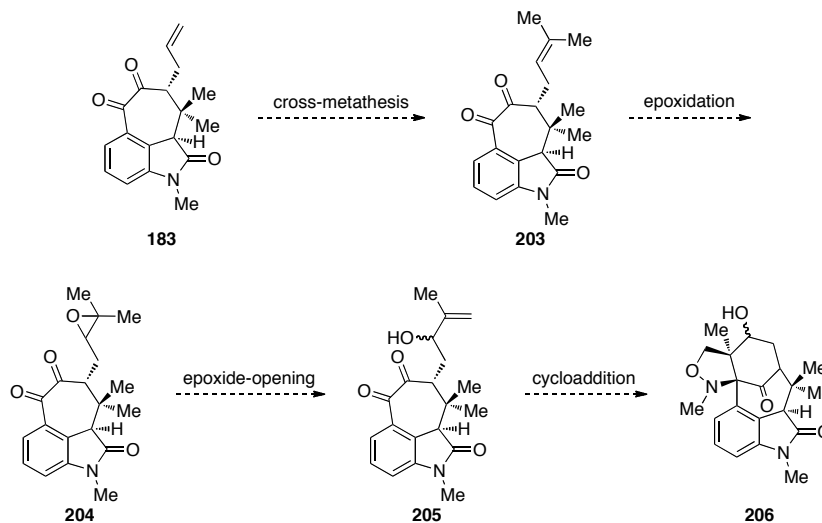
Scheme 2.3.1



2.3.2 Model System: Attempted Installation of Quaternary Center via Nitron Cycloaddition and Epoxide-opening.

To quickly assess the viability of simultaneously installing a quaternary center and a bicyclo[4.3.1] system via a nitron-mediated dipolar cycloaddition, we devised a simplified model system (Scheme 2.3.2). We believed that a cross-metathesis of terminal olefin **183** with a suitable coupling partner would provide trisubstituted alkene **203**. An epoxidation and epoxide-opening sequence (**203** → **205**) would then give requisite 1,1-disubstituted olefin **205**. Nitron formation and intramolecular dipolar cycloaddition would then deliver isoxazolidine **206**, the target model system substrate.

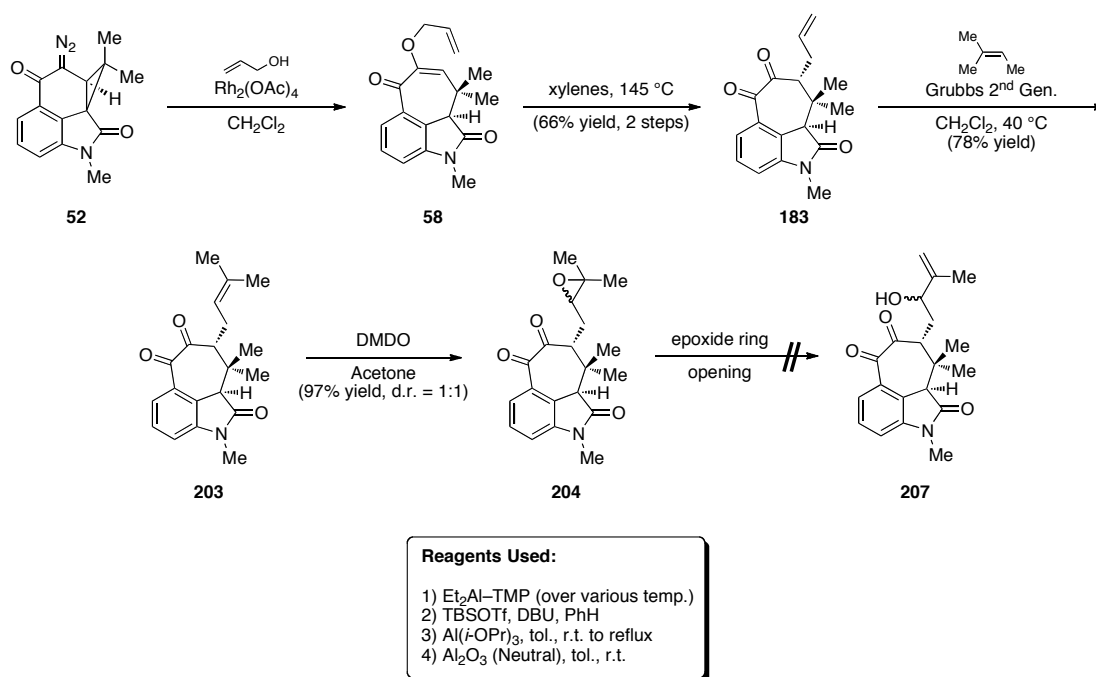
Scheme 2.3.2



In the event, we successfully conducted an O–H insertion of allyl alcohol with diazoketone **52** to produce allyl vinyl ether **58** (Scheme 2.3.3).³ Subsequent heating of allyl vinyl ether **58** in xylenes at reflux induced a Claisen rearrangement to give terminal olefin **183**. After screening several olefin cross-metathesis coupling partners, we found that 2-methyl-2-butene in the presence of Grubbs 2nd generation catalyst and terminal olefin **183** afforded our desired trisubstituted alkene **203** in excellent yield.²⁴ Epoxidation of trisubstituted alkene **203** with DMDO in acetone delivered epoxide **204** in near quantitative yield as a 1:1 mixture of diastereomers. Other oxidation conditions were screened, including *m*-CPBA; however, only Baeyer-Villiger side-products were observed.

Before we could test the nitron-mediated dipolar cycloaddition of our model system, we needed to open epoxide **204** to allylic alcohol **207**. Unfortunately, under a variety of conditions we were unable to achieve this task. Most applied conditions either resulted in exclusive isolation of starting material or complete starting material decomposition. As a result, we were forced to develop an alternate model system.

Scheme 2.3.3

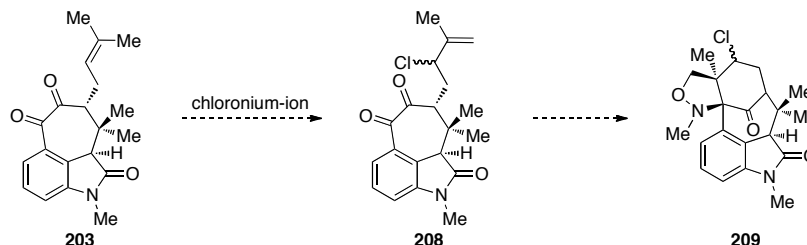


2.3.3 Model System: Installation of Quaternary Center via Nitron Cycloaddition and Chloronium-ion-mediated Elimination.

As an alternate means of arriving at a model system capable of undergoing a [3+2] dipolar cycloaddition, we turned to a chloronium ion-mediated oxidative isomerization to generate allylic chloride **208** (Scheme 2.3.4).²⁵ We were hopeful that

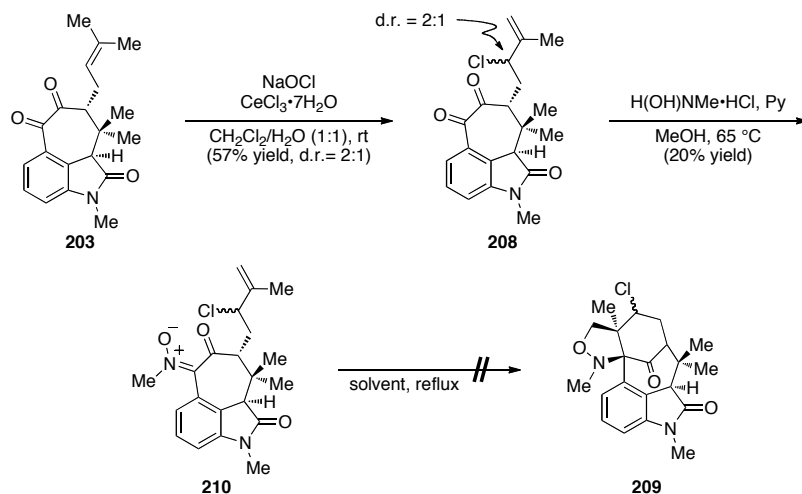
exposing compound **208** to our [3+2] dipolar cycloaddition conditions would construct isoxazolidine **209** with the secondary chloride as a functional handle for further manipulations.

Scheme 2.3.4



In the event, we discovered that when trisubstituted olefin **203** was exposed to sodium hypochlorite and cerium(III) trichloride heptahydrate, allylic chloride **208** was isolated as a 2:1 mixture of diastereomers in good yield (Scheme 2.3.5). The reaction is thought to proceed via E_1 -type elimination of a chloronium-ion intermediate to generate 1,1-disubstituted olefin **208**. Treatment of **208** with *N*-methylhydroxylamine formed nitrone **210** in low yield, presumably because of competing S_N2 or S_N2' chloride-displacement pathways. Despite the low yielding production of **210**, we attempted to induce a dipolar cycloaddition to produce isoxazolidine **209**. However, heating nitrone **210** in a variety of solvents at reflux resulted only in intractable mixture of products with no trace of desired product.

Scheme 2.3.5



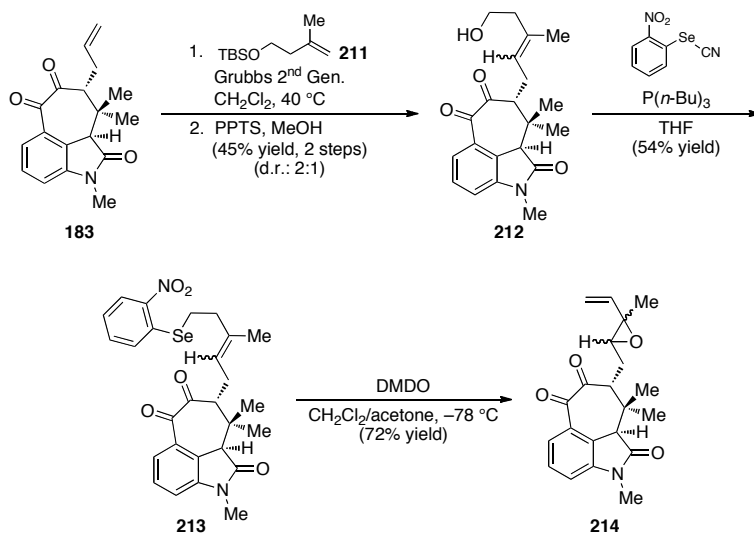
2.3.4 Attempted Installation of Quaternary Center via Nitrone Cycloaddition.

The inability to advance our model systems to substrates capable of undergoing a [3+2] dipolar cycloaddition prompted us to consider alternative routes to cyclization product **201** from intermediates along the established pathway outlined in Scheme 2.3.1. We began by directing our attention to the synthesis of the [3+2] dipolar cycloaddition precursor **202**.

Allylic alcohol **202** was prepared in a sequence that began with cross metathesis of diketone **183** and silyl ether **211** followed by silyl deprotection (Scheme 2.3.6).^{24,26} The derived alcohol **212** was isolated as an inconsequential 2:1 mixture of *E/Z*,

respectively. Selenenylation of **212** via the method of Grieco [*o*-(NO₂)C₆H₄-SeCN and P(*n*-Bu)₃] furnished selenide **213** which, upon oxidation with DMDO provided the corresponding epoxy selenoxide (not shown).²⁷⁻²⁹ As expected the latter was unstable and upon work-up underwent clean elimination to deliver vinyl epoxide **214** in good yield.³⁰

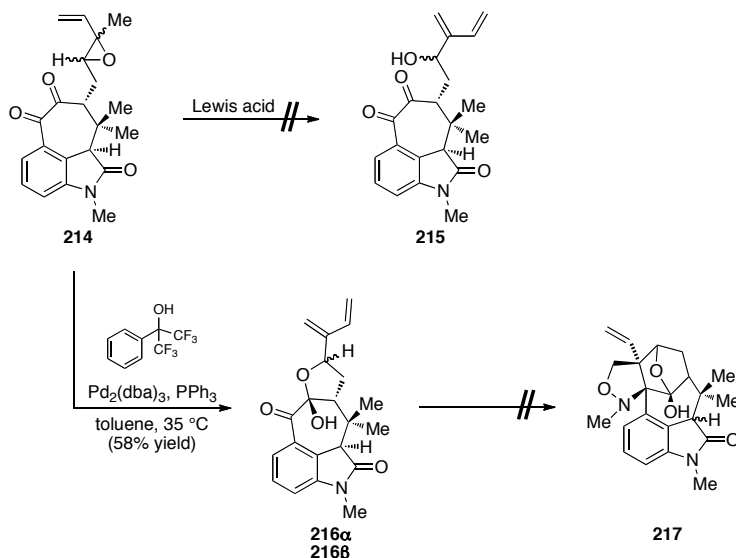
Scheme 2.3.6



Having accessed **214**, attention was turned to opening the epoxide and delivering the cycloaddition substrate (**202**). After considerable fruitless experimentation with several Lewis acids we eventually explored a palladium-catalyzed isomerization approach pioneered by Noyori³¹ and modified more recently by Radinov.³² Under Radinov's conditions, opening of vinyl epoxide **214** in the presence of a fluorinated alcohol proceeded to furnish hemiacetals **216 α** and **216 β** as an inseparable mixture of diastereomers. Although the intermediacy of the hemiacetals was expected, the effect of the altered electronics on the subsequent cycloaddition was uncertain (cf., **198** and **116**). Unfortunately, exposure of **216 α** and **216 β** to *N*-methylhydroxylamine under forcing

conditions did not produce any of the desired cycloadduct **217**. We speculate that geometric constraint of the hemi-acetal prevented the dipolar cycloaddition from occurring.

Scheme 2.3.7



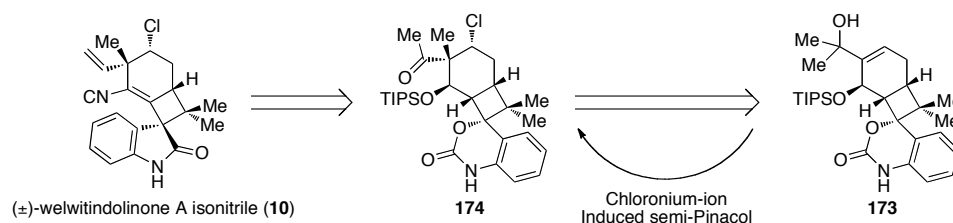
2.4 Chloronium-ion Semi-Pinacol.

2.4.1 Revised Retrosynthetic Analysis.

Ultimately, our attempts to install the quaternary center of *N*-methylwelwitindolinone C isothiocyanate (**16**) via [3+2] dipolar cycloaddition proved unsuccessful. As a result, we began to explore alternate strategies that would install the quaternary center at C12 at a later stage in the synthesis. To that end, we decided to build on familiar chemistry utilized in our welwitindolinone A isonitrile (**10**) synthesis

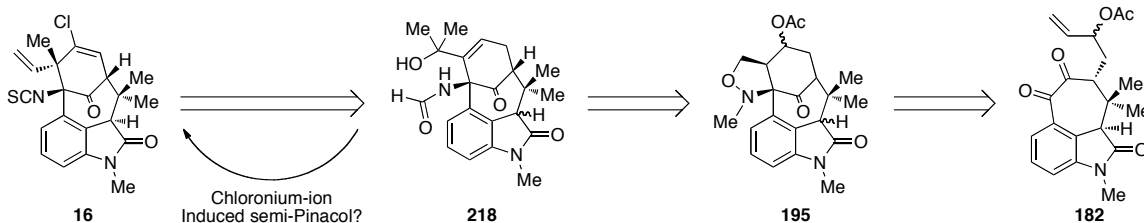
(Scheme 2.4.1).^{33,34} In the synthesis of **10**, chloronium-ion induced semi-pinacol rearrangement of tertiary allylic alcohol **173** installed the secondary chloride and quaternary center of **174**. Further functional group manipulations eventually enabled completion of the total synthesis of **10**.

Scheme 2.4.1



We believed that a chloronium-ion-induced semi-Pinacol rearrangement could be used in a similar fashion to install the quaternary center in **16** (Scheme 2.4.2). In order to test this hypothesis, we needed first to arrive at intermediate **218**, a structure containing a tertiary allylic alcohol motif poised for rearrangement. Having already established a facile approach to the core of *N*-methylwelwitindolinone C isothiocyanate (**16**) via nitrene-mediated dipolar cycloaddition, we wanted to expand and incorporate that approach into our projected chloronium-ion semi-Pinacol rearrangement strategy. Construction of alcohol **218** would proceed through N–O bond cleavage of isoxazolidine **195**, which in turn would arise from a [3+2] dipolar cycloaddition of the pendant olefin within compound **182**.

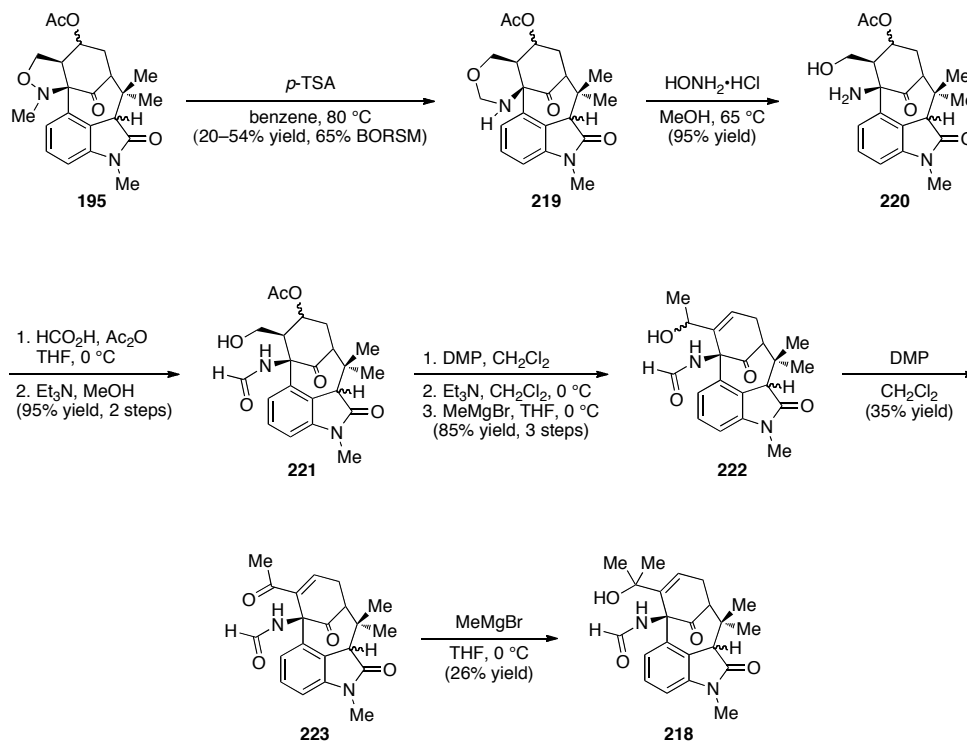
Scheme 2.4.2



2.4.2 Construction of the Requisite Tertiary Alcohol.

As illustrated in Scheme 2.4.3, isoxazolidine **195** was advanced first by rearrangement to the corresponding aminal (**219**). Conversion of **195** to **219** was poor; however, the remaining starting material was isolated and recycled, thereby providing enough material to move forward. Subsequent treatment of **219** with hydroxylamine hydrochloride produced amino-alcohol **220** in 95% yield. To set the stage for eventual introduction of the bridgehead isonitrile, **220** was bis-formylated.^{35,36} Selective deformylation of the derived formates produced alcohol **221** that, in a three-step process involving oxidation with Dess–Martin periodinane (DMP),³⁷ base-induced elimination to the enal, and addition of methyl magnesium bromide, was converted to secondary alcohol **222** as an inconsequential mixture of diastereomers. In practice, the instability of the intermediates produced in this three-step sequence to silica gel required that the sequence be performed without purification. Finally, oxidation of alcohol **222** to enone **223**, followed by addition of methyl magnesium bromide provided desired tertiary allylic alcohol **218**, albeit in low yield.

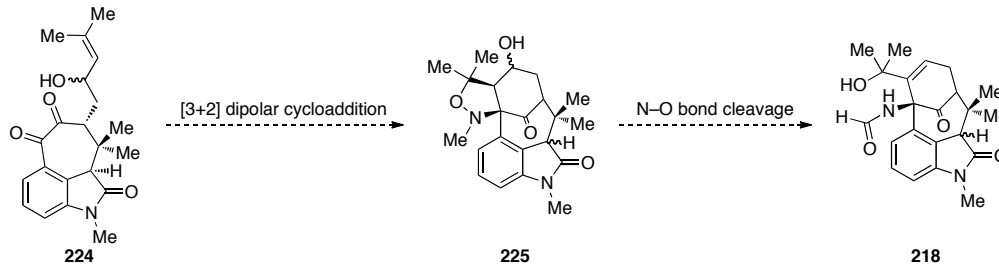
Scheme 2.4.3



2.4.3 Attempted Alternate Route to Tertiary Alcohol.

In an attempt to improve the synthesis of **218** as outline in Scheme 2.4.3, we devised a possible alternate route (Scheme 2.4.4). We envisioned a [3+2] dipolar cycloaddition of trisubstituted olefin **224**, having the requisite gem-dimethyls of tertiary allylic alcohol **218** embedded within the dipolarophile tether, to generate isoxazolidine **225**. Cleavage of the N–O bond of the corresponding isoxazolidine (**225**) would lead directly to tertiary allylic alcohol **218**.

Scheme 2.4.4

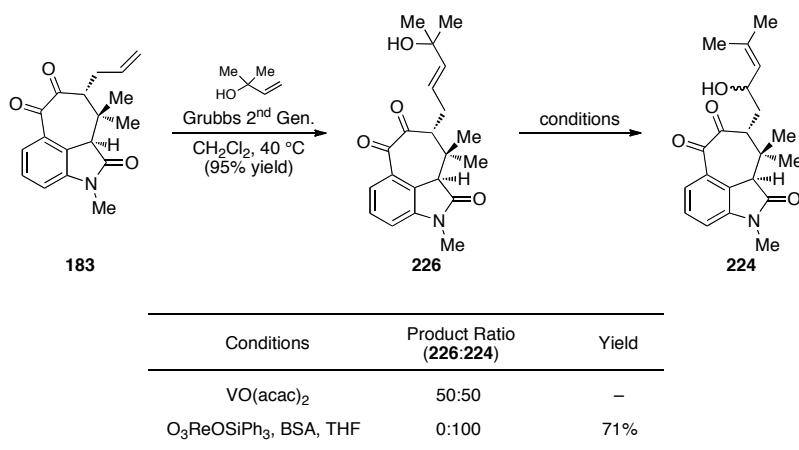


In the event, a Grubbs 2nd generation catalyst-mediated cross metathesis of terminal olefin **183** with 2-methyl-3-buten-2-ol produced allylic alcohol **226** in excellent yield (Scheme 2.4.5).²⁴ Allylic transposition of tertiary alcohol **226** to secondary alcohol **224** proved more difficult than anticipated. Our first attempts to acylate alcohol **226** and transpose the allylic acetate failed due to our inability to functionalize the tertiary alcohol. We then turned to metal-mediated allylic transpositions of alcohols and found that standard VO(acac)₂ conditions gave a 1:1 mixture of transposed product to starting material (**224:226**).³⁸ Efforts to separate and recycle the mixture were made, but recovery was inefficient, and we eventually pursued more exotic methods for transposition.

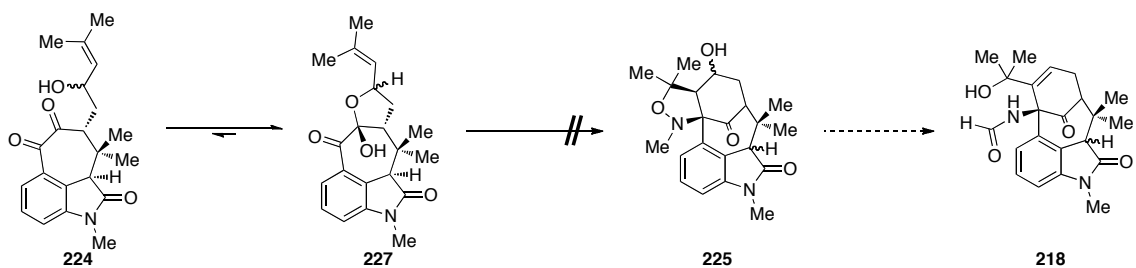
In 2005, Grubbs and Morrill outlined the utility of O₃ReOSiPh₃ as an efficient catalyst for 1,3-isomerizations of allylic alcohols.³⁹ They related that proper solvent choice and the presence of *N,O*-bis(trimethylsilyl)acetamide (BSA) delivered less-hindered allylic alcohols with high selectivity. They proposed that the difference in rate of silylation of primary, secondary, and tertiary alcohols with BSA controlled the equilibrium of transposed product to starting material. Delighted by this finding, we applied the reported reaction conditions to our system and found that after some optimization we could transpose **226** to allylic alcohol **224** in good yield and high

regioselectivity. Unfortunately, we were unable to prevent hydrolysis of the secondary, in-situ generated silyl ether (not shown), and collapse of the resultant alcohol onto the corresponding carbonyl to generate acetal **227** was unavoidable (Scheme 2.4.6). As in our earlier model systems (see Scheme 2.3.7 for comparison), formation of acetal **227** prevented a [3+2] dipolar cycloaddition from occurring, and we were thus unable to advance our strategy. As a result, we returned to our original route to **218** (Scheme 2.4.3).

Scheme 2.4.5



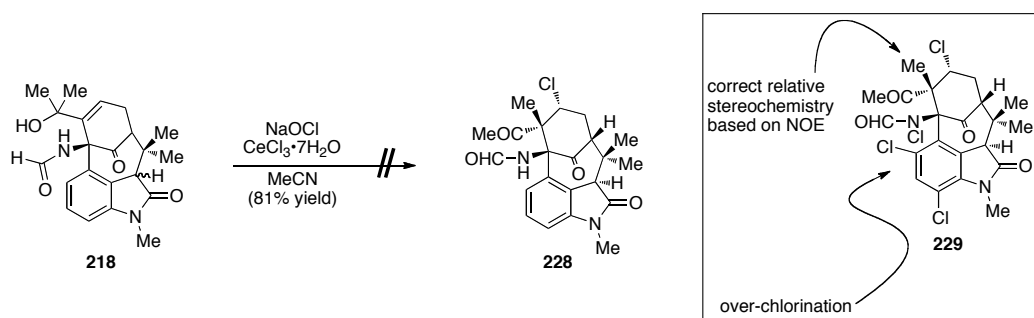
Scheme 2.4.6



2.4.4 Installation of Quaternary Center via Chloronium-ion Semi-Pinacol.

Despite its poor overall yield, the unoptimized synthetic sequence leading to **218** provided sufficient material to explore the proposed halonium ion-induced semi-pinacol rearrangement. In the event, exposure of **218** to $\text{CeCl}_3 \cdot 7\text{H}_2\text{O}$ and NaOCl was found not to produce the expected product **228**, but rather undesired product **229** (Scheme 2.4.7). Extensive NMR analysis indicated that chloronium ion activation and subsequent rearrangement had occurred from what appeared to be the desired and sterically more encumbered face (see Section 2.4.4.1 for rationale). However, this transformation was accompanied by over-chlorination. Given our success in applying this type of semi-pinacol in the welwitindolinone A (**10**) synthesis (Scheme 2.4.1), we were both surprised and disappointed by the indiscriminate reactivity observed. Recent efforts to overcome this problem by limiting stoichiometry of the oxidant revealed that the aromatic system in substrate **218** reacts first, followed by the formamide and then the trisubstituted olefin.

Scheme 2.4.7

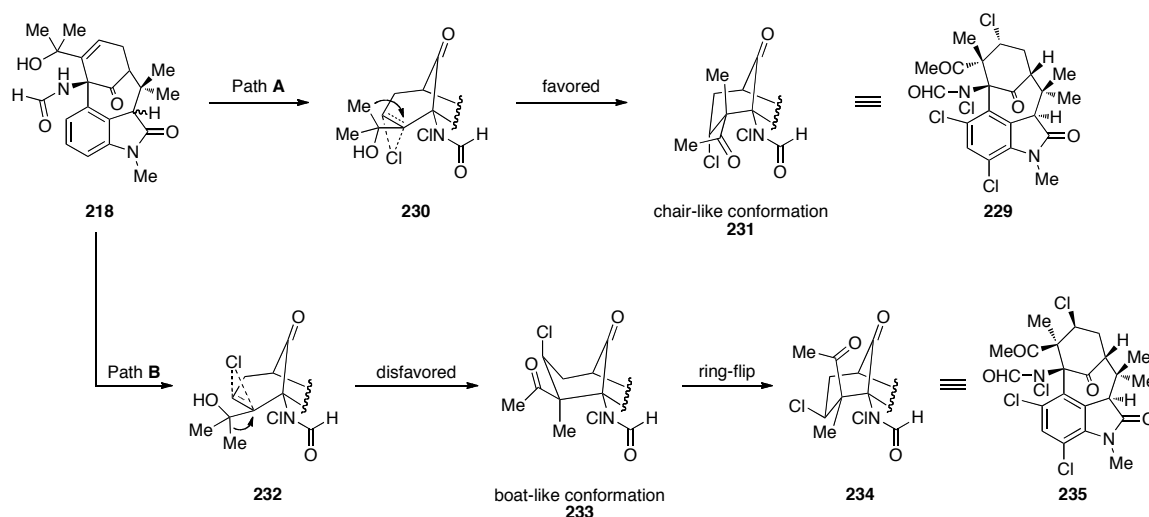


2.4.4.1 Relative Stereochemical Rationale of Chloronium-ion semi-Pinacol Rearrangement.

At first, the relative stereochemical outcome of the chloronium-ion semi-Pinacol rearrangement seemed counterintuitive (see Scheme 2.4.7 for referenced reaction). The chloronium-ion appeared to approach from the more hindered face of the trisubstituted olefin in **218**. This pathway is represented by Path A in Scheme 2.4.8. In this process, the chloronium-ion approaches from the bottom face of the olefin represented by intermediate **230**. A methyl-shift then may occur antiperiplanar to the chloronium-ion in a chair-like transition state to directly generate conformer **231** that is equivalent to the observed product **229**. To further support our rationalization, we address the approach of a chloronium-ion from the top face of the olefin (**218**).

As shown in Path B (Scheme 2.4.8), if the chloronium-ion approaches from the top face of olefin **232**, a methyl-shift occurring antiperiplanar to the chloronium-ion would proceed through a boat-like transition state leading to the energetically disfavored boat-like conformer **233**. A ring-flip would then be necessary to arrive at the more favored chair conformer **234**. 3-D structure **234** is equivalent to 2-D structure **235**, which is not observed in the reaction.

Scheme 2.4.8



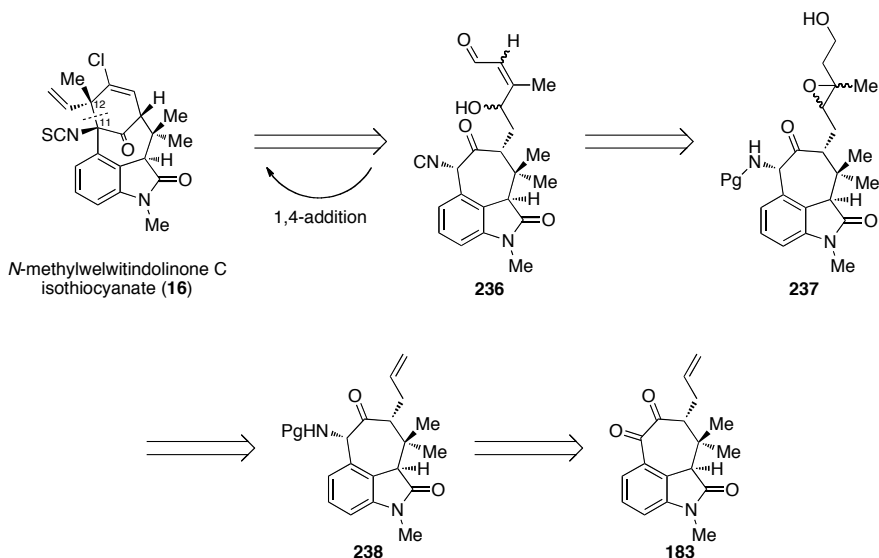
2.5 Michael Addition Approach.

2.5.1 Retrosynthetic Analysis.

With the unfortunate turn of events in our attempt to install the quaternary center of **16** via a chloronium-ion semi-Pinacol rearrangement (see Section 2.4), we formulated a new synthetic strategy towards *N*-methylwelwitindolinone C isothiocyanate (**16**) (Scheme 2.5.1). Our plan depended on an intramolecular Michael addition of the derived enolate of the α -isonitrile ketone within **236** onto the pendant enal to forge the C–C bond between C11 and C12.⁴⁰ Additional functional group manipulations would then provide **16**. Construction of the γ -hydroxy enal motif of **236** would arise from the oxidation and epoxide ring-opening of epoxy alcohol **237**. Isonitrile formation from the corresponding protected amine would complete the synthesis of **236**. We envisioned a cross-metathesis

of pendant olefin **238** with a functionalized olefin to provide a skeletal appendage for conversion to **237**. The protected α -amino ketone (**238**) would arise through a reductive amination of an intermediate imine starting from diketone **183**.

Scheme 2.5.1

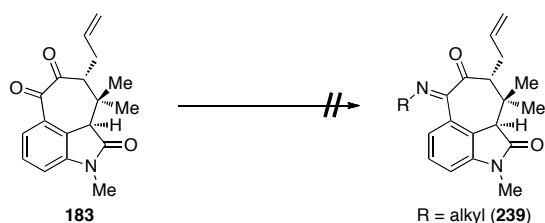


2.5.2 Indium-Mediated Reductive Amination.

We began the synthesis of the Michael precursor by exploring reductive amination conditions to build **238** in Scheme 2.5.1. This seemingly straightforward transformation proved more difficult than anticipated (Scheme 2.5.2). Ultimately, we were unable to condense a primary amine onto the benzylic carbonyl of **183** to make keto-imine **239**. We speculated that primary amines were not nucleophilic enough to form our requisite imine. Given this result, we considered condensation of *O*-alkylated

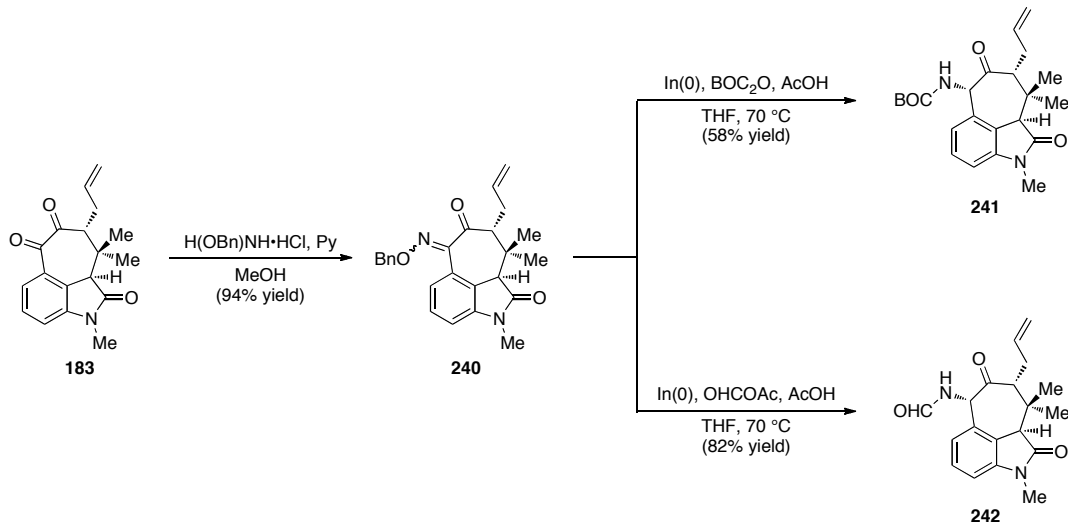
hydroxylamines to form oxime ethers; here, exploitation of the α -effect would increase nucleophilicity while still maintaining the necessary nitrogen functionality.

Scheme 2.5.2



In 2001, Moody and coworkers described a direct conversion of ketones to protected secondary amines through the use of an indium(0)-mediated reductive amination of oxime ethers.⁴¹ We decided to apply this method to our current strategy. Our findings are outlined in Scheme 2.5.3. Condensation of **183** with *O*-benzylhydroxylamine formed the corresponding *O*-benzyloxime ether (**240**) in near quantitative yield. We were elated to find that exposure of oxime ether **240** to indium(0), acetic acid, and either BOC₂O or formic acetic anhydride at 70 °C in THF gave the protected secondary amines **241** and **242**, respectively, in good yield. Having established an efficient method for assembly of **238**, we turned our attention to the conversion of formamide **242** into the necessary isonitrile moiety.

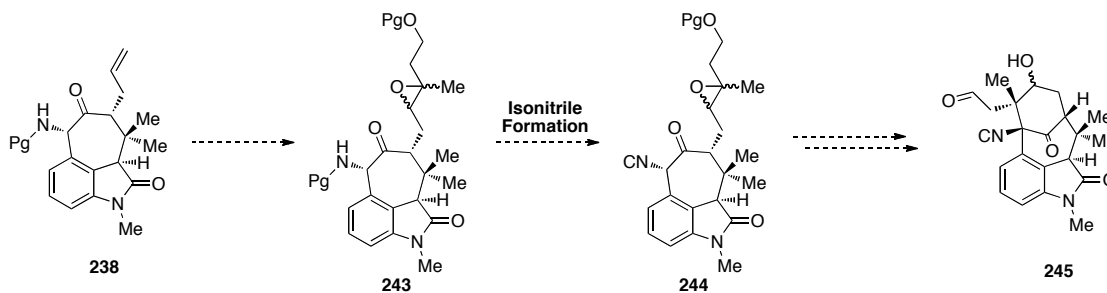
Scheme 2.5.3



2.5.3 Attempted Formation of an Isonitrile from **242**.

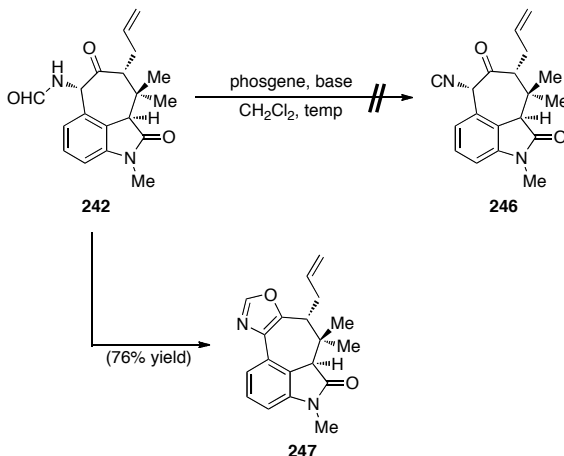
Ultimately, we planned to reveal the isonitrile of **244** after installation of the pendant protected epoxy alcohol within **243** (Scheme 2.5.4). This strategy, if successful, would eventually lead to core structure **245**, a compound containing enough functionality for the completion of **16**. However, rather than pursuing conditions to form the isonitrile moiety at a later stage, we decided to use formamide **242** as a test substrate to optimize the reaction conditions for later implementation.

Scheme 2.5.4



According to standard methods of isonitrile preparations, formamides can be converted to isonitriles when exposed to phosgene and an amine base. Unfortunately, when formamide **242** was treated with phosgene and triethylamine, we did not isolate any of our desired isonitrile (**246**) (Scheme 2.5.5). Instead, we isolated oxazole **247** as the exclusive product. Attempts were made to avoid oxazole formation by varying the base and reaction temperature, but all proved unsuccessful.

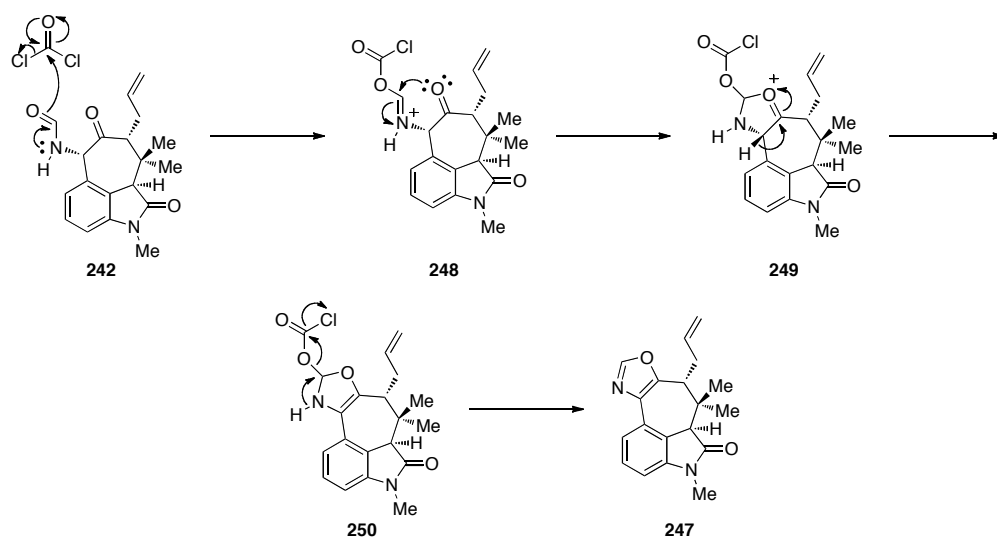
Scheme 2.5.5



Entry	base	temp (°C)	Isonitrile (246)	Oxazole (247)	S.M. (242)
1	Et ₃ N	rt	–	100	–
2	Et ₃ N	0	–	100	–
3	Et ₃ N	–78	–	100	–
4	DTBMP	–78	–	–	100
5	DTBMP	0	–	100	–

The formation of oxazole **247** can be rationalized by the mechanism outlined in Scheme 2.5.6. Initial addition of formamide within **242** onto phosgene generates iminium **248**, which is intercepted by the adjacent carbonyl to form oxocarbenium **249**. Beta-deprotonation would quench the oxocarbenium, giving intermediate **250**. A final push of electrons from nitrogen to extrude carbon dioxide and HCl would result in the formation of oxazole **247**.

Scheme 2.5.6

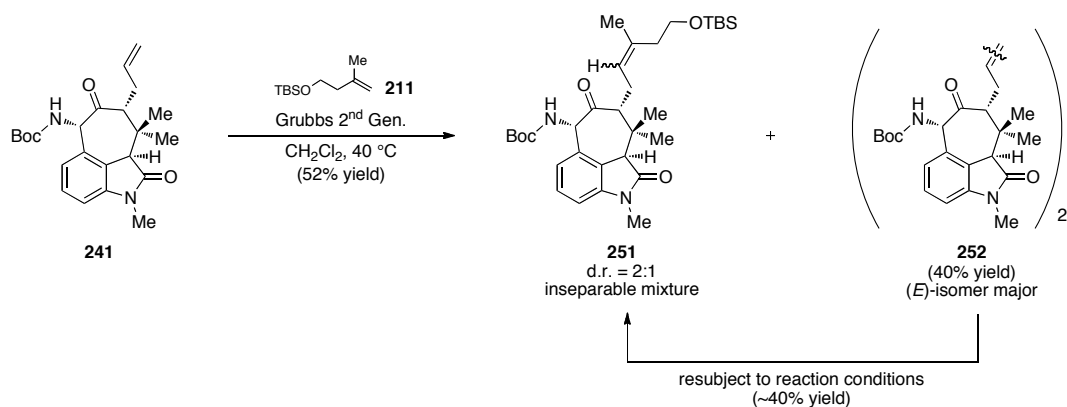


2.5.4 Trisubstituted Olefin Formation: Cross-Metathesis.

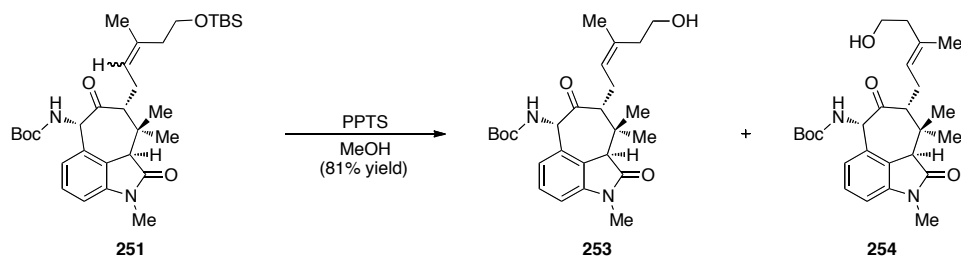
Despite our failures to convert formamide **242** to the corresponding isonitrile **246**, we decided to attempt the projected Michael addition without performing the isonitrile. To that end, we needed to construct the functionalized side-chain present in structure **243** of Scheme 2.5.4. Starting with olefin **241**, a Grubbs 2nd generation-mediated cross metathesis with homo allylic silyl ether **211**⁴² gave trisubstituted olefin **251** as an

inseparable, 2:1 mixture of diastereomers in a 52% yield (Scheme 2.5.7). The mass balance of the reaction was accounted for by isolation of dimer **252** in 40% yield. Fortunately, dimer **252** could be resubjected to the reaction conditions to produce trisubstituted olefin **251** in approximately 40% yield. Although we could not separate the diastereomers of **251** at this point, we discovered that upon deprotection of the silyl enol ether **251** with PPTS in methanol, we could separate the olefin isomers as alcohols **253** and **254** (Scheme 2.5.8).

Scheme 2.5.7



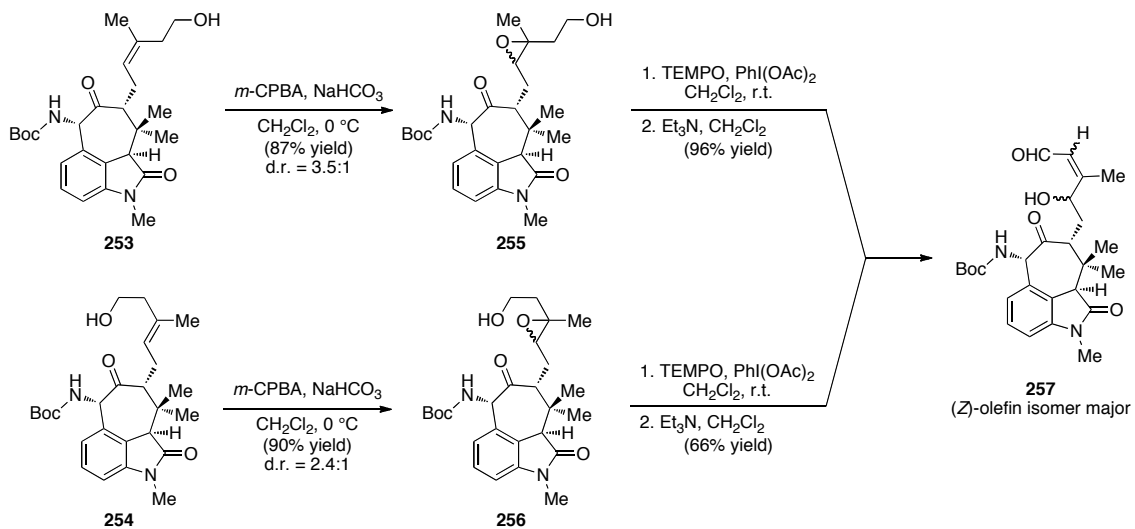
Scheme 2.5.8



2.5.5 Formation of Requisite γ -Hydroxy Enal 257.

Having separated alcohols **253** and **254**, we were poised for smooth formation of requisite γ -hydroxy enal **257** (Scheme 2.5.9). Alcohol **253** was exposed to *m*-CPBA in the presence of NaHCO₃ to deliver epoxy alcohol **255** in 87% yield as 3.5:1 mixture of diastereomers. Oxidation of alcohol **255** to the intermediate aldehyde (not shown) and subsequent treatment with triethylamine provided targeted γ -hydroxy enal **257**. Because of the similarities between alcohols **253** and **254**, the same chemistry for the conversion of alcohol **253** to γ -hydroxy enal **257** was used to transform alcohol **254** to γ -hydroxy enal **257** with comparable yields and selectivities.

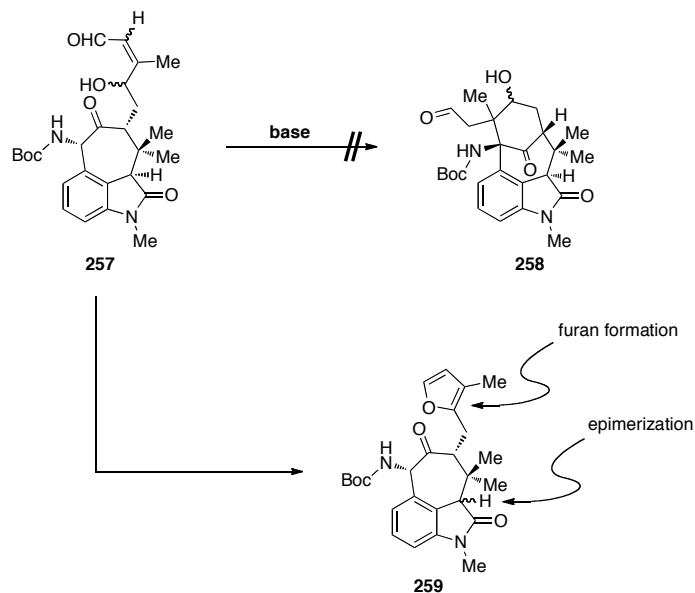
Scheme 2.5.9



2.5.6 Attempted Michael Additions.

Establishment of an efficient route to γ -hydroxy enal **257** set the stage to test our projected Michael addition. Although **257** was less ideal a substrate than α -isonitrile ketone **236** (*vide supra*) to test our hypothesis, we believed that γ -hydroxy enal **257** was still capable of undergoing cyclization upon exposure to excess base. However, when γ -hydroxy enal **257** was treated with excess base, no cyclization product (**258**) was observed (Scheme 2.5.10). Only trace amounts of furan **259** were isolated from the complex product mixture.

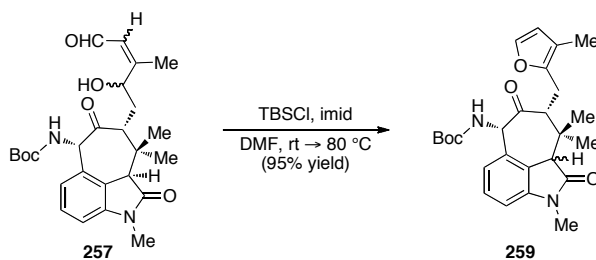
Scheme 2.5.10



In an attempt to circumvent the deleterious formation of the furan moiety in compound **259**, we aimed to protect the secondary alcohol of γ -hydroxy enal **257** (Scheme 2.5.11). Unfortunately, treatment of γ -hydroxy enal **257** with TBSCl and

imidazole in DMF at 80 °C resulted in complete conversion to furan **259**. With the propensity of γ -hydroxy enal **257** to undergo cyclization to the corresponding furan, we abandoned this route and pursued alternative means for the construction of the welwitindolinone alkaloids.

Scheme 2.5.11



2.6 Conclusion.

In summary, three related routes were attempted for the synthesis of *N*-methylwelwitindolinone C isothiocyanate (**16**). The first route highlighted the utility of a [3+2] dipolar cycloaddition to construct the core of **16**. Expansion of this method to include installation of a quaternary center in a single step was considered but proved unsuccessful. In a second strategy, we aimed to install the requisite quaternary center at C12 via a chloronium-ion-mediated semi-Pinacol rearrangement. In the event, we successfully installed a quaternary center, but also irreversibly overchlorinated the molecule (see structure **229**). Our attention was then directed towards a third strategy which projected to build the bicyclo[4.3.1] system and quaternary center in a single

operation using a Michael addition. Unfortunately, this strategy was inherently flawed and resulted in unforeseen oxazole (Scheme 2.5.5) and furan (Scheme 2.5.10) formation.

2.7 Experimental Section.

2.7.1 Material and Methods.

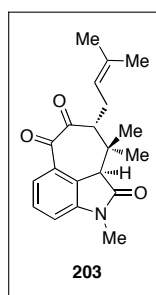
Unless otherwise stated, reactions were magnetically stirred in flame-dried glassware under an atmosphere of nitrogen. Triethylamine (Et₃N) and methanol were dried over calcium hydride and freshly distilled. Benzene, tetrahydrofuran, dichloromethane, toluene, and diethyl ether were dried using a solvent purification system manufactured by SG Water U.S.A., LLC using technology based upon that originally described by Grubbs *et al.*⁴³ Reagent grade DMF, DMSO, acetone, and 1,2-dichloroethane were supplied by Fischer Scientific and purchased from the Colorado State Chemistry Stockroom. All other commercially available reagents were used as received.

Unless otherwise stated, all reactions were monitored by thin-layer chromatography (TLC) using Silicycle glass-backed extra hard layer, 60 Å plates (indicator F-254, 250 µm). Column or flash chromatography was performed with the indicated solvents using Silicycle SiliaFlash® P60 (230-400 mesh) silica gel as the stationary phase. Chromatography was conducted in accordance with the guidelines reported by Still *et al.*⁴⁴ All melting points were obtained on a Gallenkamp capillary melting point apparatus (model: MPD350.BM2.1) and are uncorrected. Infrared spectra were obtained using a

Nicolet Avatar 320 FTIR or Bruker Tensor 27 FTIR. ^1H and ^{13}C NMR spectra were recorded on a Varian Inova 400, Varian Inova 400 autosampler, or Varian Inova 300 spectrometer. Chemical shifts (δ) are reported in parts per million (ppm) relative to internal residual solvent peaks from indicated deuterated solvents. Coupling constants (J) are reported in Hertz (Hz) and are rounded to the nearest 0.1 Hz. Multiplicities are defined as: s = singlet, d = doublet, t = triplet, q = quartet, quint. = quintuplet, m = multiplet, dd = doublet of doublets, ddd = doublet of doublet of doublets, dddd = doublet of doublet of doublet of doublets, br = broad, app = apparent, par = partial. High-resolution mass spectra were performed at the Central Instrument Facility by Donald L. Dick of Colorado State University. Single-crystal X-ray analyses were performed by Susie Miller and Brian Newell of Colorado State University.

2.7.2 Preparative Procedures:

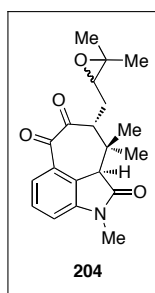
Preparation of Trisubstituted Alkene 203.



Trisubstituted Alkene 203. Diketone **183** (99 mg, 0.333 mmol, 1.0 equiv.) and 2-methyl-2-butene (0.25 mL, 0.999 mmol, 3.0 equiv.) were diluted in CH_2Cl_2 (13.9 mL)

and stirred for 10 minutes. Grubbs 2nd generation catalyst (14 mg, 0.016 mmol, 0.05 equiv.) was then added and the reaction was stirred at reflux overnight (approx. 12 hours). Upon completion as indicated by TLC, the reaction was concentrated and immediately purified via column chromatography (20% EtOAc/hexanes) to give the resulting trisubstituted alkene **203** (84 mg, 78% yield) as a yellow crystalline solid: m.p. 160-162 °C; FTIR (thin film/NaCl) 2971, 2933, 1717, 1604, 1473, 1372, 1338, 1300, 1271 cm⁻¹; ¹H NMR (300 MHz, CDCl₃) δ 7.65 (dd, *J* = 0.9, 8.1 Hz, 1H), 7.49 (dt, *J* = 0.9, 7.8 Hz, 1H), 7.1 (d, *J* = 7.8 Hz, 1H), 4.86-4.8 (m, 1H), 3.3 (s, 1H), 3.22 (s, 3H), 2.84 (dd, *J* = 2.4, 11.4 Hz, 1H), 2.7 (ddd, *J* = 7.5, 13.2, 20.7 Hz, 1H), 2.11 (dd, *J* = 6.0, 13.5 Hz, 1H), 1.58 (s, 3H), 1.56 (s, 3H), 1.47 (s, 3H), 0.9 (s, 3H); ¹³C NMR (75 MHz, CDCl₃) δ 205.4, 192.8, 174.5, 145.1, 134.6, 129.6, 129.2, 128.7, 120.7, 120.7, 113.3, 58.1, 53.1, 38.5, 26.5, 25.8, 24.6, 22.8, 21.0, 17.7; HRMS (EI) *m/z* 326.1749 [calcd for C₂₀H₂₄NO₃ (M⁺) 326.1751].

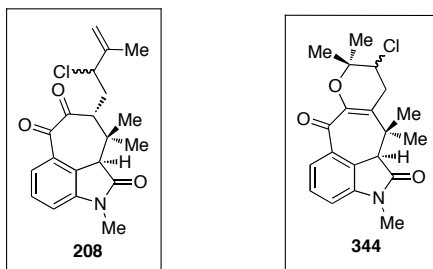
Preparation of Epoxide **204**.



Epoxide 204. In a flask open to air, trisubstituted alkene **203** (52 mg, 0.16 mmol, 1.0 equiv.) was diluted acetone (1.60 mL) and cooled to -78 °C. Freshly made

dimethyldioxirane in acetone (7 mL, approx. 0.07–0.09 M) was added rapidly. The solution was stirred at $-78\text{ }^{\circ}\text{C}$ for 30 minutes and then gradually warmed to room temperature. The reaction was then concentrated *in vacuo* and subsequently purified by flash chromatography (20% EtOAc/hexanes eluent) to give diastereomeric epoxide **204** (53 mg, 97% yield) as a yellow solid: m.p. 139–142 $^{\circ}\text{C}$; FTIR (thin film/NaCl) 2972, 2933, 2253, 1717, 1604, 1473, 1420, 1373, 1338, 1301, 1272 cm^{-1} ; ^1H NMR (400 MHz, CDCl_3) δ 7.72 (dd, $J = 8.4, 8.0$ Hz, 2H), 7.52 (dt, $J = 2.4, 8.0$ Hz, 2H), 7.13 (dd, $J = 4.0, 8.0$ Hz, 2H), 3.36 (s, 1H), 3.35 (s, 1H), 3.24 (s, 6H), 3.11 (dd, $J = 2.4, 11.6$ Hz, 1H), 3.0 (dd, $J = 2.0, 11.2$ Hz, 1H), 2.62 (dd, $J = 5.6, 7.6$ Hz, 1H), 2.5 (dd, $J = 4.4, 7.6$ Hz, 2H), 2.39 (ddd, $J = 4.4, 11.6, 13.6$ Hz, 2H), 2.29–2.23 (m, 2H), 1.75 (ddd, $J = 2.0, 6.0, 14.0$ Hz, 1H), 1.47 (s, 6H), 1.24 (s, 6H) 1.23 (s, 6H) 0.92 (s, 3H), 0.9 (s, 3H); ^{13}C NMR (100 MHz, CDCl_3) δ 210.3, 210.2, 204.9, 192.2, 174.5, 174.4, 145.2, 145.1, 129.8, 129.7, 129.2, 128.7, 121.0, 113.5, 113.3, 62.6, 62.2, 60.3, 59.7, 55.0, 54.7, 53.1, 53.0, 38.6, 38.5, 26.6, 25.4, 25.3, 25.2, 24.7, 22.9, 22.7, 21.1, 20.9, 18.9, 18.6; HRMS (EI) m/z 342.1703 [calcd for $\text{C}_{20}\text{H}_{24}\text{NO}_4$ (M^+) 342.17].

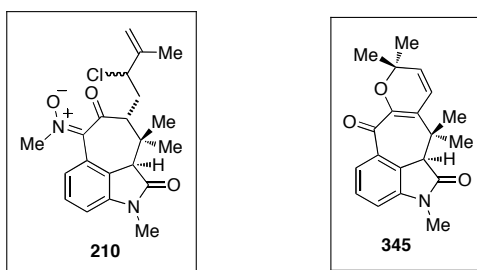
Preparation of Allylic Chloride 208.



Allylic Chloride 208. To a solution of trisubstituted alkene **203** (84 mg, 0.258 mmol, 1.0 equiv.) in $\text{CH}_2\text{Cl}_2:\text{H}_2\text{O}$ (1.43:1.43 mL) was added cerium(III) chloride heptahydrate (125 mg, 0.336 mmol, 1.3 equiv.). The solution was stirred for 5 minutes before bleach (0.39 mL, 0.336 mmol, 1.3 equiv.) was added dropwise. After 1.5 hrs TLC analysis indicated the reaction complete. Saturated Na_2SO_3 was added and the mixture was stirred vigorously, extracted with CH_2Cl_2 , and dried over MgSO_4 . After filtration and concentration, purification via column chromatography (20% EtOAc/hexanes, then 5% EtOAc/benzene) gave allylic chloride **208** (53 mg, 57% yield) as a mixture of diastereomers: FTIR (thin film/ NaCl) 2976, 2937, 1716, 1650, 1605, 1472, 1420, 1373, 1340, 1300, 1271 cm^{-1} ; ^1H NMR (400 MHz, CDCl_3) δ 7.68 (d, $J = 8.4$ Hz, 1H), 7.56 (d, $J = 8.4$ Hz, 1H), 7.52 (t, $J = 8.0$ Hz, 1H), 7.38 (t, $J = 8.0$, 1H), 7.13 (d, $J = 7.6$ Hz, 1H), 6.96 (d, $J = 7.6$ Hz, 1H), 4.96 (s, 1H), 4.86 (s, 1H), 4.07 (dd, $J = 4.4, 9.6$ Hz, 1H), 3.87 (dd, $J = 7.2, 10$ Hz, 1H), 3.69 (s, 1H), 3.32 (s, 1H), 3.24 (s, 3H), 3.23 (s, 3H), 3.17 (d, $J = 10$ Hz, 1H), 2.71 (dd, $J = 6.4, 10$ Hz, 1H), 2.56 (ddd, $J = 4.8, 11.2, 14.4$ Hz, 1H), 1.92 (dd, $J = 9.6, 12.4$ Hz, 1H), 1.75 (s, 3H), 1.72 (s, 3H), 1.54 (s, 3H), 1.45 (s, 3H), 1.27 (s,

3H), 0.92 (s, 3H), 0.79 (s, 3H); ^{13}C NMR (100 MHz, CDCl_3) δ 204.1, 192.0, 174.3, 145.1, 143.7, 143.3, 133.2, 131.5, 129.9, 129.2, 128.8, 128.5, 126.6, 122.1, 120.9, 115.2, 113.5, 111.0, 76.4, 65.2, 60.0, 55.0, 53.1, 53.0, 52.9, 41.9, 38.7, 33.4, 27.0, 26.7, 26.6, 24.1, 22.6, 21.3, 21.1, 17.3, 16.8, 16.7; HRMS (EI) m/z 360.1371 [calcd for $\text{C}_{20}\text{H}_{23}\text{ClNO}_3$ (M $^+$) 360.1361]. A trace impurity was identified as **dihydropyran 344**. FTIR (thin film/NaCl) 3468, 2975, 2928, 2855, 1716, 1604, 1472, 1420, 1373, 1340, 1301, 1272 cm^{-1} ; ^1H NMR (400 MHz, CDCl_3) δ 7.74 (d, $J = 8.0$, 1H), 7.56 (t, $J = 8.0$ Hz, 1H), 7.15 (d, $J = 8.0$ Hz, 1H), 3.56 (dd, $J = 2.0$, 11.6 Hz, 1H), 3.39 (s, 1H), 3.34 (dd, $J = 2.0$, 11.6 Hz, 1H), 3.26 (s, 3H), 2.67 (ddd, $J = 2.0$, 11.2, 13.6 Hz, 1H), 1.77 (ddd, $J = 2.0$, 11.6, 13.6 Hz, 1H), 1.49 (s, 3H), 1.32 (s, 3H), 1.31 (s, 3H), 0.944 (s, 3H); ^{13}C NMR (100 MHz, CDCl_3) δ 205.0, 192.1, 174.4, 145.2, 129.9, 129.2, 128.7, 121.1, 113.6, 72.9, 71.5, 55.2, 53.2, 38.7, 29.6, 27.0, 26.6, 25.8, 22.6, 21.3; HRMS (EI) m/z 360.1362 [calcd for $\text{C}_{20}\text{H}_{23}\text{ClNO}_3$ (M $^+$) 360.1361].

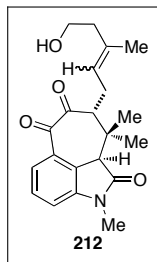
Preparation of Nitrone 210.



Nitron 210 and Pyran 345. To a solution of allylic chloride **208** (53 mg, 0.148 mmol, 1.0 equiv.) in MeOH (9.8 mL) was added *N*-methylhydroxylamine hydrochloride

(80 mg, 0.957 mmol, 6.5 equiv.) and pyridine (80 μ L, 0.972 mmol, 6.6 equiv.). The resulting mixture was heated at reflux until TLC analysis indicated the reaction complete (approx. 2hrs). The solution was then concentrated, taken up in EtOAc, filtered over a cotton plug, and concentrated. Purification via column chromatography (20% EtOAc/hexanes) gave a 3:2 mixture of nitrone **210** (cacl'd 11.6 mg, 20% yield) and pyran **345** (cacl'd 6.4 mg, 14% yield) as an intractable mixture (18 mg isolated, 34% total yield). The mixture was characterized as follows: FTIR (thin film/NaCl) 2974, 2935, 1711, 1672, 1649, 1606, 1505, 1468, 1392, 1372, 1330, 1301, 1255 cm^{-1} ; ^1H NMR (400 MHz, CDCl_3) δ 8.14 (d, $J = 8.0$ Hz, 1H), 7.6 (d, $J = 8.0$ Hz, 1H), 7.43 (t, $J = 8.0$ Hz, 1H), 7.39 (t, $J = 8.0$ Hz, 1H), 6.96 (d, $J = 7.6$ Hz, 1H), 6.88 (d, $J = 7.6$ Hz, 1H), 6.19 (d, $J = 9.6$ Hz, 1H), 5.78 (d, $J = 9.6$ Hz, 1H), 4.94 (s, 1H), 4.87 (s, 1H), 4.16-4.08 (m, 1H), 4.14 (s, 3H), 3.69 (s, 1H), 3.24 (s, 3H), 3.18 (s, 3H), 3.08 (s, 1H), 2.89 (d, $J = 10.8$ Hz, 1H), 2.60 (ddd, $J = 6.0, 10.8, 14$ Hz, 1H), 1.84 (dd, $J = 8.4, 14$ Hz, 1H), 1.78 (s, 3H), 1.74 (s, 3H), 1.55 (s, 3H), 1.34 (s, 3H), 1.33 (s, 3H), 0.85 (s, 3H), 0.78 (s, 3H); ^{13}C NMR (100 MHz, CDCl_3) δ 197.4, 184.4, 175.0, 174.6, 144.3, 144.2, 144.1, 143.4, 134.2, 133.6, 132.5, 128.7, 128.5, 127.5, 126.3, 126.0, 123.3, 122.7, 121.9, 114.5, 110.8, 109.3, 74.3, 65.8, 56.7, 55.4, 52.9, 52.5, 43.9, 41.0, 33.9, 28.0, 26.6, 26.2, 25.6, 23.6, 21.4, 20.8, 20.4, 17.6; HRMS (EI) m/z 389.1624 [cacl'd for $\text{C}_{21}\text{H}_{26}\text{ClN}_2\text{O}_3$ (M^+) 389.1626]; HRMS (EI) m/z 324.1595 [cacl'd for $\text{C}_{20}\text{H}_{22}\text{NO}_3$ (M^+) 324.1594].

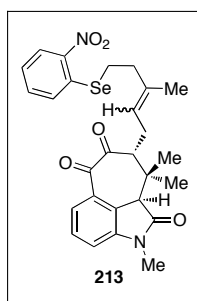
Preparation of Diketone 212.



Diketone 212. Diketone **183** (187 mg, 0.63 mmol, 1.0 equiv.) and olefin **211** (882 mg, 4.40 mmol, 7.0 equiv.) were diluted in CH_2Cl_2 (15.7 mL) and stirred for 10 minutes. Grubbs 2nd generation catalyst (54 mg, 0.063 mmol, 0.1 equiv.) was then added and the reaction was stirred at reflux overnight (approx. 12 hours). Upon completion as indicated by TLC, the reaction was concentrated and immediately purified via column chromatography (20% EtOAc/hexanes) to give the resulting coupled adduct (193 mg, 0.411 mmol). The coupled adduct was taken up in MeOH (41 mL) before pyridinium *p*-toluenesulfonate (21 mg, 0.082 mmol, 0.2 equiv.) was added. The reaction was stirred at room temperature over 12 hours whereupon TLC indicated the consumption of starting material. The reaction was concentrated, re-dissolved in EtOAc, washed with sat. NaHCO_3 , brine, and dried over Na_2SO_4 . Purification of the concentrated mixture by flash chromatography (50% EtOAc/hexanes) gave diketone product **212** (104 mg, *E/Z*: 2:1, 47% yield, 2 steps) as a yellow oil: FTIR (thin film/ NaCl) 3420, 2935, 1715, 1604, 1473, 1372, 1339, 1300, 1272 cm^{-1} ; ^1H NMR (400 MHz, CDCl_3) δ 7.70 (d, $J = 8.0$ Hz, 1H), 7.69 (d, $J = 8.0$ Hz, 1H), 7.49 (t, $J = 8.0$ Hz, 2H), 7.29 (d, $J = 7.6$ Hz, 2H), 5.04-4.98 (m,

2H), 3.68-3.57 (m, 4H), 3.37 (s, 1H), 3.36 (s, 1H), 3.24 (s, 6H), 2.90-2.86 (m, 2H), 2.82-2.74 (m, 2H), 2.37-2.25 (m, 2H), 2.22-2.05 (m, 6H), 1.64 (s, 6H), 1.52 (s, 3H), 1.5 (s, 3H), 0.93 (s, 6H); ^{13}C NMR (100 MHz, CDCl_3) δ 205.9, 193.6, 174.5, 145.3, 135.2, 129.7, 129.0, 128.9, 124.2, 123.9, 120.92, 120.87, 113.5, 113.4, 60.6, 60.2, 58.3, 58.2, 53.4, 53.2, 43.0, 38.6, 38.3, 35.1, 26.6, 24.6, 24.5, 23.4, 23.0, 22.9, 21.3, 21.2, 15.9; HRMS (EI) m/z 356.1862 [calcd for $\text{C}_{21}\text{H}_{26}\text{NO}_4$ (M^+) 356.1856].

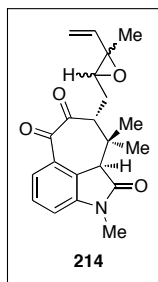
Preparation of Selenide **213**.



Selenide 213. A solution of alcohol **212** (60 mg, 0.17 mmol, 1.0 equiv.) in THF (1.69 mL) was treated with *o*-nitrophenylselenocyanate (46 mg, 0.20 mmol, 1.2 equiv.) at room temperature. The mixture was stirred for 10 minutes before tri-*n*-butylphosphine (50.5 μL , 0.20, 1.2 equiv.) was added. Upon completion as indicated by TLC (approx. 2 hours) an aliquot of sat. NH_4Cl was added. The resulting brown mixture was extracted with Et_2O , washed with brine, dried over MgSO_4 , and concentrated *in vacuo*. Purification of the concentrated mixture by flash chromatography (30% EtOAc /hexanes) gave selenide **213** (49 mg, 54% yield) as a yellow oil. The major diastereomer was characterized as follows: FTIR (thin film/ NaCl) 2970, 2930, 1716, 1604, 1513, 1473,

1332, 1303, 1271 cm^{-1} ; ^1H NMR (400 MHz, CDCl_3) δ 8.30 (d, $J = 8.4$ Hz, 1H), 7.71 (d, $J = 8.0$ Hz, 1H), 7.58-7.49 (m, 3H), 7.31 (t, $J = 8.0$ Hz, 1H), 7.13 (d, $J = 7.6$ Hz, 1H), 5.02 (t, $J = 7.2$ Hz, 1H), 3.39 (s, 1H), 3.26 (s, 3H), 2.99-2.88 (m, 3H), 2.81 (ddd, $J = 8.0, 13.2, 13.2$ Hz, 1H), 2.39-2.35 (m, 2H), 2.15 (dd, $J = 6.0, 13.6$ Hz, 1H), 1.70 (s, 3H), 1.53 (s, 3H), 0.96 (s, 3H); ^{13}C NMR (100 MHz, CDCl_3) δ 205.6, 192.8, 174.5, 147.0, 145.2, 136.9, 133.8, 129.8, 129.3, 128.8, 126.6, 125.4, 122.9, 120.9, 113.4, 58.1, 53.3, 38.6, 38.2, 26.6, 24.6, 23.0, 21.2, 16.0; HRMS (EI) m/z 563.1060 [calcd for $\text{C}_{27}\text{H}_{28}\text{N}_2\text{NaO}_5\text{Se}$ (M^+) 563.1056].

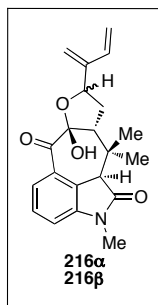
Preparation of Vinyl Epoxide 214.



Vinyl Epoxide 214. In a flask open to air, selenide **213** (49 mg, 0.09, 1.0 equiv.) was diluted CH_2Cl_2 (7 mL) and cooled to -78 $^\circ\text{C}$. Freshly made dimethyldioxirane in acetone (7 mL, approx. 0.07–0.09 M) was added rapidly. The solution was stirred at -78 $^\circ\text{C}$ for 30 minutes and then gradually warmed to room temperature. The reaction was then concentrated *in vacuo* and subsequently purified by flash chromatography (20% EtOAc/hexanes eluent) to give diastereomeric vinyl epoxide **214** (23 mg, 72% yield) as a pale yellow solid. The mixture of diastereomers were characterized as follows: FTIR

(thin film/NaCl) 2970, 1716, 1604, 1473, 1373, 1339, 1300, 1272 cm^{-1} ; ^1H NMR (400 MHz, CDCl_3) δ 7.72 (d, $J = 8.0$ Hz, 2H), 7.52 (t, $J = 8.0$ Hz, 2H), 7.13 (d, $J = 8.0$ Hz, 2H), 5.82 (dd, $J = 11.2, 17.6$ Hz, 1H), 5.61 (dd, $J = 10.8, 17.6$ Hz, 1H), 5.29 (d, $J = 17.2$ Hz, 2H), 5.17 (d, $J = 10.8$ Hz, 2H), 3.39 (s, 1H), 3.38 (s, 1H), 3.25 (s, 6H), 3.14-3.10 (m, 2H), 2.70 (dd, $J = 3.6, 8.4$ Hz, 1H), 2.59 (dd, $J = 4.0, 7.6$ Hz, 1H), 2.47 (ddd, $J = 4.0, 11.6, 13.6$ Hz, 1H), 2.36 (ddd, $J = 3.6, 11.6, 14.0$ Hz, 1H), 1.59-1.53 (m, 2H), 1.49 (s, 3H), 1.45 (s, 3H), 1.37 (s, 3H), 1.36 (s, 3H), 0.93 (s, 3H), 0.88 (s, 3H); ^{13}C NMR (100 MHz, CDCl_3) δ 204.7, 192.1, 174.5, 145.2, 140.0, 135.5, 129.9, 129.3, 128.7, 121.1, 118.0, 116.5, 113.5, 63.4, 63.1, 62.1, 60.8, 54.7, 53.1, 38.8, 26.6, 25.4, 24.9, 22.8, 21.8, 21.1, 15.3; HRMS (EI) m/z 376.1526 [calcd for $\text{C}_{21}\text{H}_{23}\text{NNaO}_4$ (M^+) 376.1519].

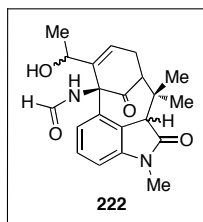
Preparation of Hemiacetals **216 α** and **216 β** .



Hemiacetals 216 α and 216 β . Triphenylphosphine (20 mg, 75.0 μmol , 0.5 equiv.) and tris(dibenzylideneacetone)-dipalladium(0)-chloroform (7 mg, 7.5 μmol , 0.05 equiv) were combined and diluted with toluene (0.8 mL). The deep purple mixture changed to a deep yellow after 1 hour. 1,1,1,3,3,3-Hexafluoro-2-phenyl-2-propanol (25.3 μL , 0.15 mmol, 1.0 equiv.) was then added. After 10 minutes the mixture turned a deep

red-orange and was added via cannula into a vial containing vinyl epoxide **214** (53 mg, 0.15 mmol, 1.0 equiv.) The reaction was then submerged in a 35 °C oil bath and left overnight (approx. 12 hours) to react. After completion as indicated by TLC, the reaction was rapidly concentrated and immediately purified by flash chromatography (20% EtOAc/hexanes) to give diastereomeric acetals **216** (31 mg, 58% yield) as an off white solid. The mixture of diastereomers was characterized as follows: FTIR (thin film/NaCl) 3377, 2926, 1699, 1604, 1372, 1339, 1298, 1216 cm^{-1} ; ^1H NMR (400 MHz, CDCl_3) δ 7.64 (d, $J = 8.0$ Hz, 2H), 7.43 (t, $J = 8.0$ Hz, 2H), 7.04 (d, $J = 8.0$ Hz, 2H), 6.46 (dd, $J = 11.2, 18.0$ Hz, 1H), 6.34 (dd, $J = 11.6, 18.4$ Hz, 1H), 5.45 (s, 1H), 5.3-5.02 (m, 8H), 4.72 (m, 1H), 4.14 (s, 1H), 4.08 (s, 1H), 3.24 (s, 3H), 3.23 (s, 3H), 3.03 (d, $J = 11.6$ Hz, 2H), 2.78 (m, 1H), 2.33-2.15 (m, 4H), 1.96-1.91 (m, 1H), 1.67 (s, 3H), 1.63 (s, 3H), 0.85 (s, 3H), 0.77 (s, 3H); ^{13}C NMR (100 MHz, CDCl_3) δ 196.6, 196.5, 175.9, 146.1, 145.9, 144.8, 136.5, 136.1, 131.3, 131.1, 129.0, 128.9, 127.9, 127.8, 122.2, 121.9, 114.7, 114.4, 114.2, 112.2, 112.1, 103.2, 102.6, 78.0, 75.9, 53.6, 52.7, 52.6, 50.5, 35.4, 35.2, 33.3, 31.1, 26.4, 25.3, 25.2, 23.8, 23.7; HRMS (EI) m/z 376.1519 [calcd for $\text{C}_{21}\text{H}_{23}\text{NNaO}_4$ (M⁺) 376.1519].

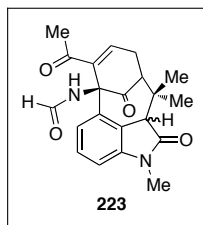
Preparation of Alcohol 222.



Alcohol 222. A solution of alcohol **221** (207 mg, 0.5 mmol, 1.0 equiv.) in CH_2Cl_2 (10 mL) was treated with Dess-Martin periodinane (319 mg, 0.75 mmol, 1.5 equiv.) and stirred at room temperature for 30 minutes, at which point TLC indicated the reaction complete. The reaction was cooled to 0 °C before saturated NaHSO_3 (5 mL) and saturated NaHCO_3 (5 mL) were added. The two layers were separated and the organic extract was washed with brine, dried over Na_2SO_4 , filtered and concentrated. The crude reaction mixture was diluted in CH_2Cl_2 (10 mL) and stirred at 0 °C before triethylamine (77 μL , 0.55 mmol, 1.1 equiv.) was added. After 30 minutes acetic acid (31 μL , 0.55 mmol, 1.1 equiv.) was added and the reaction was partitioned between CH_2Cl_2 (20 mL) and saturated NaHCO_3 (20 mL). The organic layer was washed with brine, dried over Na_2SO_4 , filtered and concentrated. The crude reaction mixture, diluted in THF (10 mL) was cooled to 0 °C. A 3.0 M solution of methyl magnesium bromide in Et_2O (0.37 mL, 1.11 mmol, 3.0 equiv.) was added and the reaction was stirred for 30 minutes. Upon consumption of starting material, the reaction was quenched with 1 N NH_4Cl , extracted with EtOAc , washed with brine, and dried over Na_2SO_4 . The resulting mixture was purified by flash chromatography (90% EtOAc /hexanes) to give secondary alcohol **222**

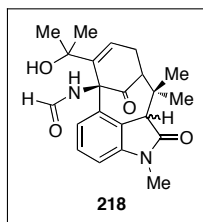
as a mixture of diastereomers (134 mg, 73% yield, 3 steps). The complex mixture was carried through the next step and characterized.

Preparation of Enone **223**.



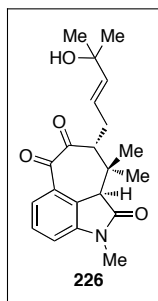
Enone 223. A solution of alcohol **222** (20 mg, 0.05 mmol, 1.0 equiv.) in CH₂Cl₂ (1.9 mL) was treated with Dess-Martin periodinane (73 mg, 0.17 mmol, 3.0 equiv.) and stirred at room temperature for 8 hours, at which point TLC indicated the reaction complete. The reaction was cooled to 0 °C before saturated NaHSO₃ (2 mL) and saturated NaHCO₃ (2 mL) were added. The two layers were separated and the organic extract was washed with brine, dried over Na₂SO₄, filtered and concentrated. Purification by flash chromatography (75% EtOAc/hexanes) gave enone **223** (7 mg, 35% yield) as a pale yellow oil. FTIR (thin film/NaCl) 3329, 3055, 2970, 2917, 1731, 1698, 1609, 1465, 1368, 1340, 1266, 1243 cm⁻¹; ¹H NMR (400 MHz, CDCl₃) δ 8.14 (d, *J* = 1.2 Hz, 1H), 7.25 (t, *J* = 8.0 Hz, 1H), 7.04-7.02 (m, 1H), 6.9 (s, 1H), 6.70 (d, *J* = 8.0 Hz, 1H), 3.88 (s, 1H), 3.15 (s, 3H), 2.58-2.49 (m, 2H), 2.45 (s, 3H), 2.36-2.28 (m, 1H), 1.68 (s, 3H), 0.94 (s, 3H); ¹³C NMR (100 MHz, CDCl₃) δ 201.1, 174.9, 160.1, 142.8, 134.6, 129.5, 126.0, 120.9, 107.2, 69.9, 51.8, 51.7, 37.7, 29.2, 27.8, 27.4, 26.3, 20.6; HRMS (EI) *m/z* 389.1480 [calcd for C₂₁H₂₂N₂NaO₄ (M⁺) 389.1472].

Preparation of Allylic Alcohol 218.



Allylic Alcohol 218. A solution of enone **233** (66 mg, 0.18 mmol, 1.0 equiv.) in THF (8 mL) was cooled to 0 °C. A 3.0 M solution of methyl magnesium bromide in Et₂O (0.30 mL, 0.90 mmol, 5.0 equiv.) was added and the reaction was stirred for 7 hours. Upon consumption of starting material, the reaction was quenched with 1 N NH₄Cl, extracted with EtOAc, washed with brine, and dried over Na₂SO₄. The resulting mixture was purified by flash chromatography (2% MeOH/CHCl₃) to give allylic alcohol **218** (26 mg, 26% yield) as a yellow oil. ¹H NMR (400 MHz, DMSO-d₆) δ 9.42 (s, 1H), 8.02 (s, 1H), 7.27 (t, *J* = 8.0 Hz, 1H), 7.18 (d, *J* = 8.0 Hz, 1H), 6.85 (d, *J* = 7.6 Hz, 1H), 6.06 (s, 1H), 5.81-5.79 (m, 1H), 3.80 (s, 1H), 3.10 (s, 3H), 2.31-2.18 (m, 2H), 1.79-1.73 (m, 1H), 1.55 (s, 3H), 1.47 (s, 3H), 1.35 (s, 3H), 0.76 (s, 3H); ¹³C NMR (100 MHz, DMSO-d₆) δ 201.7, 174.5, 160.1, 147.3, 141.5, 136.4, 128.6, 125.3, 124.4, 121.1, 106.5, 73.0, 70.9, 51.3, 51.2, 36.5, 31.4, 30.2, 28.5, 25.8, 25.2, 19.8; HRMS (EI) *m/z* 405.1789 [calcd for C₂₂H₂₆N₂NaO₄ (M⁺) 405.1785].

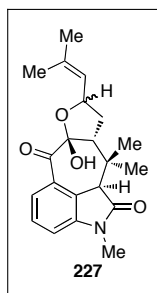
Preparation of Allylic Alcohol 226.



Allylic Alcohol 226. Diketone **183** (30 mg, 0.101 mmol, 1.0 equiv.) was diluted in CH₂Cl₂ (0.63 mL) before 2-methyl-3-buten-2-ol (42.2 μL, 0.404 mmol, 4.0 equiv.) was added and the mixture was stirred for 10 minutes. Grubbs 2nd generation catalyst (5 mg, 0.006 mmol, 0.06 equiv.) was then added and the reaction was stirred at reflux for 3hrs. Upon completion as indicated by TLC, the reaction was concentrated and immediately purified via column chromatography (15–20% EtOAc/CH₂Cl₂) to give the resulting allylic alcohol **226** (34 mg, 95% yield) as a light green foam: FTIR (thin film/NaCl) 3480, 2973, 2933, 2252, 1716, 1604, 1473, 1420, 1372, 1340, 1300, 1272, 1235 cm⁻¹; ¹H NMR (300 MHz, CDCl₃) δ 7.67 (dd, *J* = 0.9, 8.1 Hz, 1H), 7.51 (dt, *J* = 0.9, 7.8 Hz, 1H), 7.12 (d, *J* = 7.5 Hz, 1H), 5.61 (d, *J* = 15.3 Hz, 1H), 5.43 (ddd, *J* = 6.3, 7.2, 15.6 Hz, 1H), 3.34 (s, 1H), 3.24 (s, 3H), 2.93 (dd, *J* = 2.4, 11.4 Hz, 1H), 2.73 (dddd, *J* = 0.9, 7.2, 11.7, 13.5 Hz, 1H), 2.18 (dddd, *J* = 1.2, 2.4, 6.3, 13.8 Hz, 1H), 1.72 (s, 1H), 1.48 (s, 3H), 1.23 (s, 6H), 0.91 (s, 3H); ¹³C NMR (75 MHz, CDCl₃) δ 205.2, 192.8, 174.4, 145.2, 141.5, 129.7, 129.1, 128.8, 123.0, 120.8, 113.5, 70.6, 57.7, 53.3, 38.4, 29.7, 29.6, 28.3, 26.6, 22.9, 21.0; HRMS (EI) *m/z* 378.168 [calcd for C₂₁H₂₅NNaO₄ (M⁺)

378.1676].

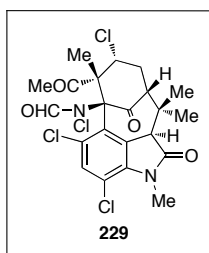
Preparation of Hemiacetal **227**.



Hemiacetal 227. To a solution of $\text{O}_3\text{ReOSiPh}_3$ (14 mg, 0.027 mmol, 0.03 equiv.) in THF (2.2 mL) was added a solution of allylic alcohol **226** (315 mg, 0.887 mmol, 1.0 equiv.) in THF (2.2 mL). *N,O*-bis(trimethylsilyl)acetamide (0.26 mL, 1.064 mmol, 1.2 equiv.) was then added and the mixture was stirred for 10 minutes before TLC analysis indicated the reaction complete. Concentration and purification via column chromatography (30% EtOAc/hexanes) gave hemiacetal **227** (223 mg, 71% yield) as an inseparable mixture of diastereomers and as an amorphous white solid: FTIR (thin film/NaCl) 3368, 2969, 2930, 2882, 1697, 1604, 1468, 1372, 1341, 1299 cm^{-1} ; ^1H NMR (400 MHz, CDCl_3) δ 7.61 (dd, $J = 1.2, 8.0$ Hz, 2H), 7.42 (dt, $J = 0.8, 7.6$, Hz, 2H), 7.02 (dd, $J = 0.8, 7.6$, Hz, 2H), 5.31 (dd, $J = 1.2, 8.8$ Hz, 1H), 5.11-5.09 (m, 2H), 4.69 (ddd, $J = 6.0, 9.6, 9.6$ Hz, 1H), 4.12 (d, $J = 4.4$ Hz, 2H), 3.34 (s, 2H), 3.23 (d, $J = 1.2$, 6H), 2.60 (ddd, $J = 7.2, 10.8, 10.8$ Hz, 1H), 2.32 (t, $J = 9.6$ Hz, 1H), 2.21-2.02 (m, 4H), 1.72 (s, 3H), 1.68 (s, 3H), 1.66 (s, 6H), 1.65 (s, 3H), 1.64 (s, 3H), 0.82 (s, 3H), 0.79 (s, 3H); ^{13}C NMR (100 MHz, CDCl_3) δ 196.7, 196.3, 176.1, 144.7, 136.9, 136.1, 131.4, 128.8, 127.8,

125.8, 125.4, 122.1, 112.1, 112.0, 103.1, 102.4, 75.5, 74.1, 53.7, 52.9, 52.6, 52.2, 35.5, 35.4, 33.0, 31.9, 26.4, 25.9, 25.4, 25.3, 23.8, 23.2, 18.3; ; HRMS (EI) m/z 378.168 [calcd for $C_{21}H_{25}NNaO_4$ (M^+) 378.1676].

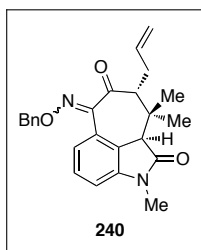
Preparation of Chlorinated Product 229.



Chlorinated Product 229. Tertiary allylic alcohol **218** (51 mg, 0.133 mmol, 1.0 equiv.) was diluted in CH_3CN (10 mL) and stirred at 0 °C. Cerium(III) chloride heptahydrate (149 mg, 0.40 mmol, 3.0 equiv.) was added followed by addition of a 0.1 M aqueous solution of sodium hypochlorite (10.7 mL, 1.07 mmol, 8.0 equiv.). The reaction was stirred from 0 °C to room temperature over 9 hours whereupon TLC indicated consumption of starting material. The reaction was cooled to 0 °C before saturated sodium sulfite (10 mL) was added and stirred for 10 minutes. Chloroform was added and the layers were separated. The aqueous layer was extracted twice more with chloroform and the organic partitions were combine, washed with brine, and dried over Na_2SO_4 . Purification of the filtrate by flash chromatography (33% EtOAc/hexanes) furnished chlorinated product **229** (49 mg, 71% yield) as a colorless foam. 1H NMR (400 MHz, $CDCl_3$) δ 8.05 (s, 1H) 7.41 (s, 1H), 5.03-4.98 (dd, $J = 9.2, 11.6$ Hz, 1H), 3.54 (s, 3H), 3.02 (s, 1H), 2.63-2.57 (dd, $J = 9.6, 10.4$ Hz, 1H), 2.53-2.45 (ddd, $J = 8.8, 10.8, 14.0$ Hz,

1H), 2.27 (s, 3H), 2.0 (s, 3H), 1.85-1.76 (ddd, $J = 9.2, 11.4, 14.0$ 1H), 1.71 (s, 3H), 0.80 (s, 3H); ^{13}C NMR (125 MHz, CDCl_3) δ 206.5, 175.7, 171.7, 160.0, 140.3, 132.7, 132.6, 128.2, 127.4, 117.3, 90.3, 75.8, 60.8, 58.0, 54.4, 52.4, 40.6, 34.0, 30.1, 29.9, 26.8, 26.4, 26.0, 22.0, 21.4, 14.6, 14.5; HRMS (EI) m/z 541.0233 [calcd for $\text{C}_{22}\text{H}_{22}\text{Cl}_4\text{N}_2\text{NaO}_4$ (M^+) 541.0226].

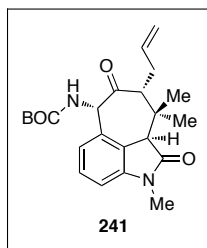
Preparation of *O*-Benzyl Oxime Ether 240.



***O*-Benzyl Oxime Ether 240a and 240b.** Diketone **183** (208 mg, 0.700 mmol, 1.0 equiv.) was diluted in methanol (4.66 mL) before benzylhydroxylamine hydrochloride (128 mg, 0.804 mmol, 1.15 equiv.) was added. The solution was stirred at room temperature for 10 minutes whereupon pyridine (125 μL , 1.549 mmol, 2.2 equiv.) was added. The heterogenous mixture was stirred at room temperature until starting material was consumed as indicated by TLC (approx. 3hrs). The reaction was concentrated, diluted with water, extracted with EtOAc, washed with brine, and dried over MgSO_4 . After filtration and concentration, purification via column chromatography (10–15% EtOAc/hexanes) gave *O*-benzyl oxime ethers **240a** and **240b** (265.0 mg, 94% combined yield). **240a**. The first diastereomer to elute was isolated as an off white amorphous solid:

FTIR (thin film/NaCl) 3077, 3033, 2972, 2936, 2873, 1715, 1642, 1604, 1562, 1497, 1470, 1389, 1371, 1337, 1300, 1281, 1238 cm^{-1} ; ^1H NMR (400 MHz, CDCl_3) δ 7.96 (d, $J = 8.1$ Hz, 1H), 7.28-7.27 (m, 6H), 6.87 (d, $J = 7.8$ Hz, 1H), 5.66 (dddd, $J = 6.6, 10.2, 12.6, 16.8$ Hz, 1H), 5.42 (dd, $J = 12.0, 28.5$ Hz, 2H), 4.98 (d, $J = 17.7$ Hz, 1H), 4.93 (d, $J = 10.2$ Hz, 1H), 3.15 (s, 1H), 3.14 (s, 3H), 2.83 (ddd, $J = 6.3, 11.7, 17.7$ Hz, 1H), 2.79 (s, 1H), 2.06 (dd, $J = 6.3, 12.6$ Hz, 1H), 1.37 (s, 3H), 0.79 (s, 3H); ^{13}C NMR (100 MHz, CDCl_3) δ 198.9, 174.9, 152.9, 144.3, 136.1, 135.6, 128.4, 128.3, 128.2, 125.6, 124.0, 116.6, 109.6, 78.6, 57.6, 52.5, 41.7, 30.1, 26.0, 21.6, 20.4; HRMS (EI) m/z 403.2007 [calcd for $\text{C}_{25}\text{H}_{27}\text{N}_2\text{O}_3$ (M $^+$) 403.2016]. **240b**. The second diastereomer to elute was isolated as an off white amorphous solid: FTIR (thin film/NaCl) 3073, 3032, 2974, 2930, 2873, 1713, 1610, 1466, 1369, 1336, 1299, 1241, 1208 cm^{-1} ; ^1H NMR (300 MHz, CDCl_3) δ 7.55 (d, $J = 6.0$ Hz, 1H), 7.40-7.29 (m, 6H), 6.84 (d, $J = 6.0$ Hz, 1H), 5.66-5.56 (m, 1H), 5.27 (s, 2H), 4.95 (d, $J = 12.6$ Hz, 1H), 4.83 (d, $J = 8.1$ Hz, 1H), 3.22 (s, 1H), 3.19 (s, 3H), 2.72 (s, 2H), 2.10 (s, 1H), 1.45 (s, 3H), 0.82 (s, 3H); ^{13}C NMR (75 MHz, CDCl_3) δ 200.3, 175.0, 167.4, 144.8, 137.2, 135.7, 129.0, 128.5, 128.4, 128.2, 128.1, 125.2, 118.3, 116.7, 109.0, 77.9, 52.7, 41.7, 30.8, 26.3, 22.3; HRMS (EI) m/z 403.2017 [calcd for $\text{C}_{25}\text{H}_{27}\text{N}_2\text{O}_3$ (M $^+$) 403.2016].

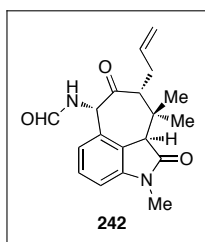
Preparation of *N*-Boc-Protected Amino Ketone **241**.



***N*-Boc-Protected Amino Ketone 241.** A solution of *O*-benzyl oxime ethers **240a** and **240b** (192 mg, 0.477 mmol, 1.0 equiv.) in THF (6.28 mL) was treated with di-*tert*-butoxy-dicarboxylate (385 mg, 1.765 mmol, 3.7 equiv.), acetic acid (190 μ L, 3.268 mmol, 6.85 equiv), and indium(0) powder (300 mg, 2.605 mmol, 5.46 equiv.). The resulting mixture was heated at 71 $^{\circ}$ C overnight (approx. 12hrs). During the course of the reaction, the indium(0) powder coagulated indicating the reaction was near complete. After 12hr, TLC analysis indicated the reaction was complete. The heterogeneous mixture was filtered over celite, washed with NaHCO₃, and dried over MgSO₄. Purification via chromatography (15% EtOAc/hexanes) gave *N*-Boc-protected amino ketone **241** (111.0 mg, 58% yield) as a white powder: m.p. 190-192.5 $^{\circ}$ C; FTIR (thin film/NaCl) 3339, 2977, 2935, 2904, 1699, 1642, 1610, 1469, 1390, 1369, 1343, 1304, 1278, 1246 cm⁻¹; ¹H NMR (400 MHz, CDCl₃) δ 7.33-7.27 (m, 2H), 6.74 (d, *J* = 8.4 Hz, 1H), 5.64 (dddd, *J* = 6.8, 6.8, 10.0, 16.8 Hz, 1H), 5.50 (d, *J* = 5.2 Hz, 1H), 5.29 (d, *J* = 6.8 Hz, 1H), 5.00 (d, *J* = 16.4 Hz, 1H), 4.96 (d, *J* = 10.4 Hz, 1H), 3.08 (s, 3H), 2.95 (s, 1H), 2.67 (d, *J* = 12.0 Hz, 1H), 2.62 (ddd, *J* = 7.2, 12.0, 18.8 Hz, 1H), 2.07 (dd, *J* = 6.4, 12.0 Hz, 1H), 1.39 (s, 9H), 1.34 (s, 3H), 0.71 (s, 3H); ¹³C NMR (100 MHz, CDCl₃) δ

208.6, 175.0, 155.6, 144.2, 135.3, 133.6, 129.2, 124.0, 123.4, 117.5, 107.4, 80.1, 80.0, 79.9, 64.8, 56.8, 52.2, 40.7, 31.1, 28.3, 26.1, 21.8, 20.4; HRMS (EI) m/z 299.1754 [calcd for $C_{18}H_{23}N_2O_2$ (M^+) 299.1754].

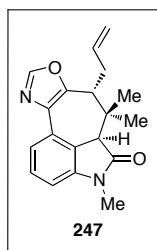
Preparation of Formamide **242**.



Formamide 242. A solution of *O*-benzyl oxime ethers **240a** and **240b** (227 mg, 0.564 mmol, 1.0 equiv.) in THF (5.0 mL) was treated with acetoformate (0.28 mL, 2.087 mmol, 3.7 equiv.), acetic acid (221 μ L, 3.863 mmol, 6.85 equiv), and indium(0) powder (305 mg, 2.65 mmol, 5.46 equiv.). The resulting mixture was heated at 71 °C overnight (approx. 12hrs). During the course of the reaction, the indium(0) powder coagulated indicating the reaction was near complete. After 12hr, TLC analysis indicated the reaction was complete. The heterogeneous mixture was filtered over celite, washed with $NaHCO_3$, and dried over $MgSO_4$. Purification via chromatography (40% EtOAc/hexanes) gave formamide **242** (151 mg, 82% yield) as a white powder: m.p. 184.6-186.2; FTIR (thin film/ $NaCl$) 3307, 2973, 2937, 2878, 1700, 1610, 1517, 1469, 1417, 1372, 1342, 1301, 1273, 1236 cm^{-1} ; 1H NMR (300 MHz, $CDCl_3$) δ 8.29 (s, 1H), 7.38-7.34 (m, 2H), 6.94 (d, J = 7.8 Hz, 1H), 6.81 (dd, J = 2.4, 6.3Hz, 1H), 5.78 (d, J = 8.1 Hz, 1H), 5.69 (dddd, J = 6.9, 6.9, 13.6, 17.1 Hz, 1H), 5.05 (dd, J = 1.2, 17.1 Hz, 1H), 5.01 (d, J = 9.9

Hz, 1H), 3.13 (s, 3H), 3.02 (s, 1H), 2.79 (dd, $J = 2.4, 11.7$ Hz, 1H), 2.66 (ddd, $J = 7.5, 12.9, 12.9$ Hz, 1H), 2.15 (ddd, $J = 0.9, 6.3, 13.2$ Hz, 1H), 1.38 (s, 3H), 0.77 (s, 3H); ^{13}C NMR (75 MHz, CDCl_3) δ 208.0, 175.0, 161.0, 144.3, 135.1, 132.9, 129.5, 124.2, 123.6, 117.9, 107.7, 61.8, 57.0, 52.3, 41.0, 31.1, 26.2, 21.8, 20.5; HRMS (EI) m/z 327.1711 [calcd for $\text{C}_{19}\text{H}_{23}\text{N}_2\text{O}_3$ (M^+) 327.1703].

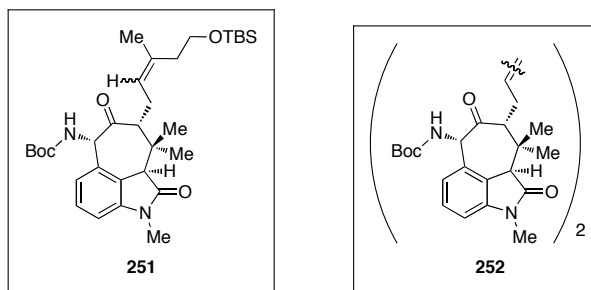
Preparation of Oxazole 247.



Oxazole 247. A solution of formamide **242** (25 mg, 0.077 mmol, 1.0 equiv.) in CH_2Cl_2 (2.25 mL) was treated with triethylamine (30 μL , 0.199 mmol, 2.6 equiv.) and stirred for 10 minutes at room temperature. A 20% solution of phosgene in toluene (122 μL , 0.23 mmol, 3.0 equiv.) was then added dropwise. The solution was allowed to react for 2hrs whereupon TLC analysis indicated the reaction complete. An aliquot of saturated NaHCO_3 was then added and the solution was extracted with CH_2Cl_2 , washed with brine, and dried over Na_2SO_4 . After filtration and concentration, purification via column chromatography (30% Et_2O /hexanes) gave oxazole **247** (18 mg, 76% yield) as a white amorphous solid: FTIR (thin film/ NaCl) 3077, 2976, 2874, 1778, 1710, 1640, 1608, 1593, 1526, 1467, 1393, 1370, 1353, 1331, 1298, 1269, 1224 cm^{-1} ; ^1H NMR (400 MHz,

CDCl₃) δ 7.85 (s, 1H), 7.78 (d, *J* = 8.0 Hz, 1H), 7.7 (d, *J* = 7.6 Hz, 1H), 7.78 (s, 1H), 7.47 (t, *J* = 8.0 Hz, 1H), 7.39 (t, *J* = 8.0 Hz, 1H), 6.87 (d, *J* = 8.0 Hz, 1H), 6.77 (d, *J* = 7.6 Hz, 1H), 5.85-5.67 (m, 2H), 5.12 (dd, *J* = 1.2, 17.2 Hz, 2H), 5.03 (d, *J* = 11.6 Hz, 2H), 3.70 (s, 1H), 3.23 (s, 3H), 3.22 (s, 3H), 2.99 (s, 1H), 2.93 (dd, *J* = 4.4, 7.2 Hz, 1H), 2.85-2.78 (m, 1H), 2.66-2.56 (m, 1H), 2.47 (dt, *J* = 7.6, 15.2 Hz, 1H), 2.35-2.29 (m, 4H), 1.65 (s, 3H), 1.41 (s, 3H), 0.94 (s, 3H), 0.70 (s, 3H); ¹³C NMR (100 MHz, CDCl₃) δ 193.7, 175.9, 175.2, 151.7, 150.8, 149.8, 144.8, 143.9, 142.8, 136.2, 136.0, 131.9, 129.0, 128.4, 127.8, 127.3, 126.1, 124.1, 122.8, 121.5, 120.2, 119.0, 117.3, 117.2, 108.1, 106.8, 73.0, 54.35, 53.26, 50.2, 46.9, 38.1, 34.2, 29.9, 26.5, 26.4, 25.9, 25.0, 23.6, 22.2; HRMS (EI) *m/z* 309.1594 [calcd for C₁₉H₂₁N₂O₂ (M⁺) 309.1598].

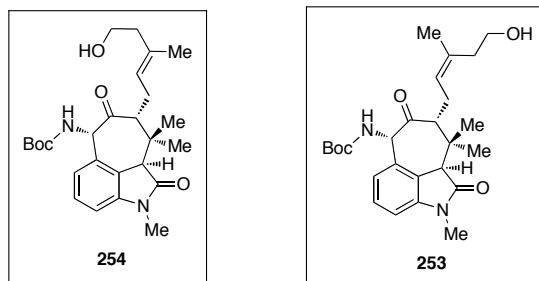
Preparation of Trisubstituted Olefin **251** and Dimer **252**.



Trisubstituted Olefin 251. *N*-Boc-protected amino ketone **241** (233 mg, 0.585 mmol, 1.0 equiv.) was diluted in CH₂Cl₂ (20 mL) before protected homo-allylic alcohol **211** (821 mg, 4.093 mmol, 7.0 equiv.) was added and the solution was stirred for 10 minutes. Grubbs 2nd generation catalyst (25 mg, 0.029 mmol, 0.06 equiv.) was then added and the reaction was stirred at reflux for 5hrs whereupon the reaction was deemed

complete by TLC analysis. Two drops of DMSO were added to the mixture that was stirred for 2hrs at which point the solution was concentrated. Purification via column chromatography (20–40% EtOAc/hexanes) gave trisubstituted olefin **251** (174 mg, 52% yield) as a pale yellow foam: FTIR (thin film/NaCl) 3339, 2958, 2931, 2858, 2252, 1715, 1610, 1470, 1390, 1368, 1341, 1304, 1276, 1250 cm^{-1} ; ^1H NMR (400 MHz, CDCl_3) δ 7.40 (d, $J = 5.6$, 1H), 7.35 (dd, $J = 6.0$, 6.0 Hz, 1H), 6.78 (d, $J = 6.4$ Hz, 1H), 5.4 (s, 1H), 5.34 (d, $J = 9.6$ Hz, 1H), 5.02 (dd, $J = 7.6$, 13.6 Hz, 1H), 3.63 (t, $J = 5.6$ Hz, 1H), 3.62 (ddd, $J = 2.4$, 6.0, 7.6 Hz, 1H), 3.16 (s, 3H), 3.05 (s, 1H), 3.04 (s, 1H), 2.67 (ddd, $J = 6.0$, 9.2, 15.2 Hz, 1H), 2.64 (s, 1H), 2.31-2.26 (m, 1H), 2.18 (t, $J = 5.6$ Hz, 1H), 2.09-2.03 (m, 1H), 1.67 (s, 1H), 1.66 (s, 1H), 1.58 (s, 2H), 1.45 (s, 9H), 1.43 (s, 3H), 1.32-1.22 (m, 1H), 0.87 (d, $J = 3.6$ Hz, 9H), 0.77 (s, 3H), 0.03 (s, 6H); ^{13}C NMR (100 MHz, CDCl_3) δ 209.3, 175.3, 155.7, 144.4, 135.4, 135.2, 133.9, 133.8, 129.3, 126.1, 124.3, 123.7, 123.3, 122.9, 107.5, 80.1, 64.9, 62.6, 61.8, 57.6, 57.3, 52.5, 52.4, 43.2, 40.9, 35.7, 34.3, 26.2, 26.1, 25.6, 24.3, 22.5, 22.0, 20.7, 18.5, 18.4, 16.6, 14.2, -5.1; HRMS (EI) m/z 593.337 [calcd for $\text{C}_{32}\text{H}_{50}\text{N}_2\text{NaO}_5\text{Si}$ (M^+) 593.3381]. **Dimer 252.** FTIR (thin film/NaCl) 3302, 2974, 2930, 1699, 1609, 1509, 1466, 1389, 1366, 1350, 1318, 1279, 1246 cm^{-1} ; ^1H NMR (400 MHz, CDCl_3) δ 7.43 (d, $J = 7.6$ Hz, 2H), 7.35 (t, $J = 7.6$ Hz, 2H), 6.77 (d, $J = 7.6$ Hz, 2H), 5.55 (s, 2H), 5.29 (s, 2H), 5.26 (s, 2H), 3.15 (s, 6H), 3.04 (s, 2H), 2.70 (d, $J = 11.2$ Hz, 2H), 2.59 (dd, $J = 4.0$, 13.6 Hz, 2H), 2.03 (d, $J = 13.2$ Hz, 2H), 1.43 (s, 18H), 1.39 (s, 6H), 0.74 (s, 6H); ^{13}C NMR (100 MHz, CDCl_3) δ 208.7, 175.3, 155.9, 144.3, 133.9, 130.0, 129.3, 124.3, 123.6, 107.4, 80.1, 65.0, 56.9, 52.5, 40.9, 30.0, 28.5, 26.2, 21.9, 20.7; HRMS (EI) m/z 791.3988 [calcd for $\text{C}_{44}\text{H}_{56}\text{N}_4\text{NaO}_8$ (M^+) 791.399].

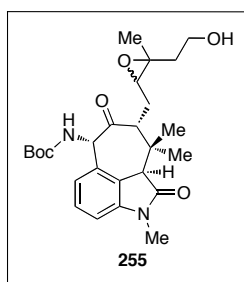
Preparation of Alcohol **254** and Alcohol **253**.



Alcohol 254 and Alcohol 253. To a solution of trisubstituted olefin **251** (174 mg, 0.305 mmol, 1.0 equiv.) in methanol (18.0 mL) was added PPTS (26 mg, 0.10 mmol, 0.33 equiv.). The solution was stirred for 4hrs whereupon consumption of starting material was indicated by TLC analysis. The reaction was concentrated, taken up in EtOAc and water, extracted with EtOAc, washed with sat. NaHCO₃ then brine, and dried over MgSO₄. After filtration and concentration, the mixture was purified via silica gel column chromatography (30% EtOAc/hexanes) to give alcohols **254** and **253** (combined 113 mg, 81% yield). **254**. The first compound to elute was isolated as a white foam (70 mg, 50% yield): FTIR (thin film/NaCl) 3325, 2976, 2935, 1699, 1610, 1510, 1469, 1390, 1369, 1342, 1280, 1249 cm⁻¹; ¹H NMR (300 MHz, CD₃CN) δ 7.39 (t, *J* = 7.8 Hz, 1H), 7.14 (d, *J* = 8.1 Hz, 1H), 6.88 (d, *J* = 7.5 Hz, 1H), 5.81 (d, *J* = 8.1 Hz, 1H), 5.18 (d, *J* = 8.7 Hz, 1H), 5.06 (dt, *J* = 1.2, 8.1 Hz, 1H), 3.6-3.44 (m, 2H), 3.11 (s, 3H), 3.07 (s, 1H), 2.86-2.79 (m, 1H), 2.69-2.54 (m, 2H), 2.16 (s, 1H), 2.12 (t, *J* = 6.3 Hz, 2H), 1.56 (s, 3H), 1.41 (s, 9H), 1.39 (s, 1H), 1.36 (s, 3H), 0.73 (s, 3H); ¹³C NMR (100 MHz, CDCl₃) δ 209.1, 175.2, 156.2, 144.4, 134.9, 132.4, 129.2, 124.2, 124.1, 123.8, 107.5, 80.7, 65.4,

59.6, 57.1, 52.6, 43.3, 40.5, 30.4, 28.4, 26.2, 25.6, 22.0, 20.7, 15.5; HRMS (EI) m/z 479.2517 [calcd for $C_{26}H_{36}N_2NaO_5$ (M⁺) 479.2516]. **253**. The second compound to elute was isolated as a white solid (43 mg, 31% yield): m.p. 173.5-174.5 °C; FTIR (thin film/NaCl) 3343, 2971, 2933, 2873, 1700, 1610, 1495, 1469, 1390, 1369, 1344, 1304, 1278, 1247 cm^{-1} ; ¹H NMR (300 MHz, CD₃CN) δ 7.39 (t, J = 7.8 Hz, 1H), 7.17 (d, J = 7.8 Hz, 1H), 6.89 (d, J = 7.5 Hz, 1H), 5.76 (s, 1H), 5.20 (dd, J = 2.7, 11.4 Hz, 1H), 5.09 (t, J = 7.8 Hz, 1H), 3.51 (dd, J = 6.9, 12.6 Hz, 2H), 3.11 (s, 3H), 3.09 (s, 1H), 2.69 (dd, J = 2.1, 11.7 Hz, 1H), 2.59 (ddd, J = 7.5, 13.5, 20.4 Hz, 1H), 2.51 (t, J = 5.7 Hz, 1H), 2.31 (ddd, J = 6.9, 6.9, 13.2 Hz, 1H), 2.11 (ddd, J = 6.6, 6.6, 13.5 Hz, 1H), 1.96 (s, 1H), 1.65 (s, 3H), 1.41 (s, 9H), 1.35 (s, 3H), 0.73 (s, 3H); ¹³C NMR (100 MHz, CDCl₃) δ 210.8, 209.5, 175.2, 155.9, 144.4, 135.9, 134.8, 133.5, 129.3, 128.4, 125.7, 124.4, 124.2, 123.7, 107.6, 80.3, 65.1, 60.6, 57.5, 52.5, 40.9, 35.1, 34.4, 30.5, 29.8, 28.4, 26.3, 25.4, 23.7, 22.0, 21.3, 20.7; HRMS (EI) m/z 479.2516 [calcd for $C_{26}H_{36}N_2NaO_5$ (M⁺) 479.2516].

Preparation of Epoxy Alcohol **255**.

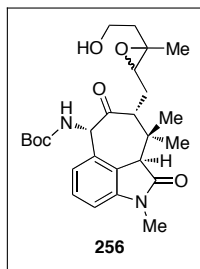


Epoxy Alcohol 255a and 255b. To a solution of alcohol **253** (43 mg, 0.094 mmol, 1.0 equiv.) in CH₂Cl₂ (10 mL) was added saturated NaHCO₃ (17 mL) and cooled

to 0 °C. *m*-CPBA (40 mg, 0.178 mmol, 1.89 equiv.) was then added and the reaction was stirred for 3hrs at 0 °C whereupon TLC indicated consumption of starting material. An aliquot of a saturated solution of Na₂S₂O₃ was then added and the solution was extracted with CH₂Cl₂, washed with NaHCO₃, and dried over Na₂SO₄. After filtration and concentration, purification via column chromatography (40–50% EtOAc/hexanes) gave epoxy alcohol **255a** and **255b** (39 mg, 87% yield) as a mixture of diastereomers and as a white foam. **255a**. FTIR (thin film/NaCl) 3326, 2976, 2935, 2877, 1700, 1611, 1517, 1469, 1391, 1369, 1342, 1304, 1281, 1249 cm⁻¹; ¹H NMR (400 MHz, CDCl₃) δ 7.37 (t, *J* = 8.8 Hz, 1H), 7.23 (d, *J* = 8.0 Hz, 1H), 6.79 (d, *J* = 7.6 Hz, 1H), 5.61 (d, *J* = 8.8 Hz, 1H), 5.21 (d, *J* = 9.2 Hz, 1H), 3.65 (s, 2H), 3.39 (s, 1H), 3.17 (s, 3H), 3.04 (s, 1H), 2.86 (dd, *J* = 2.0, 12.0 Hz, 1H), 2.83 (dd, *J* = 4.4, 8.8 Hz, 1H), 7.07 (dd, *J* = 12.8, 21.6 Hz, 1H), 1.95 (dt, *J* = 4.4, 14.8 Hz, 1H), 1.81 (d, *J* = 13.6 Hz, 1H), 1.65-1.58 (m, 1H), 1.47 (s, 9H), 1.41 (s, 3H), 1.22 (s, 3H), 0.79 (s, 3H); ¹³C NMR (100 MHz, CDCl₃) δ 208.4, 175.1, 156.5, 144.4, 132.6, 129.5, 124.1, 123.7, 107.6, 80.8, 64.5, 62.1, 61.0, 58.4, 53.8, 52.3, 41.1, 40.4, 28.4, 26.3, 21.9, 20.6, 17.1; HRMS (EI) *m/z* 495.2461 [calcd for C₂₆H₃₆N₂NaO₆ (M⁺) 495.2466]. **255b**. FTIR (thin film/NaCl) 3327, 2975, 2934, 1703, 1610, 1511, 1468, 1390, 1368, 1342, 1303, 1281, 1248 cm⁻¹; ¹H NMR (400 MHz, CDCl₃) δ 7.38-7.30 (m, 2H), 6.79 (d, *J* = 7.6 Hz, 1H), 5.78 (d, *J* = 8.4 Hz, 1H), 5.31 (d, *J* = 6.4 Hz, 1H), 3.78 (ddd, *J* = 4.8, 10.8, 16 Hz, 1H), 3.66-3.61 (m, 1H), 3.18 (s, 3H), 3.07 (s, 1H), 2.82 (dd, *J* = 5.2, 8.0 Hz, 1H), 2.79 (dd, *J* = 2.0, 14.0 Hz, 1H), 2.5-2.43 (m, 1H), 2.32 (dd, *J* = 3.2, 17.2 Hz, 1H), 1.94-1.89 (m, 1H), 1.67-1.61 (m, 2H), 1.45 (s, 12H), 1.26 (s, 3H), 0.78 (s, 3H); ¹³C NMR (100 MHz, CDCl₃) δ 209.0, 175.1, 156.3, 144.4, 133.2, 129.4, 126.1,

124.1, 123.5, 107.5, 80.6, 64.2, 61.2, 60.1, 58.9, 54.2, 52.3, 40.9, 40.5, 28.4, 26.9, 26.3, 22.2, 20.7, 16.7; HRMS (EI) m/z 495.2464 [calcd for $C_{26}H_{36}N_2NaO_6$ (M+) 495.2466].

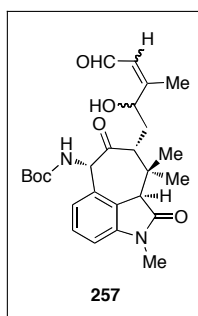
Preparation of Epoxy Alcohol 256.



Epoxy Alcohol 256a and 256b. To a solution of alcohol **254** (95 mg, 0.207 mmol, 1.0 equiv.) in CH_2Cl_2 (10 mL) was added saturated $NaHCO_3$ (17 mL) and cooled to 0 °C. *m*-CPBA (72 mg, 0.321 mmol, 1.89 equiv.) was then added and the reaction was stirred for 3hrs at 0 °C whereupon TLC indicated consumption of starting material. An aliquot of a saturated solution of $Na_2S_2O_3$ was then added and the solution was extracted with CH_2Cl_2 , washed with $NaHCO_3$, and dried over Na_2SO_4 . After filtration and concentration, purification via column chromatography (40–50% EtOAc/hexanes) gave epoxy alcohol **256a** and **256b** (88 mg, 90% yield) as a mixture of diastereomers and as a white foam. **256a.** FTIR (thin film/ $NaCl$) 3333, 2974, 2934, 2882, 1704, 1610, 1509, 1469, 1390, 1368, 1343, 1304, 1279, 1248 cm^{-1} ; 1H NMR (400 MHz, $CDCl_3$) δ 7.38-7.31 (m, 4H), 6.80 (d, J = 8.0 Hz, 1H), 6.69 (d, J = 8.8 Hz, 1H), 5.65 (d, J = 7.6 Hz, 1H), 5.48 (d, J = 8.4 Hz, 1H), 5.20 (s, 2H), 3.92-3.72 (m, 4H), 3.17 (s, 6H), 3.06 (s, 2H), 2.91 (dd, J = 2.4, 12.0 Hz, 2H), 2.7 (dd, J = 5.6, 8.4 Hz, 1H), 2.59 (dd, J = 4.8, 7.6 Hz, 1H), 2.31-

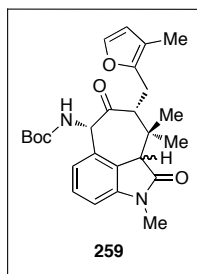
2.26 (m, 2H), 2.21 (ddd, $J = 8.8, 11.2, 14.0$ Hz, 1H), 2.0 (s, 1H), 1.81-1.67 (m, 6H), 1.46 (s, 9H), 1.45 (s, 9H), 1.42 (s, 3H), 1.40 (s, 3H), 1.33 (s, 3H), 1.32 (s, 3H), 0.78 (s, 3H), 0.76 (s, 3H); ^{13}C NMR (100 MHz, CDCl_3) δ 209.2, 175.3, 175.1, 144.5, 133.4, 132.9, 129.5, 129.3, 124.4, 124.2, 123.7, 107.7, 107.6, 80.3, 64.9, 62.5, 61.6, 61.4, 59.8, 59.5, 54.3, 54.0, 52.3, 52.1, 41.2, 41.0, 34.3, 34.1, 28.4, 26.3, 26.2, 25.7, 22.6, 22.5, 22.1, 21.9, 20.7, 20.5; HRMS (EI) m/z 495.2468 [calcd for $\text{C}_{26}\text{H}_{36}\text{N}_2\text{NaO}_6$ (M⁺) 495.2466]. **256b**. 3338, 2976, 2935, 1707, 1611, 1517, 1469, 1390, 1369, 1342, 1304, 1280, 1249 cm^{-1} ; ^1H NMR (400 MHz, CD_2Cl_2) δ 7.36 (t, $J = 8.0$ Hz, 1H), 7.2 (d, $J = 8.0$ Hz, 1H), 6.79 (d, $J = 7.6$ Hz, 1H), 5.56 (d, $J = 8.8$ Hz, 1H), 5.44 (d, $J = 8.4$ Hz, 1H), 3.60 (t, $J = 4.0$ Hz, 2H), 3.11 (s, 3H), 2.99 (s, 3H), 2.84 (dd, $J = 2.44, 12.0$ Hz, 1H), 2.74 (dd, $J = 4.4, 8.0$ Hz, 1H), 1.88 (dt, $J = 4.8, 14.4$ Hz, 1H), 1.74 (d, $J = 12.0$ Hz, 1H), 1.58-1.51 (m, 1H), 1.45 (s, 9H), 1.35 (s, 3H), 1.17 (s, 3H), 0.75 (s, 3H); ^{13}C NMR (100 MHz, CD_2Cl_2) δ 208.6, 175.2, 144.8, 133.0, 129.5, 124.0, 107.7, 80.7, 64.7, 62.1, 61.0, 58.6, 53.9, 52.4, 41.2, 40.7, 28.4, 26.4, 26.3, 21.8, 20.6, 17.1; HRMS (EI) m/z 495.2469 [calcd for $\text{C}_{26}\text{H}_{36}\text{N}_2\text{NaO}_6$ (M⁺) 495.2466].

Preparation of γ -Hydroxy Enal 257.



γ -Hydroxy Enal 257. A solution of epoxy alcohol **255** (39 mg, 0.082 mmol, 1.0 equiv.) was diluted in CH₂Cl₂ (10 mL) before BAIB (57 mg, 0.177 mmol, 2.5 equiv.) and catalytic TEMPO (2 mg, 0.013 mmol, 0.16 equiv.) were added. The reaction was stirred for 24hrs whereupon TLC analysis indicated the reaction complete. Saturated Na₂S₂O₃ was added and the mixture was extracted with CH₂Cl₂, washed with saturated NaHCO₃, and dried over Na₂SO₄. Filtration and concentration gave a yellow oil that was subsequently diluted in CH₂Cl₂ (8.0 mL) before diisopropylethylamine (100 μ L, 0.574 mmol, 7.0 equiv.) was added. The reaction was stirred for 5 minutes then concentrated. Purification via column chromatography (50–60% EtOAc/hexanes) gave γ -hydroxy enal **257** (17 mg, 96% yield) as a mixture of diastereomers. The complex mixture was carried through the next step and characterized.

Preparation of Furan 259.



Furan 259. To a solution of γ -hydroxy enal **257** (13 mg, 0.028 mmol, 1.0 equiv.) in DMF (1 mL) was added imidazole (8 mg, 0.113 mmol, 4.6 equiv.) and TBSCl (5 mg, 0.033 mmol, 1.1 equiv.). The mixture was stirred at room temperature for 10 minutes before heating at 80 °C for 1hr. Upon completion as indicated by TLC analysis, the

solution was poured into a separatory funnel containing H₂O (15 mL) and was extracted with EtOAc, washed with brine, and dried over Na₂SO₄. After filtration and concentration, purification via column chromatography (5% EtOAc/benzene) gave furan **259** (12 mg, 95% yield) as a white solid: m.p. 177.8-178.8 °C; FTIR (thin film/NaCl) 3339, 2974, 2929, 1709, 1610, 1493, 1469, 1390, 1368, 1342, 1303, 1276, 1245 cm⁻¹; ¹H NMR (400 MHz, CDCl₃) δ 7.34 (d, *J* = 6.0 Hz, 2H), 7.19 (d, *J* = 1.67 Hz, 1H), 6.78 (dd, *J* = 4.0, 4.0 Hz, 1H), 6.11 (d, *J* = 2.0 Hz, 1H), 5.33 (d, *J* = 7.6 Hz, 2H), 3.17 (s, 3H), 3.14 (s, 1H), 3.07 (dd, *J* = 11.2 Hz, 1H), 2.65 (dd, *J* = 2.4, 11.2 Hz, 1H), 2.65 (dd, *J* = 2.4, 14.4 Hz, 1H), 1.90 (s, 3H), 1.52 (s, 3H), 1.44 (s, 9H), 0.81 (s, 3H); ¹³C NMR (100 MHz, CDCl₃) δ 208.9, 175.2, 155.6, 148.0, 144.4, 140.7, 134.0, 129.3, 124.3, 123.4, 115.0, 113.1, 107.5, 80.1, 63.9, 55.5, 52.3, 40.8, 29.8, 28.4, 26.3, 23.4, 22.0, 20.5, 9.8; HRMS (EI) *m/z* 475.2202 [calcd for C₂₆H₃₂N₂NaO₅ (M⁺) 475.2203].

2.8 Notes and References

- (1) Brian M. Stoltz, 1997; Alexandra A. Holubec, 2000; Matthew M. Weiss, 2001; Sarah Reisman, 2006; Joshua J. Day, 2009; David B. Freeman 2011.
- (2) Julie Dixon, 1999; Brian D. Doan, 1998; Munenori Inoue, 2001; Hidenori Ohki, 2002; Masami Ohtsuka, 2003; Akio Kakefuda, 2006; Rishi Vaswani, 2009.
- (3) Wood, J. L.; Holubec, A. A.; Stoltz, B. M.; Weiss, M. M.; Dixon, J. A.; Doan, B. D.; Shamji, M. F.; Chen, J. M.; Heffron, T. P. "Application of Reactive Enols in

- Synthesis: A Versatile, Efficient, and Stereoselective Construction of the Welwitindolinone Carbon Skeleton” *J. Am. Chem. Soc.* **1999**, *121*, 6326–6327.
- (4) Holubec, A. A. Dissertation, 2000, Yale University.
- (5) Funk, R. L.; Horcher, L. H. M.; Daggett, J. U.; Hansen, M. M. “Facile bridged bicycloalkane synthesis via intramolecular nitron-olefin cycloaddition” *J. Org. Chem.* **1983**, *48*, 2632-2634.
- (6) Falb, E.; Bechor, Y.; Nudelman, A.; Hassner, A.; Albeck, A.; Gottlieb, H. E. “IOOC Route to Substituted Chiral Pyrrolidines. Potential Glycosidase Inhibitors” *J. Org. Chem.* **1999**, *64*, 498-506.
- (7) Katagiri, N.; Okada, M.; Morishita, Y.; Kaneko, C. “Synthesis of chiral spiro 3-oxazolin-5-one 3-oxides (chiral nitrones) *via* a nitrosoketene intermediate and their asymmetric 1,3-dipolar cycloaddition reactions leading to the EPC synthesis of modified amino acids” *Tetrahedron* **1997**, *53*, 5725-5746.
- (8) Palmisano, G.; Danieli, B.; Lesma, G.; Trupiano, F.; Pilati, T. “Oxidation of .beta.-anilinoacrylate alkaloids vincadifformine and tabersonine by Fremy's salt. A mechanistic insight into the rearrangement of *Aspidosperma* to *Hunteria eburnea* alkaloids” *J. Org. Chem.* **1988**, *53*, 1056-1064.

- (9) Rajkovic, M.; Lorenc, L.; Petrovic, I.; Milovanovic, A.; Mihailovic, M. L. "Oxidative hydrolysis and acid-catalyzed rearrangement of steroidal isoxazolidines" *Tetrahedron Lett.* **1991**, *32*, 7605-7608.
- (10) Wood, J. L.; Moniz, G. A. "Rhodium Carbenoid-Initiated Claisen Rearrangement: Scope and Mechanistic Observations" *Org. Lett.* **1999**, *1*, 371-374.
- (11) Wood, J. L.; Moniz, G. A.; Pflum, D. A.; Stoltz, B. M.; Holubec, A. A.; Dietrich, H. J. "Development of a Rhodium Carbenoid-Initiated Claisen Rearrangement for the Enantioselective Synthesis of α -Hydroxy Carbonyl Compounds" *J. Am. Chem. Soc.* **1999**, *121*, 1748-1749.
- (12) OOI, N. S.; Wilson, D. A. *Journal of Chemical Research-S* **1980**, 366-367.
- (13) Sevastya.Tk; Volodars.Lb. *Zh. Org. Khim.* **1971**, *7*, 1974.
- (14) Lebel, N. A.; Post, M. E.; Hwang, D. "Oxidation of isoxazolidines with peroxy acids. Nitrones and N-hydroxy-1,3-tetrahydrooxazines" *J. Org. Chem.* **1979**, *44*, 1819-1823.
- (15) Nicolaou, K. C.; Koide, K. "Synthetic studies on maduropeptin chromophore 1. Construction of the aryl ether and attempted synthesis of the [7.3.0] bicyclic system" *Tetrahedron Lett.* **1997**, *38*, 3667-3670.

- (16) Uemura, e. a. *Nippon Kagaku Zasshi* **1966**, *87*, 986.
- (17) Overman, L. E. “Mercury(II)- and Palladium(II)-Catalyzed [3,3]-Sigmatropic Rearrangements” *Angew. Chem., Int. Ed.* **1984**, *23*, 579-586.
- (18) Overman, L. E.; Campbell, C. B.; Knoll, F. M. “Mild procedures for interconverting allylic oxygen functionality. Cyclization-induced [3,3] sigmatropic rearrangement of allylic carbamates” *J. Am. Chem. Soc.* **1978**, *100*, 4822-4834.
- (19) These alternative conditions were employed due to the base-lability of the allylic acetate moiety within diketone **182**.
- (20) Huisgen, R. “1,3-Dipolar Cycloadditions. Past and Future” *Angew. Chem., Int. Ed.* **1963**, *2*, 565-598.
- (21) Lebel, N. A.; Banucci, “Intramolecular nitron-allene cycloadditions” *E. J. Am. Chem. Soc.* **1970**, *92*, 5278.
- (22) Padwa, A. “Intramolecular 1,3-Dipolar Cycloaddition Reactions” *Angew. Chem., Int. Ed.* **1976**, *15*, 123-136.

- (23) Crystallographic data (excluding structure factors) for the structure **200** has been deposited with the Cambridge Crystallographic Data Centre as supplementary publication nos. CCDC 763861.
- (24) Chatterjee, A. K.; Choi, T. L.; Sanders, D. P.; Grubbs, R. H. "A General Model for Selectivity in Olefin Cross Metathesis" *J. Am. Chem. Soc.* **2003**, *125*, 11360-11370.
- (25) Moreno-Dorado, F. J.; Guerra, F. M.; Manzano, F. L.; Aladro, F. J.; Jorge, Z. D.; Massanet, G. M. "CeCl₃/NaClO: a safe and efficient reagent for the allylic chlorination of terminal olefins" *Tetrahedron Lett.* **2003**, *44*, 6691–6693.
- (26) Yan, J. B.; Herndon, J. W. "Stereoselective Preparation of Vitamin D Precursors Using the Intramolecular Coupling of Alkynes and Cyclopropylcarbene–Chromium Complexes: A Formal Total Synthesis of (±)-Vitamin D₃" *J. Org. Chem.* **1998**, *63*, 2325-2331.
- (27) Grieco, P. A.; Masaki, Y.; Boxler, D. "Sesterterpenes. I. Stereospecific total synthesis of moenocinol" *J. Am. Chem. Soc.* **1975**, *97*, 1597-1599.
- (28) Grieco, P. A.; Noguez, J. A.; Masaki, Y. "Total synthesis of deoxyvernolepin" *Tetrahedron Lett.* **1975**, *16*, 4213-4216.

- (29) Nicolaou, K. C.; Zhang, H.; Ortiz, A.; Dagneau, P. "Total Synthesis of the Originally Assigned Structure of Vannusal B" *Angew. Chem., Int. Ed.* **2008**, *47*, 8605-8610.
- (30) Murray, R. W. S., M. Synthesis of Epoxides Using Dimethyldioxirane: trans-Stilbene Oxide" *Org. Synth.* **1998**, *9*, 288.
- (31) Suzuki, M.; Oda, Y.; Noyori, R. "Palladium(0) catalyzed reaction of 1,3-diene epoxides. A useful method for the site-specific oxygenation of 1,3-dienes" *J. Am. Chem. Soc.* **1979**, *101*, 1623-1625.
- (32) Kabat, M. M.; Garofalo, L. M.; Daniewski, A. R.; Hutchings, S. D.; Liu, W.; Okabe, M.; Radinov, R.; Zhou, Y. F. "Efficient Synthesis of 1 α -Fluoro A-Ring Phosphine Oxide, a Useful Building Block for Vitamin D Analogues, from (*S*)-Carvone via a Highly Selective Palladium-Catalyzed Isomerization of Dieneoxide to Dieneol" *J. Org. Chem.* **2001**, *66*, 6141-6150.
- (33) Wang, B. M.; Song, Z. L.; Fan, C. A.; Tu, Y. Q.; Chen, W. M. "Halogen Cation Induced Stereoselective Semipinacol-type Rearrangement of Allylic Alcohols: A Highly Efficient Approach to α -Quaternary β -Haloketo Compounds" *Synlett* **2003**, 1497-1499.

- (34) Reisman, S. E.; Ready, J. M.; Hasuoka, A.; Smith, C. J.; Wood, J. L. "Total Synthesis of (\pm)-Welwitindolinone A Isonitrile" *J. Am. Chem. Soc.* **2006**, *128*, 1448–1449.
- (35) Obrecht, R.; Herrmann, R.; Ugi, I. "Isocyanide Synthesis with Phosphoryl Chloride and Diisopropylamine" *Synthesis* **1985**, 400-402.
- (36) Porcheddu, A.; Giacomelli, G.; Salaris, M. "Microwave-Assisted Synthesis of Isonitriles: A General Simple Methodology" *J. Org. Chem.* **2005**, *70*, 2361-2363.
- (37) Dess, D. B.; Martin, J. C. "A useful 12-I-5 triacetoxyperiodinane (the Dess-Martin periodinane) for the selective oxidation of primary or secondary alcohols and a variety of related 12-I-5 species" *J. Am. Chem. Soc.* **1991**, *113*, 7277-7287.
- (38) Matsubara, S.; Okazoe, T.; Oshima, K.; Takai, K.; Nozaki, H. "Isomerization of Allylic Alcohols Catalyzed by Vanadium or Molybdenum Complexes" *Bull. Chem. Soc. Jpn.* **1985**, *58*, 844–849.
- (39) Morrill, C.; Grubbs, R. H. "Highly Selective 1,3-Isomerization of Allylic Alcohols via Rhenium Oxo Catalysis" *J. Am. Chem. Soc.* **2005**, *127*, 2842–2843.
- (40) We have drawn the desired stereochemical outcome of the Michael addition to illustrate our strategy and not the expected product. At this juncture, we wanted to

test the viability of this method first, and then address the issue of diastereoselectivity.

- (41) Pitts, M. R.; Harrison, J. R.; Moody, C. J. "Indium metal as a reducing agent in organic synthesis" *J. Chem. Soc., Perkin Trans. 1*, **2001**, 955–977.

- (42) Direct usage of the unprotected variant of **211** in a cross-metathesis with ketone **241** resulted in no reaction.

- (43) Pangborn, A. B.; Giardello, M. A.; Grubbs, R. H.; Rosen, R. K.; Timmers, F. J. "Safe and Convenient Procedure for Solvent Purification" *Organometallics* **1996**, *15*, 1518–1520.

- (44) Still, W. C.; Kahn, M.; Mitra, A. "Rapid chromatographic technique for preparative separations with moderate resolution" *J. Org. Chem.* **1978**, *43*, 2923–2925.

**APPENDIX ONE: SPECTRA RELEVANT
TO CHAPTER TWO**

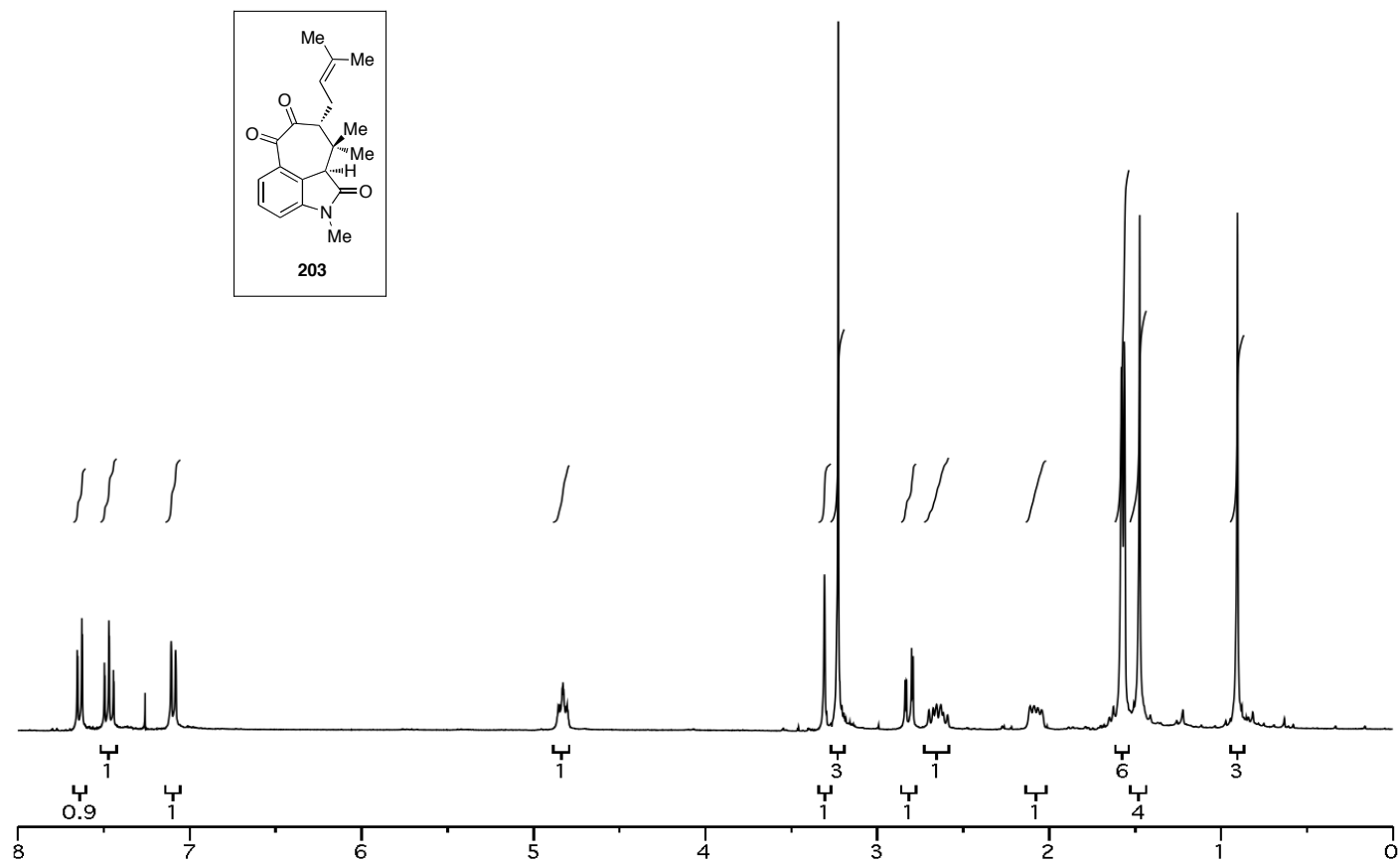


Figure A.1.1 ¹H NMR (300 MHz, CDCl₃) of compound **203**.

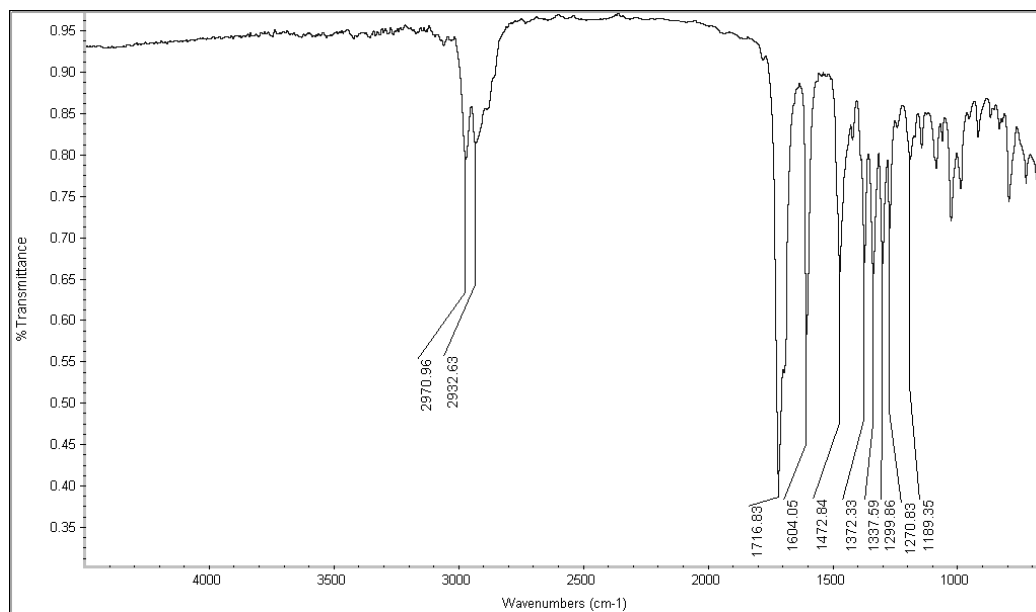


Figure A.1.2 Infrared Spectrum (thin film/NaCl) of compound **203**.

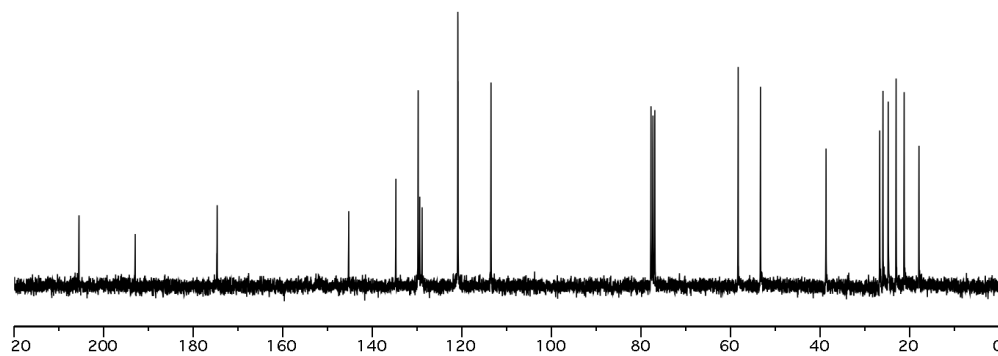


Figure A.1.3 ¹³C NMR (75 MHz, CDCl₃) of compound **203**.

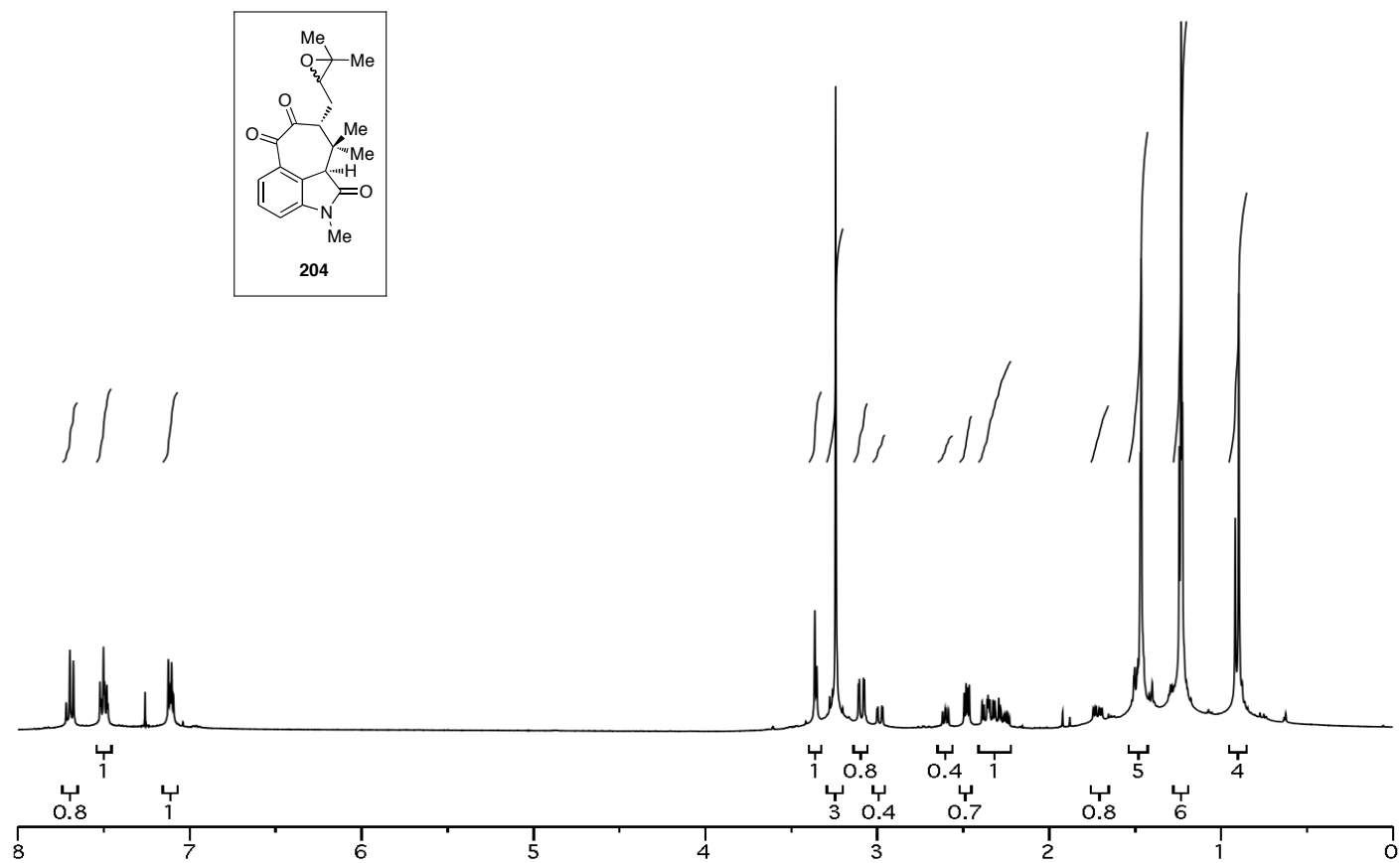


Figure A.1.4 ¹H NMR (400 MHz, CDCl₃) of compound 204.

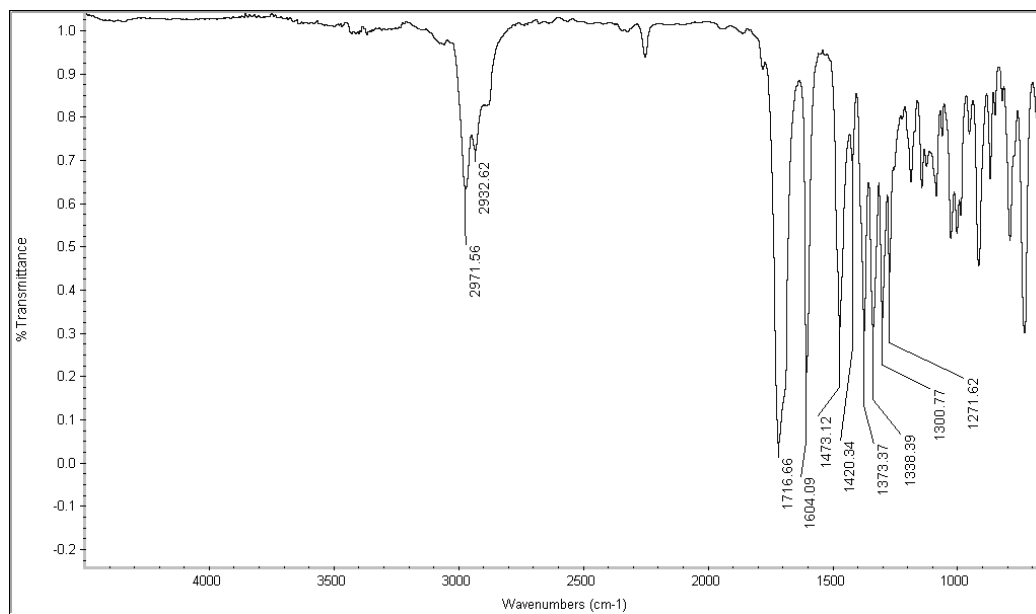


Figure A.1.5 Infrared Spectrum (thin film/NaCl) of compound **204**.

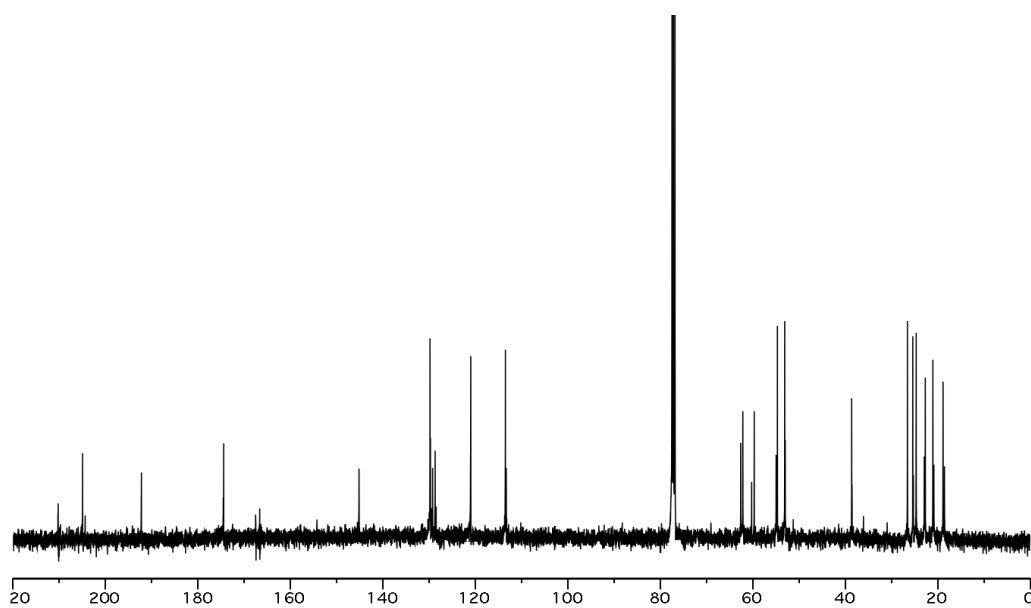


Figure A.1.6 ¹³C NMR (100 MHz, CDCl₃) of compound **204**.

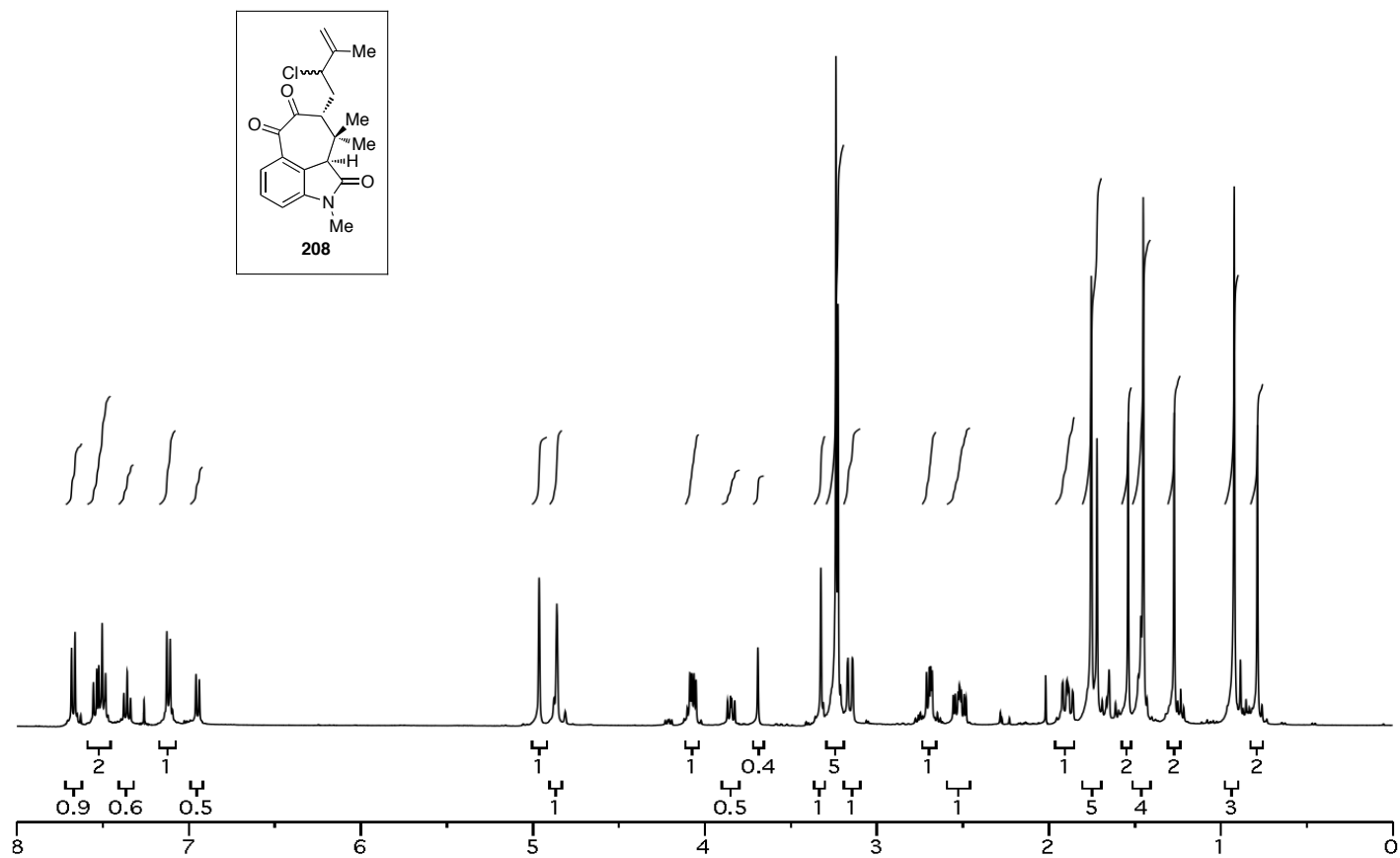


Figure A.1.7 ^1H NMR (400 MHz, CDCl_3) of compound **208**.

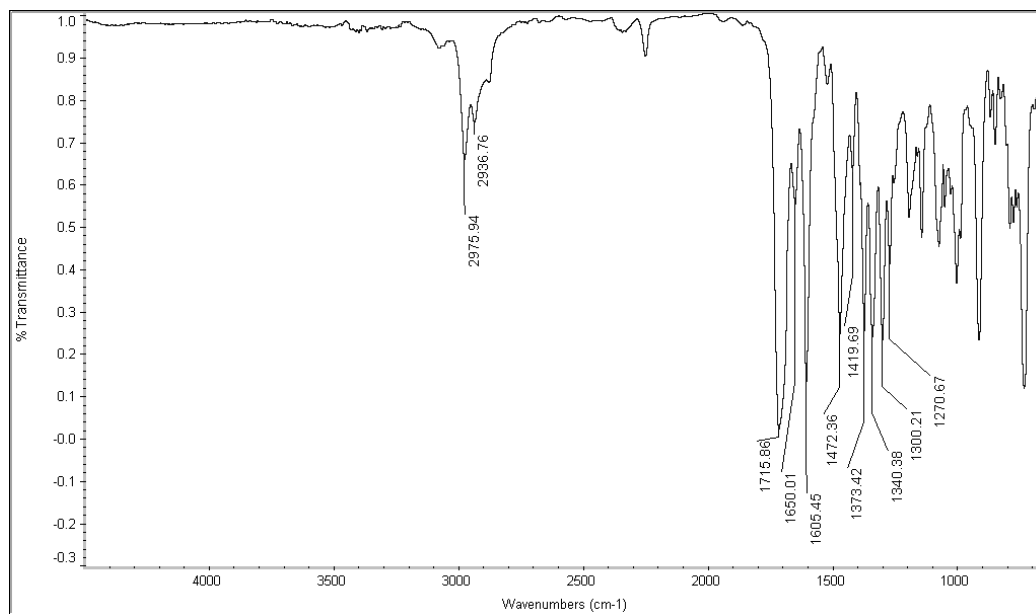


Figure A.1.8 Infrared Spectrum (thin film/NaCl) of compound **208**.

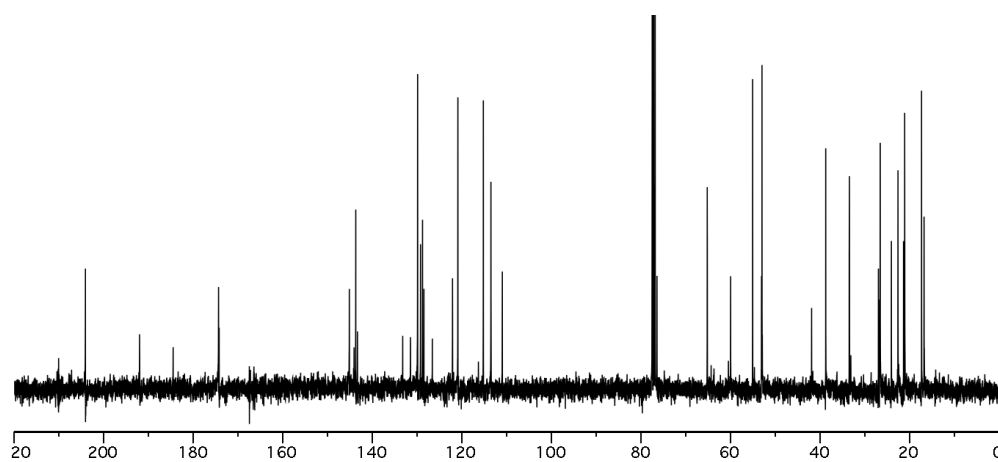


Figure A.1.9 ¹³C NMR (100 MHz, CDCl₃) of compound **208**.

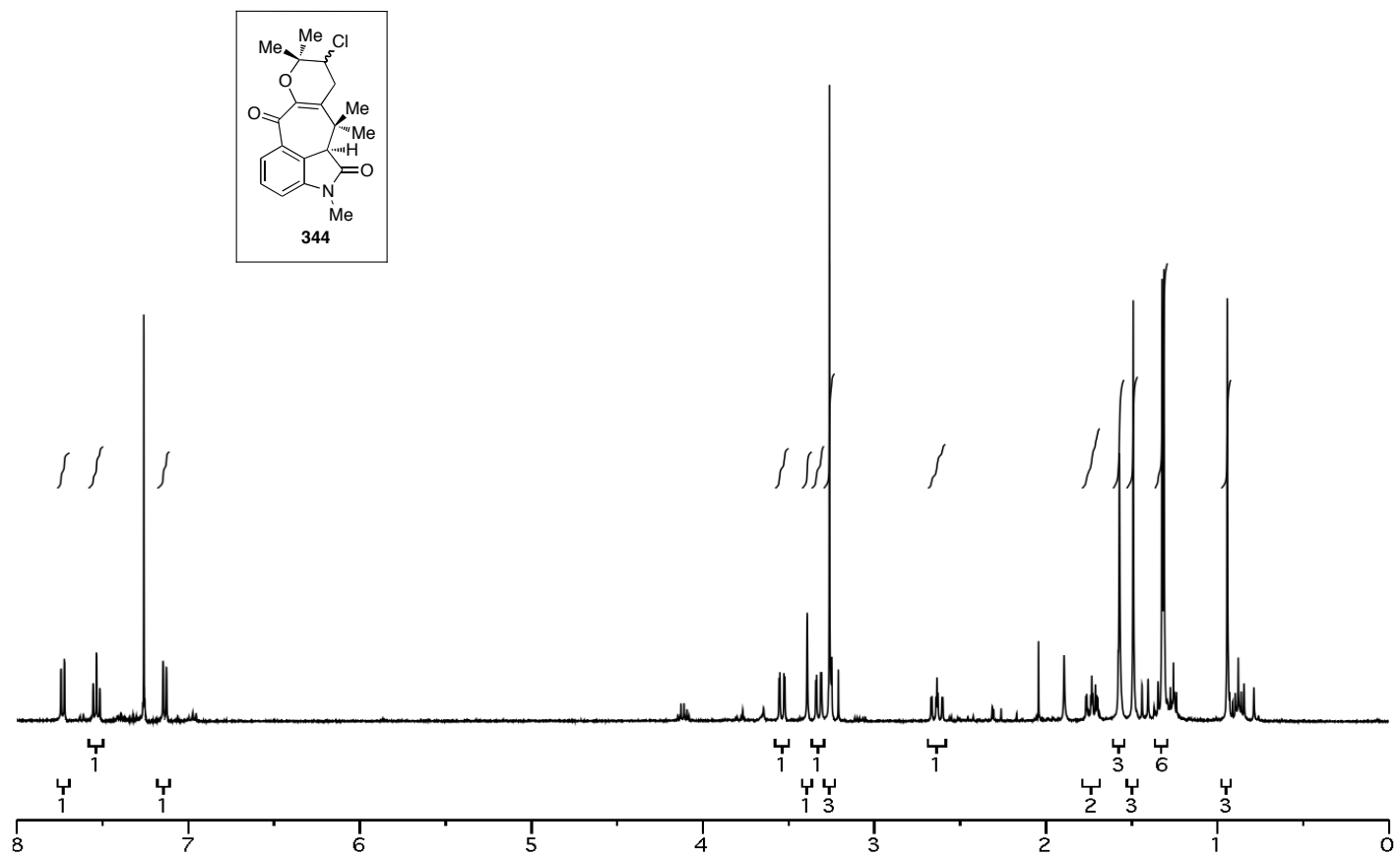


Figure A.1.10 ¹H NMR (400 MHz, CDCl₃) of compound 344.

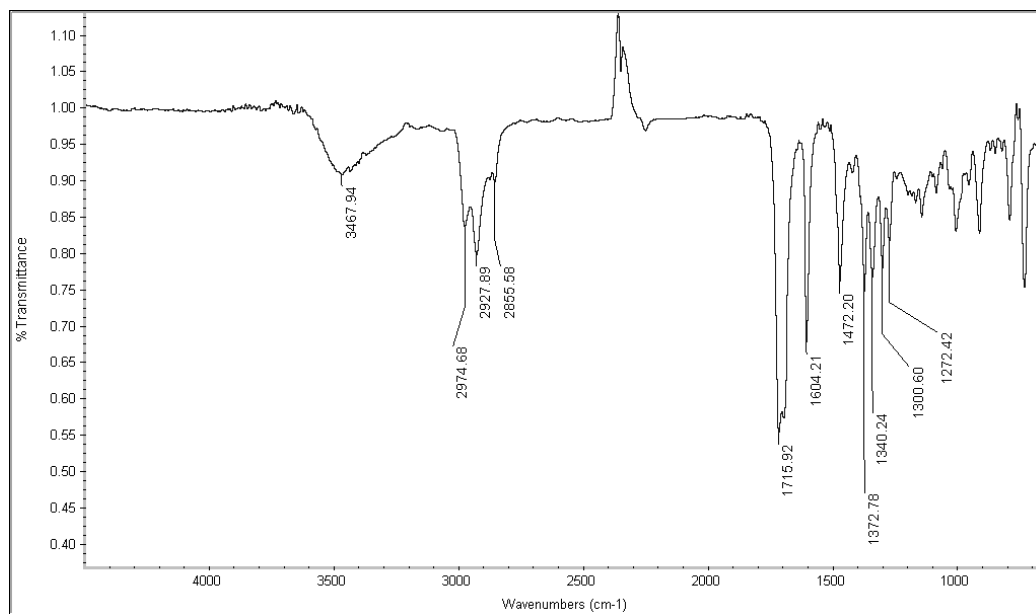


Figure A.1.11 Infrared Spectrum (thin film/NaCl) of compound **344**.

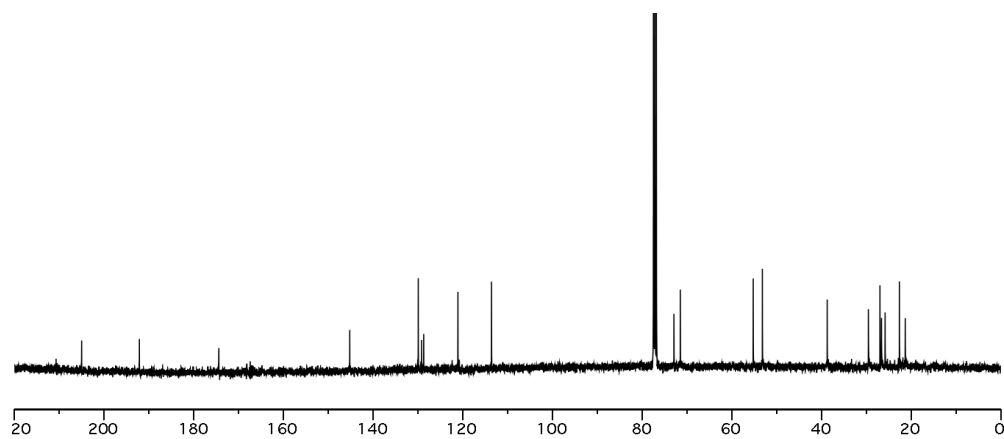


Figure A.1.12 ¹³C NMR (100 MHz, CDCl₃) of compound **344**.

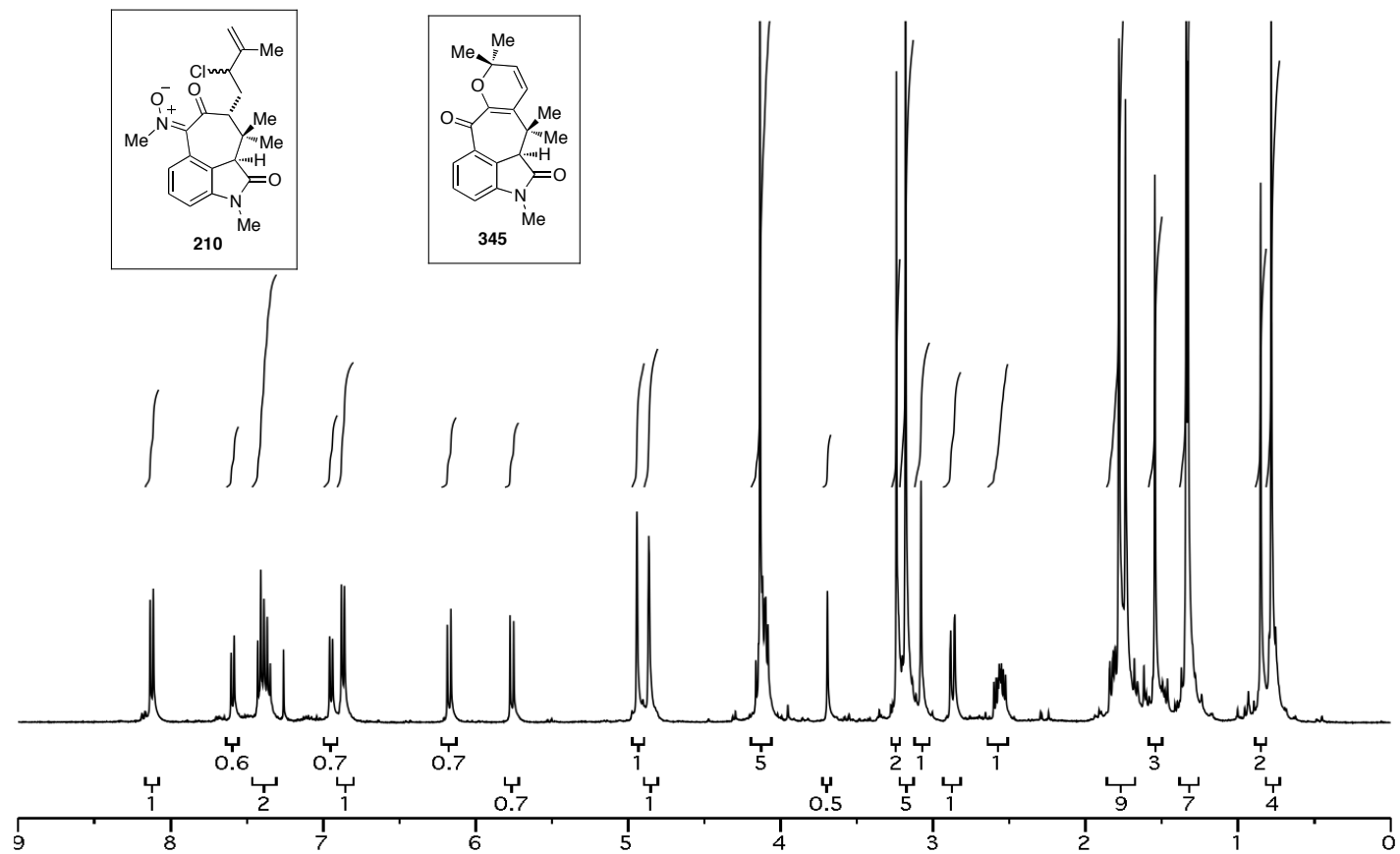


Figure A.1.13 ^1H NMR (400 MHz, CDCl_3) of compound **210** and **345**.

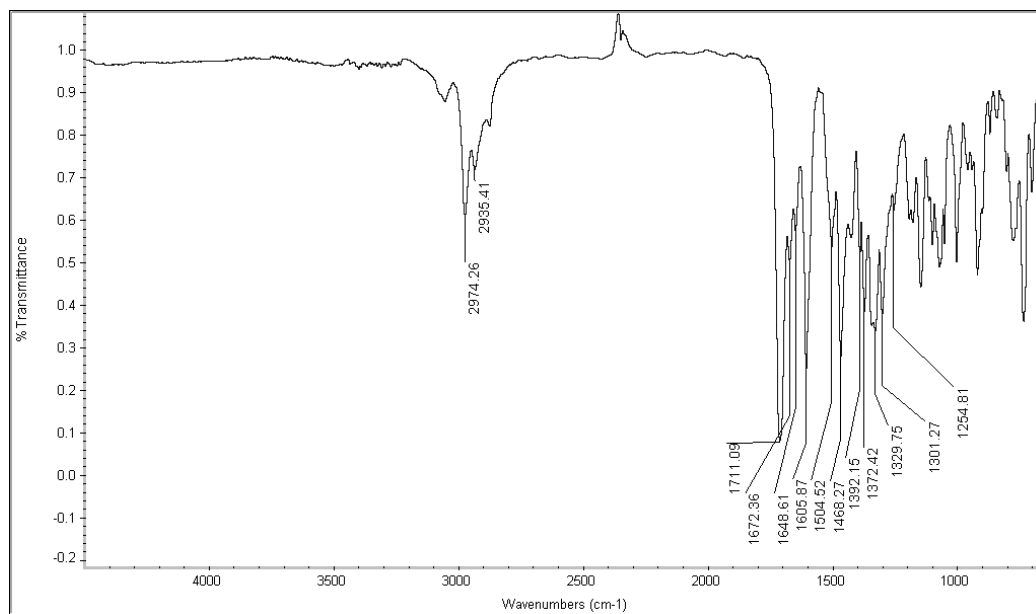


Figure A.1.14 Infrared Spectrum (thin film/NaCl) of compound **210** and **345**.

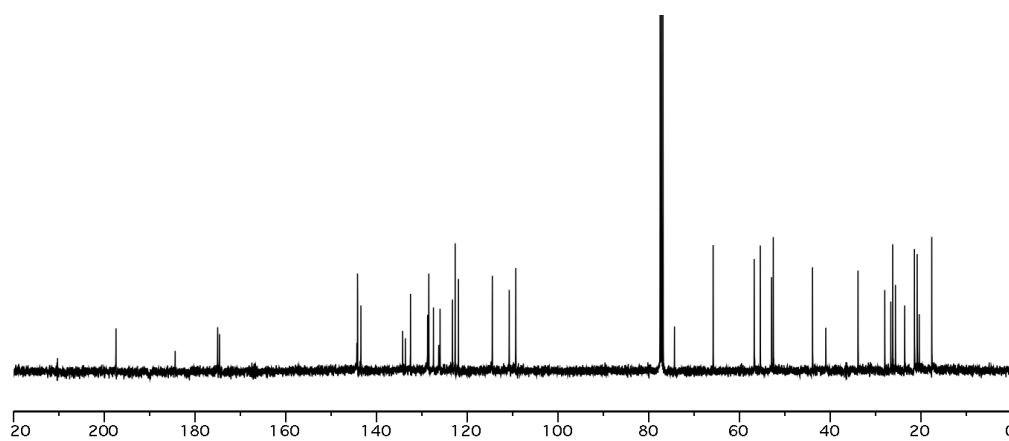


Figure A.1.15 ^{13}C NMR (100 MHz, CDCl_3) of compound **210** and **345**.

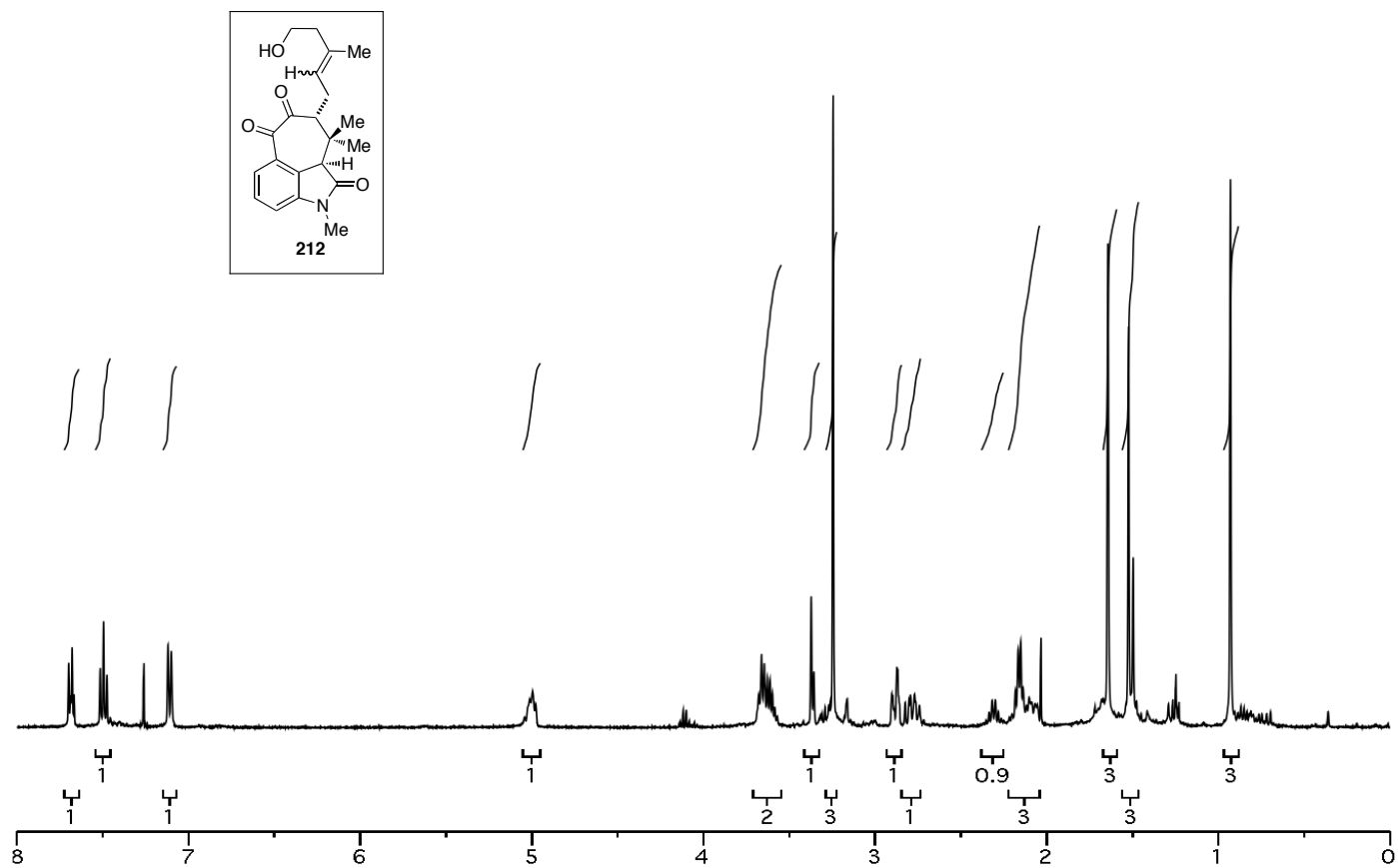


Figure A.1.16 ¹H NMR (400 MHz, CDCl₃) of compound 212.

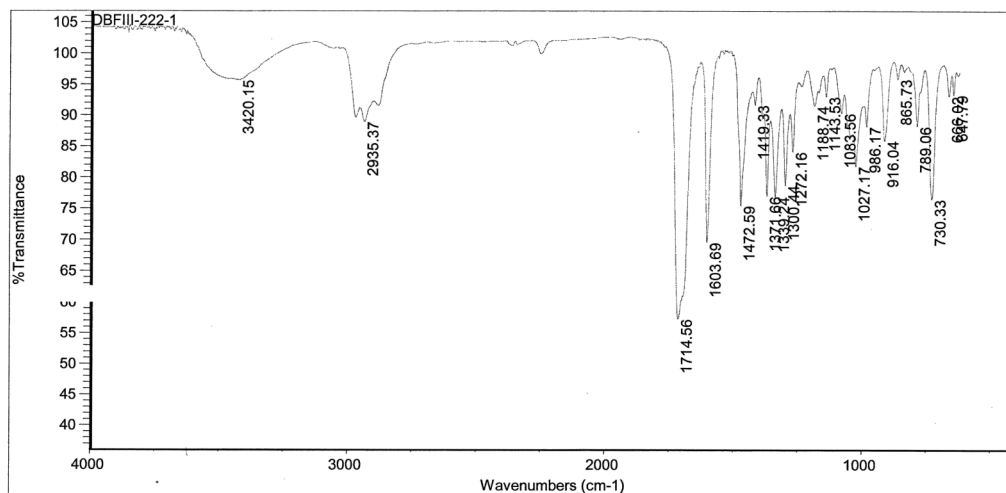


Figure A.1.17 Infrared Spectrum (thin film/NaCl) of compound **212**.

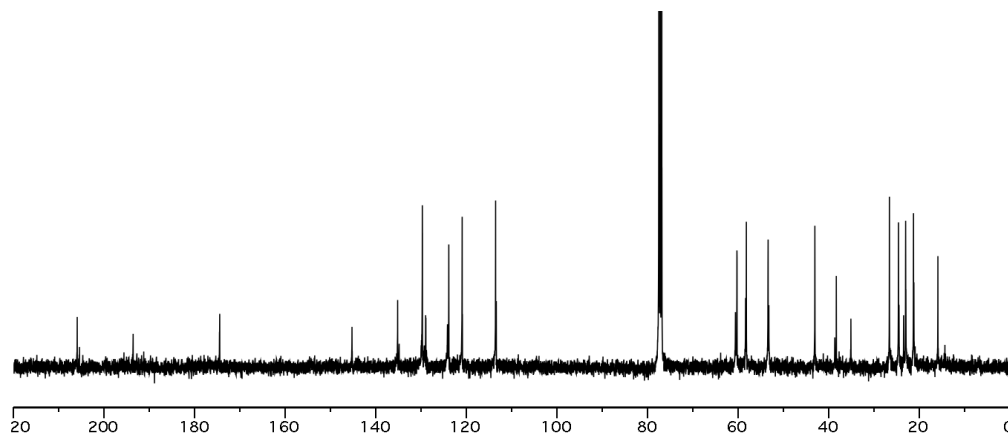


Figure A.1.18 ^{13}C NMR (100 MHz, CDCl_3) of compound **212**.

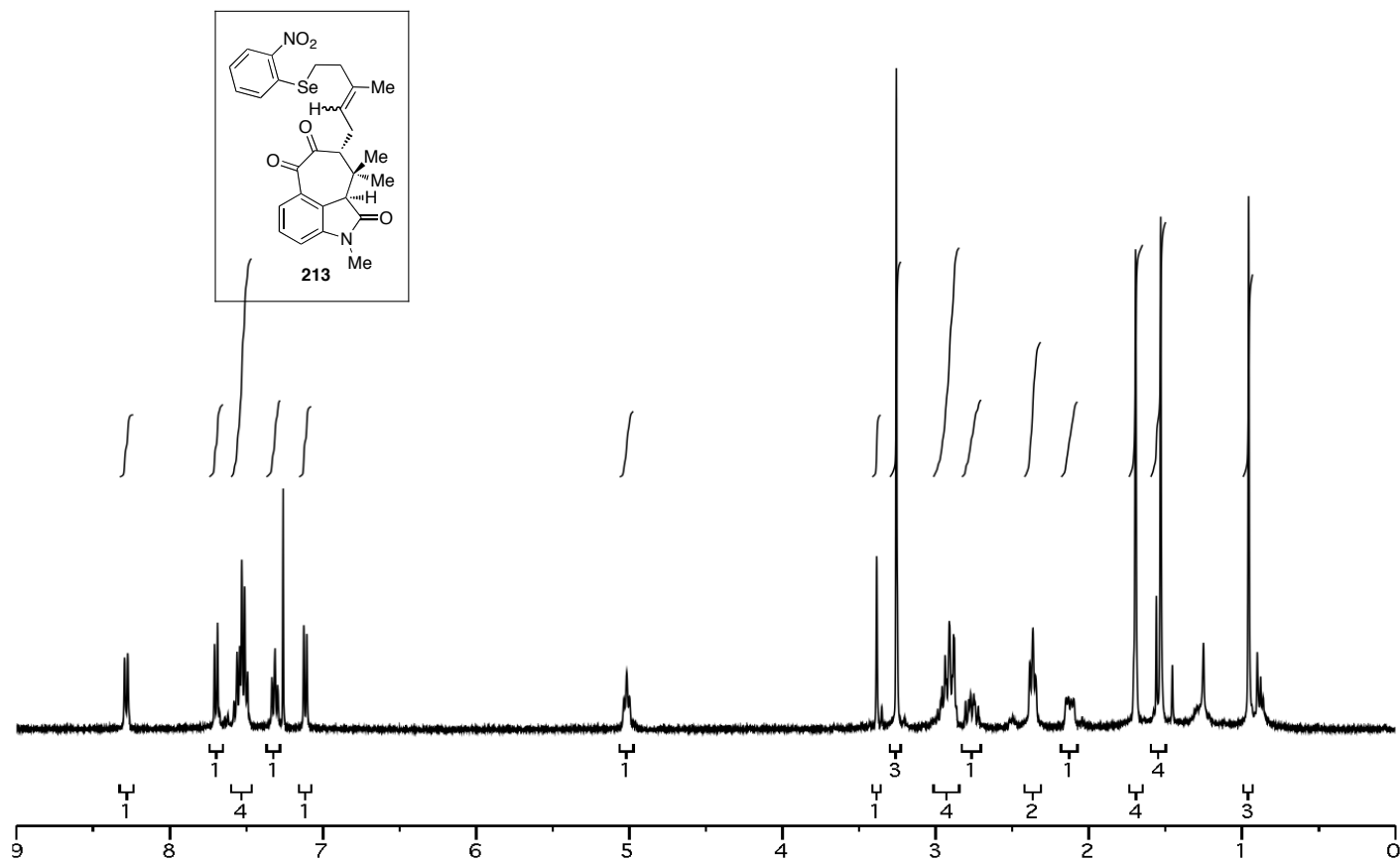


Figure A.1.19 ¹H NMR (400 MHz, CDCl₃) of compound 213.

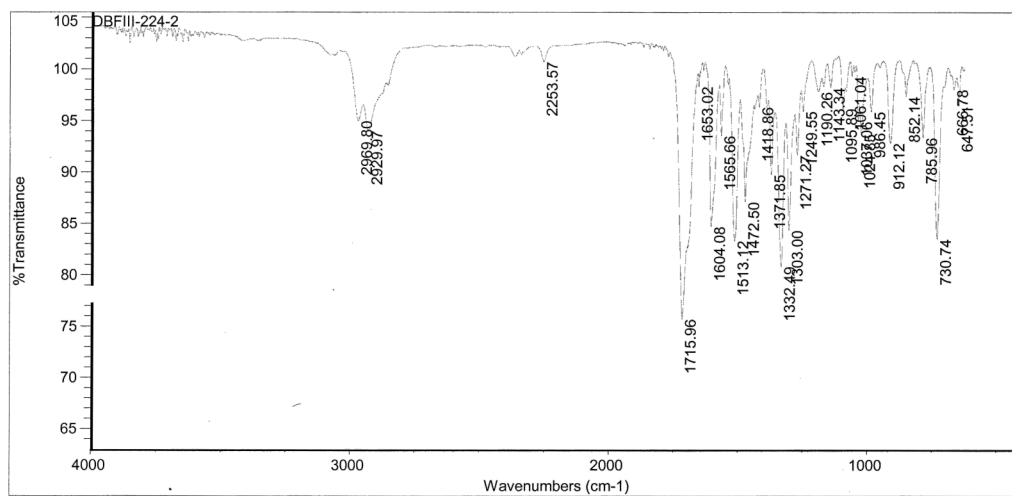


Figure A.1.20 Infrared Spectrum (thin film/NaCl) of compound **213**.

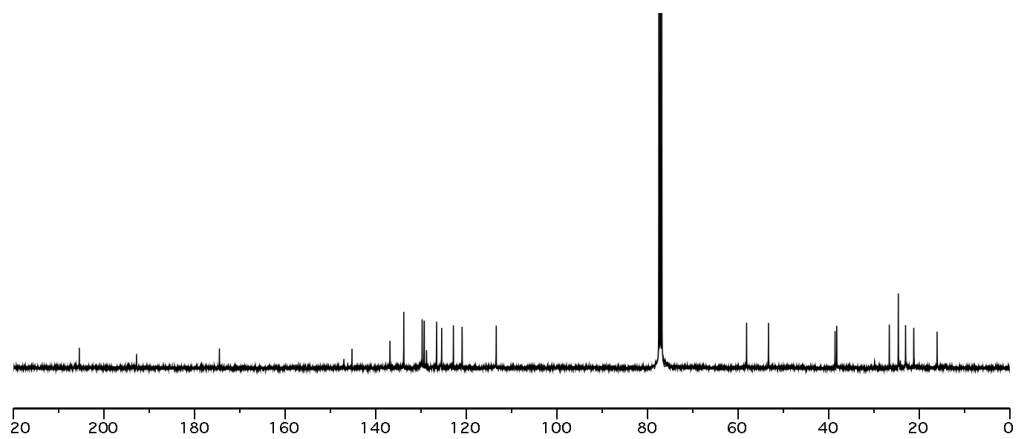


Figure A.1.21 ^{13}C NMR (100 MHz, CDCl_3) of compound **213**.

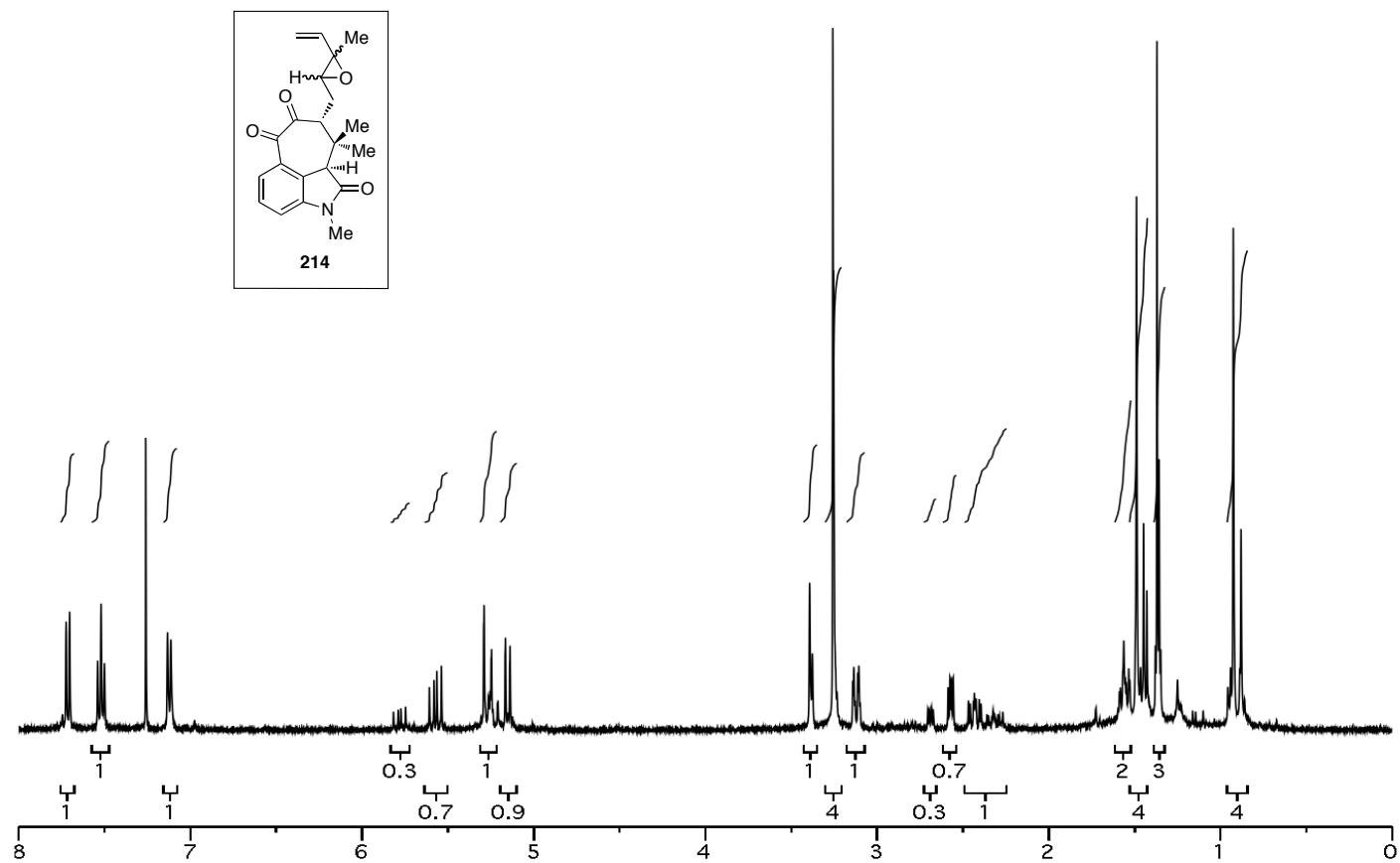


Figure A.1.22 ¹H NMR (400 MHz, CDCl₃) of compound 214.

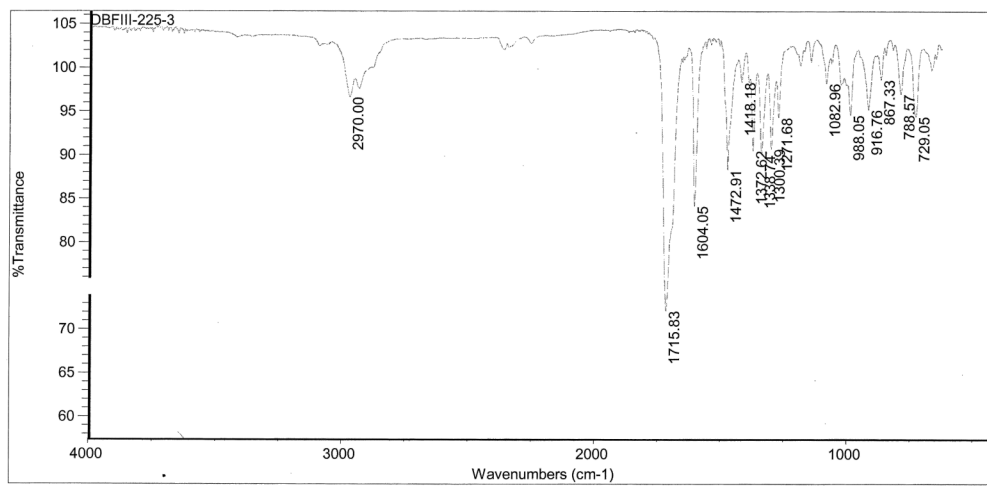


Figure A.1.23 Infrared Spectrum (thin film/NaCl) of compound **214**.

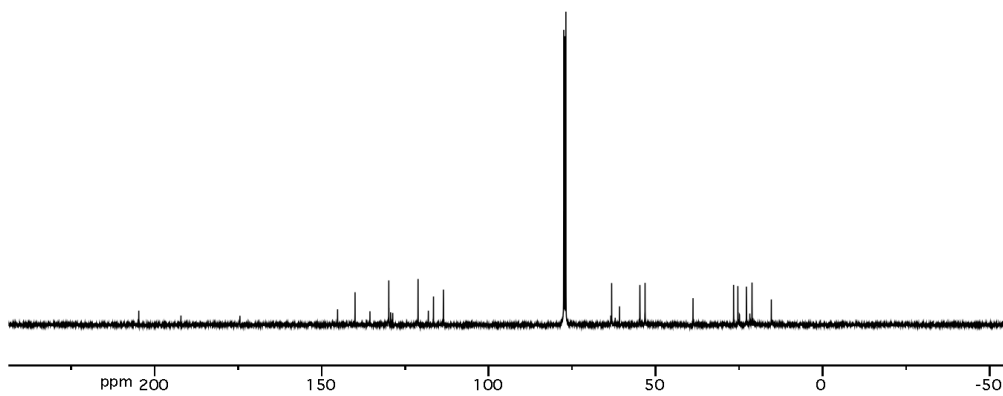


Figure A.1.24 ¹³C NMR (100 MHz, CDCl₃) of compound **214**.

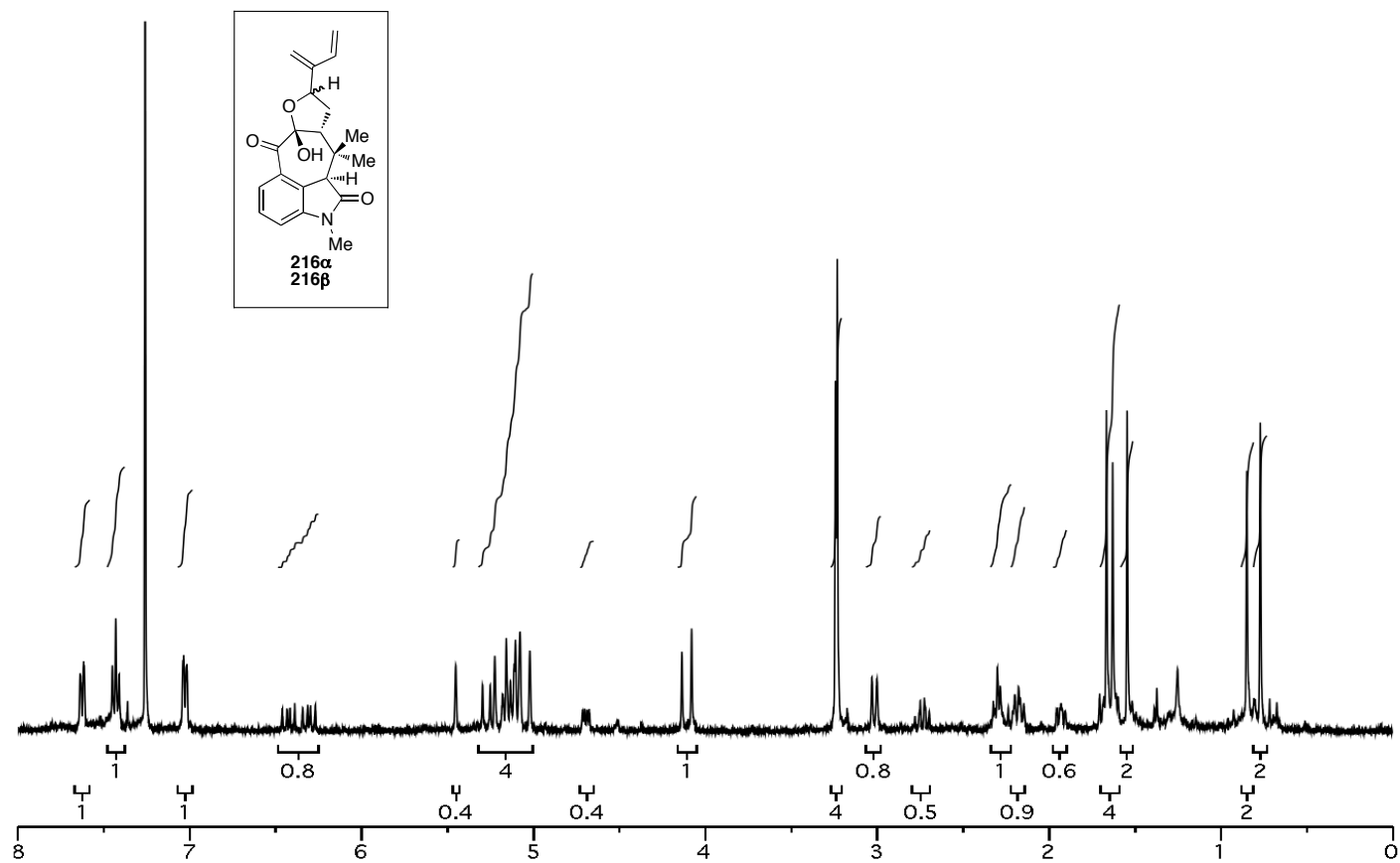


Figure A.1.25 ¹H NMR (400 MHz, CDCl₃) of compound 216.

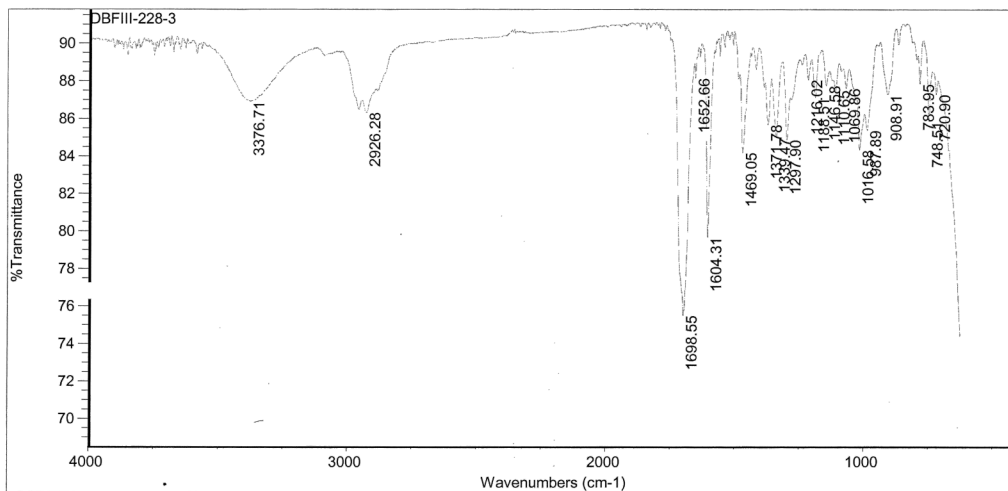


Figure A.1.26 Infrared Spectrum (thin film/NaCl) of compound **216**.

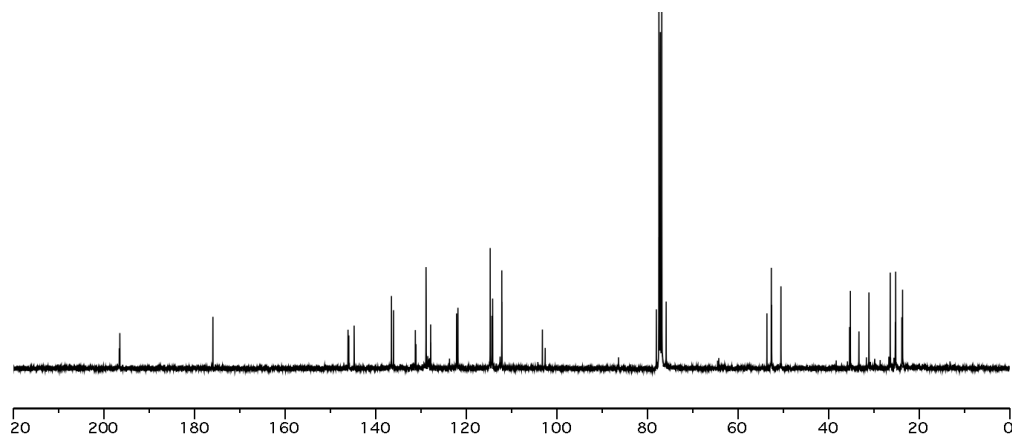


Figure A.1.27 ¹³C NMR (100 MHz, CDCl₃) of compound **216**.

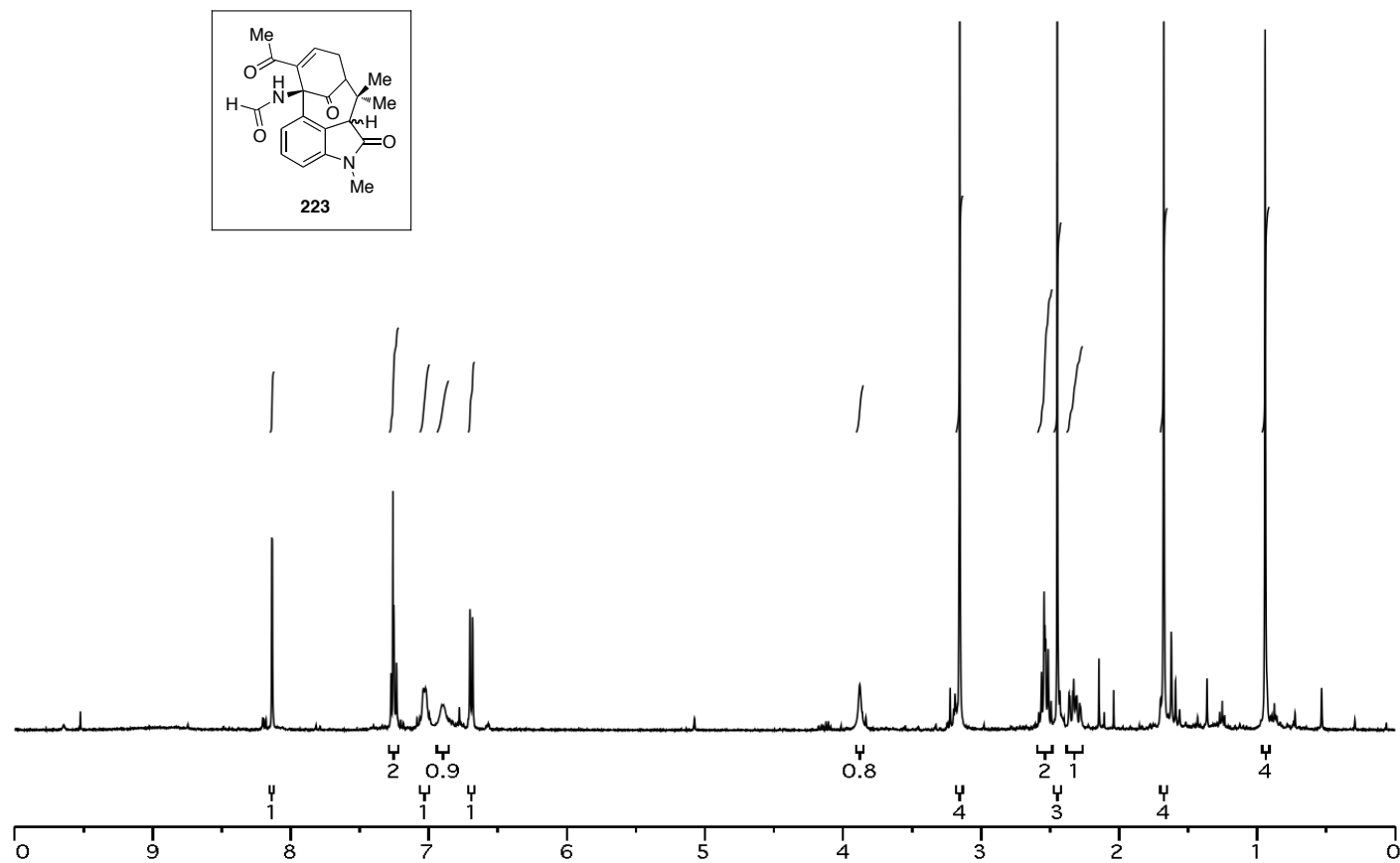


Figure A.1.28 ¹H NMR (400 MHz, CDCl₃) of compound 223.

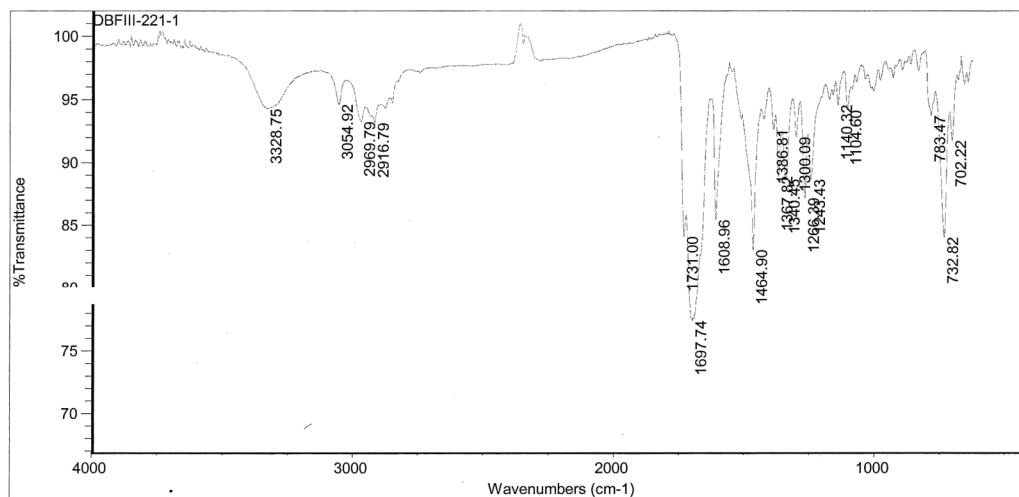


Figure A.1.29 Infrared Spectrum (thin film/NaCl) of compound **223**.

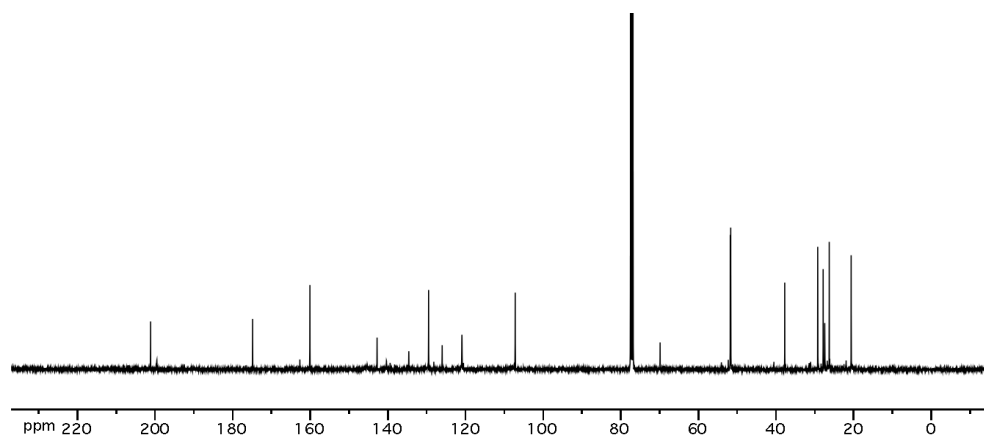


Figure A.1.30 ^{13}C NMR (100 MHz, CDCl_3) of compound **223**.

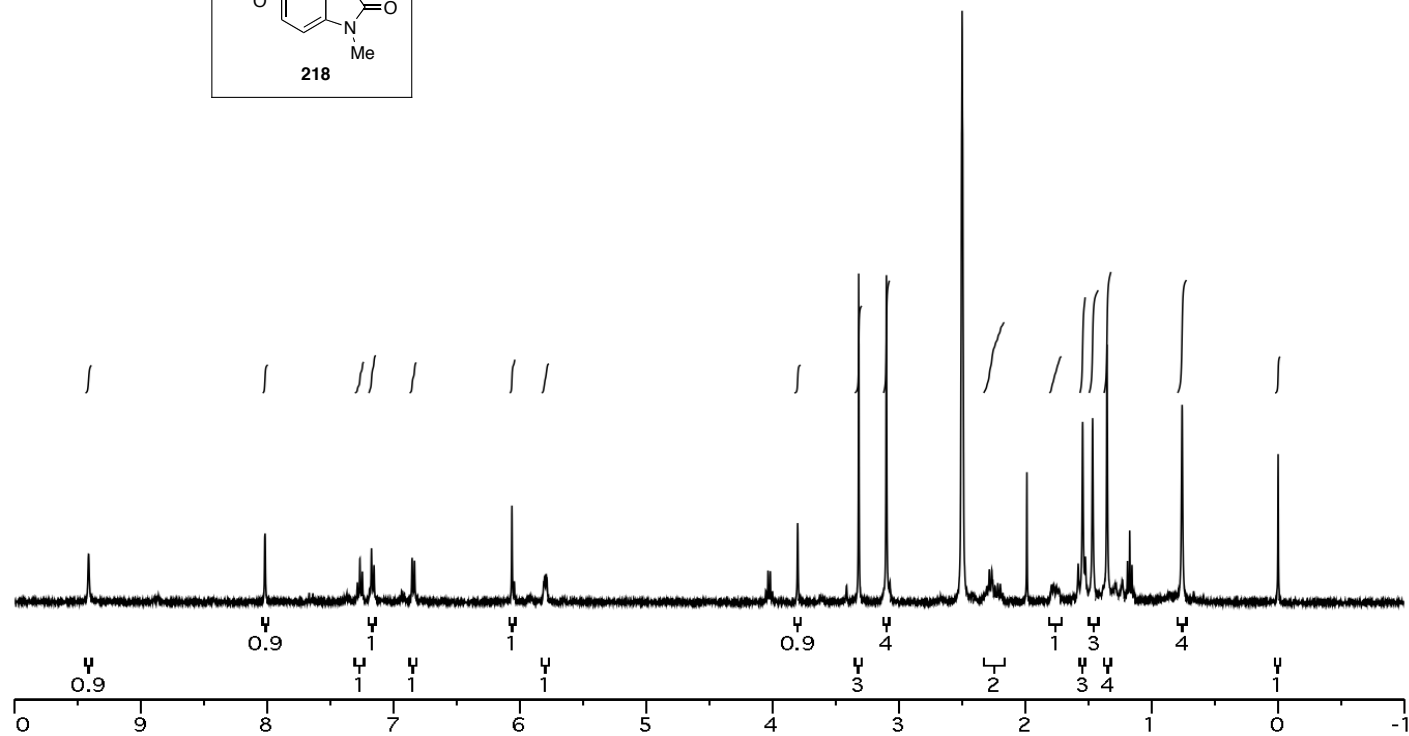
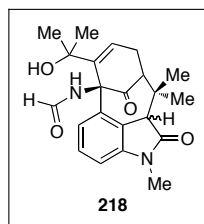


Figure A.1.31 ^1H NMR (400 MHz, CDCl_3) of compound **218**.

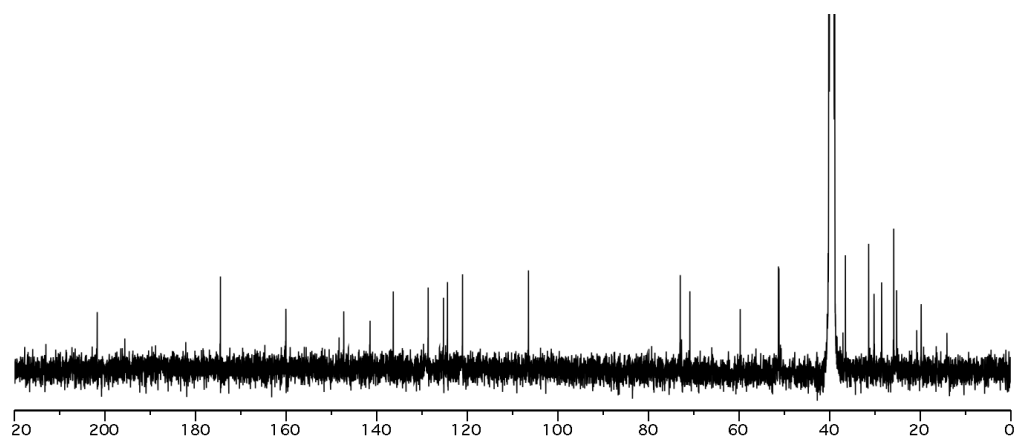


Figure A.1.32 ^{13}C NMR (100 MHz, CDCl_3) of compound **218**.

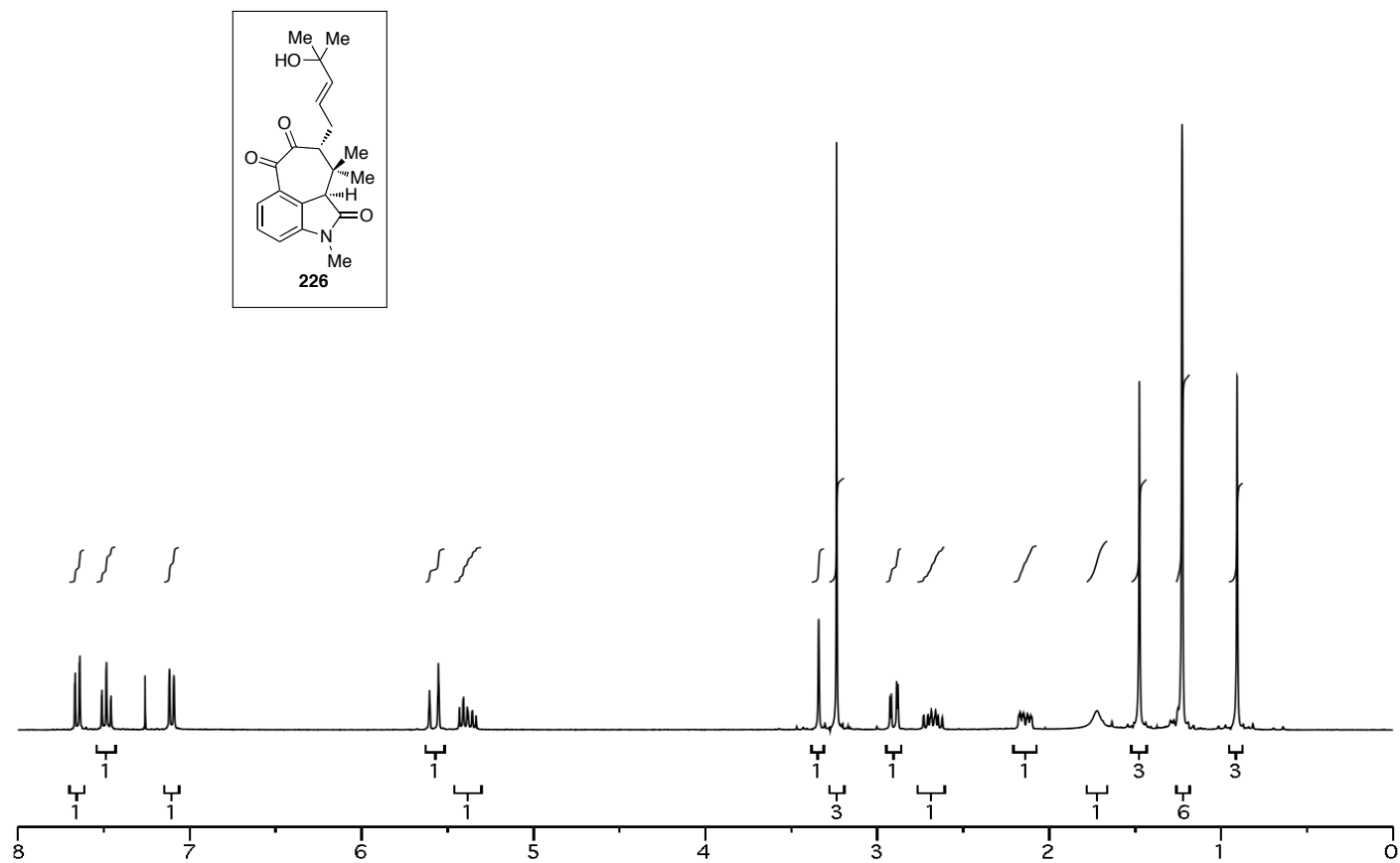


Figure A.1.33 ¹H NMR (300 MHz, CDCl₃) of compound 226.

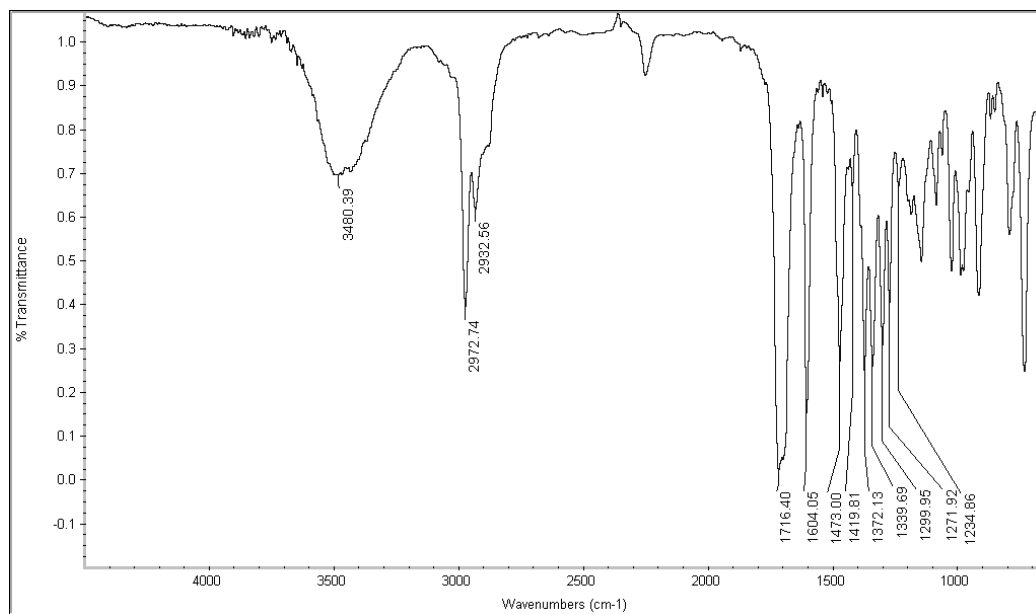


Figure A.1.34 Infrared Spectrum (thin film/NaCl) of compound 226.

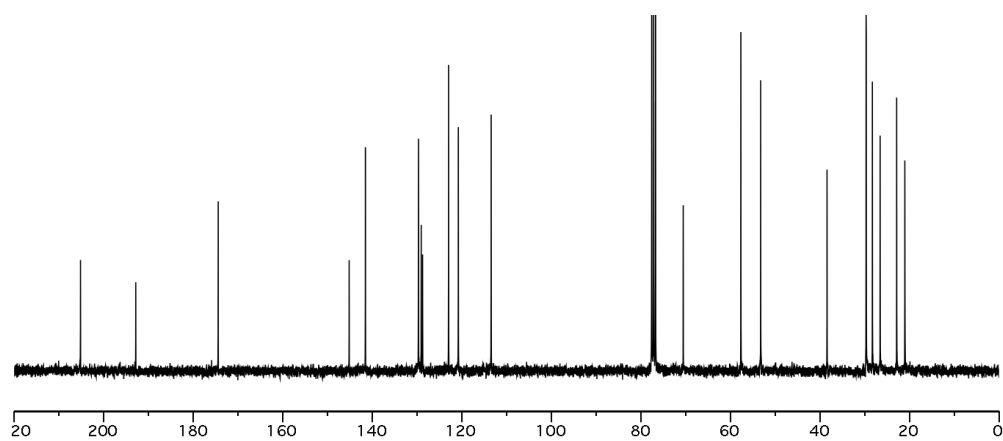


Figure A.1.35 ^{13}C NMR (75 MHz, CDCl_3) of compound 226.

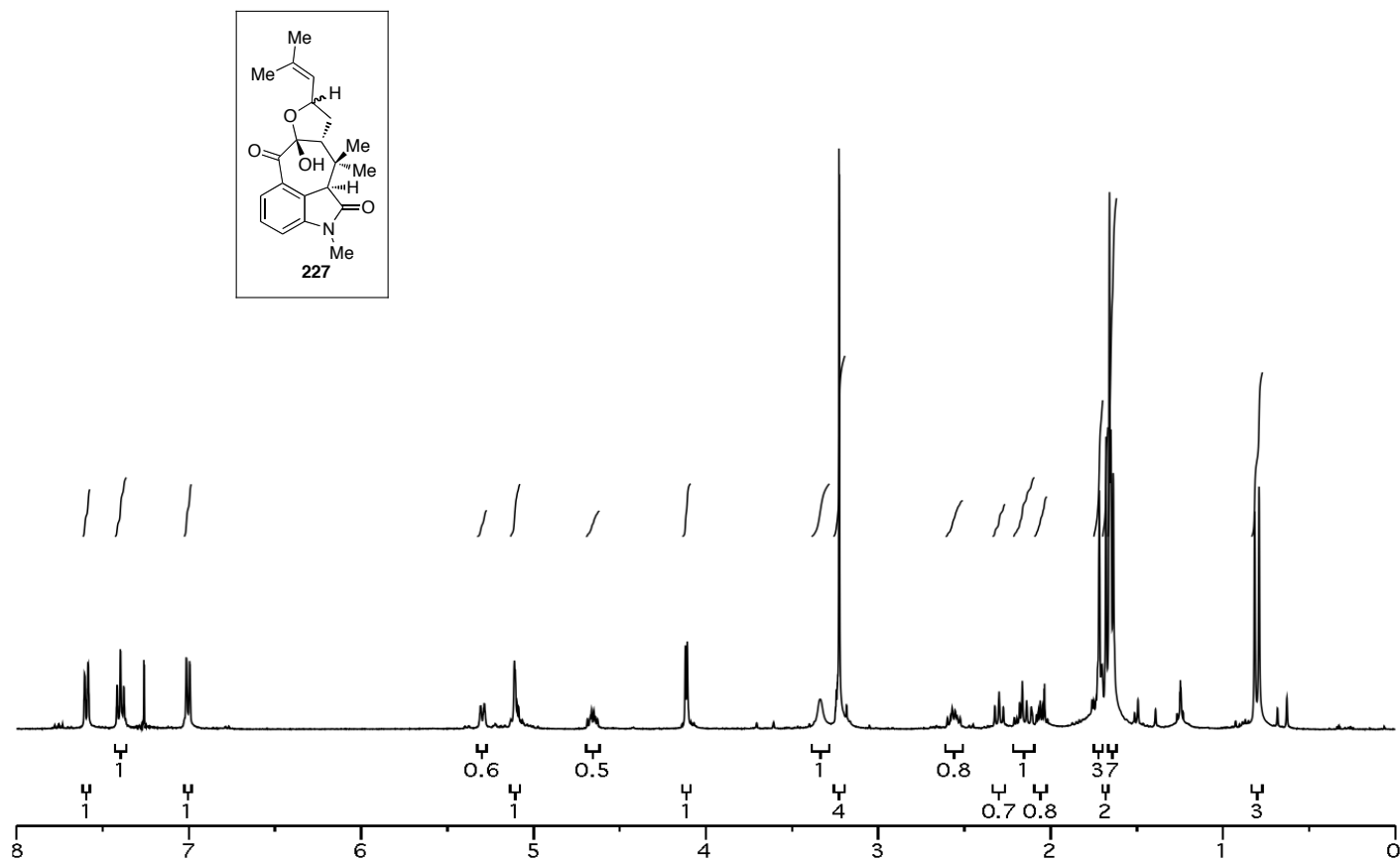


Figure A.1.36 $^1\text{H NMR}$ (400 MHz, CDCl_3) of compound 227.

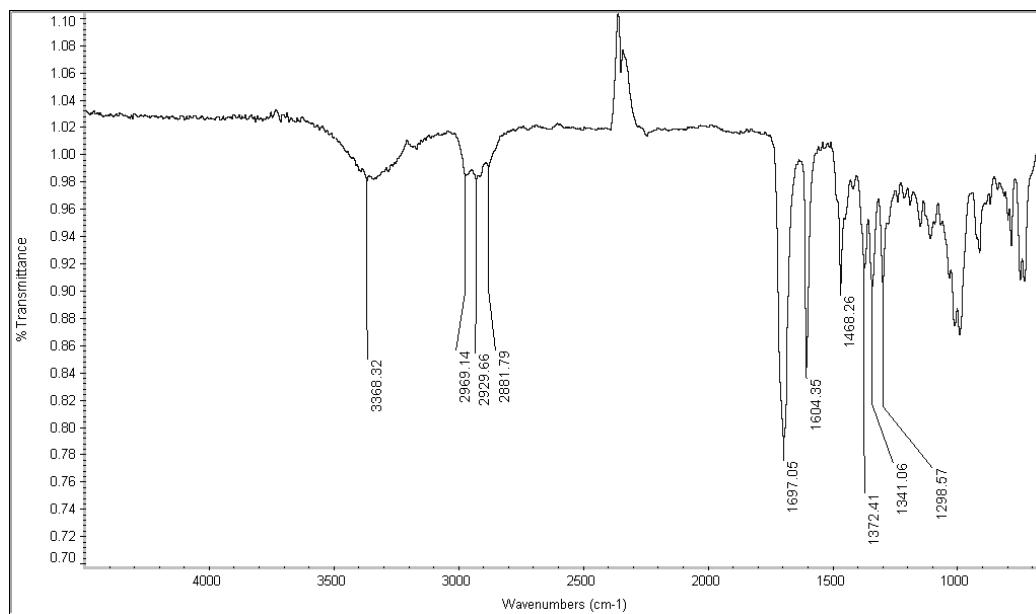


Figure A.1.37 Infrared Spectrum (thin film/NaCl) of compound **227**.

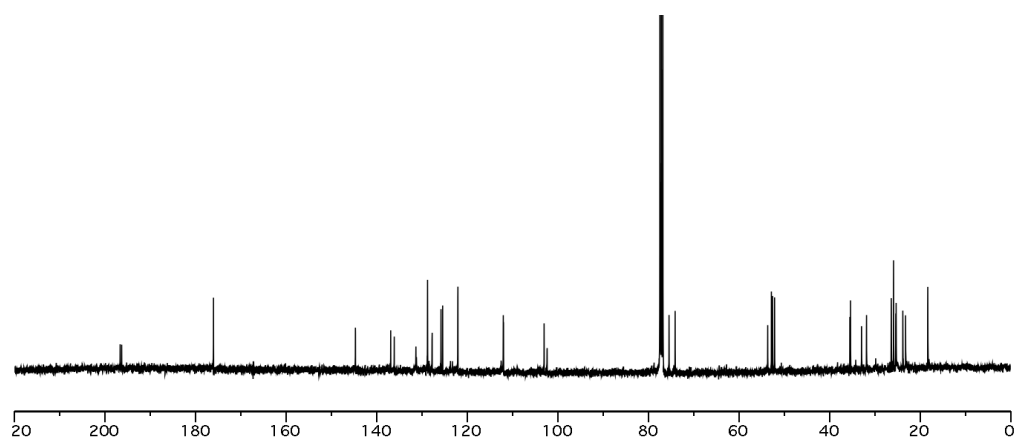


Figure A.1.38 ¹³C NMR (100 MHz, CDCl₃) of compound **227**.

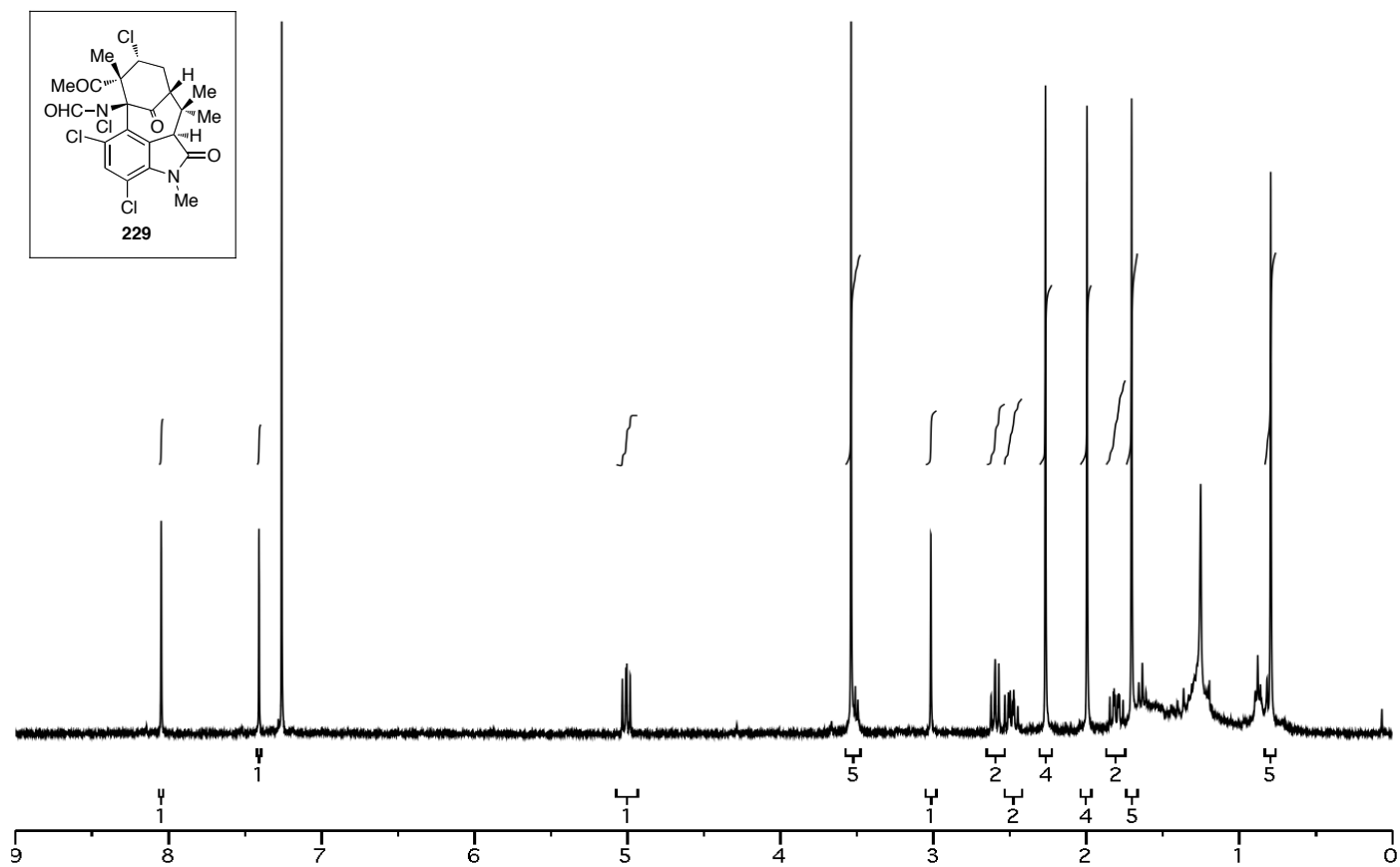


Figure A.1.39 ^1H NMR (400 MHz, CDCl_3) of compound 229.

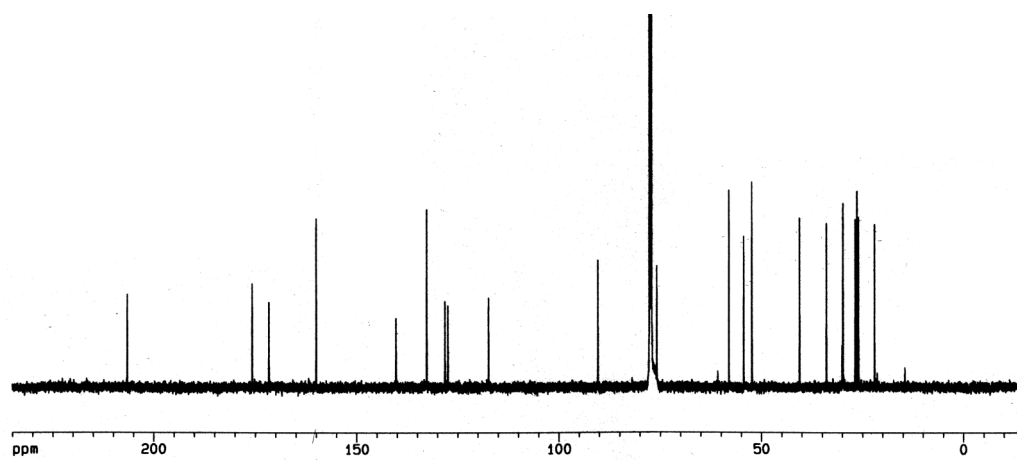


Figure A.1.40 ^{13}C NMR (100 MHz, CDCl_3) of compound **229**.

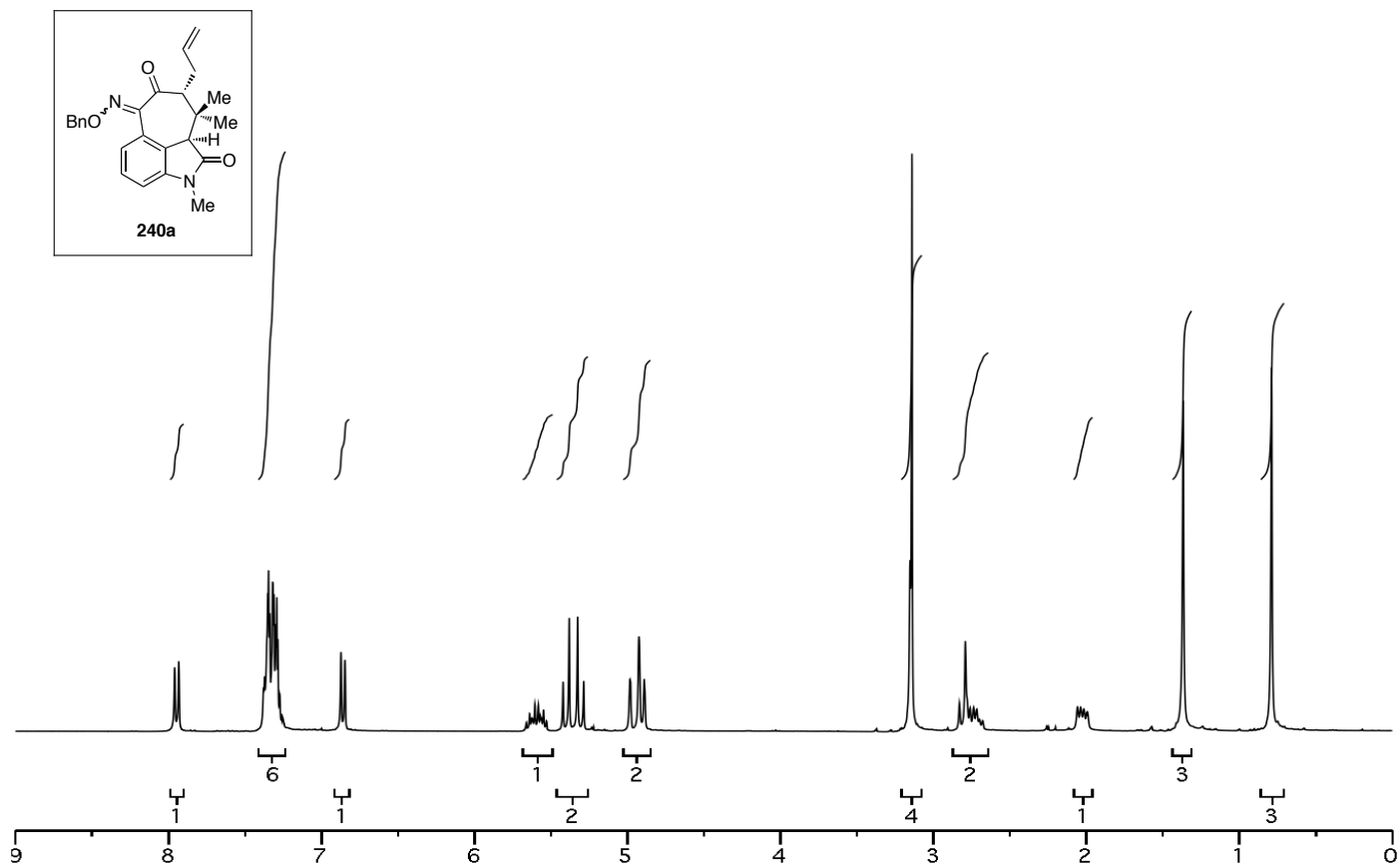


Figure A.1.41 ^1H NMR (300 MHz, CDCl_3) of compound **240a**.

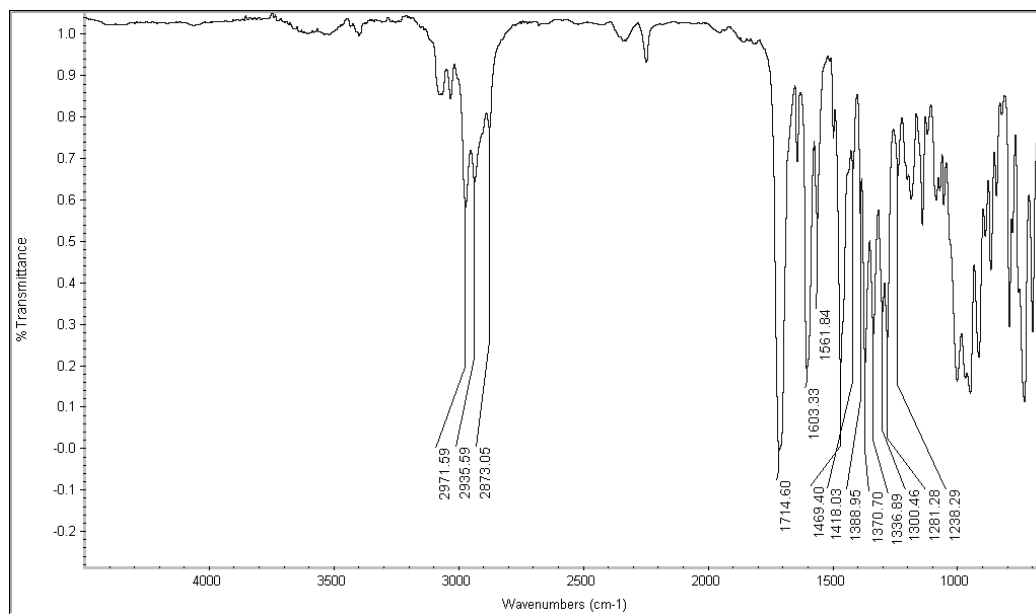


Figure A.1.42 Infrared Spectrum (thin film/NaCl) of compound **240a**.

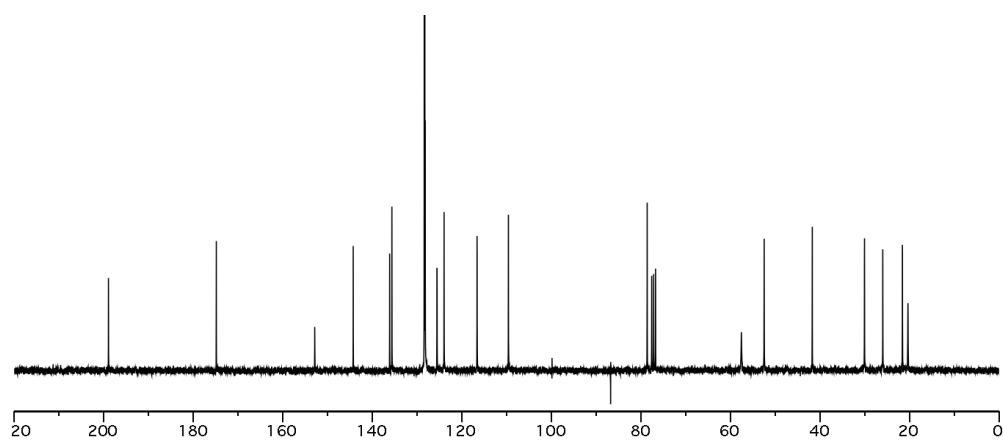


Figure A.1.43 ^{13}C NMR (75 MHz, CDCl_3) of compound **240a**.

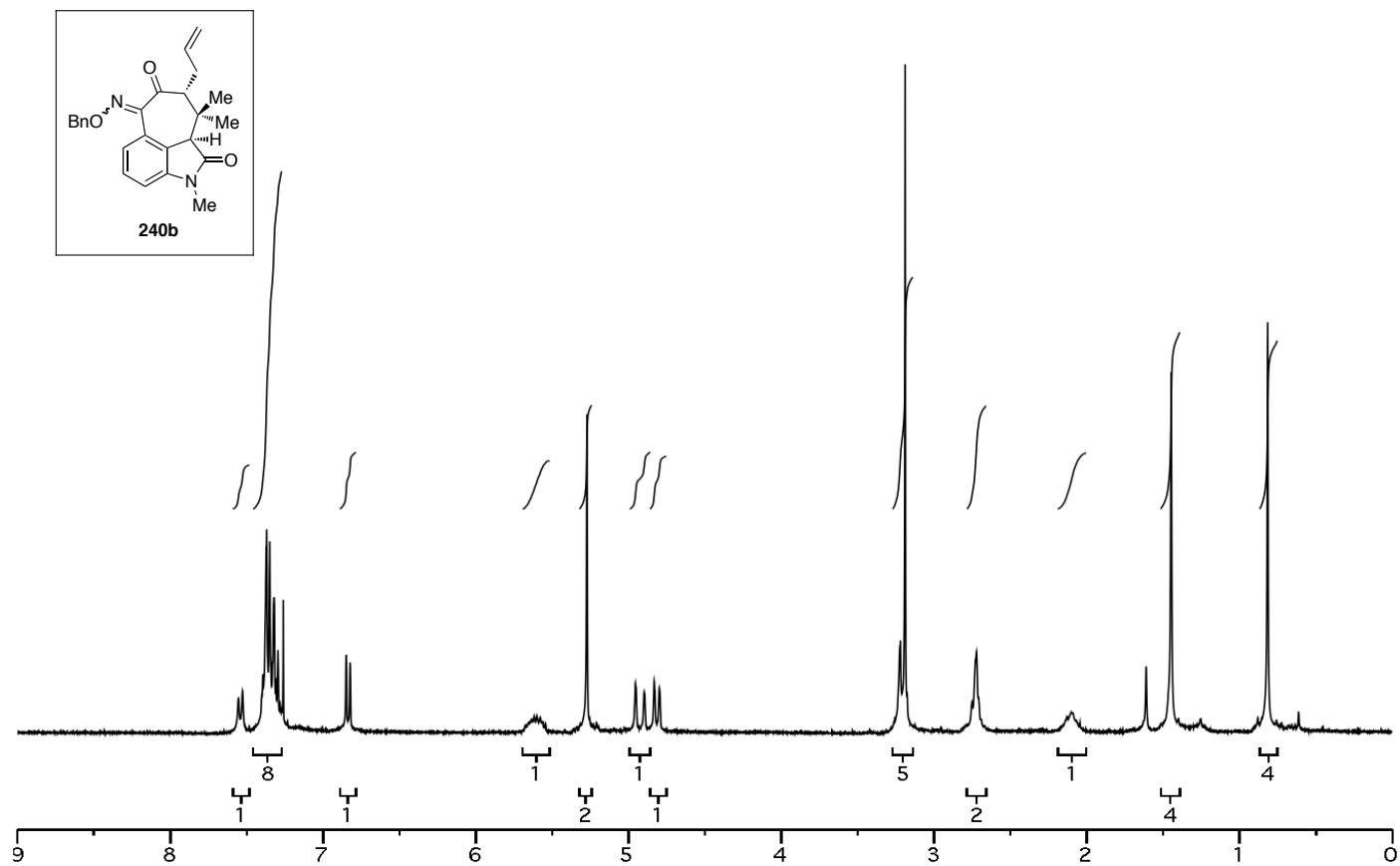


Figure A.1.44 ¹H NMR (400 MHz, CDCl₃) of compound **240b**.

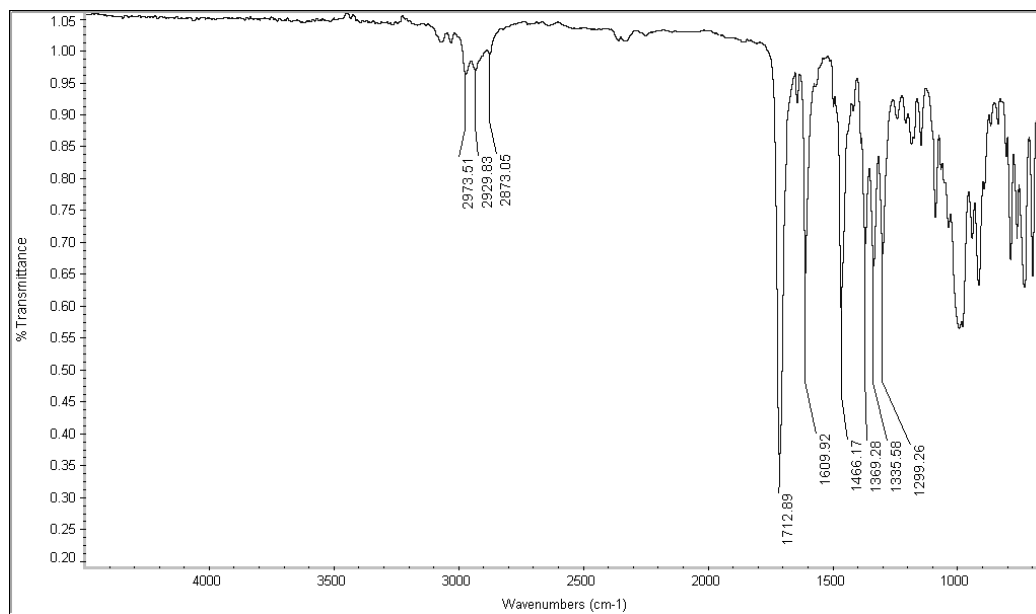


Figure A.1.45 Infrared Spectrum (thin film/NaCl) of compound **240b**.

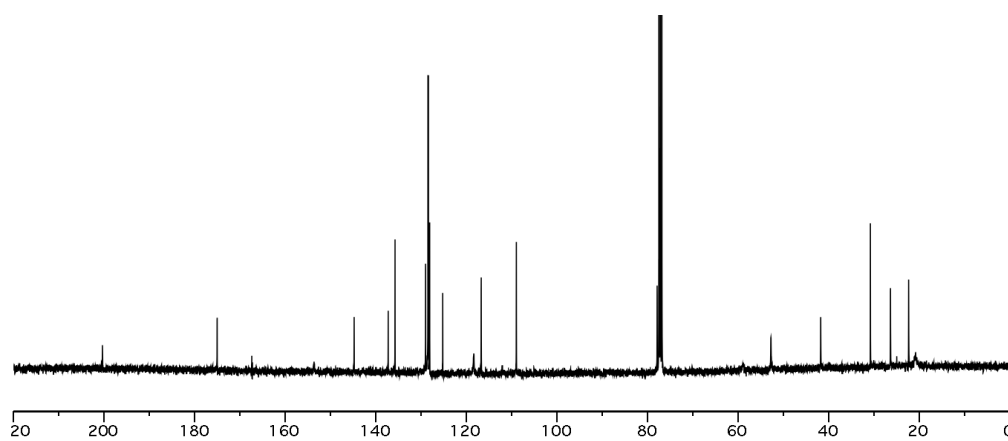


Figure A.1.46 ¹³C NMR (100 MHz, CDCl₃) of compound **240b**.

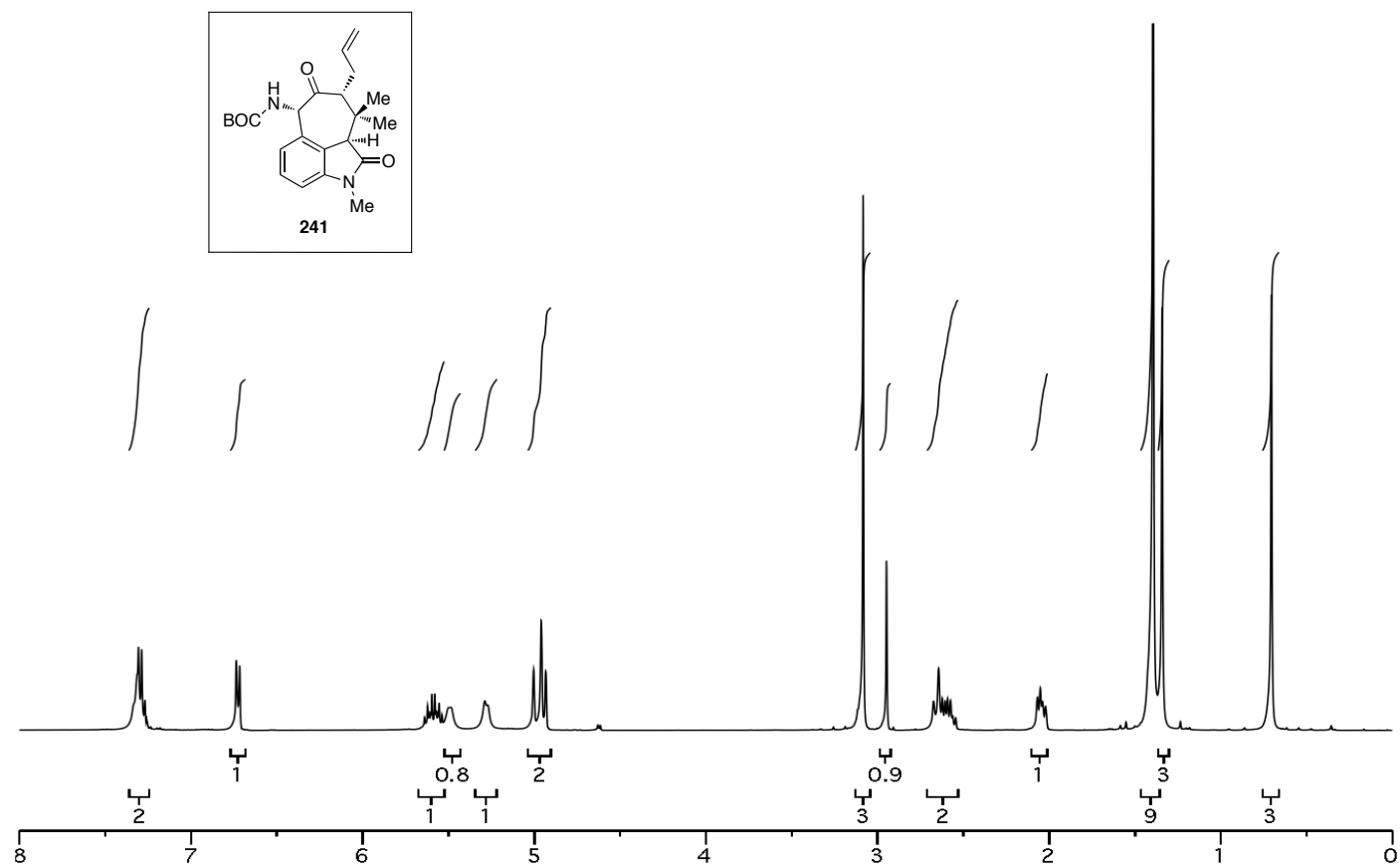


Figure A.1.47 ¹H NMR (400 MHz, CDCl₃) of compound 241.

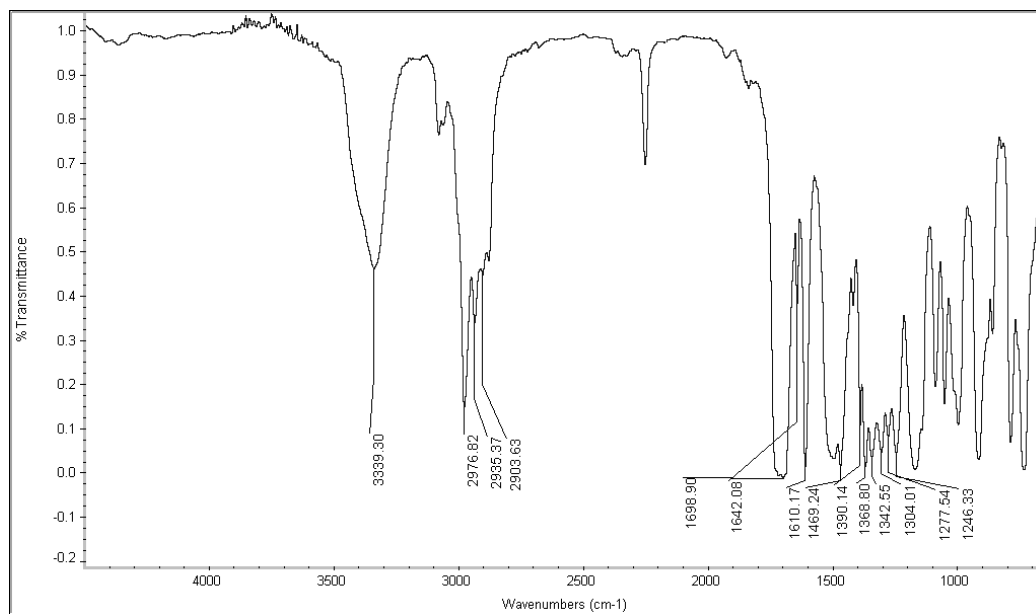


Figure A.1.48 Infrared Spectrum (thin film/NaCl) of compound **241**.

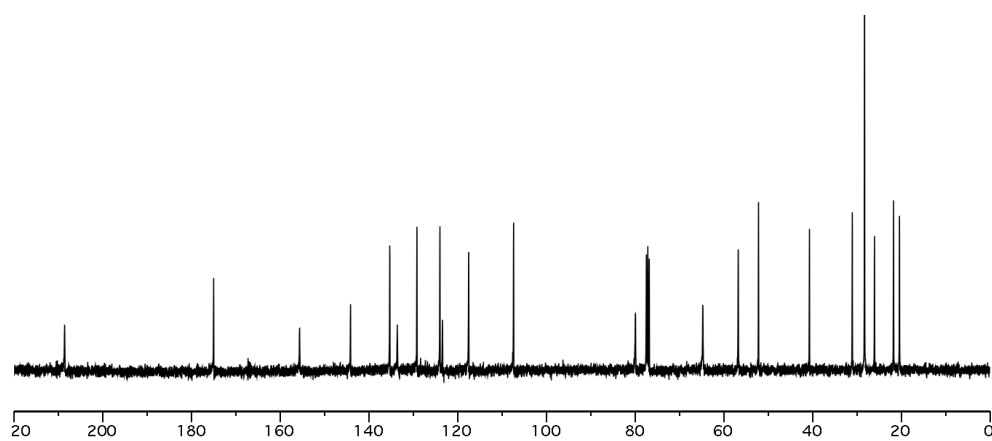


Figure A.1.49 ^{13}C NMR (100 MHz, CDCl_3) of compound **241**.

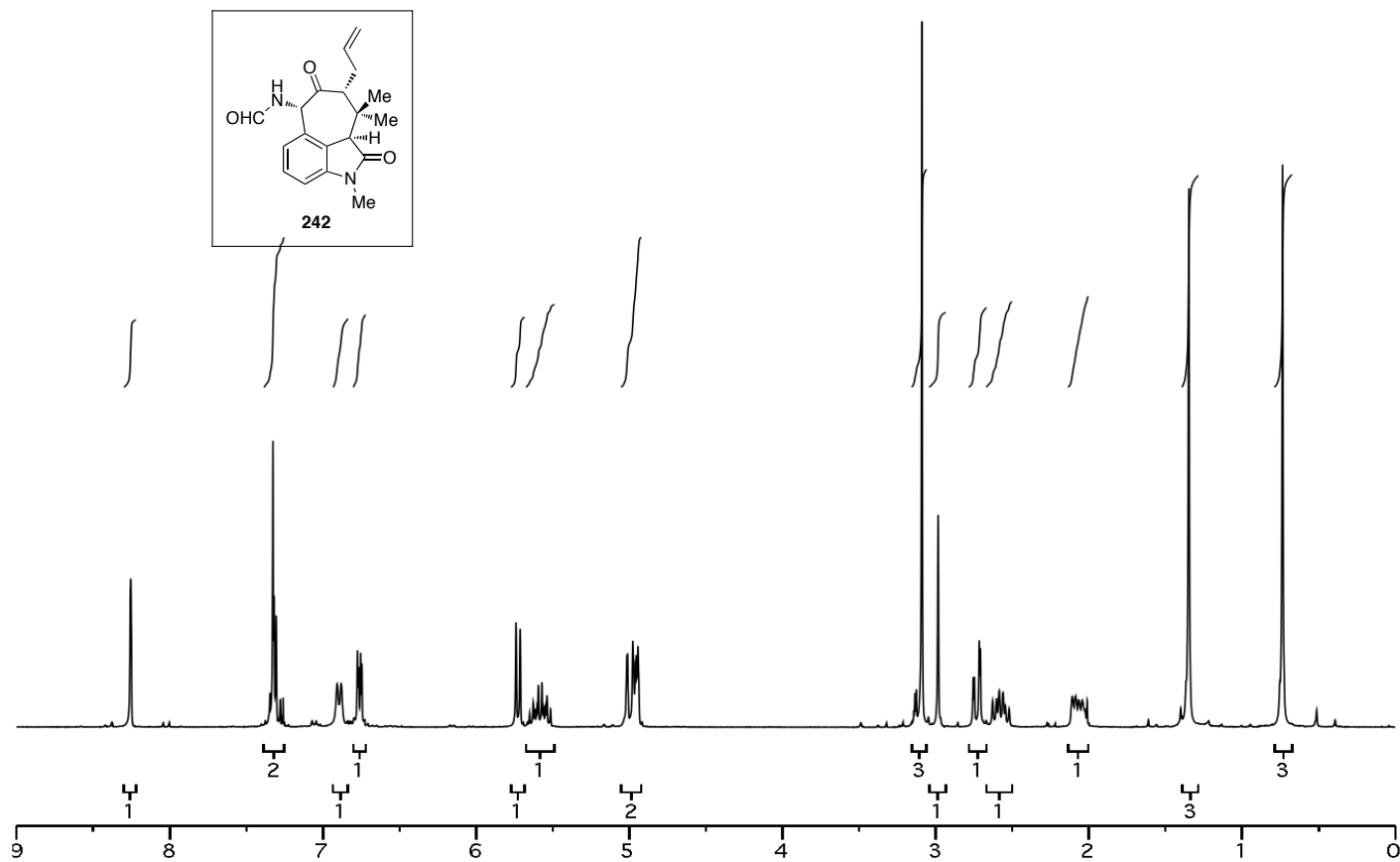


Figure A.1.50 ^1H NMR (300 MHz, CDCl_3) of compound 242.

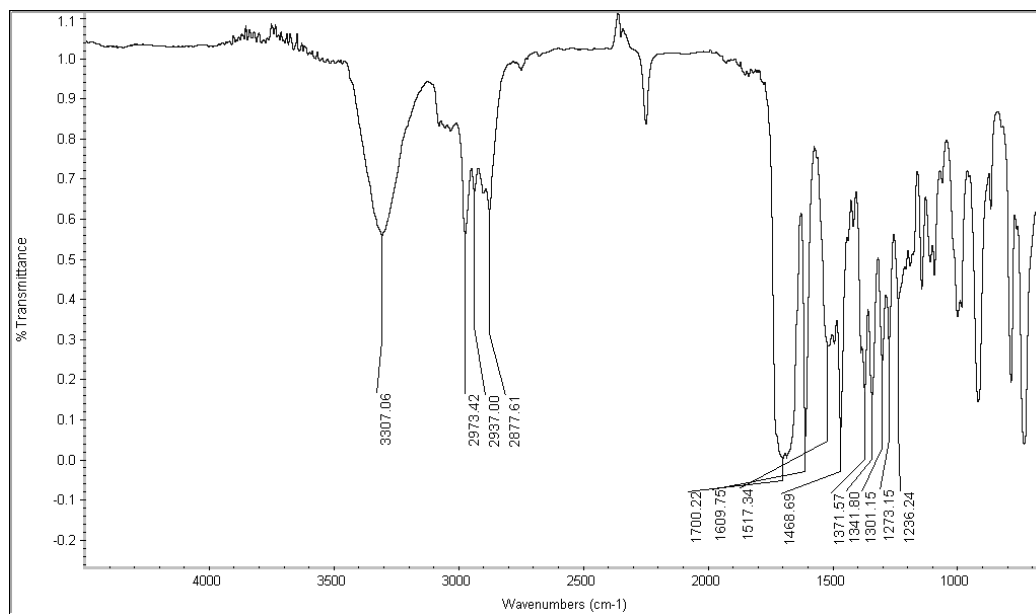


Figure A.1.51 Infrared Spectrum (thin film/NaCl) of compound **242**.

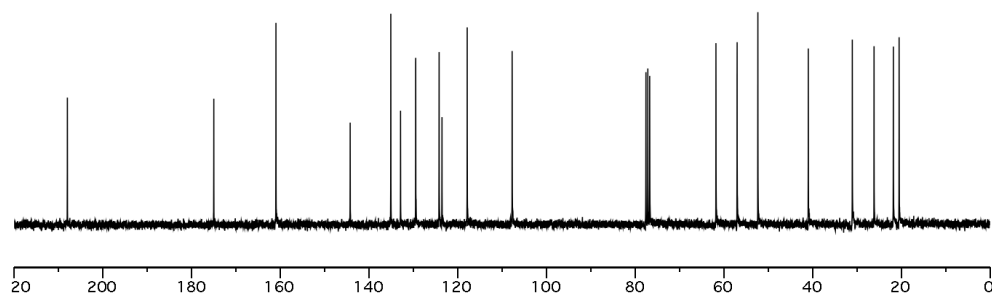


Figure A.1.52 ^{13}C NMR (75 MHz, CDCl_3) of compound **242**.

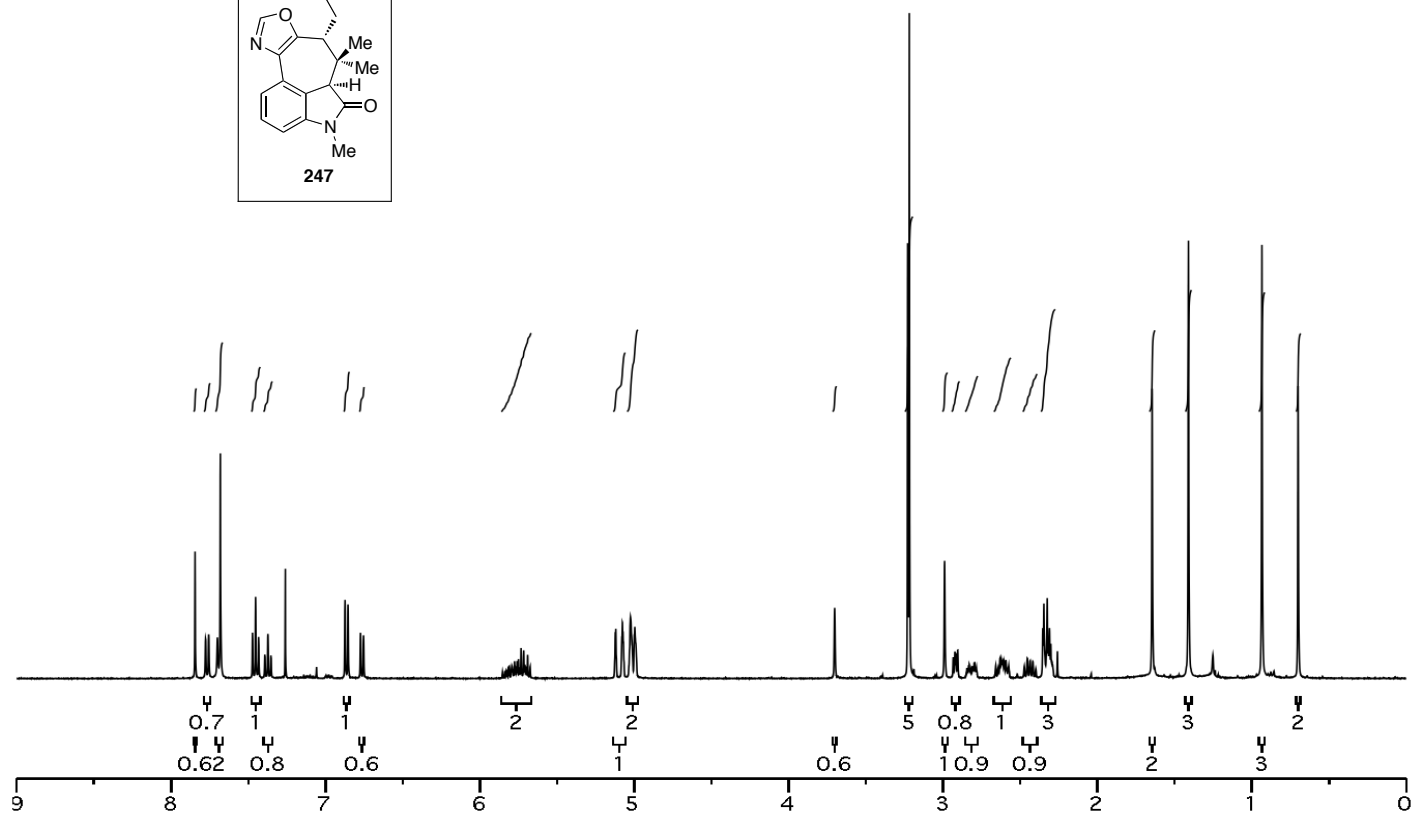
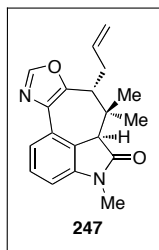


Figure A.1.53 ^1H NMR (400 MHz, CDCl_3) of compound **247**.

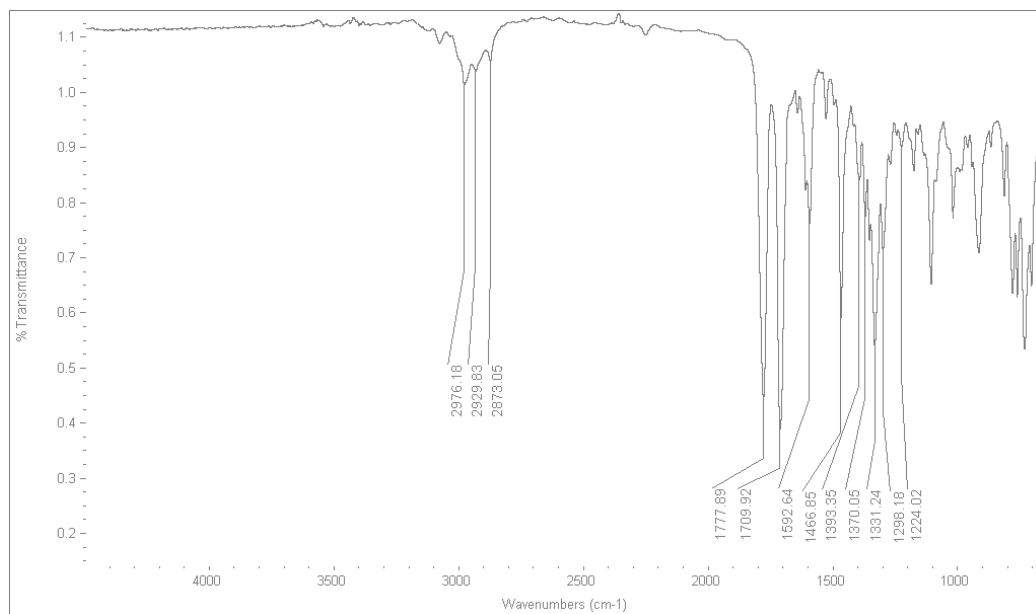


Figure A.1.54 Infrared Spectrum (thin film/NaCl) of compound **247**.

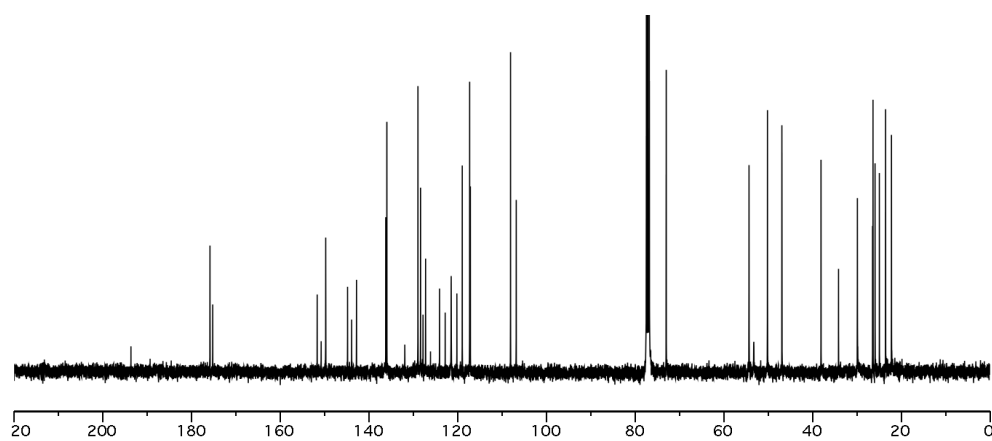


Figure A.1.55 ¹³C NMR (100 MHz, CDCl₃) of compound **247**.

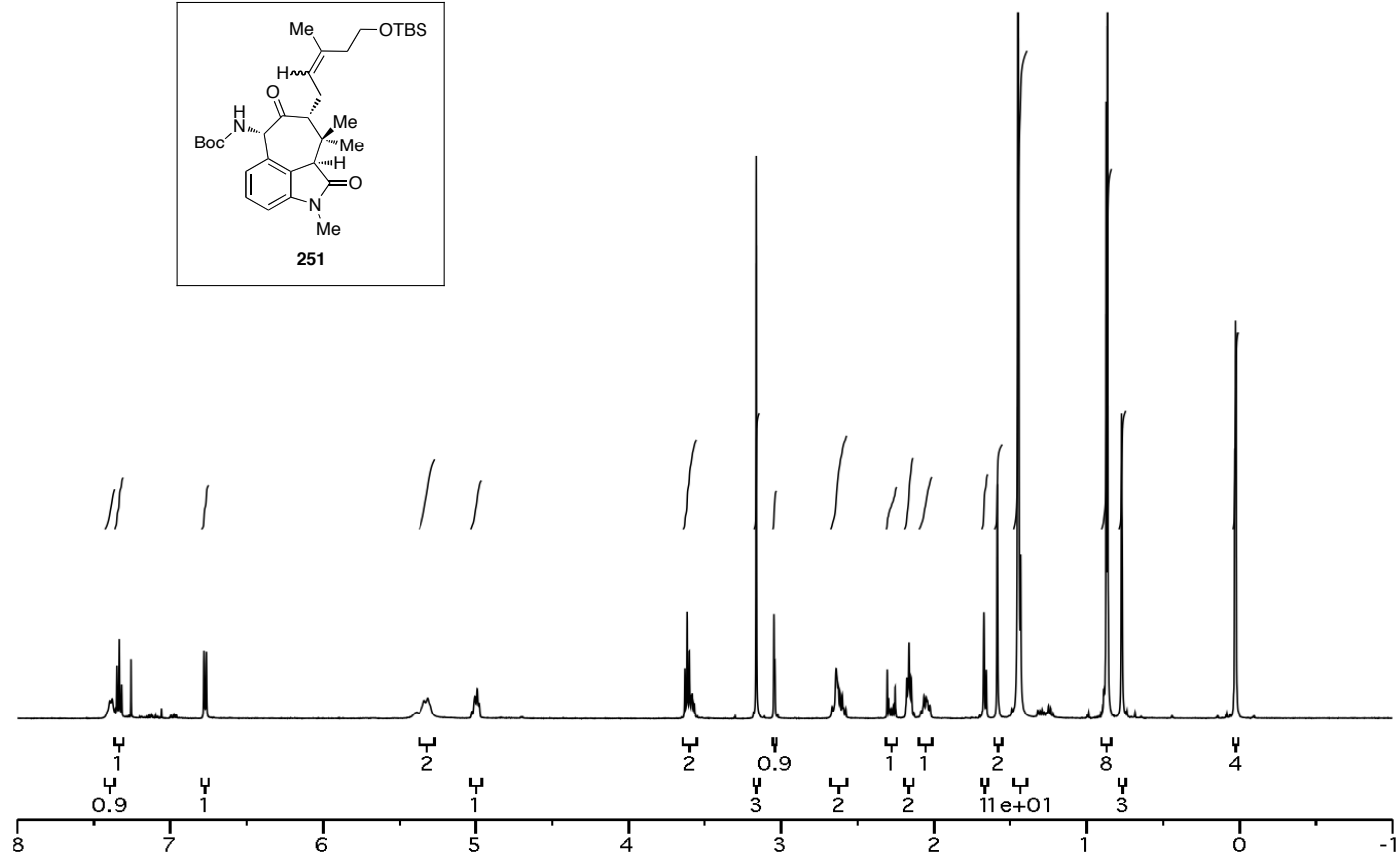
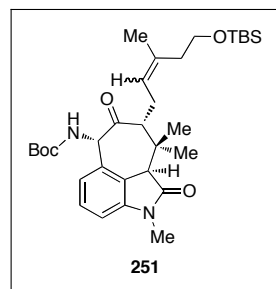


Figure A.1.56 ^1H NMR (400 MHz, CDCl_3) of compound **251**.

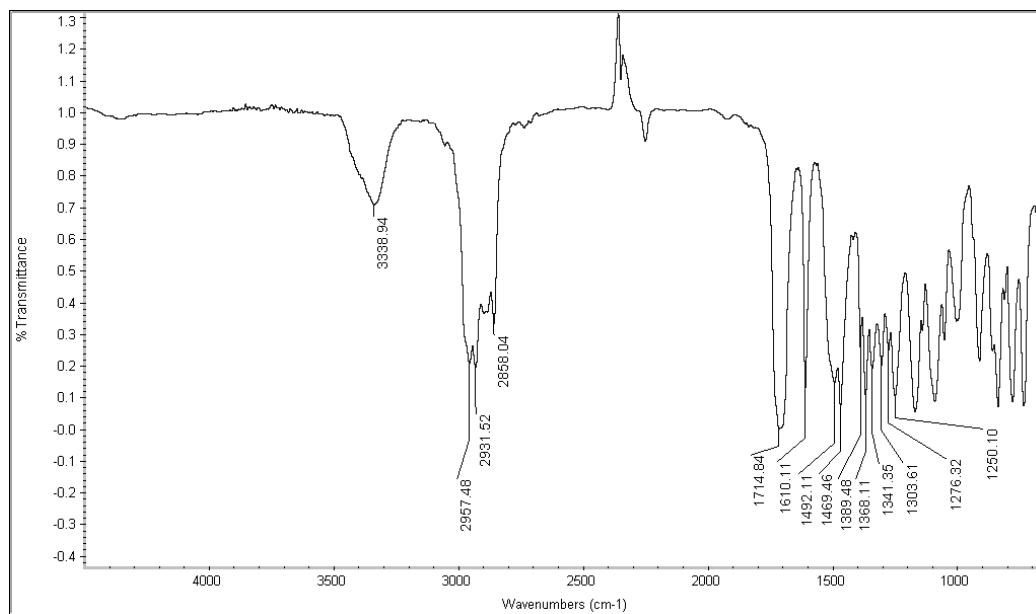


Figure A.1.57 Infrared Spectrum (thin film/NaCl) of compound **251**.

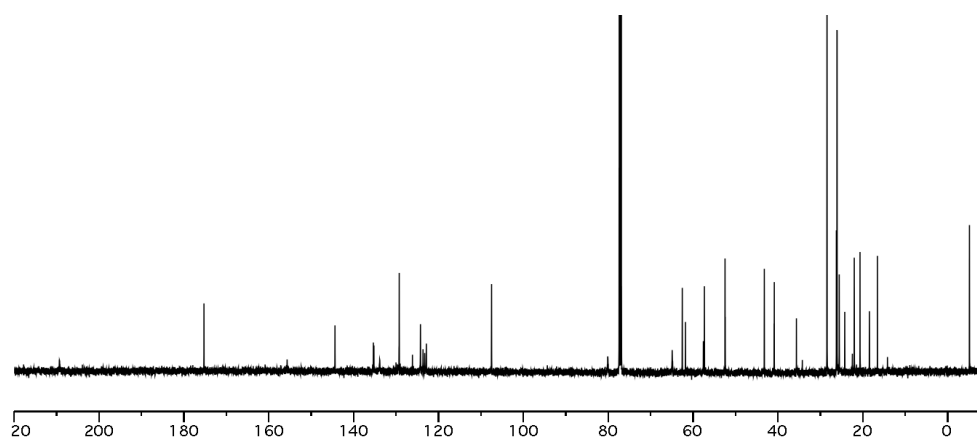


Figure A.1.58 ^{13}C NMR (100 MHz, CDCl_3) of compound **251**.

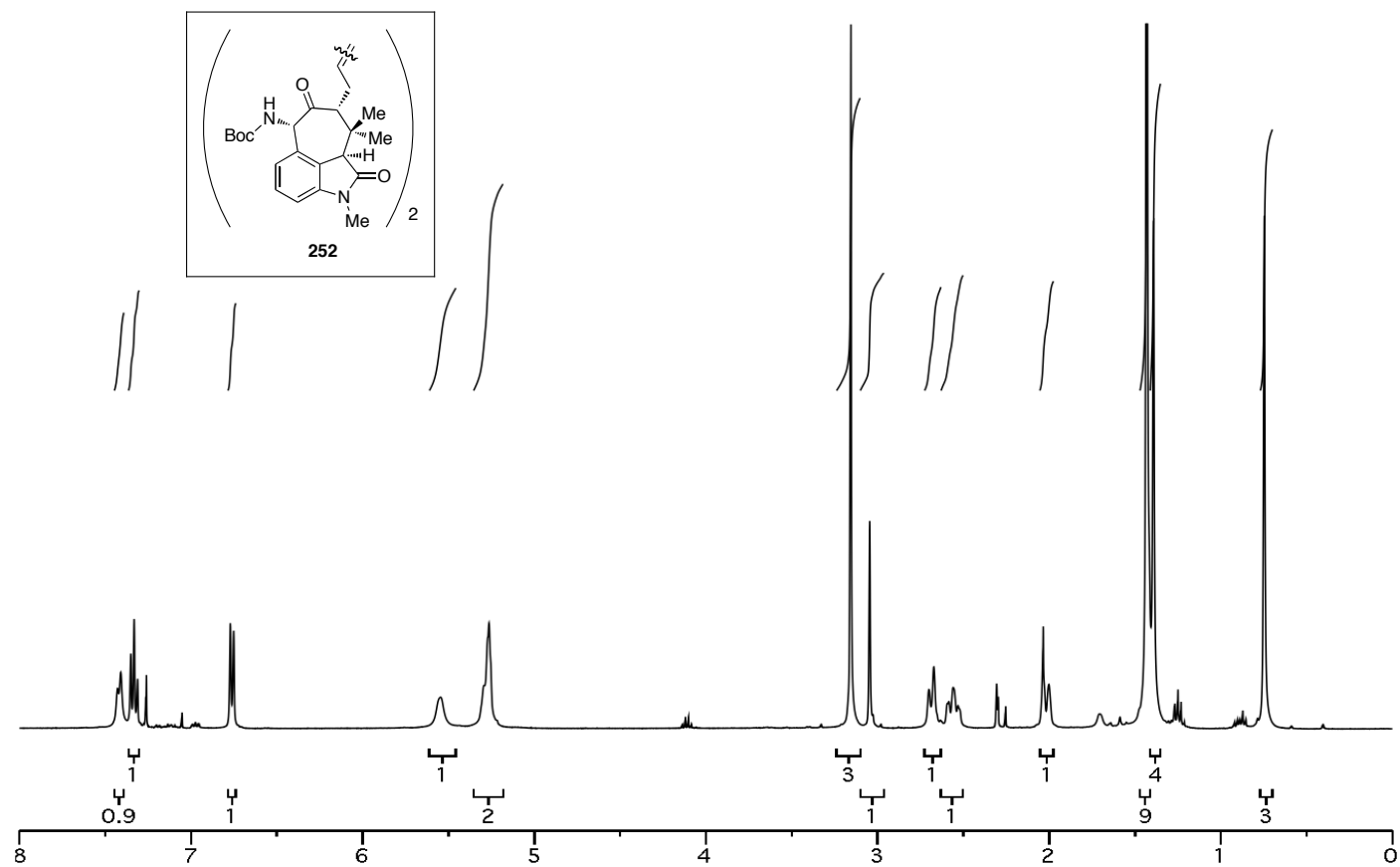


Figure A.1.59 ^1H NMR (400 MHz, CDCl_3) of compound **252**.

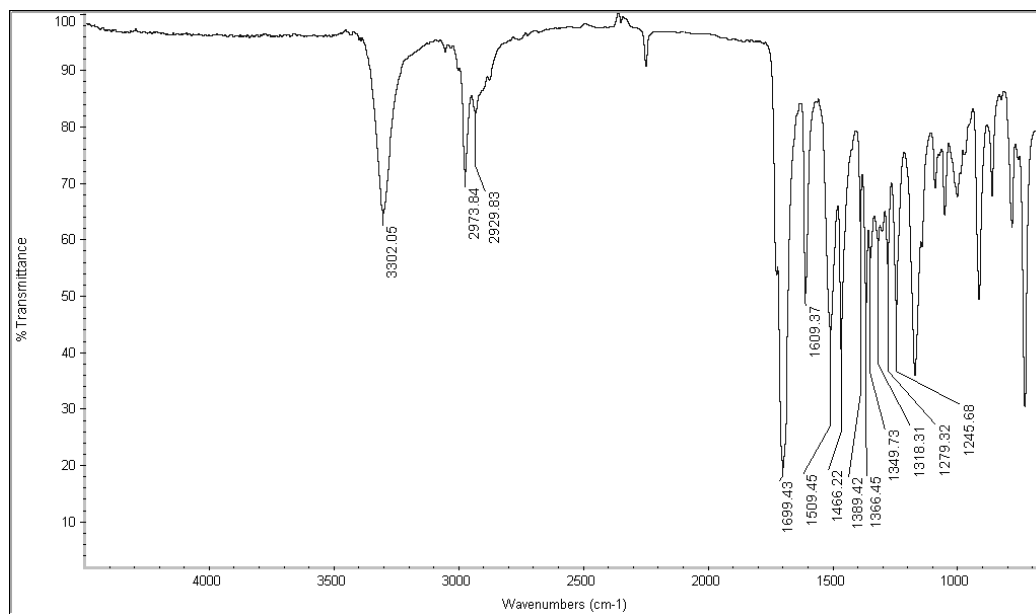


Figure A.1.60 Infrared Spectrum (thin film/NaCl) of compound **252**.

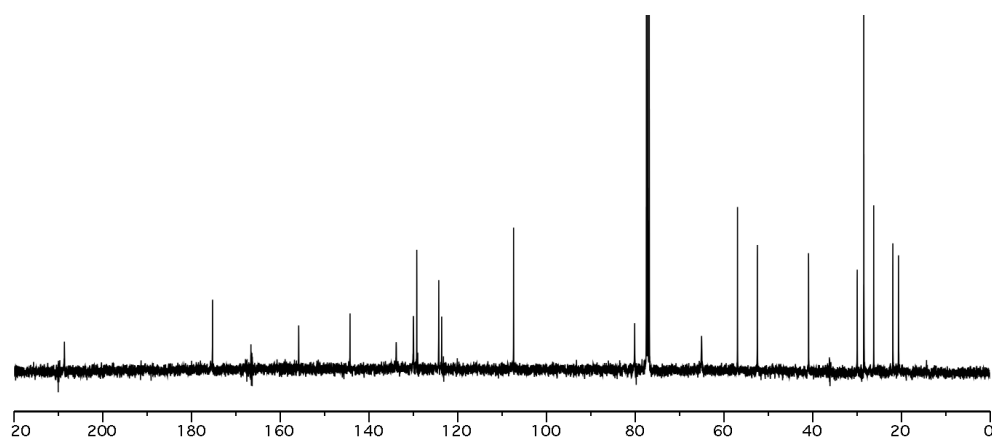


Figure A.1.61 ¹³C NMR (100 MHz, CDCl₃) of compound **252**.

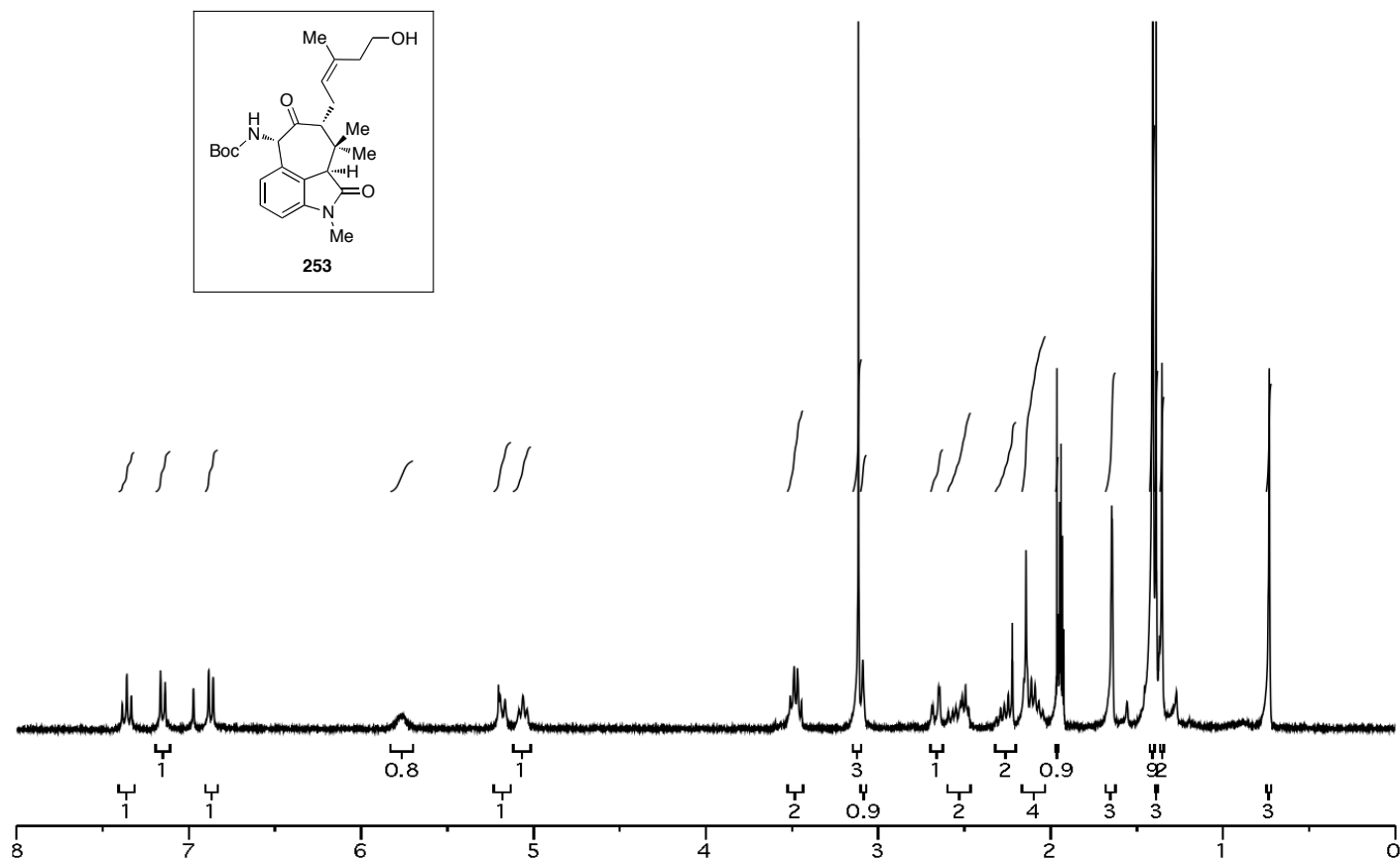


Figure A.1.62 ^1H NMR (300 MHz, CD_3CN) of compound **253**.

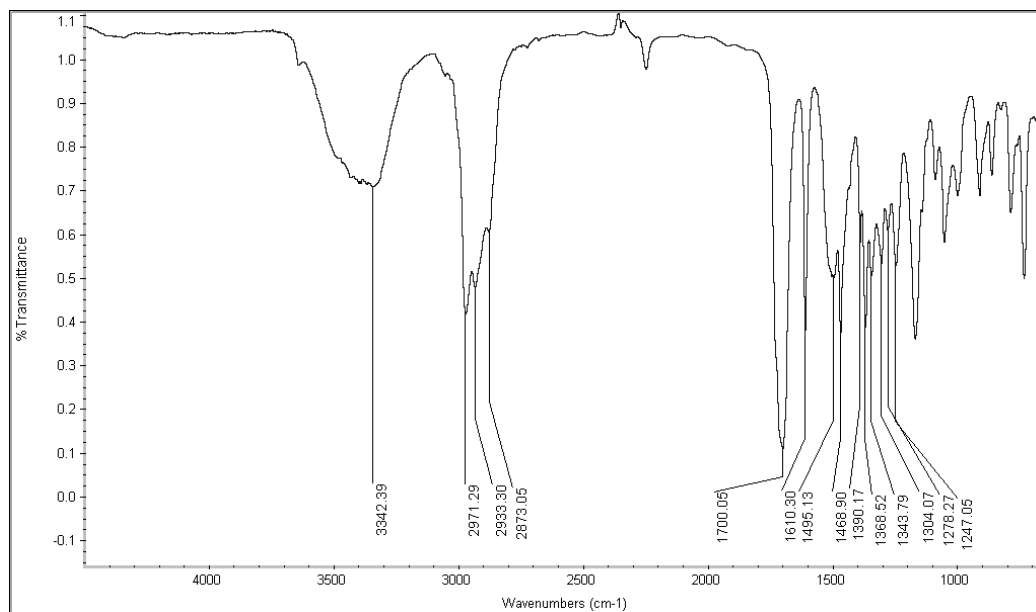


Figure A.1.63 Infrared Spectrum (thin film/NaCl) of compound **253**.

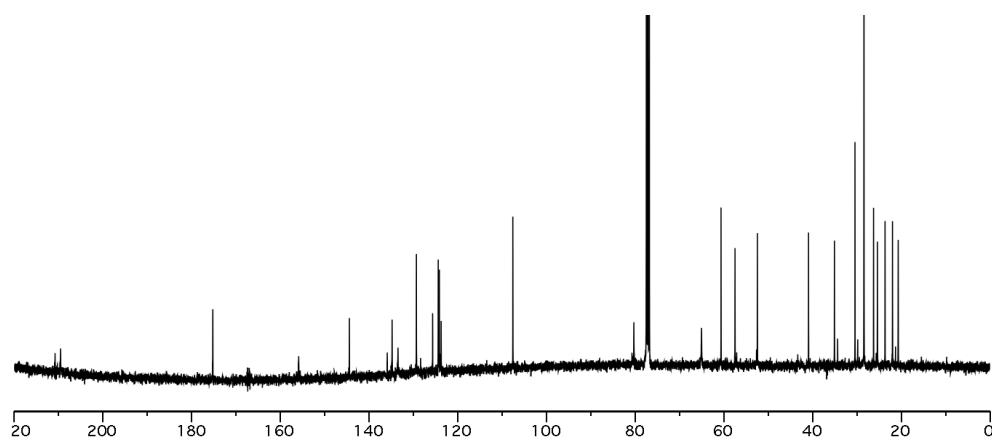


Figure A.1.64 ¹³C NMR (100 MHz, CDCl₃) of compound **253**.

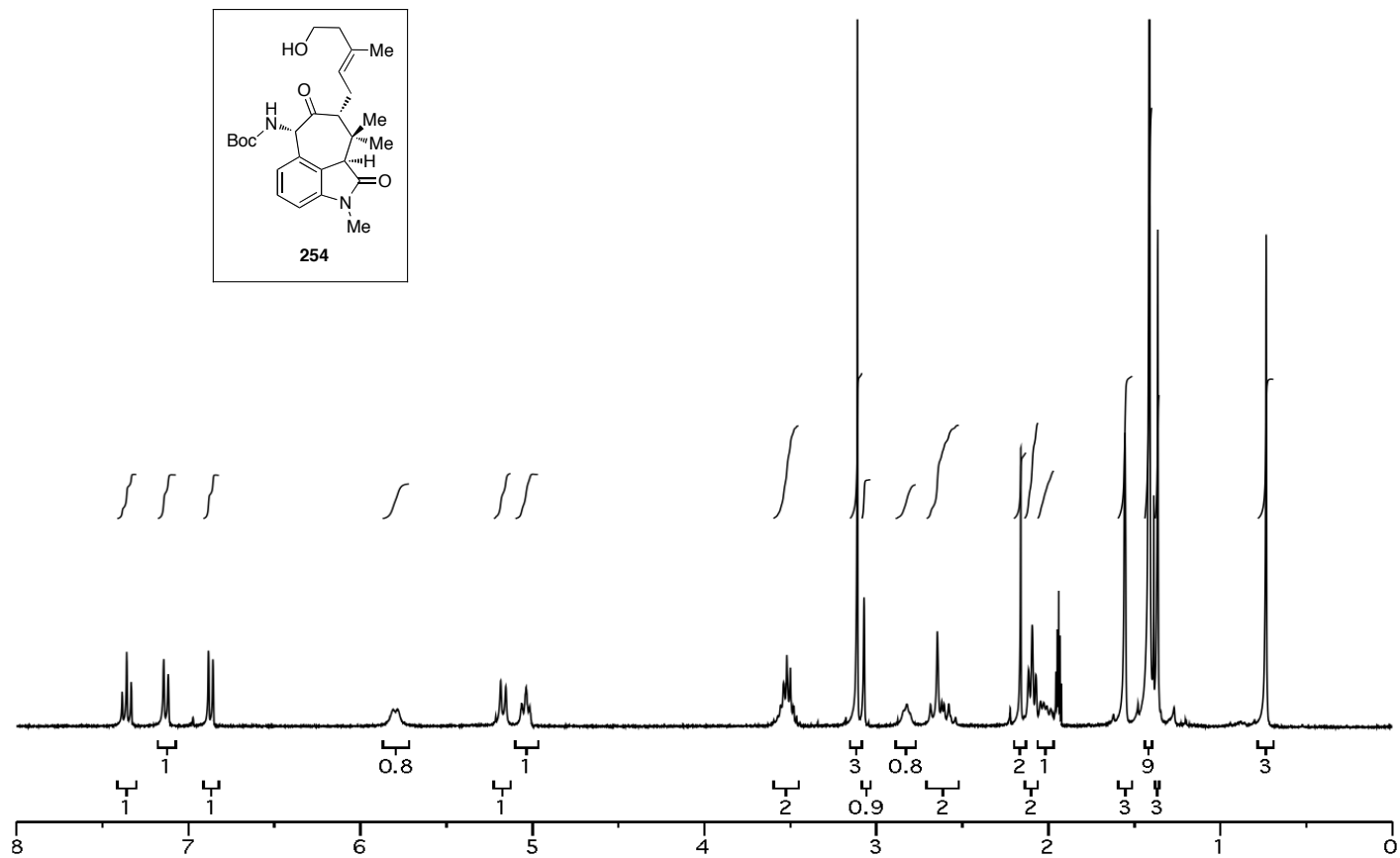


Figure A.1.65 ¹H NMR (300 MHz, CD₃CN) of compound **254**.

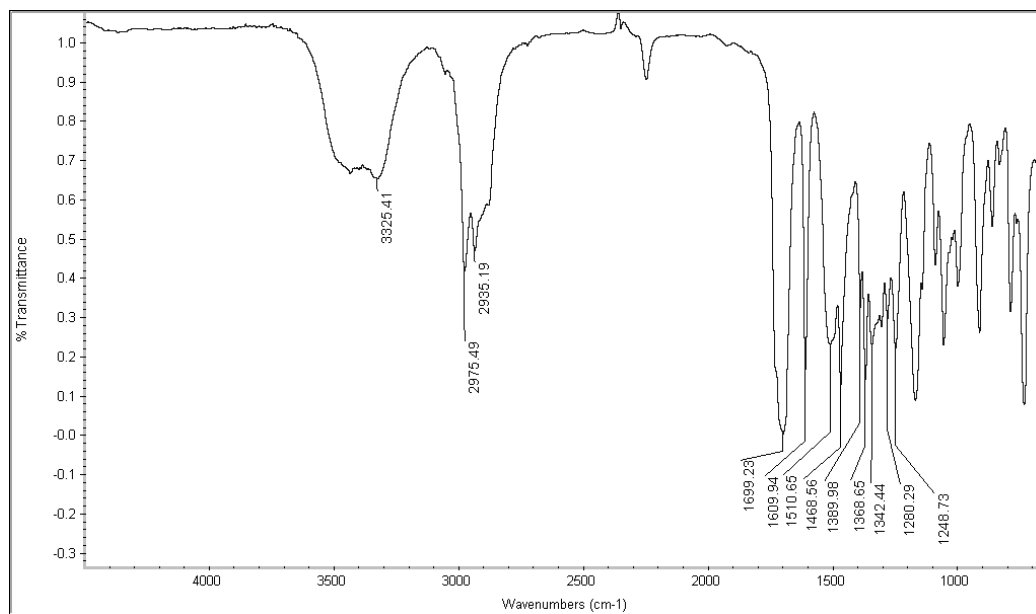


Figure A.1.66 Infrared Spectrum (thin film/NaCl) of compound **254**.

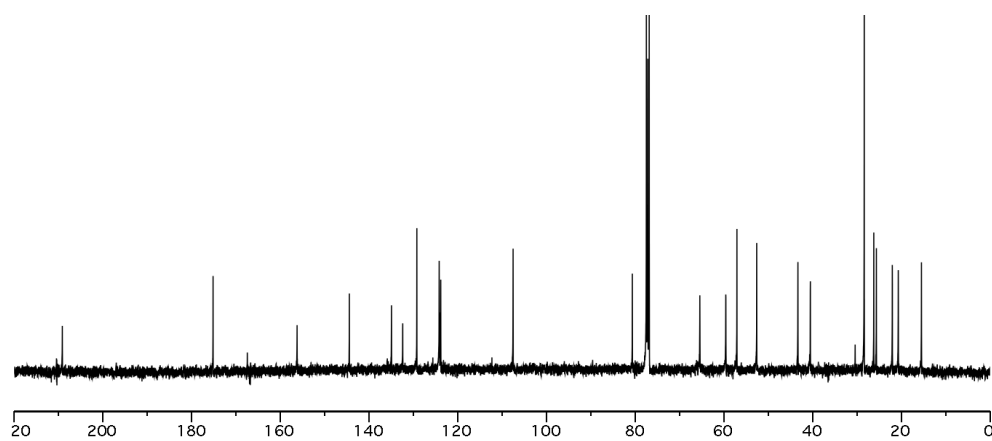


Figure A.1.67 ¹³C NMR (100 MHz, CDCl₃) of compound **254**.

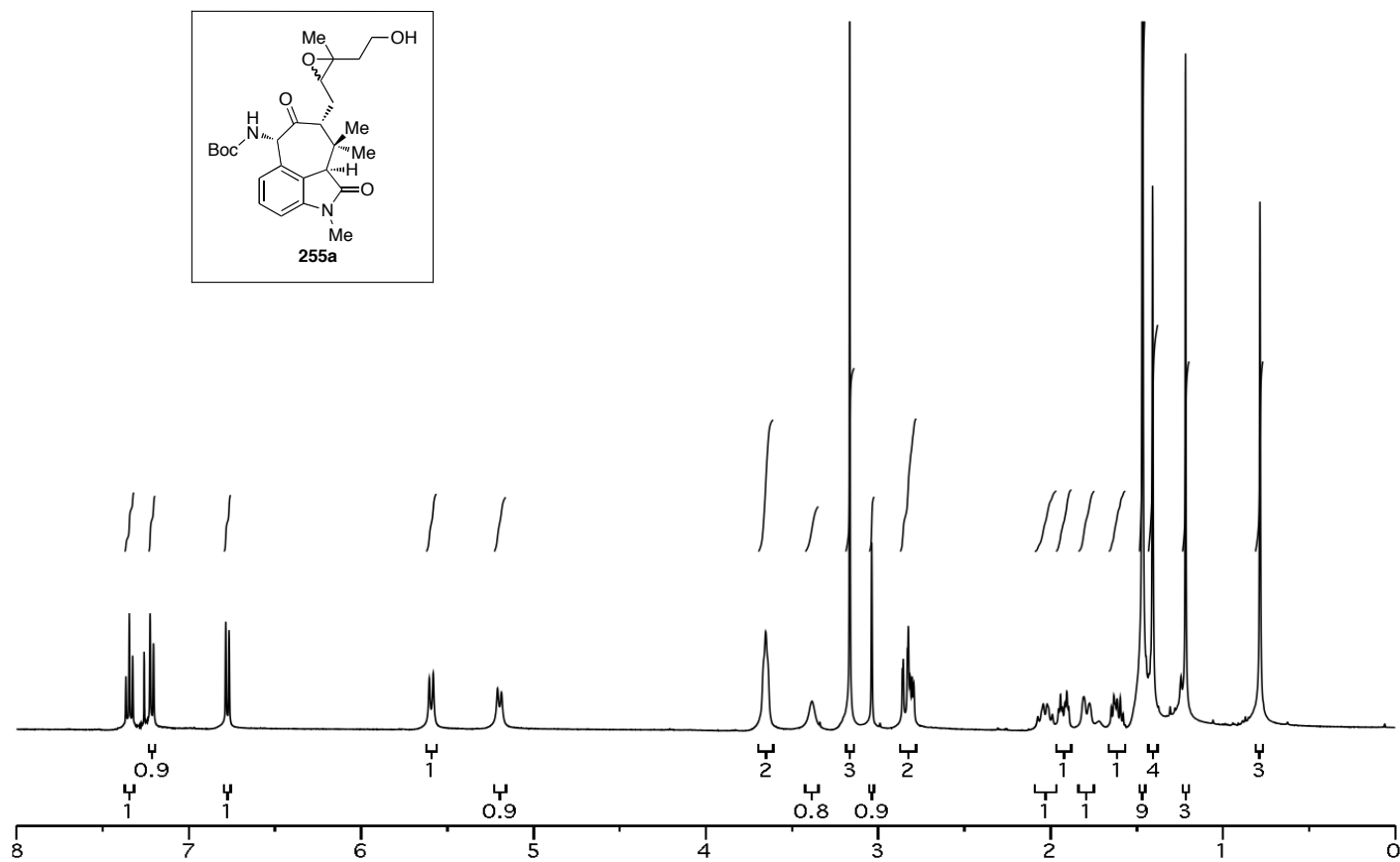


Figure A.1.68 ^1H NMR (400 MHz, CDCl_3) of compound **255a**.

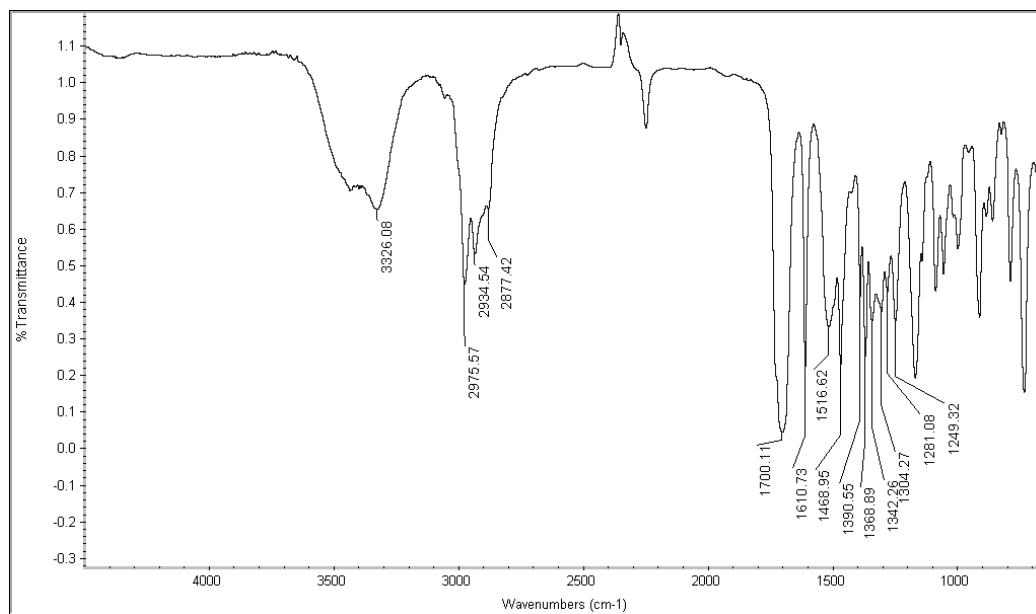


Figure A.1.69 Infrared Spectrum (thin film/NaCl) of compound **255a**.

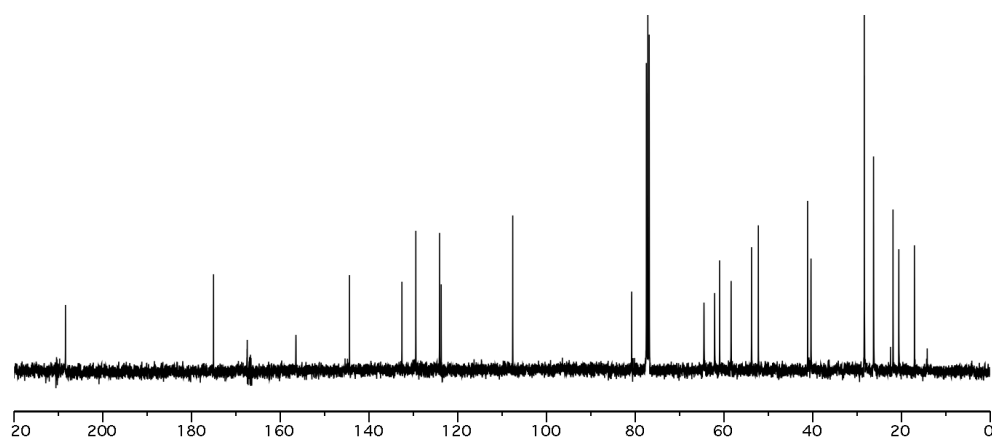


Figure A.1.70 ^{13}C NMR (100 MHz, CDCl_3) of compound **255a**.

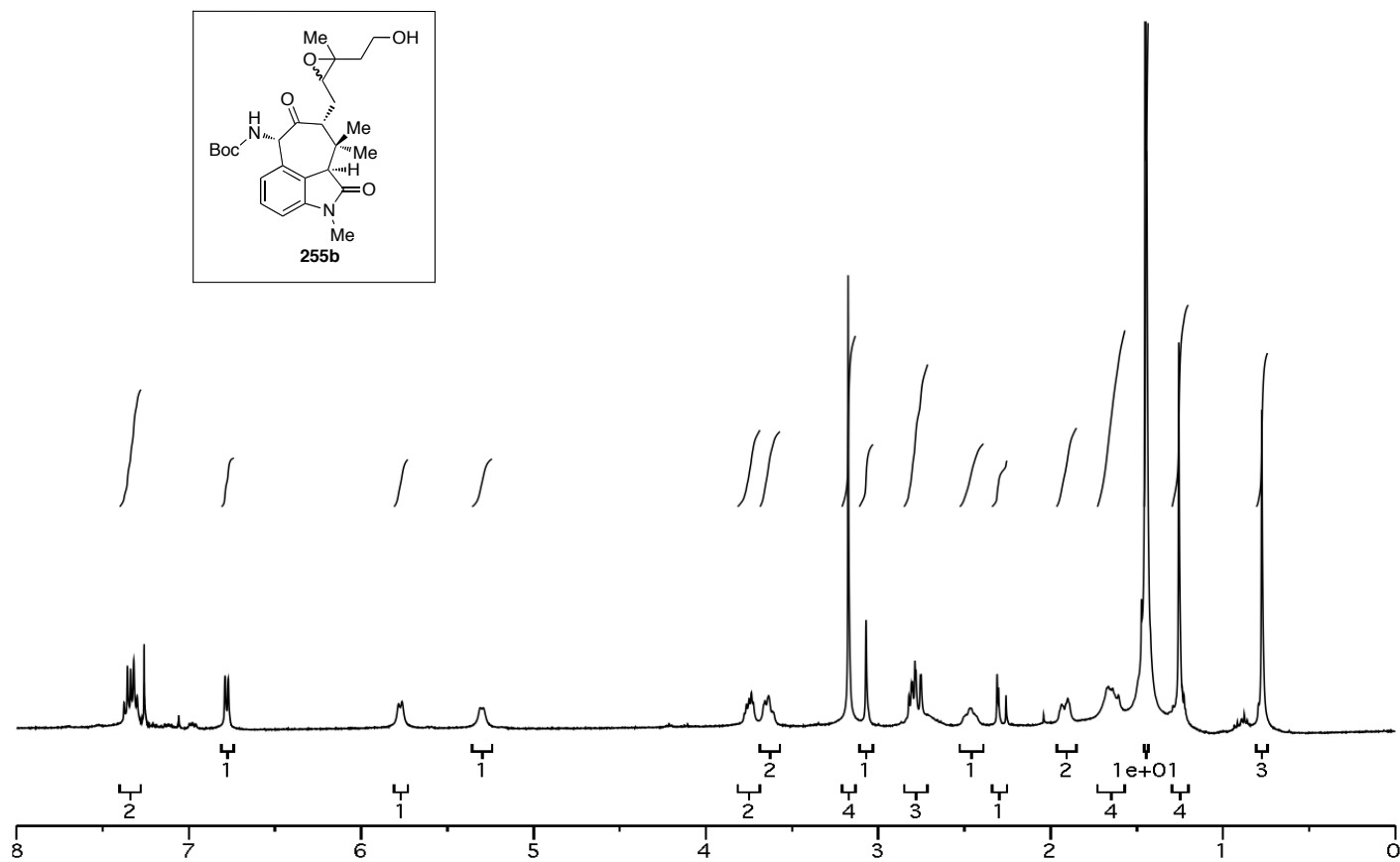


Figure A.1.71 ^1H NMR (400 MHz, CDCl_3) of compound **255b**.

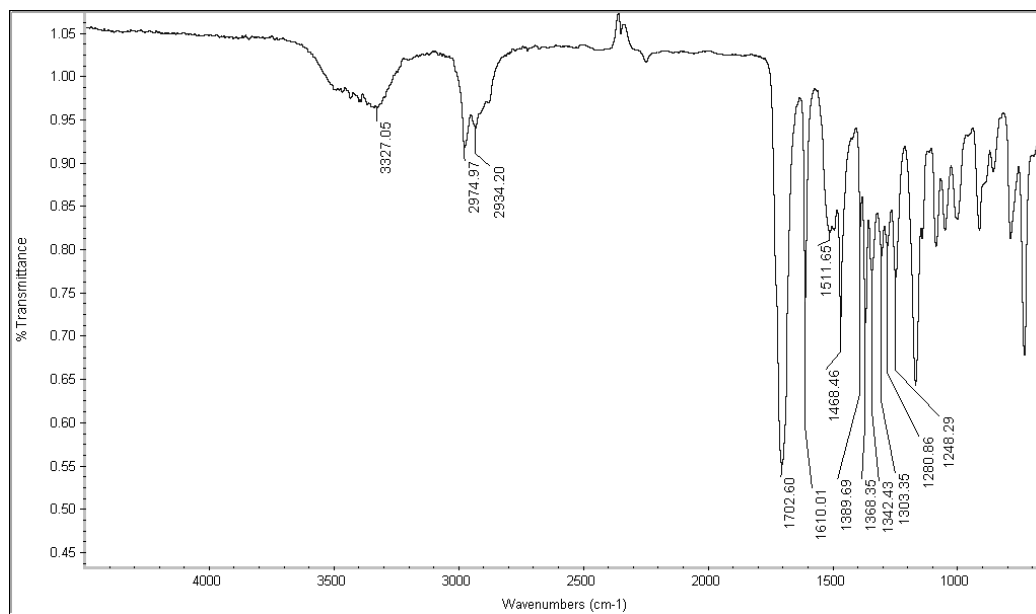


Figure A.1.72 Infrared Spectrum (thin film/NaCl) of compound **255b**.

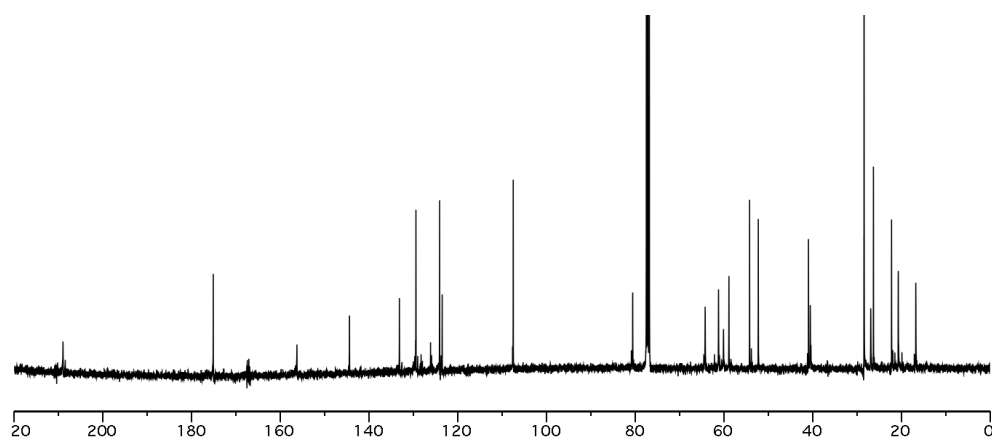


Figure A.1.73 ^{13}C NMR (100 MHz, CDCl_3) of compound **255b**.

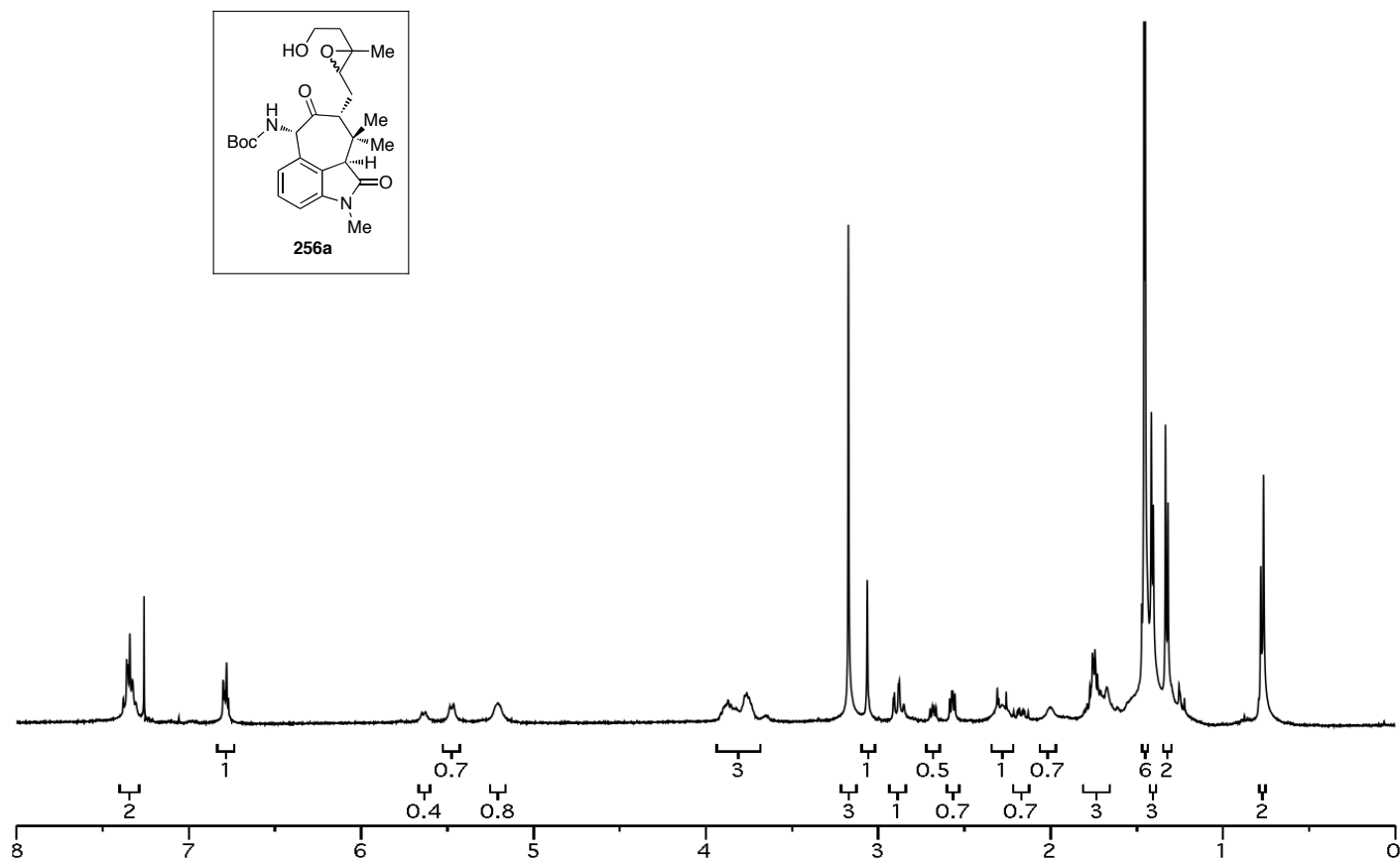


Figure A.1.74 ^1H NMR (400 MHz, CDCl_3) of compound 256a.

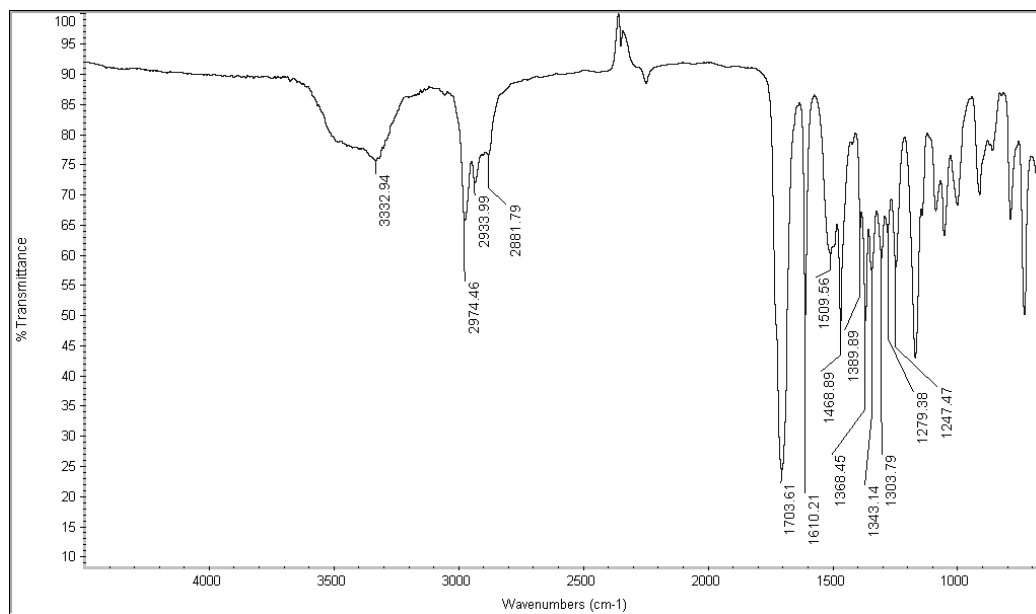


Figure A.1.75 Infrared Spectrum (thin film/NaCl) of compound **256a**.

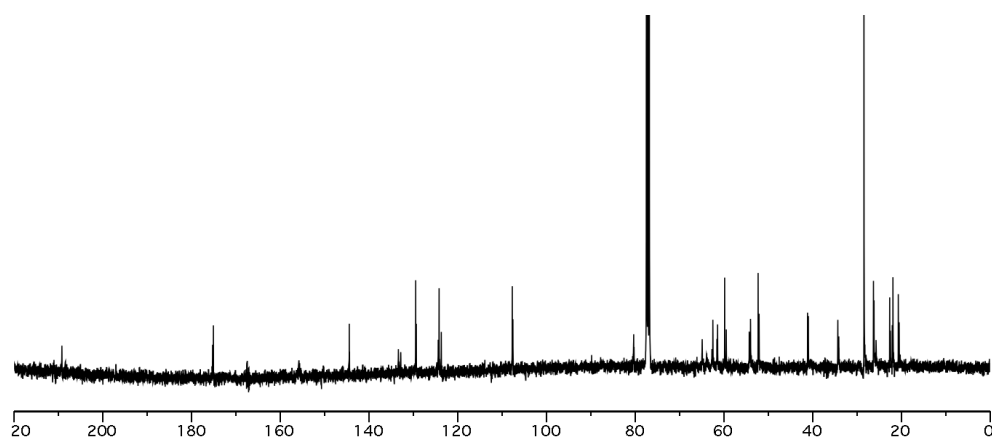


Figure A.1.76 ¹³C NMR (100 MHz, CDCl₃) of compound **256a**.

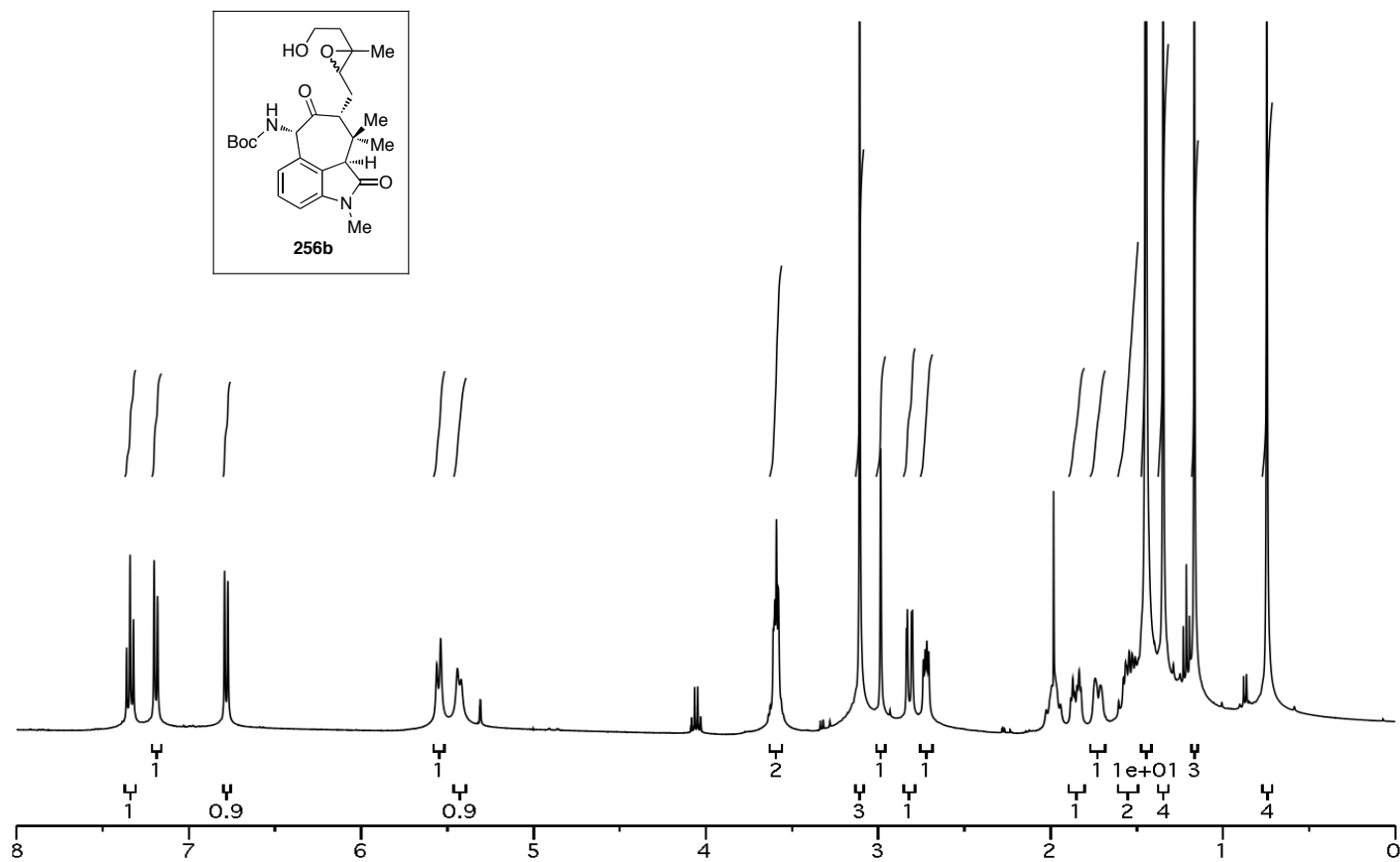


Figure A.1.77 ^1H NMR (400 MHz, CD_2Cl_2) of compound **256b**.

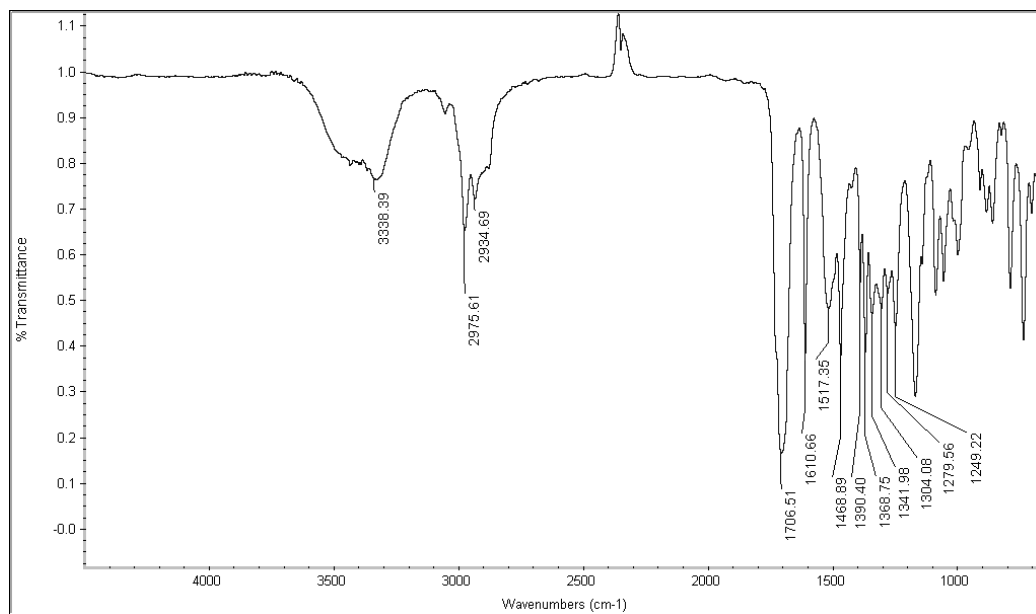


Figure A.1.78 Infrared Spectrum (thin film/NaCl) of compound **256b**.

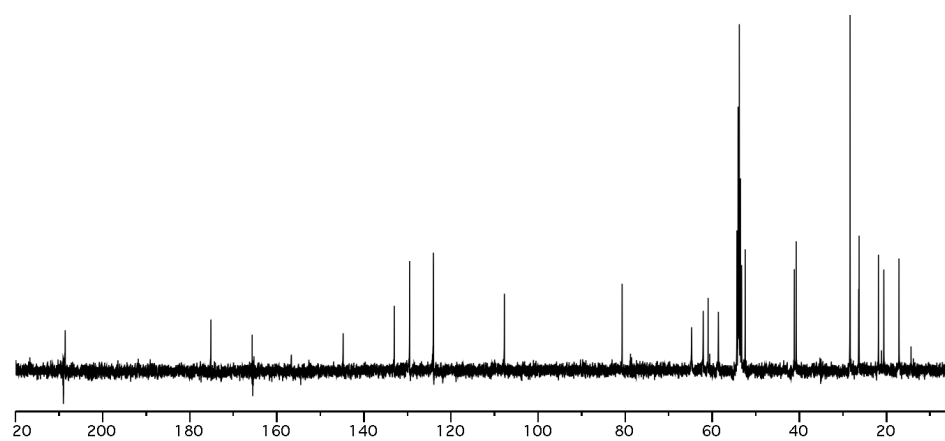


Figure A.1.79 ¹³C NMR (100 MHz, CD₂Cl₂) of compound **256b**.

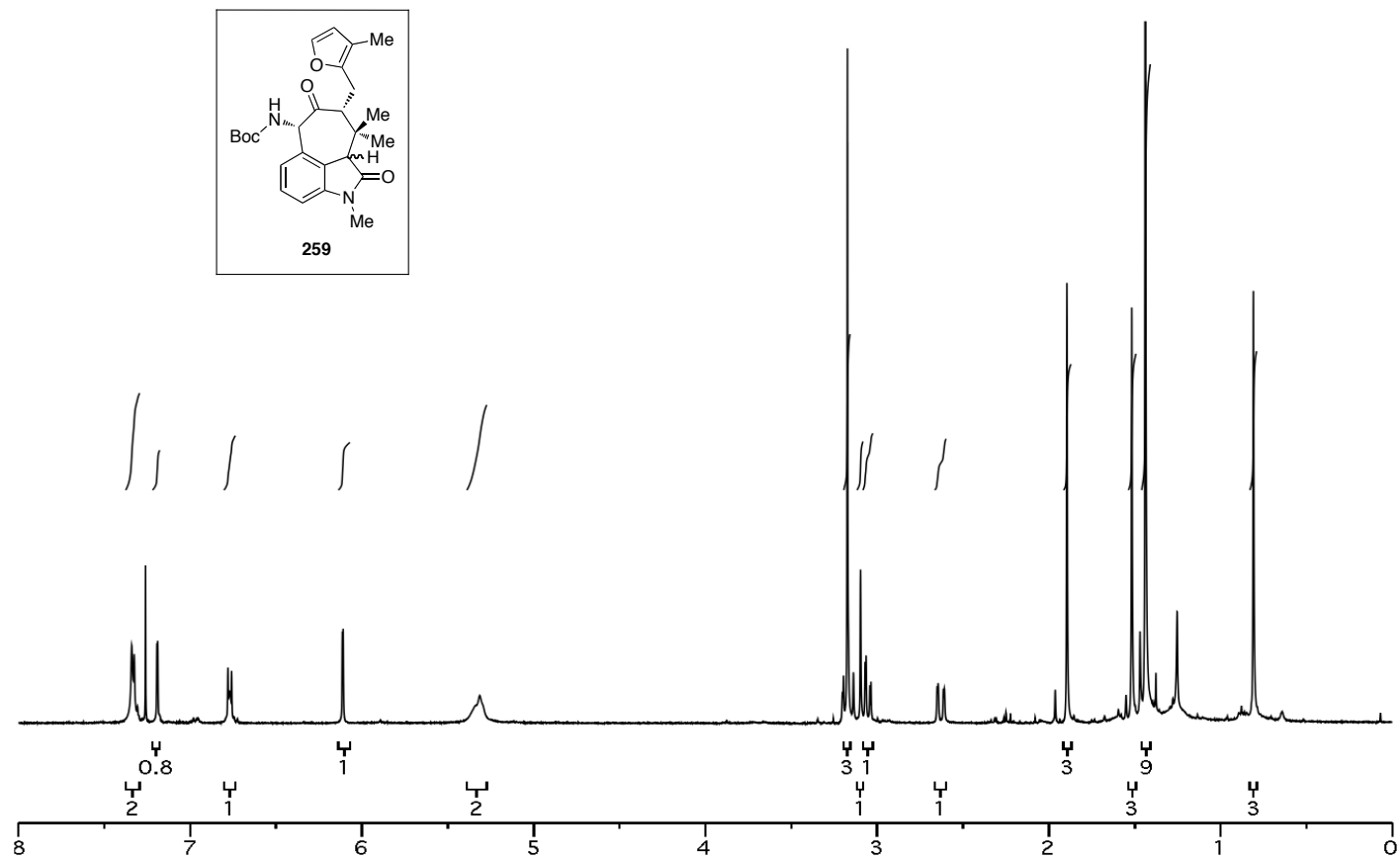


Figure A.1.80 ¹H NMR (400 MHz, CDCl₃) of compound **259**.

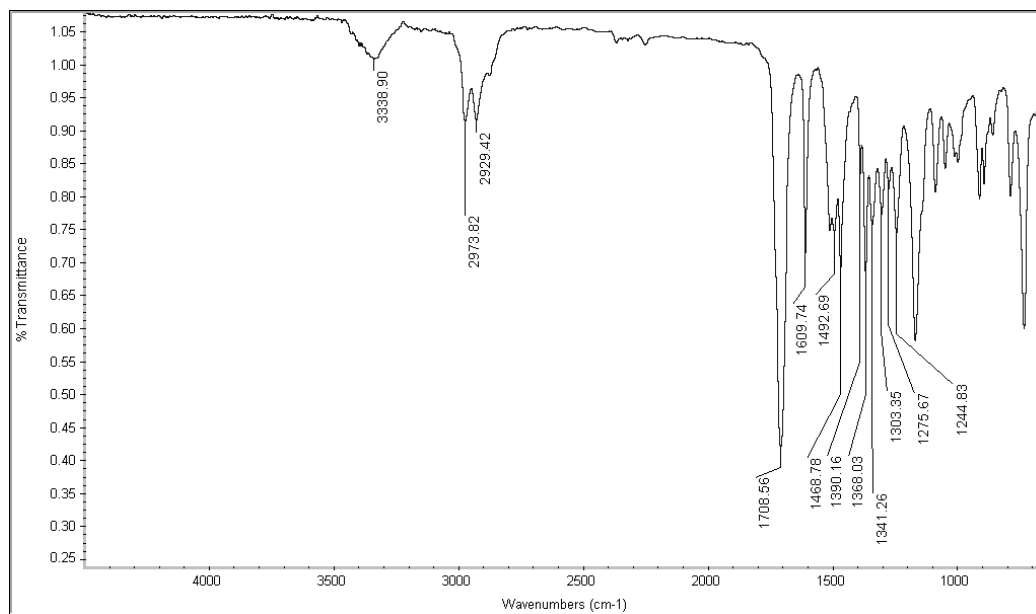


Figure A.1.81 Infrared Spectrum (thin film/NaCl) of compound **259**.

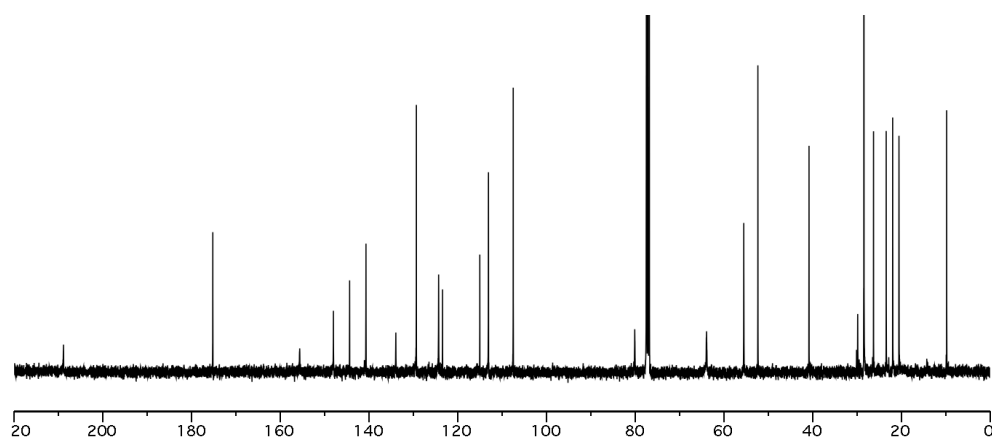


Figure A.1.82 ^{13}C NMR (100 MHz, CDCl_3) of compound **259**.

Chapter 3

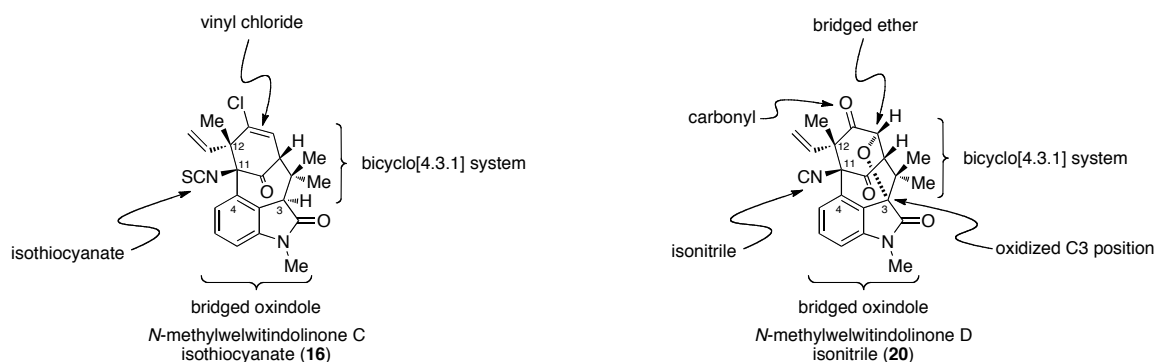
***N*-Methylwelwitindolinone D Isonitrile and the Advent of a Tandem O–H Insertion Conia-ene Cyclization**

3.1 Initial Considerations.

Although our attempts thus far were unsuccessful for the synthesis of *N*-methylwelwitindolinone C isothiocyanate (**16**), our resolve was unwavering. We were determined to devise a new approach to accessing **16** that drew from the lessons of our previous routes. To that end, we began by directing our attention to the entire welwitindolinone family as possible synthetic precursors. We believed that this approach would address the inherent similarities among the family, including the bicyclo[4.3.1] system, the bridged oxindole, and the C12 quaternary center, by presenting the same synthetic challenges in a new light.

After considering several welwitindolinone congeners, *N*-methylwelwitindolinone D isonitrile (**20**) presented itself as an exciting new synthetic target. Structurally, the core of **20** is the same as **16** containing a bicyclo[4.3.1] system and bridged oxindole (see Figure 3.1.1 for comparison). However, an oxidized C3 position that forms a bridged spiro-ether distinguishes **20** from the welwitindolinone family. We speculated that we could exploit this inherent difference for its construction through a convergent process. We envisioned that the coupling of a functionalized cyclohexane piece and an oxindole would forge the embedded tetrahydrofuran ring system that would then be used to direct the completion of **20**.

Figure 3.1.1

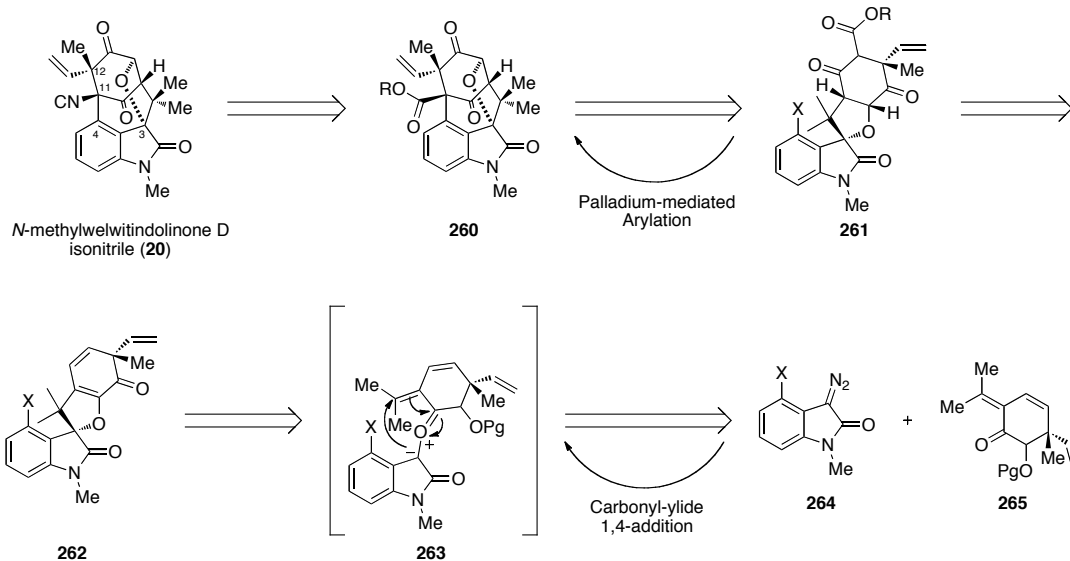


3.2 Carbonyl-ylide Approach.

3.2.1 Retrosynthetic Analysis.

As outlined in Scheme 3.2.1, our plan for completing *N*-methylwelwitindolinone D isonitrile (**20**) depends on the late stage installation of the isonitrile through a Curtius rearrangement of **260**.^{1,2} A key palladium-mediated intramolecular arylation reaction of β -keto ester **261** would forge the core of **20** represented by structure **260**.³ Access to β -keto ester **261** would be achieved through a four-step process involving hydroboration of the disubstituted olefin in **262**, oxidation of the resulting secondary hydroxyl group, acylation of the ketone, and a reduction of the enone (not shown). Spiro-dihydrofuran **262** would arise via metal catalyst carbonyl-ylide 1,4-addition (**263**)⁴ of diazoisatin **264** and enone **265**.

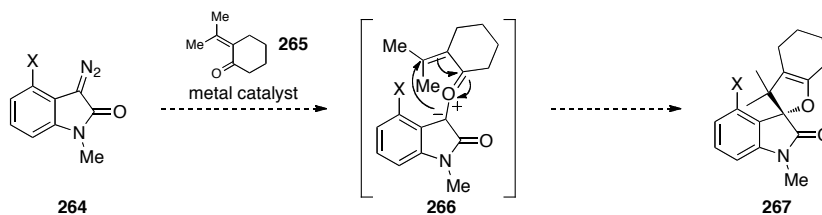
Scheme 3.2.1



3.2.2 Carbonyl-ylide Model System.

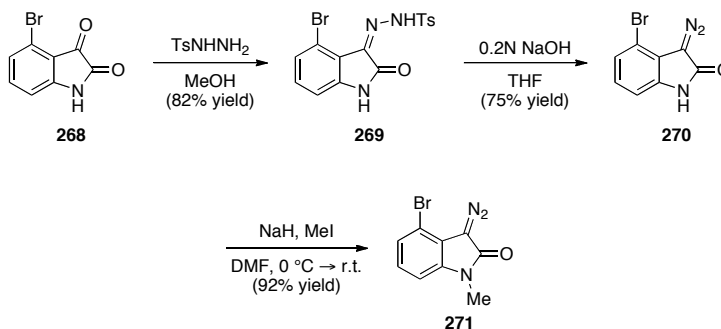
Before committing resources to our synthetic strategy, we wanted to investigate the viability of a metal-catalyzed carbonyl-ylide 1,4-addition. To that end, we proposed a model system that would incorporate diazoisatin (**264**) and a simplified enone coupling partner (**265**) (Scheme 3.2.2). We projected that when a metal catalyst, such as rhodium(II) acetate dimer, was added to a mixture of diazoisatin **264** and enone **265**, dediazotization of **264** would result in the formation of intermediate oxonium ylide **266** (catalyst omitted for clarity). Oxonium ylide **266** would then undergo a sequential 1,4-addition to construct spiro-oxindole **267**.

Scheme 3.2.2



We began our model system with the construction of a diazoisatin piece similar to diazoisatin **268** (Scheme 3.2.3).^{5,6} Starting from commercially available 4-bromoisatin (**268**), a three-step procedure involving condensation of tosylhydrazide (**268** → **269**), base induced diazo-formation (**269** → **270**), and methylation (**270** → **271**) generated our desired diazoisatin **271** with a single purification in excellent overall yield.

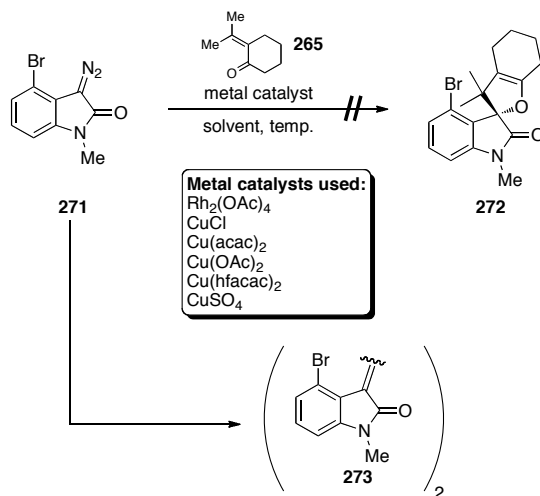
Scheme 3.2.3



With diazoketone **271** in hand, we attempted to implement a metal-catalyzed carbonyl-ylide 1,4-addition reaction (Scheme 3.2.4). Unfortunately, when diazoketone **271** was exposed to enone **265** in the presence of a variety of catalysts, desired spiroindole **272** was not produced. Instead, we exclusively observe dimer product **273** that

rapidly decomposes to hydrolyzed side products upon attempted isolation. We hypothesize that under the reaction conditions, oxonium-ylide formation (see Section 3.2.3) was reversible and when dissociated, the carbenoid species dimerizes.

Scheme 3.2.4

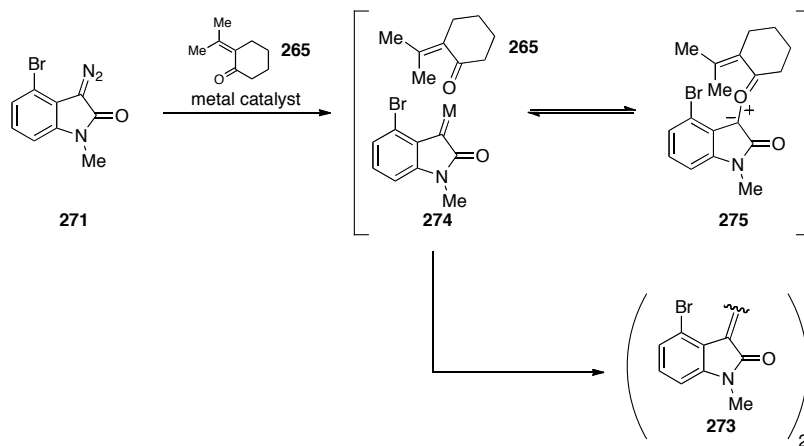


3.2.3 A Redesigned Coupling Partner Leads to New Reaction Sequence.

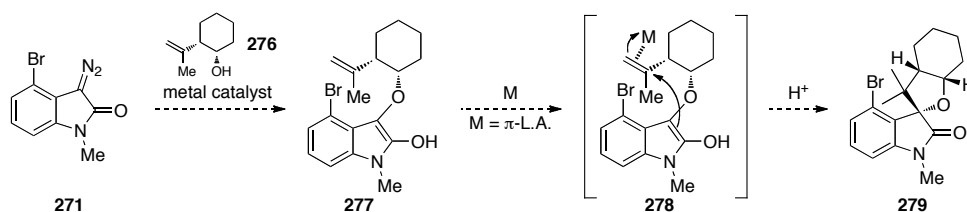
As illustrated in Scheme 3.2.5, we speculated that our carbonyl-ylide model system failed due to the equilibrium between metal-carbenoid **274** and oxonium-ylide **275**. Presumably, dimerization of **274** was faster than the projected intramolecular 1,4-addition of oxonium-ylide **275**, which was supported by the reaction outcome. To avoid dimerization, we decided to change our model system to incorporate an initial O–H insertion where reversibility would be slower than the oxonium-ylide case (Scheme 3.2.6). To that end, we designed a two-step sequence that would begin with a metal-catalyzed O–H insertion of homo-allylic alcohol **276** with diazoisatin **271** to form enol

ether **277**. Treatment of **277** with a π -Lewis acid would initiate a cyclization to form a metalated spiro-oxindole (not shown) that upon protonolysis would deliver spiro-oxindole **279**, a compound equivalent to spiro-oxindole **267**.

Scheme 3.2.5



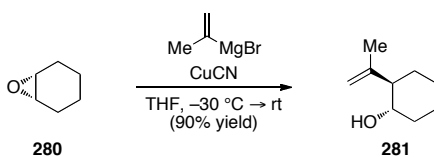
Scheme 3.2.6



Implementation of our new model system started with the creation of a homo-allylic alcohol (Scheme 3.2.7). Simple exposure of iso-propenylmagnesium bromide to cyclohexene oxide (**280**) in the presence of CuCN provided trans-related homo allylic alcohol **281** in excellent yield.⁷ At this point, rather than conducting a Mitsunobu reaction to reverse the alcohol stereochemistry, we decided to conduct the O–H insertion (Scheme 3.2.8). Surprisingly, predicted O–H insertion product **282** was not observed, but rather

spiro-oxindole **283** was exclusively isolated, albeit in moderate yield. To confirm our finding, we obtained an X-ray crystal of **283** as shown in Figure 3.2.1. Further examination of this reaction revealed it to be an O–H insertion sequential Conia-ene cyclization, an extension the O–H insertion tandem 3,3- and 2,3-rearrangement chemistry developed in our lab.⁸⁻¹⁰

Scheme 3.2.7



Scheme 3.2.8

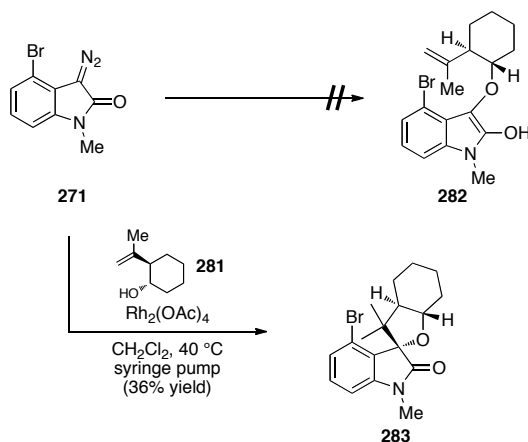
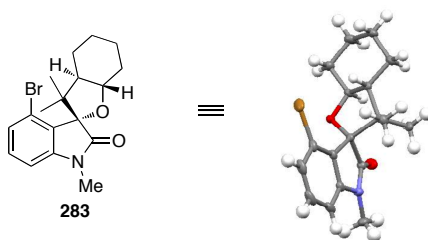


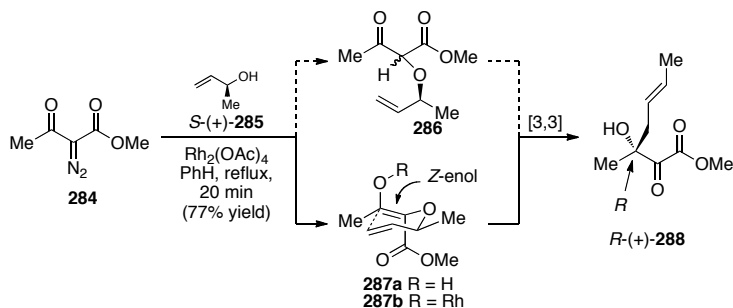
Figure 3.2.1



3.3 O–H Insertion and Conia-ene Cyclization Background.

3.3.1 O–H Insertion Claisen Rearrangement.

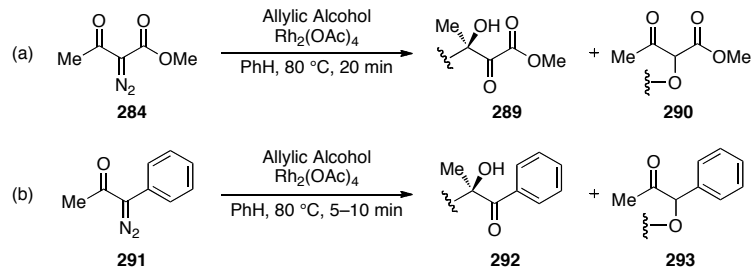
Scheme 3.3.1

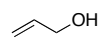
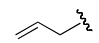
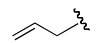
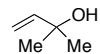
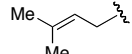
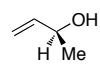
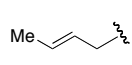
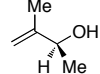
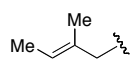
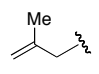
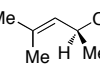
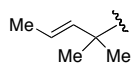
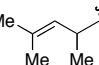
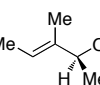
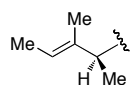
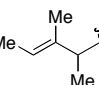
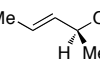
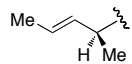


First published in 1999 by our laboratory, the rhodium catalyzed O–H insertion/Claisen rearrangement was developed to provide a method for the assembly of β -hydroxy esters (for example compound **288**, Scheme 3.3.1).⁸ We initially planned to execute this sequence in a two-step process wherein the O–H insertion product α -allyloxy- β -ketoester **286** would be isolated and subjected to a subsequent thermal

rearrangement to provide desired α -hydroxy ketone **288**. However, we discovered that under the reaction conditions, **284** proceeded directly to **288** in a highly stereoselective manner. We proposed and confirmed experimentally that this process proceeds through an O–H insertion event that delivers reactive enol **287** and not the anticipated α -allyloxy- β -ketoester **286**. These efforts revealed for the first time that rhodium-mediated O–H insertion reactions of α -diazoketones proceed via initial proton transfer to oxygen. As illustrated in Scheme 3.3.2 the scope of the reaction with acyclic α -diazoketones and both chiral and achiral allylic alcohols is broad. Additional mechanistic investigations revealed that the rate of Claisen rearrangement was unaffected by Rh(II).⁹ Kinetic studies were performed over a range of 5–90% conversion, and first-order kinetics were observed.

Scheme 3.3.2

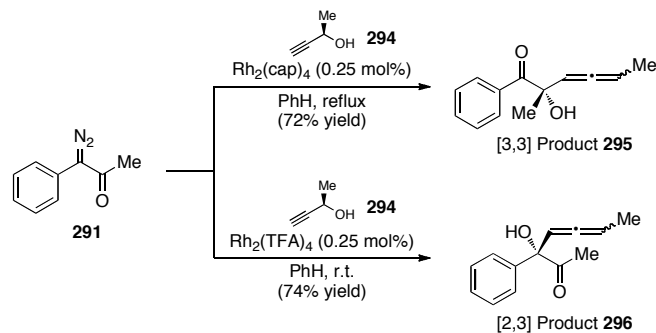


Entry	Allylic Alcohol	[ee]	[3,3] Product (yield) [ee]	Insertion Product (yield)
1a 1b			 (45) (77)	 (34) (0)
2a 2b			 (71) (72)	---
3a 3b		[98] [98]	 (77) [95] (77) [94]	---
4a 4b		[82] [82]	 (70) [77] (76) [79]	 (8) (0)
5a 5b		[75] [75]	 (68) [54] (70) [45]	 (12) (0)
6a 6b		[92] [92]	 (63) [90] (67) [91]	 (12) (0)
7a 7b		[98] [98]	 (73) [98] (80) [97]	---

Although catalyst does not affect the [3,3] rearrangement of the intermediate α -allyloxy enols, we discovered that the Rh(II) catalyst does influence the related rearrangement of propargylic alcohols.¹⁰ Incorporating a propargylic alcohol into the O–H insertion sequence gives α -hydroxy allenes **295** and **296** (Scheme 3.3.3) via the transient propargyloxy enols (not shown). This process not only provides the opportunity to access the expected [3,3] product (**295**) but also a [2,3] product (**296**). Importantly, the distribution of [3,3] and [2,3] products can be controlled by catalyst identity. As illustrated in Scheme 3.3.3, propargyloxy enols undergo a [3,3] rearrangement to the

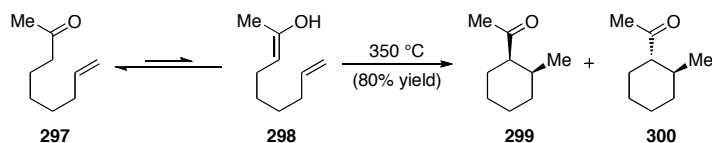
corresponding allene when exposed to $\text{Rh}_2(\text{cap})_4$ and a [2,3] rearrangement when exposed to $\text{Rh}_2(\text{TFA})_4$. Control experiments indicate that the [2,3]-pathway is mediated by Rh(II).

Scheme 3.3.3



3.3.2 Conia-ene Cyclization.

Scheme 3.3.4

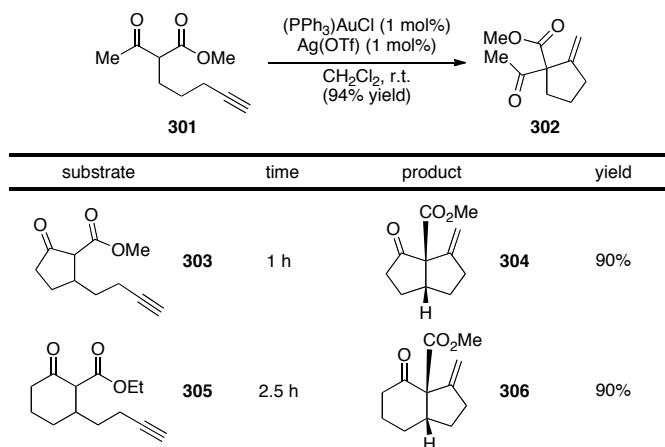


Having explored the mechanism and scope of the O–H insertion/Claisen rearrangement, we aim to explore the related O–H insertion/Conia-ene cyclization. Conia reviewed the thermal cyclizations of unsaturated carbonyl compounds in 1975.¹¹ He highlighted a variant to the “classic” ene reaction, reviewed by Hoffman in the late 60’s.¹² In a six-electron process known as the Conia-ene cyclization, thermolysis initiates a stereospecific, enol 1,5-hydrogen shift with a pendant olefin to forge new ring systems (Scheme 3.3.4).¹³ The review by Conia addresses the limitation of the Conia-ene to

simple substrates imposed by the necessity for high reaction temperatures. Over the past ten years, there have been significant advances improving reaction conditions for the Conia-ene cyclization. In particular transition metal catalysts have provided decreased reaction temperatures; however, many require prior enolate generation,¹⁴ strong acid,¹⁵ or photochemical activation.¹⁶

3.3.3 Recent Advances in the Conia-ene Cyclization.

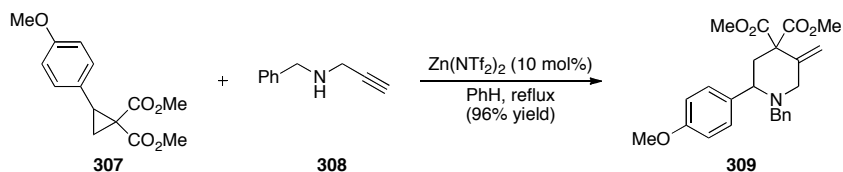
Scheme 3.3.5



More recently, Conia-ene cyclizations have been accomplished under truly mild conditions. In 2004 Toste reported a gold(I)-catalyzed Conia-ene reaction of β -ketoesters with alkynes at room temperature with low catalyst loading.¹⁷ As illustrated in Scheme 3.3.5, treatment of methyl acetoacetate **301** with 1.0 mol% of $(\text{PPh}_3)\text{AuCl}$ and 1.0 mol% of $\text{Ag}(\text{OTf})$ in dichloromethane at room temperature gives cycloadduct **302**. Toste's study of substrate scope revealed that acyclic and cyclic substrates both proceed with high diastereoselectivity. In addition Toste further expanded the utility of the Conia-

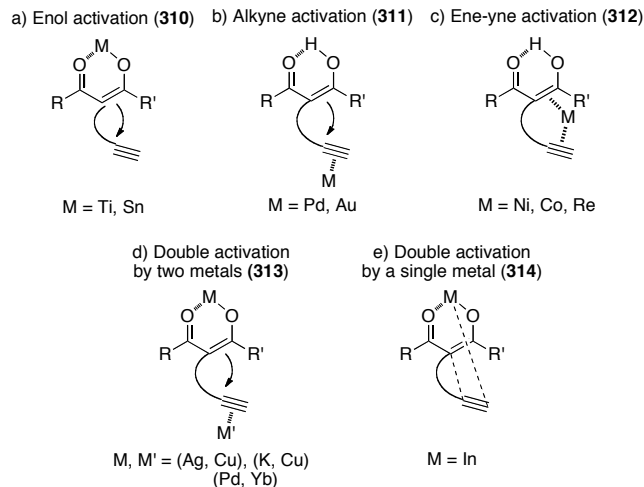
ene cyclization in an enantioselective modification that used chiral phosphine ligands in a palladium/ytterbium triflate catalyst system (not shown).¹⁸

Scheme 3.3.6



Although powerful, the utility of Toste's method has yet to be demonstrated beyond the formation of carbocycles. Given the prevalence of heterocycles in pharmaceuticals, this is an obvious and potentially important extension that warrants further investigation and could provide a concise method for heterocycle construction. Recent work by Kerr, wherein a Conia-ene cyclization has been used to form piperidines, exemplifies efforts in this direction.¹⁹ In this multi-step, one-pot procedure Zn(NTf₂)₂ catalyzes the tandem nucleophilic cyclopropane ring-opening/Conia-ene cyclization process to provide functionalized piperidines (Scheme 3.3.6).

Figure 3.3.1



Others have contributed to this field by exploring other transition metals such as Zn,²⁰ Cu,^{14c} Ni,²¹ In,²² and Re²³ and through mechanistic elucidation. Nakamura and coworkers presented a brief outline of the five suggested mechanistic pathways through which metal-mediated Conia-ene cyclizations proceed (Figure 3.3.1): a) enol activation, b) alkyne activation, c) ene-yne activation, d) double activation by two metals, and e) double activation by a single metal.^{22a} Nakamura also categorizes metals by the mechanistic pathway to which they correspond. In the metal catalyzed Conia-ene cyclization, alkynes predominate as the ene component in most literature examples. This preferential use of alkynes is attributed to the ease with which they are activated by metals.

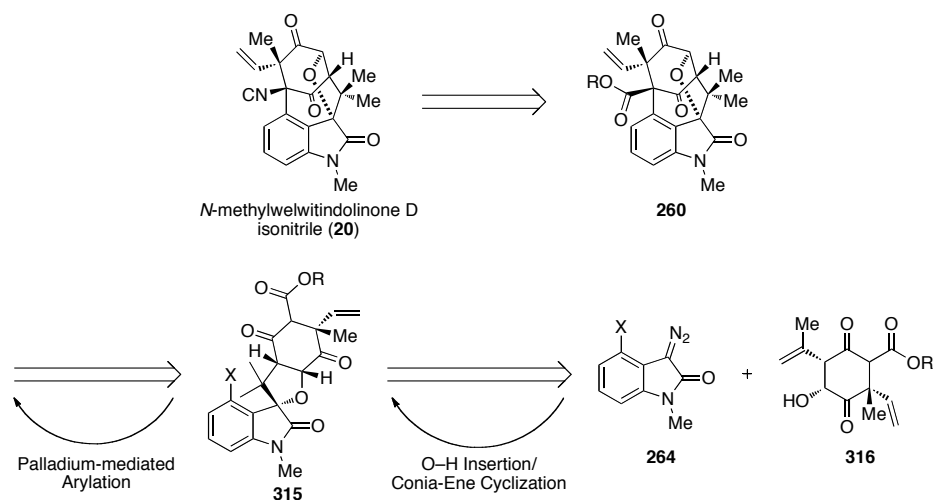
3.4 *N*-Methylwelwitindolinone D isonitrile and a Tandem O–H Insertion Conia-ene Cyclization.

3.4.1 Retrosynthetic Analysis.

In the course of exploring alternate strategies towards the synthesis of the welwitindolinone alkaloids, we discovered a new reaction sequence that could easily access the spiro tetrahydrofuran embedded within *N*-methylwelwitindolinone D isonitrile (**20**). This observation prompted the creation of a retrosynthetic analysis that highlights the utility of a tandem O–H insertion Conia-ene cyclization.

Aligned with our retrosynthetic strategy outlined in Scheme 3.4.1, our new strategy would rely on a late stage Curtius rearrangement of ester **260** to install the bridgehead nitrogen required for completion of **20**. Formation of the welwitindolinone core would arise through an intramolecular palladium-mediated arylation of the β -keto ester embedded within spiro-tetrahydrofuran **315**. Spiro-tetrahydrofuran **315** would be constructed through an O–H insertion Conia-ene cyclization of diazoisatin **264** and functionalized homo-allylic alcohol **316**.

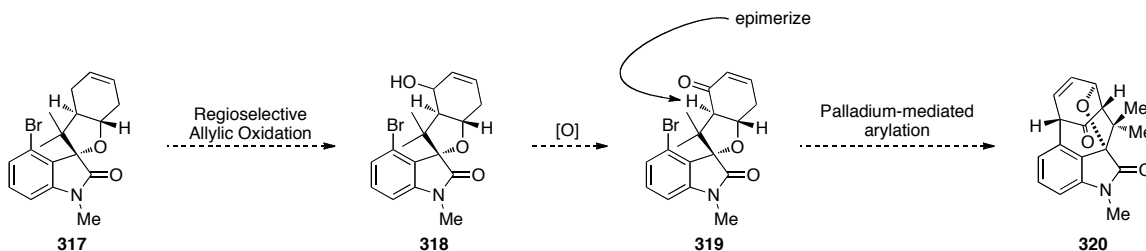
Scheme 3.4.1



3.4.2 Model System.

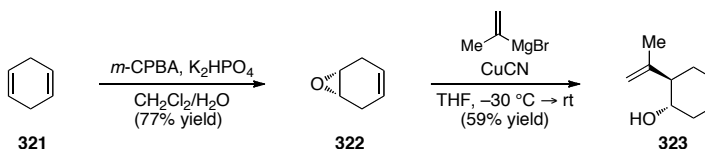
Before committing resources to our planned synthetic route (see section 3.4.1, Scheme 3.4.1), we wanted to test the viability of construction the welwitindolinone D core. To that end, we devised a model system that would exploit the O–H insertion tandem Conia-ene cyclization of a simple homo-allylic alcohol to arrive at spiro-oxindole **320** (Scheme 3.4.2). A projected regioselective allylic oxidation²⁴ of **320** would create allylic alcohol **318** and subsequent oxidation would provide enone **319**, a substrate poised for an intramolecular arylation. Exposure of enone **319** to Heck-type conditions would initiate an in situ epimerization of the indicated proton forcing the enone to come into close proximity of the aryl bromide facilitating closure to core **320**.

Scheme 3.4.2



In order to implement our strategy, we had to first direct our attention to the creation of spiro-tetrahydrofuran **317**. As depicted in Scheme 3.4.3, we began with the creation of a more functionalized homo-allylic alcohol (see Scheme 3.2.7 for comparison of homo-allylic alcohols). A mono-epoxidation of 1,4-cyclohexadiene (**321**) with *m*-CPBA in a buffered solution created epoxide **322**.²⁵ Opening of epoxide **322** with a copper catalyzed iso-propenylmagnesium bromide addition then delivered our requisite homo-allylic alcohol **323**.⁷

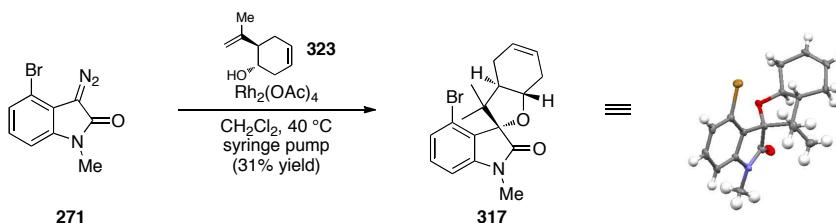
Scheme 3.4.3



Establishment of an efficient means to our desired homo-allylic alcohol **323** provided us with the opportunity to advance our model system. Fortunately, our key O–H insertion Conia-ene cyclization of diazoisatin **271** with homo-allylic alcohol **323** successfully forged spiro-tetrahydrofuran **317** (Scheme 3.4.4). An X-ray crystal structure

of **317** was obtained and confirmed the consistent relative stereochemical outcome as compared to **283** (Scheme 3.2.9).

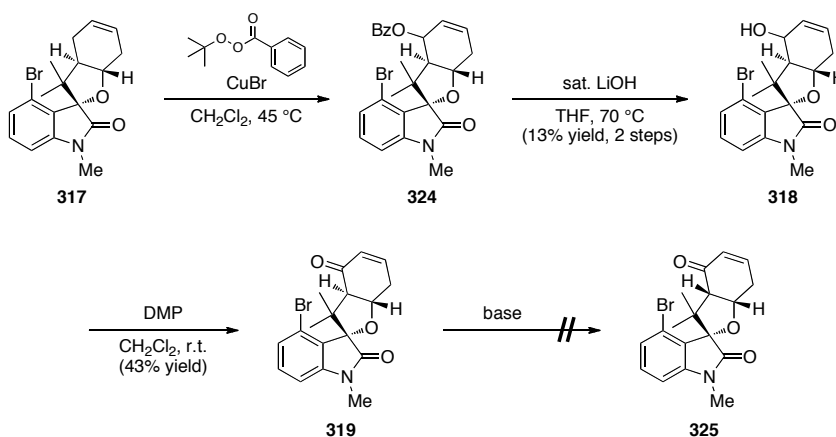
Scheme 3.4.4



With spiro-tetrahydrofuran **317** in hand, regioselective allylic oxidation of the disubstituted olefin within **317** was attempted but proved more difficult than anticipated. Initially we turned to Riley conditions for the allylic oxidation.²⁴ We speculated that the electronic effect of the electronegative oxygen present in the tetrahydrofuran ring would differentiate the allylic carbons by deactivating the undesired site from hydrogen abstraction. Unfortunately, Riley oxidation conditions provided complex mixtures and we were forced to pursue more exotic conditions.

Karasch and Sasnovsky reported the oxidation of allylic carbons to allylic alcohols through the use of *tert*-butyl benzoylperoxide and copper(I) bromide.^{26,27} Applying this method to our system, we found that we could produce allylic benzoylate **324** regioselectively. Subsequent treatment of **324** with a 40% solution of LiOH gave allylic alcohol **318** in low yield over two steps. Oxidation of allylic alcohol **318** with Dess-Martin periodinane then gave enone **319**.²⁸ Unfortunately, when we exposed enone **319** to basic conditions we were unable to effect an epimerization and the reaction produced an aromatized product mixture.

Scheme 3.4.5



3.4.2.1 Exploration of Reaction Conditions.

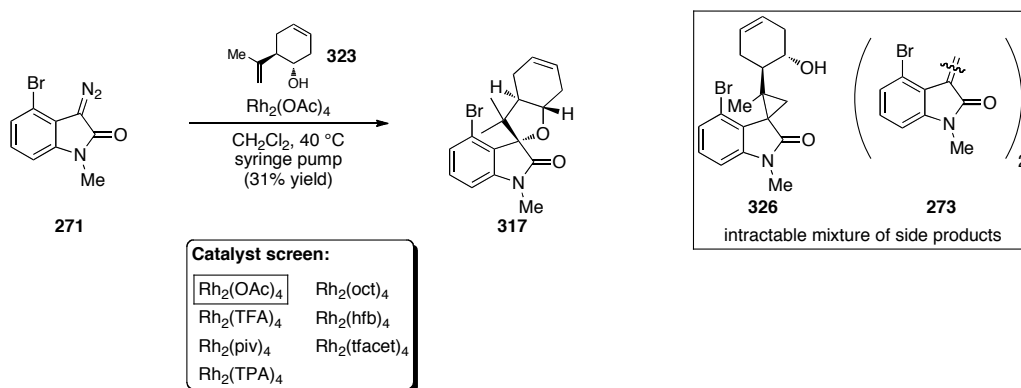
With the deleterious inability to epimerize **319** in our model system, we decided to investigate the reaction conditions of the O–H insertion Conia-ene cyclization. We hoped that if we optimized the yields of the earlier steps we could provide enough material for reaction screening to eventually circumvent aromatization and form the targeted welwitindolinone D core (**320**, Scheme 3.4.2).

To begin, we first attempted to isolate and identify the major side-product of the O–H insertion Conia-ene cyclization of diazoisatin **271** and alcohol **323** (Scheme 3.4.6). Upon purification of the reaction, we were able to identify but not isolate an intractable mixture of cyclopropanation products (**326**) and dimer products represented by **273**. This observation then led to a quick catalyst screen. After considerable efforts, we found that rhodium(II) acetate dimer gave the best results. This was not surprising considering the O–H insertion Claisen rearrangement chemistry that was developed in our laboratory

determined rhodium(II) acetate dimer to be the optimal catalyst in their system. Further analysis of the catalyst screen revealed that the more bulky rhodium(II) dimer ligands, such as triphenyl acetate and pivylate, favored cyclopropanation over O–H insertion.

Other modifications of the reaction conditions were also attempted including solvent screens and addition restrictions. We found that if we varied the solvent among methylene chloride, toluene, or benzene we obtained comparable results. Dilution or concentration of the reaction mixture also gave indistinguishable observations, thus proving the optimization of the production of spiro-THF **317** difficult.

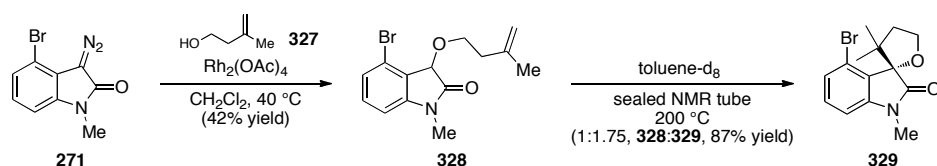
Scheme 3.4.6



Because of the problematic optimization of the formation of spiro-THF **317**, we were worried that the reaction sequence was inherently flawed. To prove to ourselves that the poor yielding reaction wasn't universal, we decided to modify the substrate pairing. Depicted in Scheme 3.4.7 is our first alteration. We exposed diazoisatin **271** to homoallylic alcohol **327** in the presence of rhodium(II) acetate dimer and isolated O–H insertion product **328** in 42% yield. Subsequent heating of **328** in deuterated toluene at

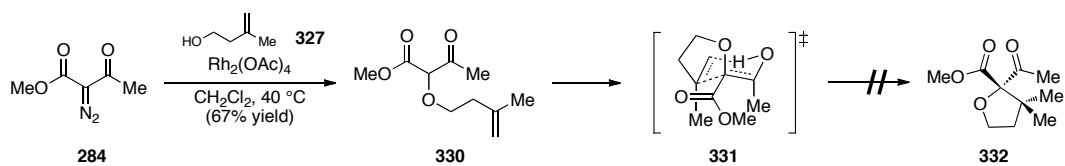
200 °C in a sealed NMR tube gave spiro-cycle **329** after 48 hours as a 1:1.75 mixture of starting material to product, respectively.

Scheme 3.4.7



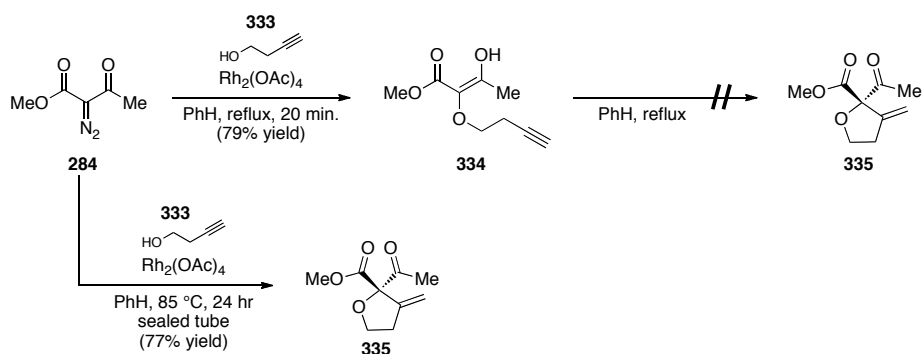
To further prove to ourselves that the low yield of the reaction sequence in Scheme 3.4.6 (**271** → **317**) was a result of substrate pairing (alcohol vs. diazo compound), we changed diazoisatin **271** to methyl diazoacetylacetate **284** (Scheme 3.4.8). Under the same reaction conditions as seen in Scheme 3.4.6, we initiated an O–H insertion to provide β -keto ester **330** in 67% yield, a 25% yield increase from the diazoisatin reaction. However, subsequent heating of β -keto ester **330** failed to deliver expected spiro-cycle **332**. We believe that an inherent 1,3-diaxial interaction within the transition state **331** prevented the cyclization. Substitution of homo allylic alcohol **327** with homo propargylic alcohol **333** (see Scheme 3.4.9) circumvented this problem and supports our speculation that the O–H insertion of diazoisatin **271** is the problematic step in our model system and that the O–H insertion Conia-ene reaction sequence is not flawed.

Scheme 3.4.8



In the course of exploring the reaction conditions of the O–H insertion Conia-ene cyclization, we made an interesting observation (Scheme 3.4.9). We found that if we treated diazo **284** with homo-propargylic alcohol **333** in the presence of rhodium(II) acetate dimer we isolated enol-ether **334** after 20 min. Subsequent heating of enol-ether **334** in benzene for 24 hrs in the absence of rhodium(II) acetate dimer did not afford any desired spiro-cycle (**335**). However, when we exposed methyl diazoacetylacetate **284** to homo-propargylic alcohol **333** in the presence of rhodium(II) acetate dimer in a sealed tube heated at 85°C for 24 hrs, we exclusively isolated desired spiro-cycle **335**. This series of reactions imply that rhodium(II) facilitates the sequential Conia-ene cyclization. At this juncture, we are unsure of whether rhodium(II) acts as a π -Lewis acid, coordinating to the alkyne or as a Lewis-acid, coordinating to the oxygen thus promoting enolization.

Scheme 3.4.9



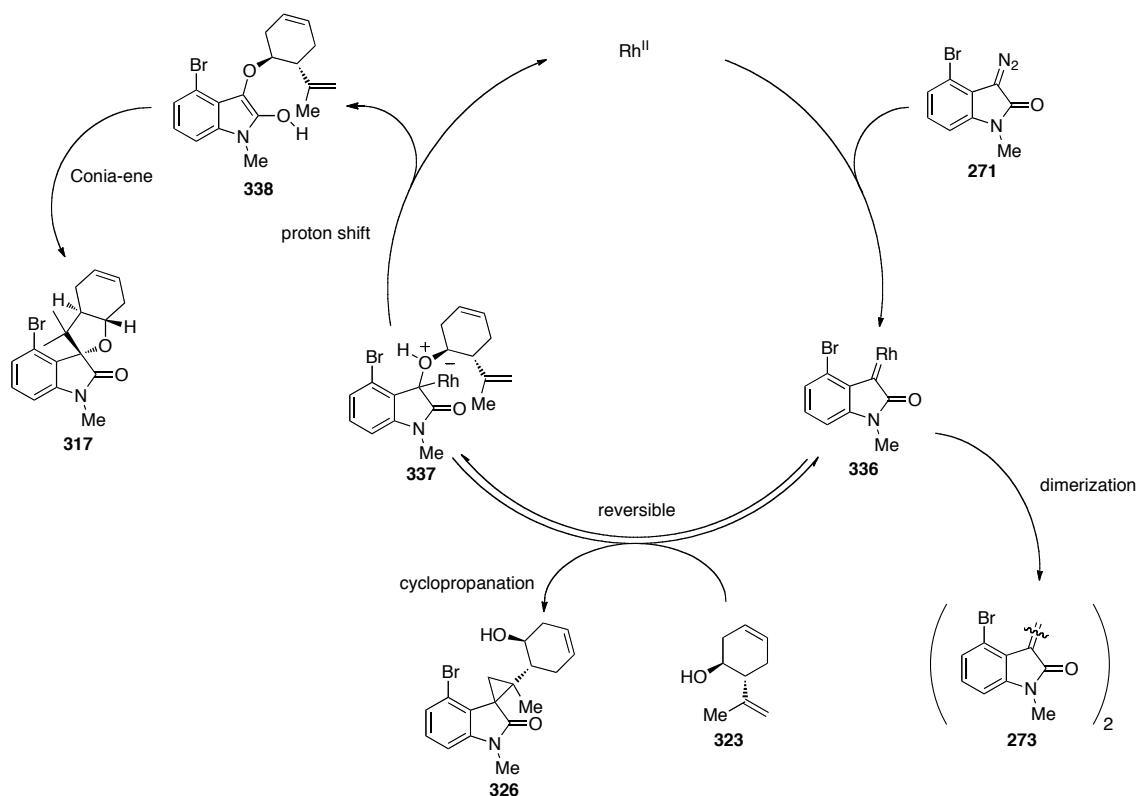
3.4.2.2 Mechanistic Rationale.

In an attempt to rationalize the product distribution of the O–H insertion Conia-ene cyclization of diazoisatin **271** and homo-allylic alcohol **323** (see Scheme 3.4.6 for reaction scheme), we devised a mechanism (Scheme 3.4.10). We believe that the rhodium(II)-mediated dediazotization of diazoisatin **271** produces rhodium carbenoid **336**. This rhodium carbenoid (**336**) can then undergo a dimerization to give representative dimer adduct **273**, thus removing reacting starting material and partially explaining a decreased yield.

As homo-allylic alcohol **323** is slowly added to the reaction flask, rhodium carbenoid **336** can form oxonium ylide **337** or cyclopropanation adducts **326**. Because literature precedence has shown oxonium ylide formations to be reversible,²⁹ we believe that the reversibility of oxonium ylide **326** formation siphons off the rhodium carbenoid **336** as irreversible cyclopropanation products (**326**). The remaining oxonium ylide **337** can undergo a 1,4-proton shift to deliver enol **338** and recycle the rhodium(II) catalyst. Enol **338** then can undergo a thermally induced Conia-ene cyclization.

This mechanistic rationale highlights several observations. First, the rhodium-mediated dediazotization of diazoisatin **271** to form rhodium carbenoid **336** requires heat, reflecting the stability of diazoisatin **271**. We believe that the heat required to initiate the carbenoid formation also increases the reversibility of the oxonium ylide **337** formation. Second and in accordance with the first, the product distribution suggests that cyclopropanation and dimerization are faster than the 1,4-proton shift.

Scheme 3.4.10

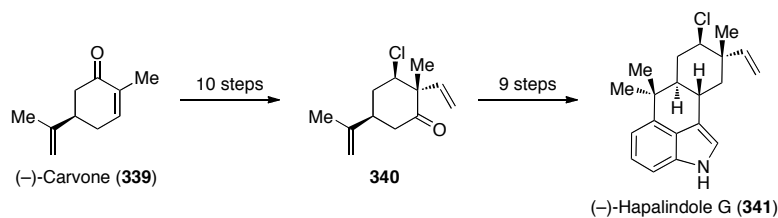


3.4.3 Attempted O–H Insertion Conia-ene Cyclization of a Complex Alcohol:

Inspiration from Fukuyama.

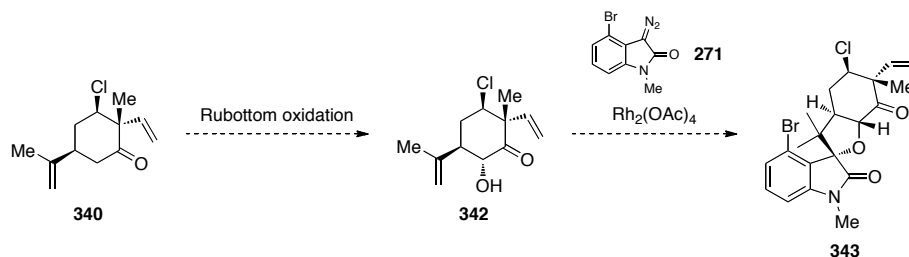
Although we were unable to optimize the O–H insertion Conia-ene cyclization of our model system, we were determined to use this method for the formation of welwitindolinone D isonitrile (**20**) despite the inherent low yield related to diazoisatin **271**. To that end and to quickly assess the viability of the O–H insertion Conia-ene cyclization of a more functionalized homo-allylic alcohol, we searched the literature for a known, suitable component.

Scheme 3.4.11



Our search eventually led to a report by Fukuyama on the first total synthesis of (-)-Hapalindole G (**341**, Scheme 3.4.11).³⁰ In this report, the synthesis of (-)-Hapalindole G (**341**) was completed in 19 steps starting from commercially available (-)-carvone (**339**). After 10 steps they arrived at ketone **340**, a substrate that we believed could be transformed into a functionalized homo-allylic alcohol required for our projected O–H insertion Conia-ene cyclization. As depicted in Scheme 3.4.12, a Rubottom oxidation of ketone **340**³¹ would provide α -hydroxy ketone **342**, the homo-allylic alcohol motif necessary for the subsequent O–H insertion Conia-ene cyclization (**342** \rightarrow **343**).

Scheme 3.4.12

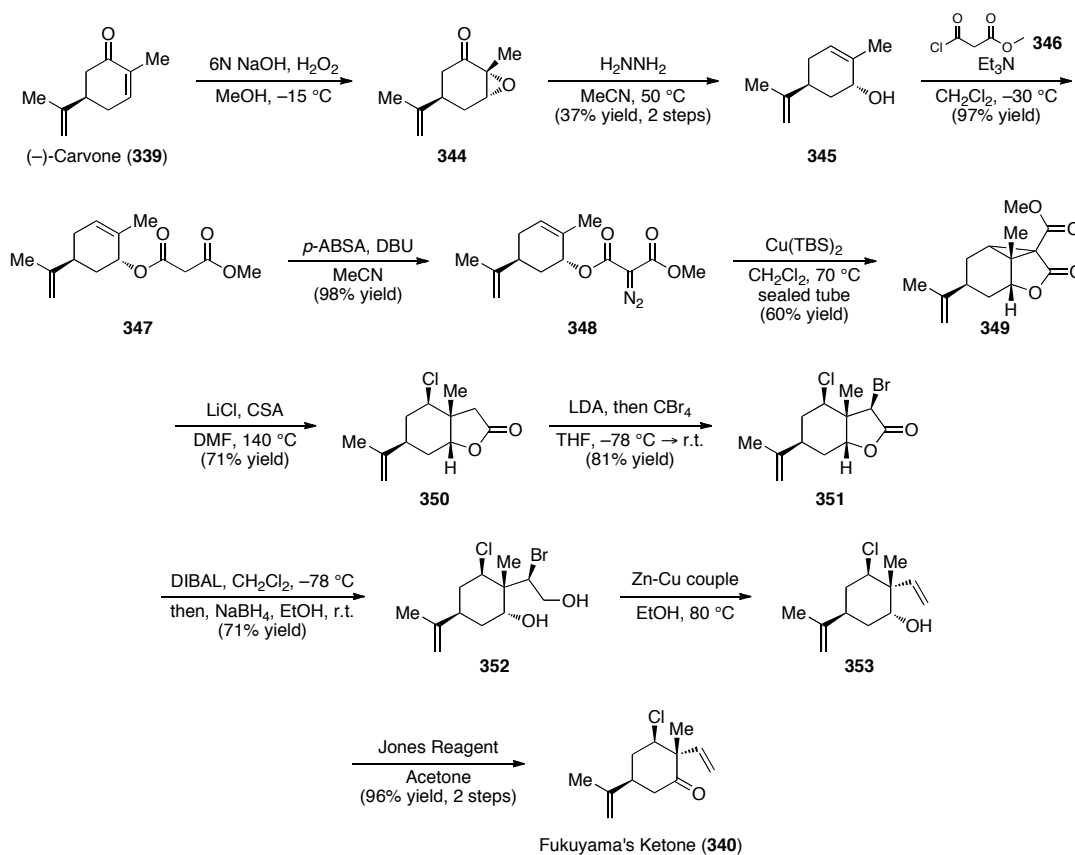


In accord with our broad strategy outlined in Scheme 3.4.12, we began by synthesizing Fukuyama's ketone **340** by following his exact route. Starting from

enantioenriched (-)-carvone (**339**), an epoxidation provided epoxy-ketone **344** where subsequent exposure to anhydrous hydrazine initiated a Wharton transposition to deliver allylic alcohol **345**. Exposure of allylic alcohol **345** to acid chloride **346** in the presence of triethylamine then gave mixed malonyl **347** in excellent yield. Subsequent diazotransfer with *p*-ABSA then created diazomalonyl **348**. Treatment of diazomalonyl **348** with Cu(TBS)₂ induced a cyclopropanation that resulted in lactone **349**.

Heating lactone **349** in DMF in the presence of LiCl and CSA opened the cyclopropane ring and induced a Krapcho decarboxylation to deliver compound **350**. Bromination of lactone **350** to bromolactone **351** followed by a reduction provided bromohydrine **352**. According to Fukuyama, this two-part reduction is necessary to avoid over reduction to the primary alcohol (not shown). Transformation of **352** with zinc-copper couple to the ethylene moiety in **353** established the desired quaternary center for welwitindolinone D isonitrile (**20**). Jones oxidation of alcohol **353** then completed the synthesis of Fukuyama's ketone (**340**).

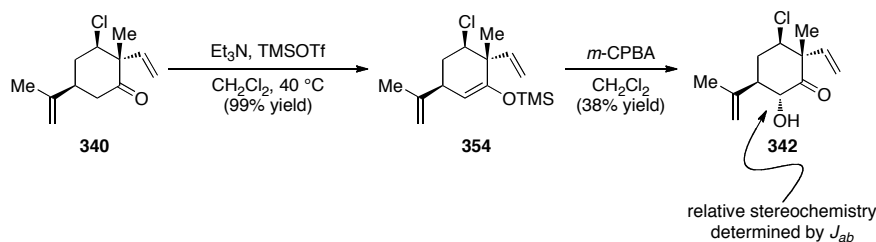
Scheme 3.4.13



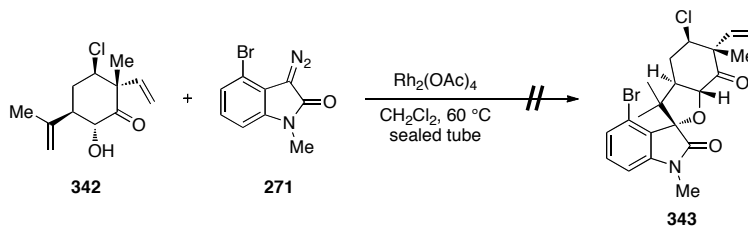
With ketone **340** in hand, we were poised to implement our planned Rubottom oxidation to form the requisite homo-allylic alcohol motif (Scheme 3.4.14). Initial attempts to form silyl enol ether **354** via deprotonation and silylation were unsuccessful. Ultimately, we found that exposure of ketone **340** to TMSOTf and triethylamine in CH₂Cl₂ at reflux delivered silyl enol ether **354** in near quantitative yield. Exposure of silyl enol ether **354** to *m*-CPBA resulted in the formation of α -hydroxy ketone **342**. The relative stereochemistry was determined via analysis of the ¹H coupling constants.

The establishment of a functionalized homo-allylic alcohol (**342**) gave us the opportunity to test the viability of the O–H insertion Conia-ene cyclization to construct welwitindolinone D isonitrile (**20**) (Scheme 3.4.15). Unfortunately, when alcohol **342** and diazoisatin **271** were subjected to the O–H insertion Conia-ene cyclization conditions, spiro-THF **343** was not observed. Crude ^1H NMR indicates an intractable mixture of cyclopropanation adducts and dimerization of diazoisatin **271**.

Scheme 3.4.14



Scheme 3.4.15



3.5 Conclusion.

After several failed attempts to construct *N*-methylwelwitindolinone C isothiocyanate (**16**), we shifted our attention to *N*-methylwelwitindolinone D isonitrile

(**20**) with the intent of accessing the entire welwitindolinone family. Our initial plan to build the embedded bridged THF-ring system via a tandem carbonyl-ylide 1,4 addition ultimately was unsuccessful, however those failures led to the discovery of a new reaction sequence, the O–H insertion Conia-ene cyclization.

Our group has conducted extensive studies in the realm of O–H insertion tandem [2,3]/[3,3] rearrangements. The discovery of the O–H insertion Conia-ene cyclization provided a nice extension to our established studies. This new tandem reaction sequence also paved a new pathway for the construction of the embedded THF-ring system within welwitindolinone D isonitrile (**20**). Brief explorations of the reaction conditions revealed diazoisatin **271** to be a poor substrate for the sequence, yet we still believed it would serve our purpose. A simple model system demonstrated the utility of this method, but elaboration to welwitindolinone core **320** proved difficult and the model system was abandoned.

An attempt to expedite the synthesis of welwitindolinone D isonitrile (**20**) led to the exploitation of a compound built by Fukuyama in 1994. A Rubottom oxidation gave the desired homo-allylic alcohol motif necessary for the implementation of our tandem O–H insertion Conia-ene cyclization. Unfortunately, our efforts to induce our tandem reaction sequence with a more functionalized alcohol failed and we were unable to proceed forward.

Despite our immediate failed attempts to gain access to the welwitindolinones via our newly discovered O–H insertion Conia-ene cyclization, considerable room for substrate exploration still remains. The next phase will explore swapping the diazo and

alcohol functionalities on the coupling partners and conducting the arylation of the coupling partners before the O–H insertion Conia-ene cyclization.

3.6 Experimental Section.

3.6.1 Material and Methods.

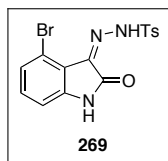
Unless otherwise stated, reactions were magnetically stirred in flame-dried glassware under an atmosphere of nitrogen. Triethylamine (Et₃N) and methanol were dried over calcium hydride and freshly distilled. Benzene, tetrahydrofuran, dichloromethane, toluene, and diethyl ether were dried using a solvent purification system manufactured by SG Water U.S.A., LLC using technology based upon that originally described by Grubbs *et al.*³² Reagent grade DMF, DMSO, acetone, and 1,2-dichloroethane were supplied by Fischer Scientific and purchased from the Colorado State Chemistry Stockroom. All other commercially available reagents were used as received.

Unless otherwise stated, all reactions were monitored by thin-layer chromatography (TLC) using Silicycle glass-backed extra hard layer, 60 Å plates (indicator F-254, 250 µm). Column or flash chromatography was performed with the indicated solvents using Silicycle SiliaFlash® P60 (230-400 mesh) silica gel as the stationary phase. Chromatography was conducted in accordance with the guidelines reported by Still *et al.*³³ All melting points were obtained on a Gallenkamp capillary melting point apparatus (model: MPD350.BM2.1) and are uncorrected. Infrared spectra were obtained using a

Nicolet Avatar 320 FTIR or Bruker Tensor 27 FTIR. ^1H and ^{13}C NMR spectra were recorded on a Varian Inova 400, Varian Inova 400 autosampler, or Varian Inova 300 spectrometer. Chemical shifts (δ) are reported in parts per million (ppm) relative to internal residual solvent peaks from indicated deuterated solvents. Coupling constants (J) are reported in Hertz (Hz) and are rounded to the nearest 0.1 Hz. Multiplicities are defined as: s = singlet, d = doublet, t = triplet, q = quartet, quint. = quintuplet, m = multiplet, dd = doublet of doublets, ddd = doublet of doublet of doublets, dddd = doublet of doublet of doublet of doublets, br = broad, app = apparent, par = partial. High-resolution mass spectra were performed at the Central Instrument Facility by Donald L. Dick of Colorado State University. Single-crystal X-ray analyses were performed by Susie Miller and Brian Newell of Colorado State University.

3.6.2 Preparative Procedures:

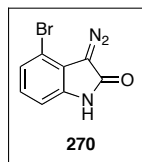
Preparation of Tosyl Hydrazone **269**.



Tosyl Hydrazone 269. 4-Bromoisatin (**268**, 1.0 g, 4.424 mmol, 1.0 equiv.) was diluted in MeOH (16.4 mL) before *p*-toluenesulfonyl hydrazide (832 mg, 4.468 mmol, 1.01 equiv.) and 2 drops of concentrated hydrochloric acid were added. The solution was

stirred for 10 minutes at room temperature and then heated at 45 °C until determined complete by TLC (approx. 1hr). The resulting suspension was concentrated, filtered, and washed with cold MeOH. Recrystallization from MeOH gave tosyl hydrazone **269** (1.383 g, 79% yield) as a yellow powder: m.p. 181.5-182 °C; FTIR (thin film/NaCl) 3137, 3072, 1709, 1619, 1582, 1439, 1395, 1355, 1322, cm^{-1} ; ^1H NMR (300 MHz, DMSO-d_6) δ 12.6 (s, 1H), 11.38 (s, 1H), 7.93 (d, $J = 8.1$ Hz, 2H), 7.43 (d, $J = 8.4$ Hz, 2H), 7.20 (d, $J = 4.2$ Hz, 2H), 6.87 (t, $J = 4.2$ Hz, 1H), 2.36 (s, 3H); ^{13}C NMR (75 MHz, DMSO-d_6) δ 161.3, 144.5, 144.0, 136.0, 134.6, 132.5, 129.7, 128.0, 126.8, 117.8, 115.6, 110.2, 21.1; HRMS (EI) m/z 393.9853 [calcd for $\text{C}_{15}\text{H}_{13}\text{BrN}_3\text{O}_3\text{S}$ (M^+) 393.9856].

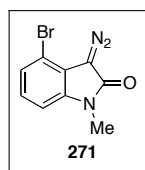
Preparation of 4-Bromo-Diazoisatin 270.



4-Bromo-Diazoisatin 270. Tosyl hydrazone **269** (1.283 g, 3.254 mmol, 1.0 equiv.) was taken up in THF (10 mL) before a 0.2*N* solution of NaOH (33 mL, 6.509, 2.0 equiv.) was added. As determined by TLC, the reaction was complete after 5 minutes. CO_2 was then bubbled through the reaction for 30 minutes. The resulting suspension was filtered, rinsed with cold water, and azeotropically dried with benzene to afford 4-bromo-diazoisatin **270** (547 mg, 70% yield) as an orange powder: FTIR (thin film/NaCl) 3135, 2104, 1684, 1616, 1580, 1487, 1444, 1413, 1380, 1313, 1252 cm^{-1} ; ^1H NMR (300 MHz, DMSO-d_6) δ 10.94 (s, 1H), 7.15 (dd, $J = 3.6, 8.0$ Hz, 1H), 7.04 (ddd, $J = 4.4, 8.0, 8.0$ Hz,

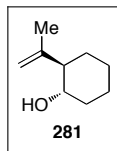
1H), 6.92 (dd, $J = 3.6, 8.0$ Hz, 1H); ^{13}C NMR (75 MHz, DMSO- d_6) δ 167.2, 134.2, 126.7, 124.3, 116.0, 113.3, 109.3; HRMS (EI) m/z 237.9608 [calcd for $\text{C}_8\text{H}_5\text{BrN}_3\text{O}$ (M+) 237.9611].

Preparation of 4-Bromo-*N*-Methyl-Diazoisatin 271.



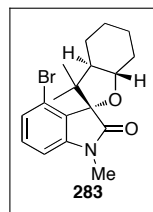
4-Bromo-*N*-Methyl-Diazoisatin 271. A solution of 4-bromo-diazoisatin **270** (66 mg, 0.277 mmol, 1.0 equiv.) in DMF (2.77 mL) was cooled to 0 °C and treated with NaH (60% by weight, 12 mg, 0.305 mmol, 1.1 equiv.). After stirring at 0 °C for 10 minutes, MeI (20 μL , 0.305 mmol, 1.1 equiv.) was added dropwise. The reaction was then slowly warmed to room temperature over 1 hr whereupon TLC indicated the consumption of starting material. 1M HCL was added followed by EtOAc and copious amounts of water (approx. 10:1 H_2O :DMF). The mixture was extracted with EtOAc, washed with brine, and dried over MgSO_4 . Purification via silica gel chromatography (15% EtOAc/hexanes) gave 4-bromo-*N*-methyl-diazoisatin **271** (62 mg, 89% yield) as an orange solid: FTIR (thin film/NaCl) 2101, 1687, 1608, 1456, 1398, 1287 cm^{-1} ; ^1H NMR (400 MHz, CDCl_3) δ 7.12 (d, $J = 8.4$ Hz, 1H), 7.02 (t, $J = 8.4$ Hz, 1H), 6.81 (d, $J = 7.6$ Hz, 1H), 3.28 (s, 3H); ^{13}C NMR (100 MHz, CDCl_3) δ 166.6, 135.7, 126.2, 125.3, 116.0, 113.9, 107.4, 94.5, 27.1; HRMS (EI) m/z 251.9768 [calcd for $\text{C}_9\text{H}_7\text{BrN}_3\text{O}$ (M+) 251.9767].

Preparation of Homo-Allylic Alcohol **281**.



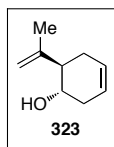
Homo-Allylic Alcohol 281. Cyclohexene oxide (1.0 mL, 9.88 mmol, 1.0 equiv.) was diluted in Et₂O (5 mL) and cooled to -30 °C before CuCN (186 mg, 2.075 mmol, 0.21 equiv.) was added. The resulting suspension was stirred for 15 minutes at -30 °C whereupon iso-propenylmagnesium bromide (0.59 M, 33.5 mL, 19.766 mmol, 2.0 equiv.) was added slowly. The reaction was warmed to room temperature over 2hrs. Upon completion as indicated by TLC (approx. 3hrs), a solution of NH₄OH:NH₄Cl (9:1) was added and stirred for 3hrs where a light blue color persisted. The solution was extracted with EtOAc, washed with brine, and dried over MgSO₄. Filtration and concentration of the solution yielded, without purification homo-allylic alcohol **281** (1.387 g, 95% yield). All characterization data has previously been reported.

Preparation of Spirocycle 283.



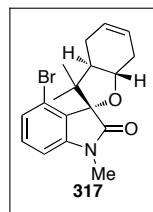
Spirocycle 283. 4-Bromo-*N*-methyl-diazoisatin **271** (57 mg, 0.226 mmol, 1.0 equiv.) and homo-allylic alcohol **281** (38 mg, 0.271 mmol, 1.2 equiv.) were diluted in CH₂Cl₂ (2.26 mL) before rhodium (II) acetate dimer (10 mg, 0.023 mmol, 0.1 equiv.) was added. The reaction vessel was sealed and heated to 60 °C. After 20 minutes the reaction vessel was cooled to room temperature whereupon TLC indicated the consumption of starting material. The reaction was concentrated, taken up in benzene and loaded directly onto a column. Purification via column chromatography (10% EtOAc/hexanes) gave spirocycle **283** (28 mg, 34% yield) as a crystalline white solid and as a single diastereomer: m.p. 131.5-132.5; FTIR (thin film/NaCl) 2936, 2863, 1732, 1604, 1579, 1453, 1394, 1370, 1339, 1288, 1243, cm⁻¹; ¹H NMR (400 MHz, CDCl₃) δ 7.10-7.03 (m, 2H), 6.67 (d, *J* = 7.2 Hz, 1H), 4.02 (ddd, *J* = 4.0, 10.8, 10.8 Hz, 1H), 3.05 (s, 3H), 2.27-2.23 (m, 1H), 2.16 (ddd, *J* = 3.2, 11.6, 11.6 Hz, 1H), 1.85 (dd, *J* = 11.6, 20.8 Hz, 2H), 1.70-1.59 (m, 2H), 1.34-1.08 (m, 4H), 1.05 (s, 3H), 0.89 (s, 3H); ¹³C NMR (100 MHz, CDCl₃) δ 179.4, 146.0, 130.2, 128.7, 127.3, 120.3, 107.2, 91.2, 83.0, 55.2, 48.6, 31.3, 26.5, 25.8, 25.3, 25.1, 24.2, 23.4; HRMS (EI) *m/z* 364.0911 [calcd for C₁₈H₂₃BrNO₂ (M⁺) 364.0907].

Preparation of Homo-Allylic Alcohol **323**.



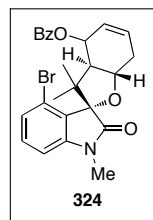
Homo-Allylic Alcohol 323. Starting from 1,4-cyclohexadiene (**321**), mono-epoxide **322** was prepared according to reported literature procedures. Mono-epoxide **322** (1.586 g, 16.498 mmol, 1.0 equiv.) was diluted in THF (8.3 mL) and cooled to $-30\text{ }^{\circ}\text{C}$ before CuCN (310 mg, 3.465 mmol, 0.21 equiv.) was added. The resulting suspension was stirred for 15 minutes at $-30\text{ }^{\circ}\text{C}$ whereupon iso-propenylmagnesium bromide (0.50 M, 66.0 mL, 32.997 mmol, 2.0 equiv.) was added slowly. The reaction was warmed to room temperature over 2hrs. Upon completion as indicated by TLC (approx. 3hrs), a solution of $\text{NH}_4\text{OH}:\text{NH}_4\text{Cl}$ (9:1) was added and stirred for 3hrs where a light blue color persisted. The solution was extracted with EtOAc, washed with brine, and dried over MgSO_4 . After filtration and concentration, purification via column chromatography of the resulting oil (5% EtOAc/hexanes) gave isopropenyl-cyclohexen-ol **323** (1.563 g, 69% yield) as a pale yellow oil: FTIR (thin film/ NaCl) 3360, 2915, 1645, 1437, 1375, 1334, 1258 cm^{-1} ; ^1H NMR (400 MHz, CDCl_3) δ 5.66-5.56 (m, 2H), 4.97 (t, $J = 1.6\text{ Hz}$, 1H), 4.92 (s, 1H), 3.83 (ddd, $J = 5.6, 9.2, 9.2\text{ Hz}$, 1H), 2.53-2.46 (m, 1H), 2.34 (ddd, $J = 6.0, 10.4, 10.4\text{ Hz}$, 1H), 2.17-2.11 (m, 2H), 2.08-1.99 (m, 1H), 1.87 (s, 1H), 1.76 (s, 3H); ^{13}C NMR (75 MHz, CDCl_3) δ 145.9, 126.1, 124.5, 113.8, 68.0, 50.2, 34.0, 30.5, 19.4; HRMS (APCI) m/z 139.112 [calcd for $\text{C}_9\text{H}_{15}\text{O}$ (M^+) 139.1117].

Preparation of Spirocycle 317.



Spirocycle 317. 4-Bromo-*N*-methyl-diazoisatin **271** (904 mg, 3.586 mmol, 1.0 equiv.) and isopropenyl-cyclohexen-ol **323** (2.422 g, 17.524 mmol, 5.0 equiv.) were diluted in CH₂Cl₂ (48 mL) before rhodium (II) acetate dimer (24 mg, 0.036 mmol, 0.01 equiv.) was added. The reaction vessel was sealed and heated to 60 °C. After 20 minutes the reaction vessel was cooled to room temperature whereupon TLC indicated the consumption of starting material. The reaction was concentrated, taken up in benzene and loaded directly onto a column. Purification via column chromatography (100% CH₂Cl₂) gave spirocycle **317** (397 mg, 30% yield) as a white powder and as a 4:1 mixture of diastereomers: m.p. 134.3-135.7 °C; FTIR (thin film/NaCl) 2962, 2917, 2850, 1730, 1603, 1579, 1453, 1345, 1326, 1287, 1241, 1213 cm⁻¹; ¹H NMR (400 MHz, CDCl₃) δ 7.13-7.06 (m, 2H), 6.71 (d, *J* = 7.2 Hz, 1H), 5.76-5.64 (m, 2H), 4.32 (ddd, *J* = 6.0, 10.4, 17.2 Hz, 1H), 3.09 (s, 3H), 2.69 (dt, *J* = 5.2, 16.4 Hz, 1H), 2.56-2.46 (m, 2H), 2.16-2.09 (m, 1H), 2.06-1.97 (m, 1H), 1.11 (s, 3H), 0.96 (s, 3H); ¹³C NMR (100 MHz, CDCl₃) δ 179.3, 146.1, 130.4, 128.7, 127.6, 127.4, 126.8, 126.7, 125.2, 124.8, 120.5, 107.3, 107.1, 91.8, 79.8, 79.3, 51.3, 50.1, 48.2, 47.0, 33.4, 32.1, 26.6, 26.2, 26.0, 25.9, 25.5, 23.8, 23.3, 21.5; HRMS (DART) *m/z* 362.0746 [calcd for C₁₈H₂₁BrNO₂ (M⁺) 362.075].

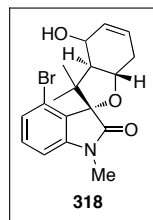
Preparation of Allylic Benzoylate 324.



Allylic Benzoylate 324. To a solution of spirocycle **317** (52 mg, 0.144 mmol, 1.0 equiv.) in CH₂Cl₂ (0.8 mL) was added rigorously dried CuBr (41 mg, 0.287 mmol, 2.0 equiv.). The resulting suspension was heated at reflux for 15 minutes then cooled to room temperature before *t*-butylperoxybenzoate (0.11 mL, 0.574 mmol, 4.0 equiv.) was slowly added. The reaction was again heated at reflux for 6hrs whereupon TLC indicated the reaction complete. Upon cooling to room temperature, an aliquot of sat. Na₂S₂O₃ was added and the mixture was stirred for 10 minutes then extracted with CH₂Cl₂, washed sat. NaHCO₃, brine, and dried over MgSO₄. After filtration and concentration, purification via column chromatography (15% EtOAc/hexanes) gave allylic benzoylate **324** (33 mg, 48% yield) as a colorless oil and as a mixture of diastereomers: FTIR (thin film/NaCl) 2965, 2932, 2869, 1727, 1604, 1580, 1453, 1350, 1329, 1269 cm⁻¹; ¹H NMR (400 MHz, CDCl₃) δ 8.07 (d, *J* = 8.0 Hz, 2H), 7.58 (t, *J* = 7.6 Hz, 1H), 7.46 (t, *J* = 8.0 Hz, 2H), 7.17-7.09 (m, 2H), 6.72 (d, *J* = 7.6 Hz, 1H), 5.89-5.76 (m, 3H), 4.49 (ddd, *J* = 5.6, 9.6, 11.6 Hz, 1H), 3.09 (s, 3H), 3.01 (t, *J* = 11.6 Hz, 1H), 2.77 (dt, *J* = 5.6, 16.8 Hz, 1H), 2.67-2.59 (m, 1H), 1.24 (s, 3H), 1.06 (s, 3H); ¹³C NMR (100 MHz, CDCl₃) δ 178.7, 166.1, 146.2, 133.3, 130.7, 130.1, 129.8, 129.7, 128.6, 128.5, 128.2, 128.1, 127.7, 127.4, 120.6, 107.5,

91.8, 71.9, 55.3, 47.9, 31.7, 27.3, 26.7, 23.5; HRMS (EI) m/z 504.0791 [calcd for $C_{25}H_{24}BrNNaO_4$ (M^+) 504.0781].

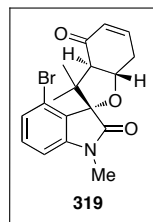
Preparation of Allylic Alcohol 318.



Allylic Alcohol 318. To a solution of allylic benzoylate **324** (33 mg, 0.068 mmol, 1.0 equiv.) in THF (2 mL) was added a saturated solution of LiOH (2 mL). The biphasic mixture was heated at 70 °C until no starting material remained as indicated by TLC (approx. 4hrs). The reaction was cooled to room temperature, extracted with EtOAc, washed with $NaHCO_3$, then brine, and dried over $MgSO_4$. After filtration and concentration, purification via column chromatography (30% EtOAc/hexanes) gave allylic alcohol **318** (7 mg, 27% yield) as an amorphous white solid: FTIR (thin film/ $NaCl$) 3436, 2968, 2926, 2877, 1724, 1605, 1580, 1453, 1392, 1349, 1289, 1246, 1216 cm^{-1} ; 1H NMR (400 MHz, $CDCl_3$) δ 7.15 (t, $J = 8.0$ Hz, 1H), 7.10 (d, $J = 7.2$ Hz, 1H), 6.71 (d, $J = 7.2$ Hz, 1H), 5.76-5.67 (m, 2H), 4.40 (d, $J = 8.0$ Hz, 1H), 4.33 (ddd, $J = 5.6, 10.4, 10.4$ Hz, 1H), 3.09 (s, 3H), 2.65-2.61 (m, 1H), 2.55 (d, $J = 10$ Hz, 1H), 2.47 (t, $J = 11.2$ Hz, 1H), 2.31 (d, $J = 10$ Hz, 1H), 1.3 (s, 3H), 1.13 (s, 3H); ^{13}C NMR (100 MHz, $CDCl_3$) δ 179.0, 146.2, 132.5, 130.6, 128.4, 127.4, 125.9, 120.6, 107.4, 91.7, 77.7, 69.4,

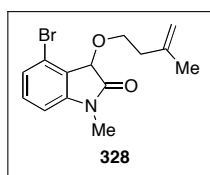
59.1, 48.2, 31.8, 27.7, 26.6, 23.3; HRMS (EI) m/z 378.0695 [calcd for $C_{18}H_{21}BrNO_3$ (M⁺) 378.0699].

Preparation of Enone 319.



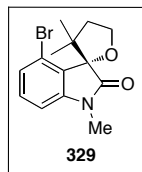
Enone 319. A solution of allylic alcohol **318** (7 mg, 0.019 mmol, 1.0 equiv.) in CH_2Cl_2 (0.62 mL) was treated with DMP (12 mg, 0.028 mmol, 1.5 equiv.) at room temperature. After 4hrs the reaction was complete as indicated by TLC. The reaction was diluted with water, extracted with EtOAc, washed with brine, and dried over $MgSO_4$. After filtration and concentration, purification via column chromatography (20% EtOAc/hexanes) gave enone **319** (3 mg, 43% yield) as a white solid: m.p. 168-169 °C; FTIR (thin film/NaCl) 2977, 2933, 2876, 1731, 1687, 1604, 1579, 1454, 1378, 1345, 1325, 1288, 1255, 1226 cm^{-1} ; 1H NMR (400 MHz, $CDCl_3$) δ 7.13-7.10 (m, 2H), 6.93 (t, J = 8.0 Hz, 1H), 6.72 (d, J = 6.8 Hz, 1H), 6.05 (d, J = 9.6 Hz, 1H), 4.71 (ddd, J = 4.8, 12.0, 12.0 Hz, 1H), 3.34 (d, J = 12.4 Hz, 1H), 3.10 (s, 3H), 3.06 (dt, J = 5.6, 18.0 Hz, 1H), 2.85 (dd, J = 10.0, 17.6 Hz, 1H), 1.36 (s, 3H), 1.17 (s, 3H); ^{13}C NMR (100 MHz, $CDCl_3$) δ 196.5, 178.3, 146.3, 145.8, 132.1, 130.9, 127.8, 127.4, 120.3, 107.6, 91.3, 77.8, 61.8, 47.7, 32.8, 26.7, 26.1, 22.7; HRMS (EI) m/z 376.0545 [calcd for $C_{18}H_{19}BrNO_3$ (M⁺) 376.0543].

Preparation of Ether 328.



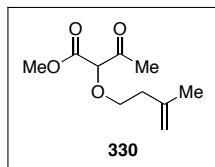
Ether 328. To a solution of 4-bromo-*N*-methyl-diazoisatin **271** (50 mg, 0.179 mmol, 1.0 equiv.) in CH₂Cl₂ (0.6 mL) was added 3-methyl-3-butene-1-ol (22 μ L, 0.214 mmol, 1.2 equiv.). The mixture was stirred for 5 minutes before rhodium(II) acetate dimer (4 mg, 0.009 mmol, 0.05 equiv.) was added. The reaction vessel was sealed and heated at 60 °C for 20 minutes whereupon the reaction was complete as indicated by TLC. The solution was concentrated, taken up in benzene, and loaded directly onto a silica gel column. Purification via column chromatography (15% EtOAc/hexanes) gave ether **328** (23 mg, 42% yield) as a colorless oil: FTIR (thin film/NaCl) 2937, 2869, 1727, 1650, 1608, 1586, 1457, 1361, 1340, 1299, 1201 cm⁻¹; ¹H NMR (400 MHz, CDCl₃) δ 7.19 (d, J = 4.4 Hz, 2H), 6.74 (t, J = 4.0 Hz, 1H), 4.82 (s, 1H), 4.79 (s, 1H), 4.78 (s, 1H), 4.04 (dd, J = 6.8, 15.6 Hz, 1H), 3.79 (dd, J = 6.8, 15.2 Hz, 1H), 3.16 (s, 3H), 2.43 (t, J = 6.8 Hz, 2H), 1.77 (s, 3H); ¹³C NMR (100 MHz, CDCl₃) δ 174.0, 146.1, 142.5, 131.5, 126.7, 124.9, 121.0, 111.8, 107.3, 76.7, 68.4, 38.1, 26.4, 22.9; HRMS (EI) m/z 310.0432 [calcd for C₁₄H₁₇BrNO₂ (M⁺) 310.0437].

Preparation of Spirocycle 329.



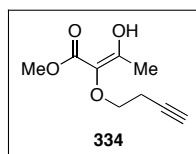
Spirocycle 329. A solution of ether **328** (15.0 mg, 0.48 mmol, 1.0 equiv.) in toluene- d_8 (0.6 mL) was placed in a Wilmad NMR tube with a J. Young valve and heated at 200 °C in an oil bath. The reaction was monitored periodically by NMR analysis. After 48hrs, NMR analysis of the reaction revealed a mixture of starting material, product and decomposition side-products. The reaction was immediately purified via column chromatography (15–20% EtOAc/hexanes) to give a mixture of **328:329** (13 mg, 87% combined yield) as a 1:1.75 mixture, respectively, and as a colorless oil. Further purification via column chromatography (3.0% EtOAc/benzene) gave **329** (5.0 mg, 34% yield) and **328** (4.0 mg, 27% yield) as colorless oils. Spirocycle **329** was characterized as follows: FTIR (thin film/NaCl) 2964, 2938, 2881, 1728, 1602, 1578, 1452, 1369, 1358, 1335, 1287, 1236 cm^{-1} ; ^1H NMR (400 MHz, CDCl_3) δ 7.18 (d, $J = 8.4$ Hz, 1H), 7.12 (t, $J = 7.6$ Hz, 1H), 6.71 (d, $J = 7.2$ Hz, 1H), 4.42 (ddd, $J = 3.6, 8.0, 8.0$ Hz, 1H), 4.37 (ddd, $J = 6.4, 8.0, 8.0$ Hz, 1H), 3.08 (s, 3H), 2.52 (ddd, $J = 11.6, 8.0, 8.0$ Hz, 1H), 2.02 (ddd, $J = 4.0, 6.4, 13.2$ Hz, 1H), 1.21 (s, 3H), 1.04 (s, 3H); ^{13}C NMR (100 MHz, CDCl_3) δ 179.2, 146.3, 130.4, 127.7, 126.9, 120.3, 107.1, 91.9, 68.5, 48.6, 39.2, 26.7, 26.2, 24.8; HRMS (EI) m/z 310.0439 [calcd for $\text{C}_{14}\text{H}_{17}\text{BrNO}_2$ (M^+) 310.0437].

Preparation of Ether 330.



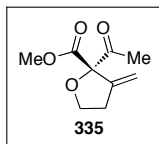
Ether 330. Starting from methylacetoacetate, diazomethylacetoacetate **284** was prepared according to reported literature procedures. To a solution of diazomethylacetoacetate **284** (54 mg, 0.380 mmol, 1.0 equiv.) in benzene (1.27 mL) was added 3-methyl-3-butene-1-ol (46 μ L, 0.456 mmol, 1.2 equiv.) The mixture was stirred for 5 minutes before rhodium(II) acetate dimer (4 mg, 0.009 mmol, 0.05 equiv.) was added. The reaction vessel was sealed and heated at 85 $^{\circ}$ C for 20 minutes whereupon the reaction was complete as indicated by TLC. The solution was loaded directly onto a silica gel column. Purification via column chromatography (10–15% EtOAc/hexanes) gave ether **284** (51.0 mg, 67% yield) as a colorless oil: FTIR (thin film/NaCl) 2956, 1754, 1729, 1651, 1438, 1357, 1262, 1201 cm^{-1} ; ^1H NMR (400 MHz, CDCl_3) δ 4.78 (s, 1H), 4.73 (s, 1H), 4.34 (s, 1H), 3.77 (s, 3H), 3.76–3.70 (m, 1H), 3.58 (dt, $J = 6.8, 8.8$ Hz, 1H), 2.38 (t, $J = 6.8$ Hz, 2H), 2.24 (s, 3H), 1.74 (s, 3H); ^{13}C NMR (100 MHz, CDCl_3) δ 202.4, 167.8, 142.0, 112.2, 85.6, 69.8, 52.8, 37.6, 26.4, 22.7; HRMS (EI) m/z 223.094 [calcd for $\text{C}_{10}\text{H}_{16}\text{NaO}_4$ (M^+) 223.0941].

Preparation of Enol Ether 334.



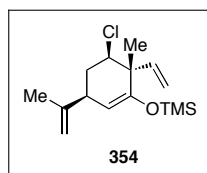
Enol Ether 334. Starting from methylacetoacetate, diazomethylacetoacetate **284** was prepared according to reported literature procedures. To a solution of diazomethylacetoacetate **284** (53 mg, 0.373 mmol, 1.0 equiv.) in benzene (1.24 mL) was added 3-butyn-1-ol (34 μ L, 0.448 mmol, 1.2 equiv.) The mixture was stirred for 5 minutes before rhodium(II) acetate dimer (1 mg, 0.002 mmol, 0.006 equiv.) was added. The reaction vessel was sealed and heated at 85 °C for 20 minutes whereupon the reaction was complete as indicated by TLC. The solution was loaded directly onto a silica gel column. Purification via column chromatography (10–15% EtOAc/hexanes) gave ether **334** (54.0 mg, 79% yield) as a colorless oil: FTIR (thin film/NaCl) 3288, 2957, 2883, 1753, 1730, 1662, 1438, 1358, 1262, 1202 cm^{-1} ; ^1H NMR (400 MHz, CDCl_3) δ 4.42 (s, 1H), 3.78 (s, 3H), 3.76-3.71 (m, 1H), 3.62 (dt, $J = 7.2, 9.2$ Hz, 1H), 2.56-2.51 (m, 2H), 2.27 (s, 3H); ^{13}C NMR (100 MHz, CDCl_3) δ 201.9, 167.4, 85.6, 80.5, 70.0, 69.3, 52.9, 26.5, 19.9; HRMS (EI) m/z 207.0629 [calcd for $\text{C}_9\text{H}_{12}\text{NaO}_4$ (M^+) 207.0628].

Preparation of THF 335.



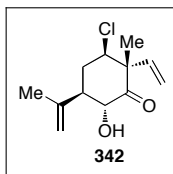
THF 335. Starting from methylacetoacetate, diazomethylacetoacetate **284** was prepared according to reported literature procedures. To a solution of diazomethylacetoacetate **284** (50 mg, 0.352 mmol, 1.0 equiv.) in benzene (1.17 mL) was added 3-butyne-1-ol (32 μ L, 0.422 mmol, 1.2 equiv.) The mixture was stirred for 5 minutes before rhodium(II) acetate dimer (1 mg, 0.002 mmol, 0.006 equiv.) was added. The reaction vessel was sealed and heated at 85 °C for 24hrs whereupon the reaction was complete as indicated by TLC. The solution was loaded directly onto a silica gel column. Purification via column chromatography (10–15% EtOAc/hexanes) gave THF **335** (50.0 mg, 77% yield) as a colorless oil: FTIR (thin film/NaCl) 2957, 2890, 1749, 1732, 1662, 1436, 1355, 1244 cm^{-1} ; ^1H NMR (400 MHz, CDCl_3) δ 5.37 (t, $J = 2.4$ Hz, 1H), 5.35 (t, $J = 2.4$ Hz, 1H), 4.14 (dd, $J = 8.4, 14.4$ Hz, 1H), 4.07 (dd, $J = 7.6, 16.0$ Hz, 1H), 3.75 (s, 3H), 2.69-2.64 (m, 2H), 2.21 (s, 3H); ^{13}C NMR (100 MHz, CDCl_3) δ 202.0, 168.8, 143.3, 112.4, 91.5, 68.6, 53.1, 32.8, 25.6; HRMS (EI) m/z 185.0808 [calcd for $\text{C}_9\text{H}_{13}\text{O}_4$ (M^+) 185.0808].

Preparation of Silyl Enol Ether 354.



Silyl Enol Ether 354.³⁵ Starting from (–)-carvone (**339**), ketone **340** was prepared according to Fukuyama's literature procedure. Ketone **340** (77 mg, 0.362 mmol, 1.0 equiv.) was diluted in CH₂Cl₂ (3.62 mL). Triethylamine (0.5 mL, 3.62 mmol, 10.0 equiv.) was added followed by TMSOTf (0.33 mL, 1.810 mmol, 5.0 equiv.) and the reaction was heated at reflux. Upon completion as indicated by TLC (approx. 30 minutes), the reaction was cooled to room temperature. An aliquot of water was added and the mixture was extracted with CH₂Cl₂ and dried over Na₂SO₄. After filtration and concentration, purification via column chromatography (100% hexanes) gave silyl enol ether **354** (83 mg, 80% yield) as a colorless oil: FTIR (thin film/NaCl) 3087, 2963, 2858, 1656, 1447, 1411, 1371, 1301, 1253, 1217 cm⁻¹; ¹H NMR (400 MHz, CDCl₃) δ 5.76 (dd, *J* = 10.8, 17.6 Hz, 1H), 5.23 (dd, *J* = 1.2, 10.8 Hz, 1H), 5.18 (dd, *J* = 0.8, 17.2 Hz, 1H), 4.79-4.78 (m, 1H), 4.76 (ddd, *J* = 1.6, 1.6, 3.2 Hz), 4.62 (dd, *J* = 0.8, 2.0 Hz, 1H), 4.15 (dd, *J* = 3.2, 12.8 Hz, 1H), 3.03 (ddd, *J* = 2.0, 5.6, 10.8 Hz, 1H), 2.18 (dddd, *J* = 0.8, 3.2, 5.6, 12.8 Hz, 1H), 1.93 (ddd, *J* = 11.2, 12.8, 12.8 Hz, 1H), 1.71 (s, 3H), 1.29 (s, 3H), 0.18 (s, 9H); ¹³C NMR (100 MHz, CDCl₃) δ 154.0, 148.1, 142.4, 115.4, 110.7, 105.4, 64.8, 47.8, 42.6, 35.2, 19.8, 17.7, 0.5.

Preparation of α -Hydroxy Ketone **342**.



α -Hydroxy Ketone 342. To a solution of silyl enol ether **354** (13 mg, 0.046 mmol, 1.0 equiv.) in CH_2Cl_2 (0.46 mL) was added *m*-CPBA (77% by weight, 11 mg, 0.048 mmol, 1.05 equiv.) at room temperature. The reaction was stirred until determined complete by TLC (approx. 3hrs) whereupon an aliquot of $\text{Na}_2\text{S}_2\text{O}_3$ was added. The resulting mixture was extracted with EtOAc, washed with NaHCO_3 and brine, and dried over MgSO_4 . After filtration and concentration, purification via column chromatography (10% EtOAc/hexanes) gave α -hydroxy ketone **342** (4 mg, 38% yield) as a colorless oil and as a single diastereomer: FTIR (thin film/ NaCl) 3486, 3086, 2948, 1715, 1647, 1447, 1415, 1377, 1285, 1252 cm^{-1} ; ^1H NMR (400 MHz, CDCl_3) δ 5.96 (dd, $J = 11.2, 17.6$ Hz, 1H), 5.43 (d, $J = 10.8$ Hz, 1H), 5.26 (d, $J = 17.2$ Hz, 1H), 4.99 (ddd, $J = 1.6, 1.6, 2.8$ Hz, 1H), 4.92 (s, 1H), 4.45 (d, $J = 11.2$ Hz, 1H), 4.08 (dd, $J = 5.2, 11.2$ Hz, 1H), 3.47 (s, 1H), 2.37-2.18 (m, 3H), 1.85 (s, 3H), 1.44 (s, 3H); ^{13}C NMR (100 MHz, CDCl_3) δ 210.3, 143.2, 137.9, 117.4, 113.9, 73.2, 63.1, 56.2, 50.9, 35.8, 19.3, 16.3; HRMS (EI) m/z 227.0842 [calcd for $\text{C}_{12}\text{H}_{16}\text{ClO}_2$ (M^+) 227.0844].

3.7 Notes and References.

- (1) Paterson, I.; Yeung, K.-S.; Ward, R. A.; Smith, J. D.; Cumming, J. G.; Lambolely, S. "The Total Synthesis of Swinholide A. Part 4: Synthesis of Swinholide A and Isoswinholide A from the Protected Monomeric Seco Acid, Pre-Swinholide A." *Tetrahedron* **1995**, *51*, 9467–9486.
- (2) Boger, D. L.; Cassidy, K. C.; Nakahara, S. "Total Synthesis of Streptonigrone" *J. Am. Chem. Soc.* **1993**, *115*, 10733–10741.
- (3) Kawatsura, M.; Hartwig, J. F. "Simple, Highly Active Palladium Catalysts for Ketone and Malonate Arylation: Dissecting the Importance of Chelation and Steric Hindrance" *J. Am. Chem. Soc.* **1999**, *121*, 1473–1478.
- (4) Storm, D. L.; Spencer, T. A. "Furan Synthesis by 1,4-Addition of Carboethoxycarbene to α -Methoxymethylene Ketones" *Tetrahedron Lett.* **1967**, *8*, 1865–1867.
- (5) Cava, M. P.; Litle, R. L.; Napier, D. R. "Condensed Cyclobutane Aromatic Systems. V. The Synthesis of Some α -Diazoindanones: Ring Contraction in the Indane Series" *J. Am. Chem. Soc.* **1958**, *80*, 2257–2263.

- (6) Muthusamy, S.; Gunanathan, C. "Rh₂(OAc)₄-Catalyzed Regioselective Intermolecular C–H Insertion Reactions: Novel Synthesis of 2-Pyrrol-3'-yloxindoles" *Synlett*, **2002**, *11*, 1783–1786.
- (7) Driver, T. G.; Franz, A. K.; Woerpal, K. A. "Diastereoselective Silacyclopropanations of Functionalized Chiral Alkenes" *J. Am. Chem. Soc.* **2002**, *124*, 6524–6525.
- (8) Wood, J. L.; Moniz, G. A.; Pflum, D. A.; Stoltz, B. M.; Holubec, A. A.; Dietrich, H. "Development of a Rhodium Carbenoid-Initiated Claisen Rearrangement for the Enantioselective Synthesis of α -Hydroxy Carbonyl Compounds" *J. Am. Chem. Soc.* **1999**, *121*, 1748–1749.
- (9) Moniz, G. A.; Wood, J. L. "Rhodium Carbonoid-Initiated Claisen Rearrangement: Scope and Mechanistic Observations" *Org. Lett.* **1999**, *1*, 371–374.
- (10) Moniz, G. A.; Wood, J. L. "Catalyst-Based Control of [2,3]- and [3,3]-Rearrangement in α -Diazoketone-Derived Propargyloxy Enols" *J. Am. Chem. Soc.* **2001**, *123*, 5095–5097.
- (11) Conia, J. M.; Le Perchec, P. "The Thermal Cyclisation of Unsaturated Carbonyl Compounds" *Synthesis*, **1975**, 1–19.

- (12) Hoffmann, H. M. R. "Ene reaction" *Angew. Chem., Int. Ed. Engl.* **1969**, *8*, 556–577.
- (13) Conia, J. M.; Leyendecker, F.; Dubois-Faget, C. "Le comportement thermique des cetonnes ethyleniques aliphatiques en fonction du nombre de carbonnes separant les deux centres insatures, et celui cis-alcoyl-2 acylcyclanes en fonction de la taille du cycle" *Tetrahedron Lett.* **1966**, *7*, 129–133.
- (14) a) Balme, G.; Bouyssi, D; Faure, R.; Gore, J.; Van Hemelryck, B. "Formation de cyclopentanes a partir de malonates δ -ethyleniques par un processus catalytique en palladium(0) stereochemie et mecanisme" *Tetrahedron* **1992**, *48*, 3891–3902.
b) McDonald, F. E.; Olson, T. C. "Group VI metal-promoted *endo*-carbocyclizations via alkyne-derived metal vinylidene carbenes" *Tetrahedron Lett.* **1997**, *38*, 7691–7692. c) Bouyssi, D.; Montiero, N.; Balme, G. "Intramolecular carbocupration reaction of unactivated alkynes bearing a stabilized nucleophile: Application to the synthesis of iridoid monoterpenes" *Tetrahedron Lett.* **1999**, *40*, 1297–1300. d) Kitagawa, O.; Suzuki, T; Inoue, T.; Watanabe, Y.; Taguchi, T. "Carbocyclization Reaction of Active Methine Compounds with Unactivated Alkenyl or Alkynyl Groups Mediated by $TiCl_4-Et_3N$ " *J. Org. Chem.* **1998**, *63*, 9470–9475.
- (15) Boaventura, M. A.; Drouin, J.; Conia, J. M. "Doubly Catalyzed Cyclization of ϵ -Acetylenic Carbonyl Compounds" *Synthesis*, **1983**, 801–804.

- (16) a) Cruciani, P.; Stammer, R.; Aubert, C.; Malacria, M. "New Cobalt-Catalyzed Cycloisomerization of ϵ -Acetylenic β -Keto Esters. Application to a Powerful Cyclization Reactions Cascade" *J. Org. Chem.* **1996**, *61*, 2699–2708. b) Cruciani, P.; Aubert, C.; Malacria, M. "Studies on diastereoselectivity of the cobalt(I) catalyzed cycloisomerization of substituted ϵ -acetylenic β -ketoester" *Tetrahedron Lett.* **1994**, *35*, 6677–6680. c) Renaud, J. L.; Aubert, C.; Malacria, M. "Cobalt-mediated cycloisomerization of δ -substituted ϵ -acetylenic β -ketoesters construction of angular triquinane by a sequence ene/Pauson-Khand reactions" *Tetrahedron* **1999**, *55*, 5113–5128.
- (17) Kennedy-Smith, J. J.; Staben, S. T.; Toste, F. D. "Gold(I)-Catalyzed Conia-Ene Reaction of β -Ketoesters with Alkynes" *J. Am. Chem. Soc.* **2004**, *126*, 4526–4527.
- (18) Corkey, B. K.; Toste, F. D. "Catalytic Enantioselective Conia-Ene Reaction" *J. Am. Chem. Soc.* **2005**, *127*, 17168–17169.
- (19) Lebold, T. P.; Leduc, A. B.; Kerr, M. A. "Zn(II)-Catalyzed Synthesis of Piperidines from Propargyl Amines and Cyclopropanes" *Org. Lett.* **2009**, *11*, 3770–3772.

- (20) Chun, Y. S.; Ko, Y. O.; Shin, H.; Lee, S. "Tandem Blaise-Alkenylation with Unactivated Alkynes: One-Pot Synthesis of α -Vinylated β -Enaminoesters from Nitriles" *Org. Lett.* **2009**, *11*, 3414–3417.
- (21) Gao, Q.; Zheng, B.; Li, J.; Yang, D. "Ni(II)-Catalyzed Conia-Ene Reaction of 1,3-Dicarbonyl Compounds with Alkynes" *Org. Lett.* **2005**, *7*, 2185–2188.
- (22) a) Itoh, Y.; Tsuji, H.; Yamagata, K.; Endo, K.; Tanaka, I.; Nakamura, M.; Nakamura, E. "Efficient Formation of Ring Structures Utilizing Multisite Activation by Indium Catalysis" *J. Am. Chem. Soc.* **2008**, *130*, 17161–17167. b) Takahashi, K.; Midori, M.; Kawano, K.; Ishihara, J.; Hatakeyama, S. "Entry to Heterocycles Based on Indium-Catalyzed Conia-Ene Reactions: Asymmetric Synthesis of (–)-Salinosporamide A" *Angew. Chem. Int. Ed.* **2008**, *47*, 6244–6246.
- (23) Kuninobu, Y.; Kawata, A.; Takai, K. "Rhenium-Catalyzed Insertion of Terminal Acetylenes into a C–H Bond of Active Methylene Compounds" *Org. Lett.* **2005**, *7*, 4823–4825.
- (24) Tsukamoto, Y.; Sato, K.; Kinoto, T.; Yanai, T. "13 β -Hydroxylation of Milbemycins by Selenium Dioxide" *Bull. Chem. Soc. Jpn.* **1992**, *65*, 3300–3307.

- (25) Perlman, N.; Albeck, A. "Efficient and Stereospecific Synthesis of (*Z*)-Hex-3-Enedioic Acid, A Key Intermediate for Gly-Gly *Cis* Olefin Isostere" *Synth. Commun.* **2000**, *30*, 4443–4449.
- (26) Kharasch, M. S.; Sosnovsky, G.; Yang, N. C. "Reactions of *t*-Butyl Perester. I. The Reaction of Peresters with Olefins" *J. Am. Chem. Soc.* **1959**, *81*, 5819–5824.
- (27) Brunel, J. M.; Billottet, L.; Letourneux, Y. "New Efficient and Totally Stereoselective Copper Allylic Benzoyloxylation of Sterol Derivatives" *Tetrahedron: Asymm.* **2005**, *16*, 3036–3041.
- (28) Dess, D. B.; Martin, J. C. "A useful 12-I-5 triacetoxyperiodinane (the Dess-Martin periodinane) for the selective oxidation of primary or secondary alcohols and a variety of related 12-I-5 species" *J. Am. Chem. Soc.* **1991**, *113*, 7277-7287.
- (29) a) Padwa, A.; Hornbuckle, S. F. "Ylide Formation from the Reaction of Carbenes and Carbenoids with Heteroatom Lone Pairs" *Chem. Rev.* **1991**, *91*, 263–309. b) Lu, C.-D.; Liu, H.; Chen, Z.-Y.; Hu, W.-H.; Mi, A.-Q. "Three-Component Reaction of Aryl Diazoacetates, Alcohols, and Aldehydes (or Imines): Evidence of Alcoholic Oxonium Ylide Intermediates" *Org. Lett.* **2005**, *7*, 83–86.
- (30) Fukuyama, T.; Chen, X. "Stereocontrolled Synthesis of (–)-Hapalindole G" *J. Am. Chem. Soc.* **1994**, *116*, 3125–3126.

- (31) Rubottom ox: Zoretic, P. A.; Wang, M.; Zhang, Y.; Shen, Z. "Total Synthesis of *d,l*-Isospongiadiol: An Intramolecular Radical Cascade Approach to Furanoditerpenes" *J. Org. Chem.* **1996**, *61*, 1806–1813.
- (32) Pangborn, A. B.; Giardello, M. A.; Grubbs, R. H.; Rosen, R. K.; Timmers, F. J. "Safe and Convenient Procedure for Solvent Purification" *Organometallics* **1996**, *15*, 1518–1520.
- (33) Still, W. C.; Kahn, M.; Mitra, A. "Rapid chromatographic technique for preparative separations with moderate resolution" *J. Org. Chem.* **1978**, *43*, 2923–2925.
- (34) Unambiguous mass could not be obtained for compound **354**.

**APPENDIX TWO: SPECTRA RELEVANT
TO CHAPTER THREE**

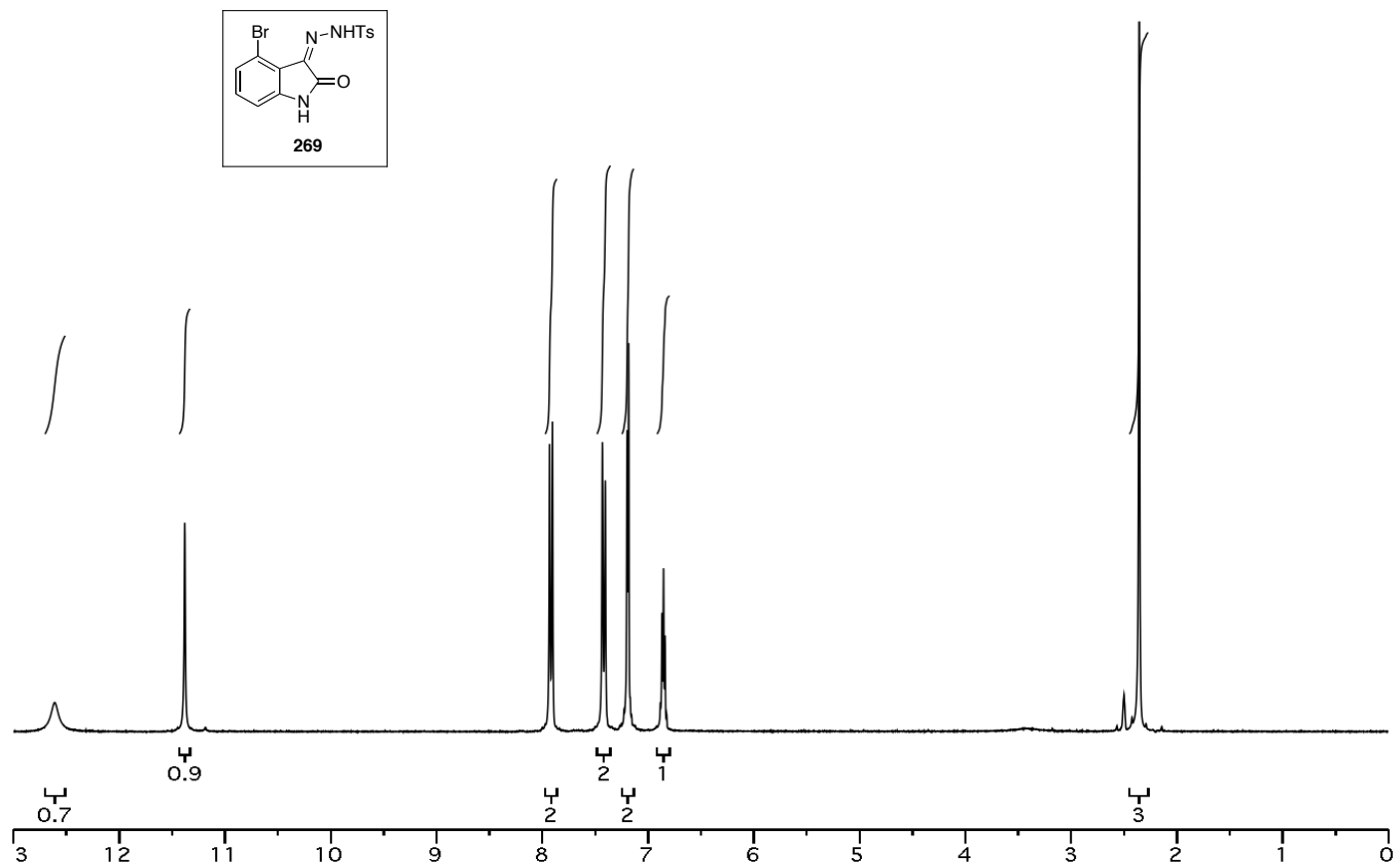


Figure A.2.1 ^1H NMR (300 MHz, DMSO-d_6) of compound **269**.

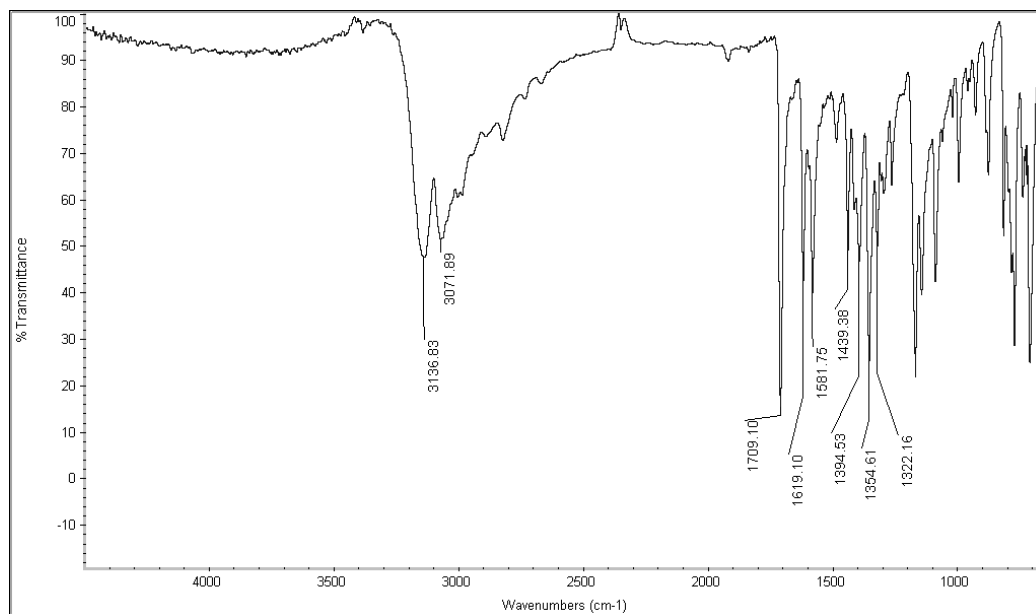


Figure A.2.2 Infrared Spectrum (KBr pellet) of compound **269**.

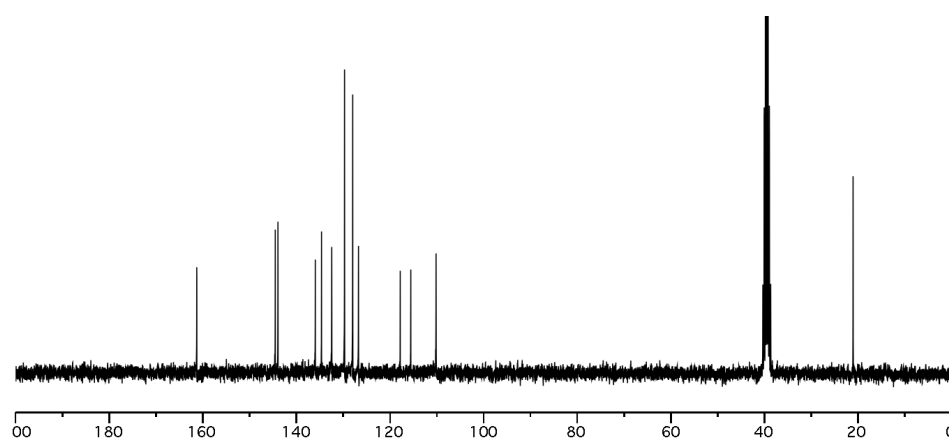


Figure A.2.3 ¹³C NMR (75 MHz, DMSO-d₆) of compound **269**.

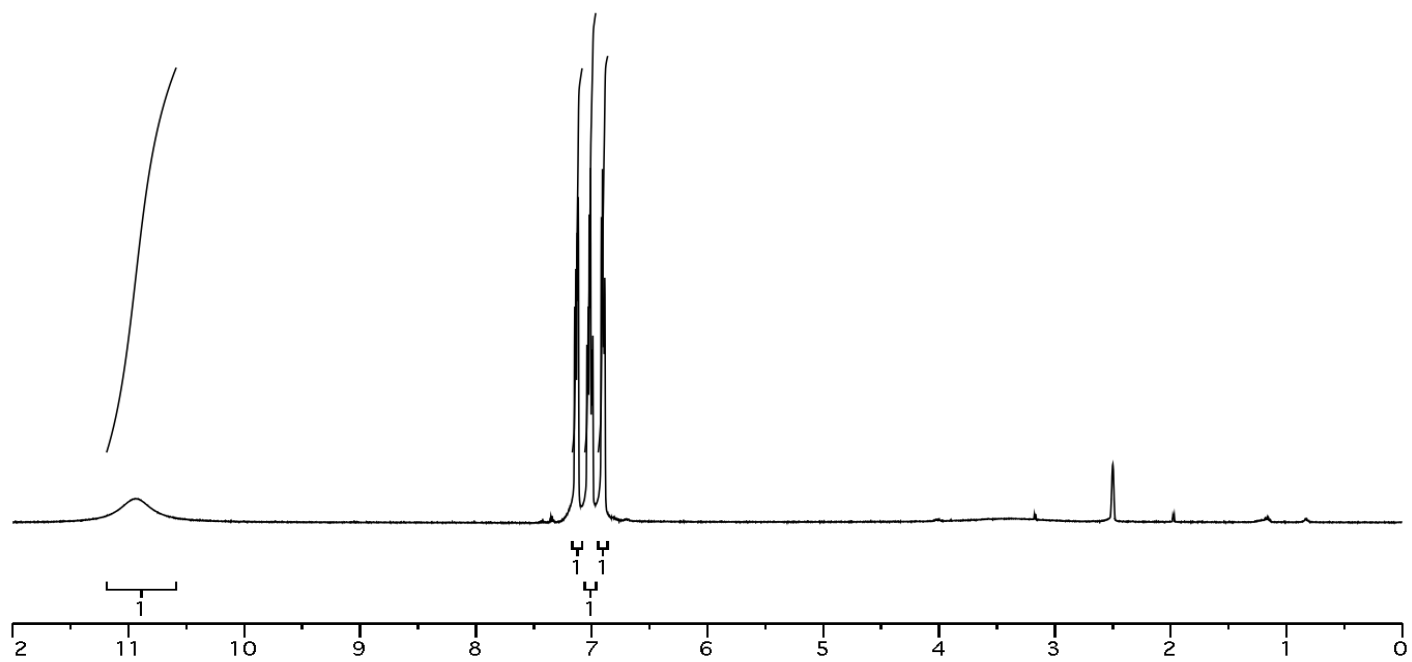
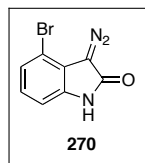


Figure A.2.4 ^1H NMR (400 MHz, DMSO-d_6) of compound **270**.

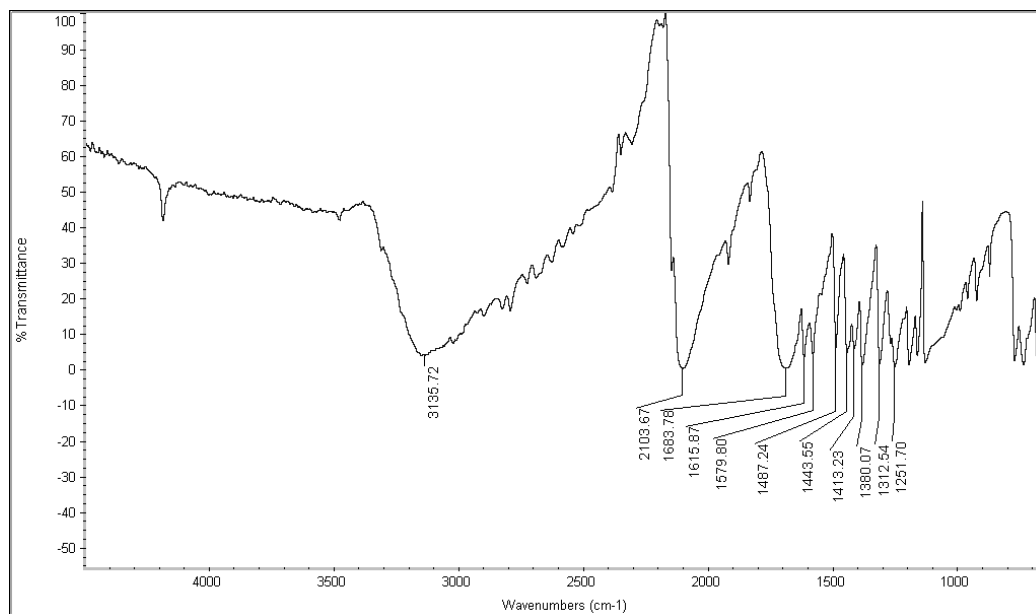


Figure A.2.5 Infrared Spectrum (thin film/NaCl) of compound **270**.

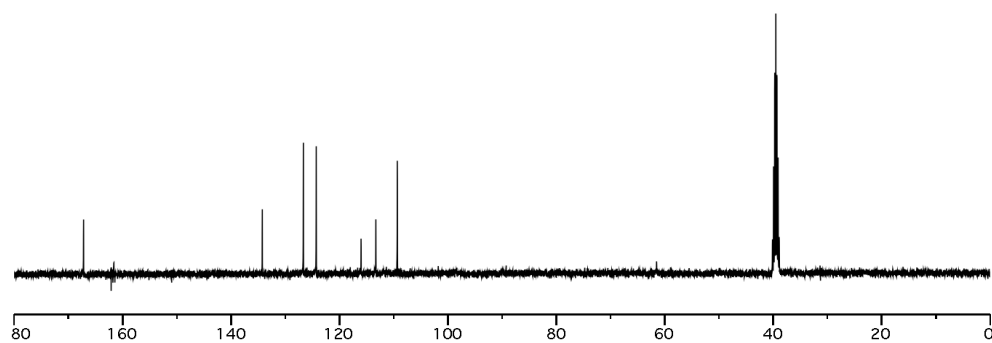


Figure A.2.6 ^{13}C NMR (100 MHz, DMSO-d_6) of compound **270**.

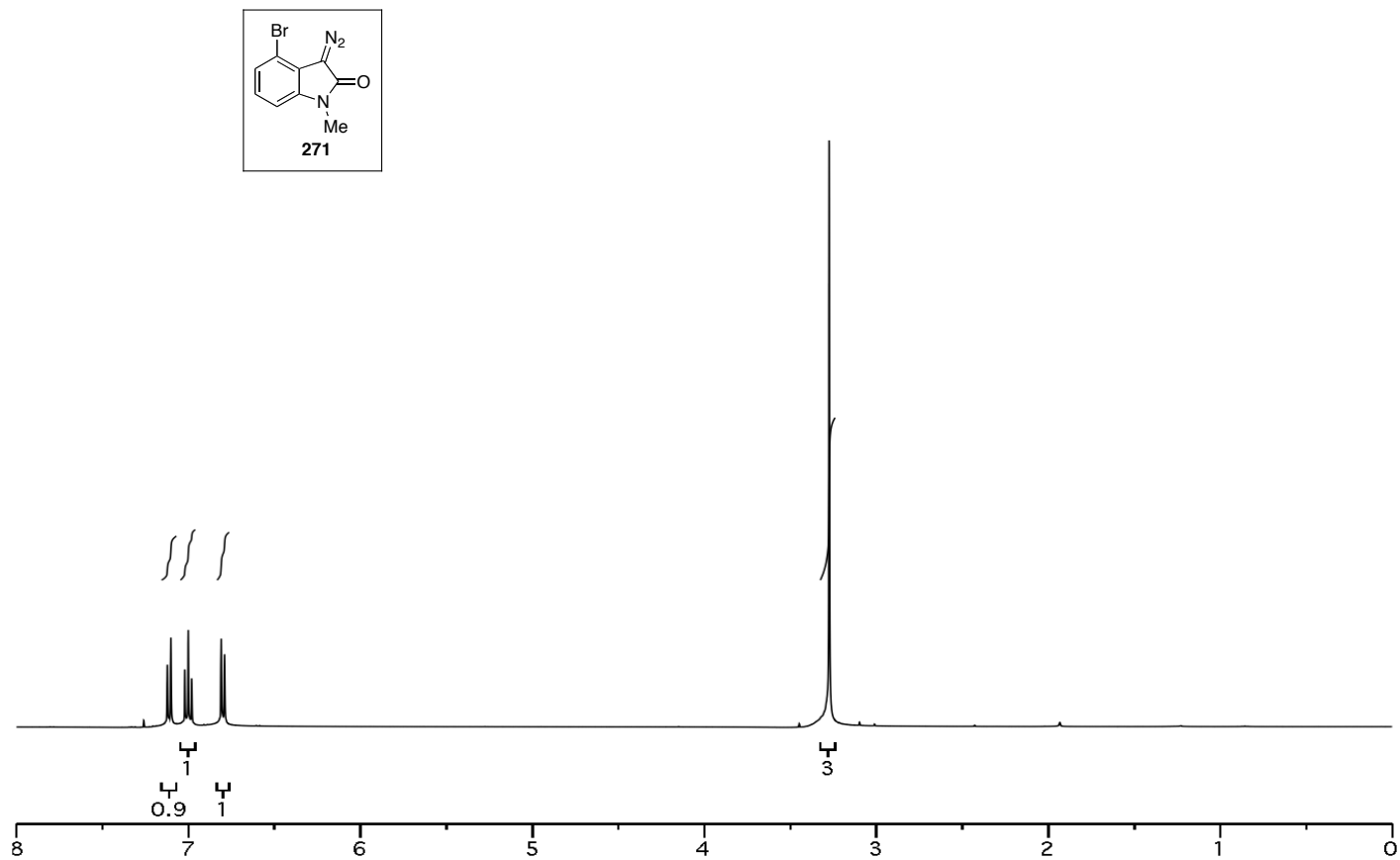


Figure A.2.7 ^1H NMR (400 MHz, CDCl_3) of compound **271**.

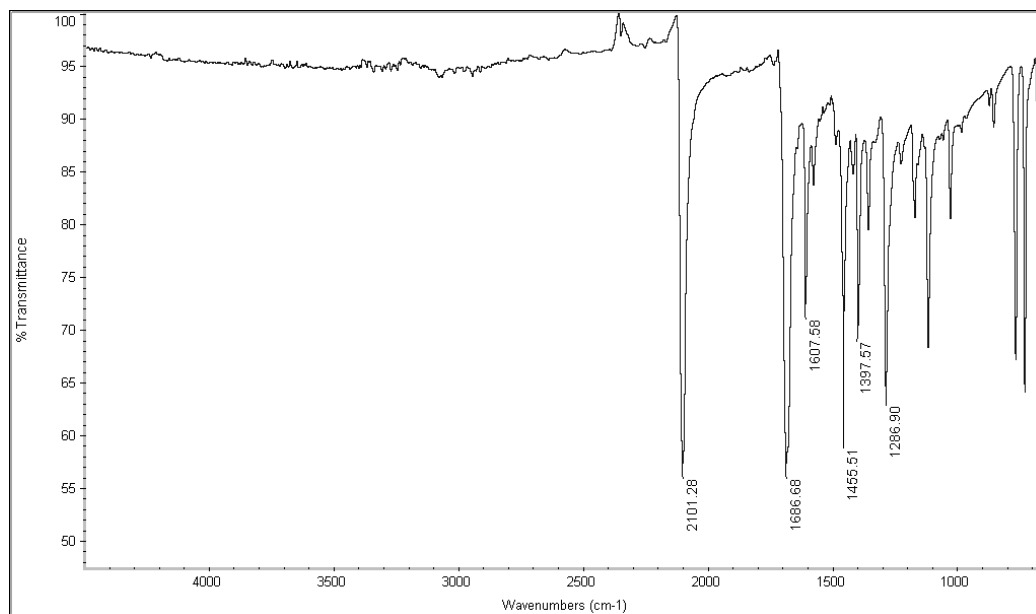


Figure A.2.8 Infrared Spectrum (thin film/NaCl) of compound **271**.

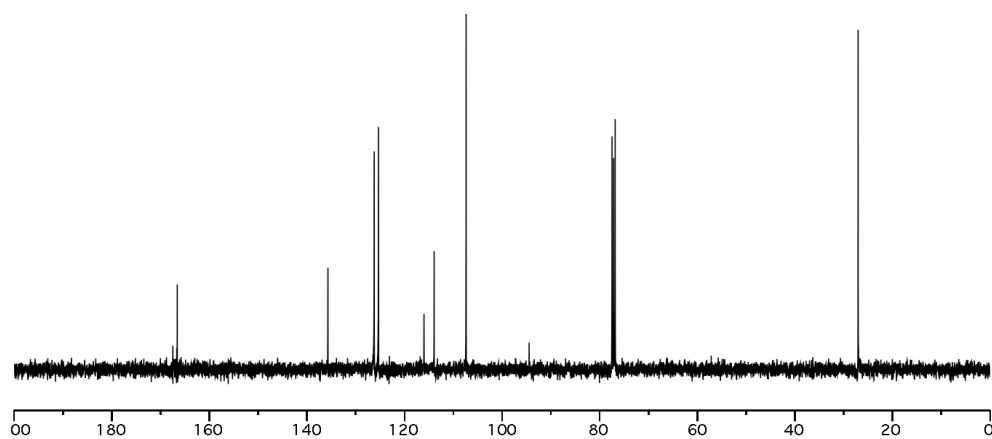


Figure A.2.9 ¹³C NMR (100 MHz, CDCl₃) of compound **271**.

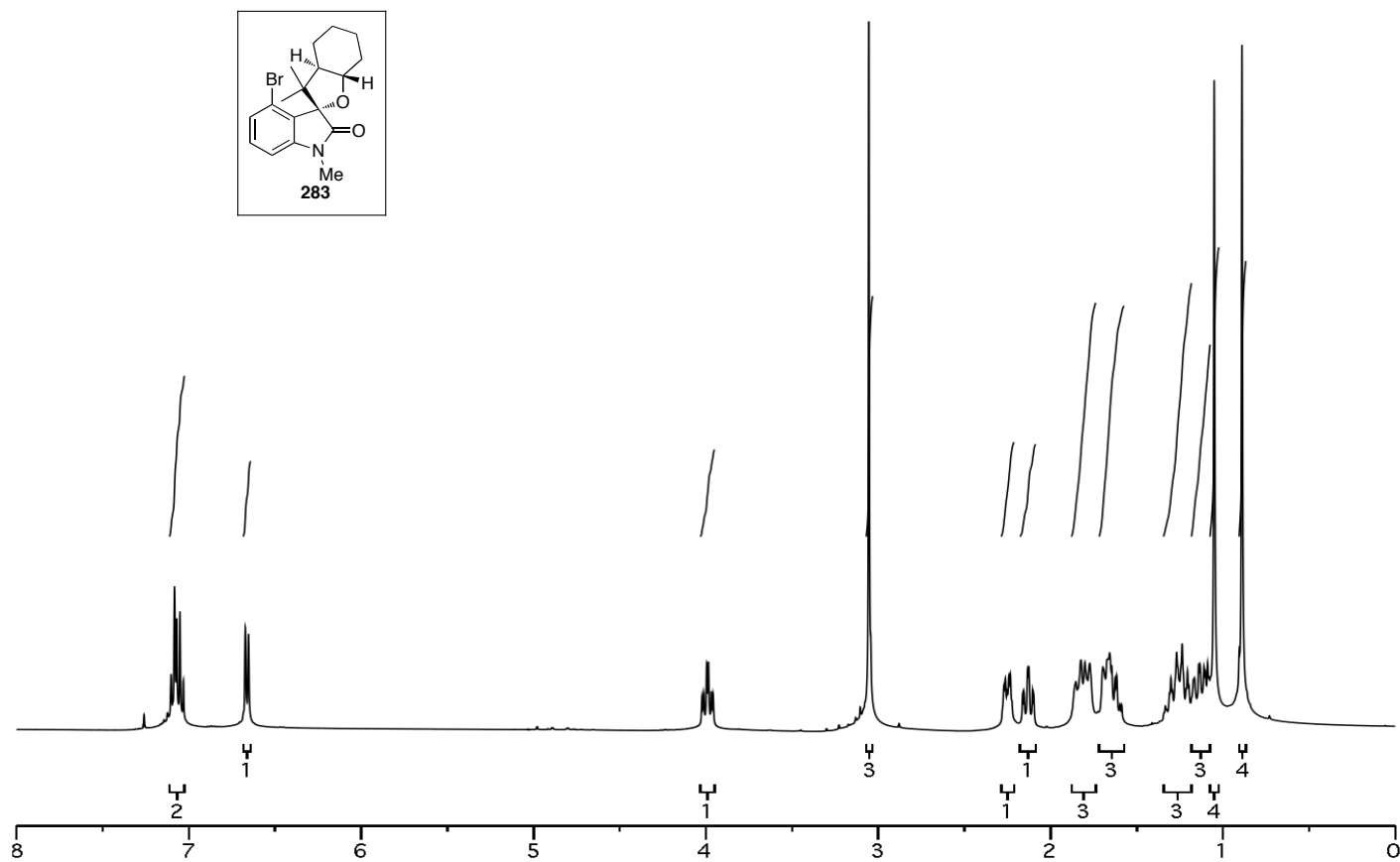


Figure A.2.10 ¹H NMR (400 MHz, CDCl₃) of compound 283.

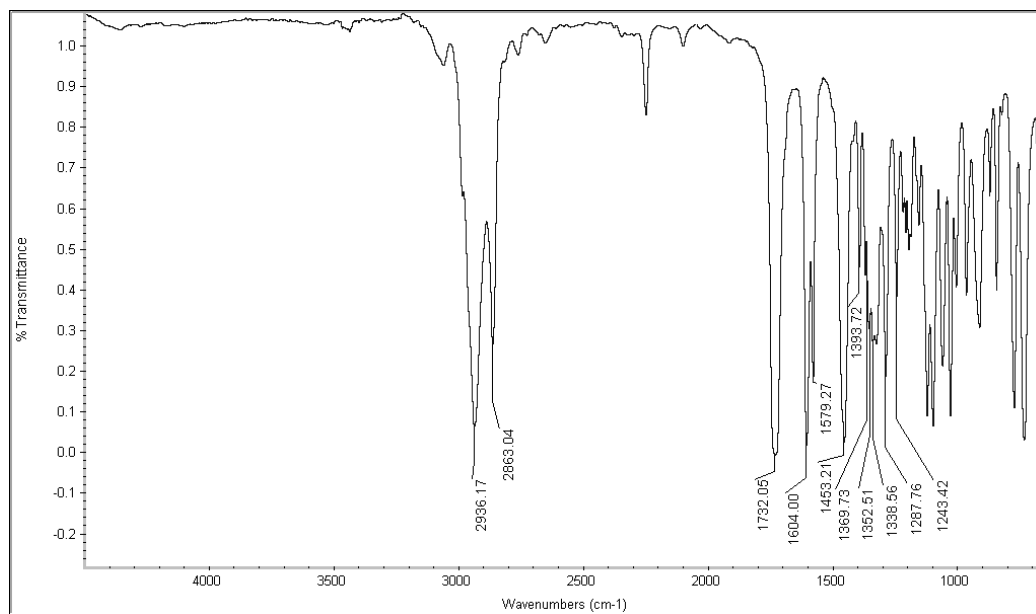


Figure A.2.11 Infrared Spectrum (thin film/NaCl) of compound **283**.

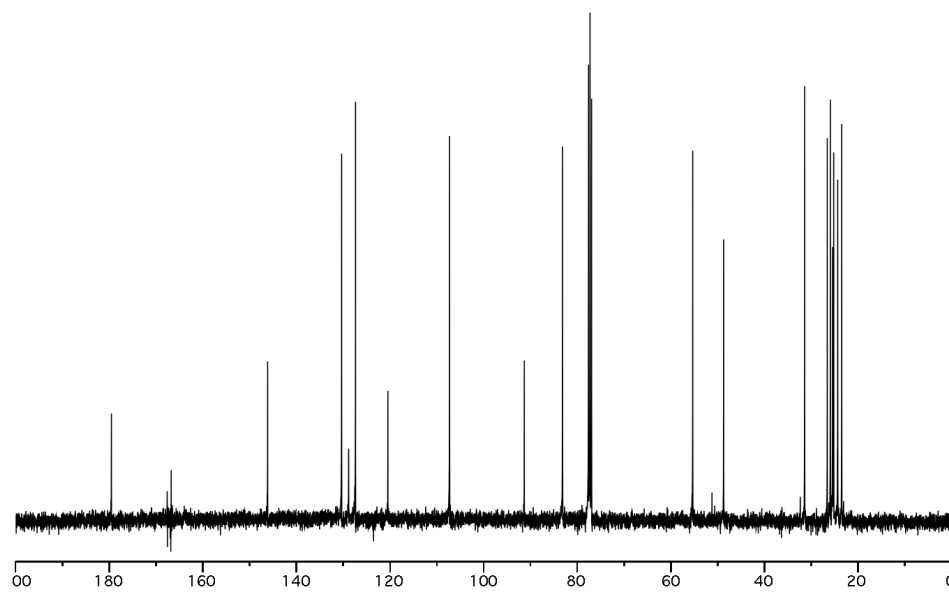


Figure A.2.12 ^{13}C NMR (100 MHz, CDCl_3) of compound **283**.

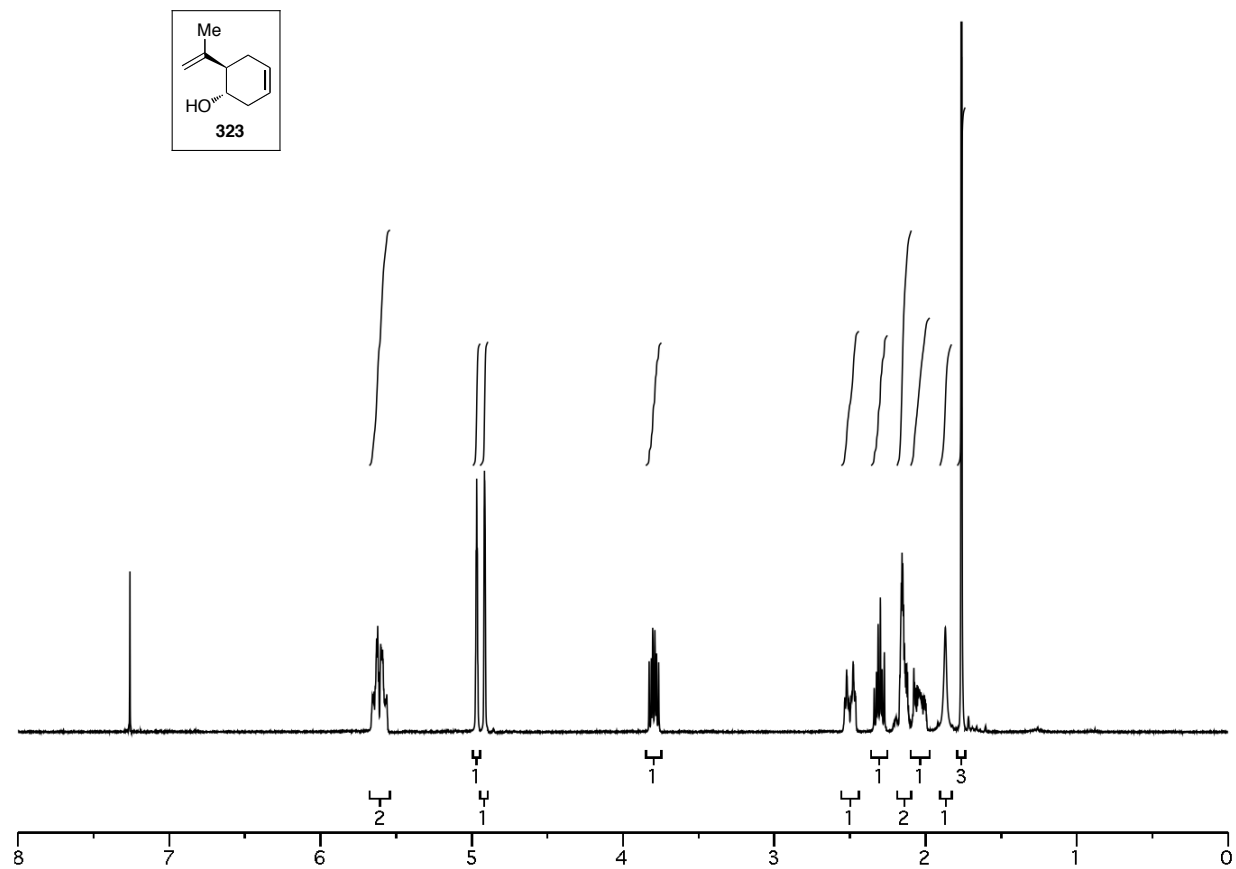


Figure A.2.13 ^1H NMR (400 MHz, CDCl_3) of compound **323**.

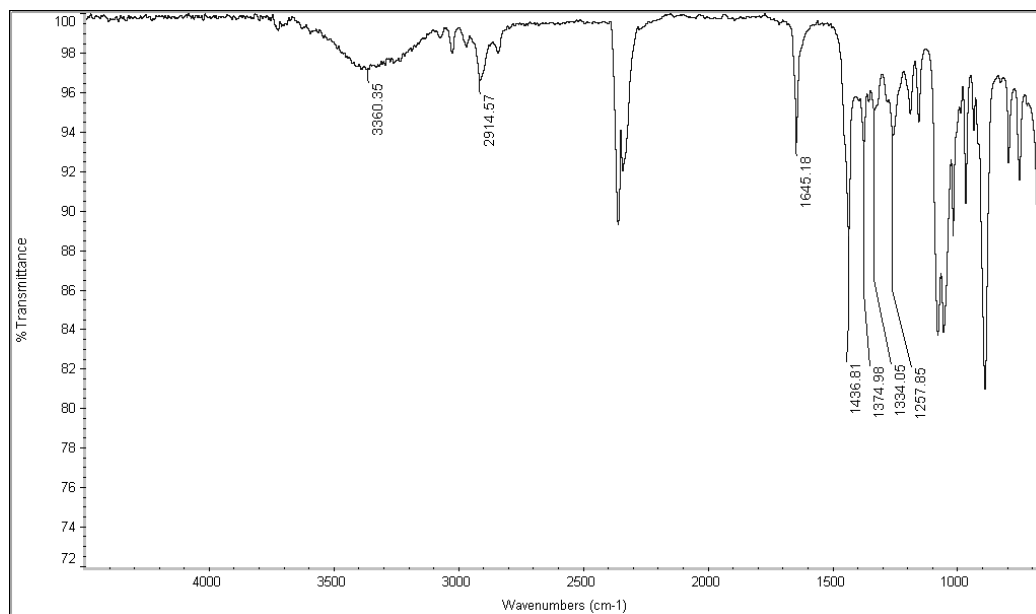


Figure A.2.14 Infrared Spectrum (thin film/NaCl) of compound **323**.

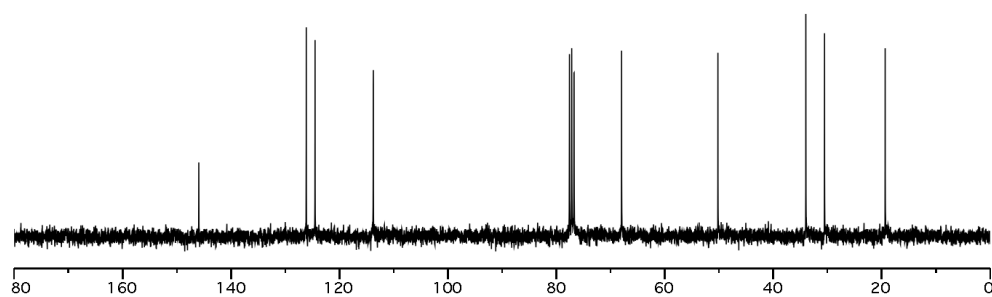


Figure A.2.15 ¹³C NMR (75 MHz, CDCl₃) of compound **323**.

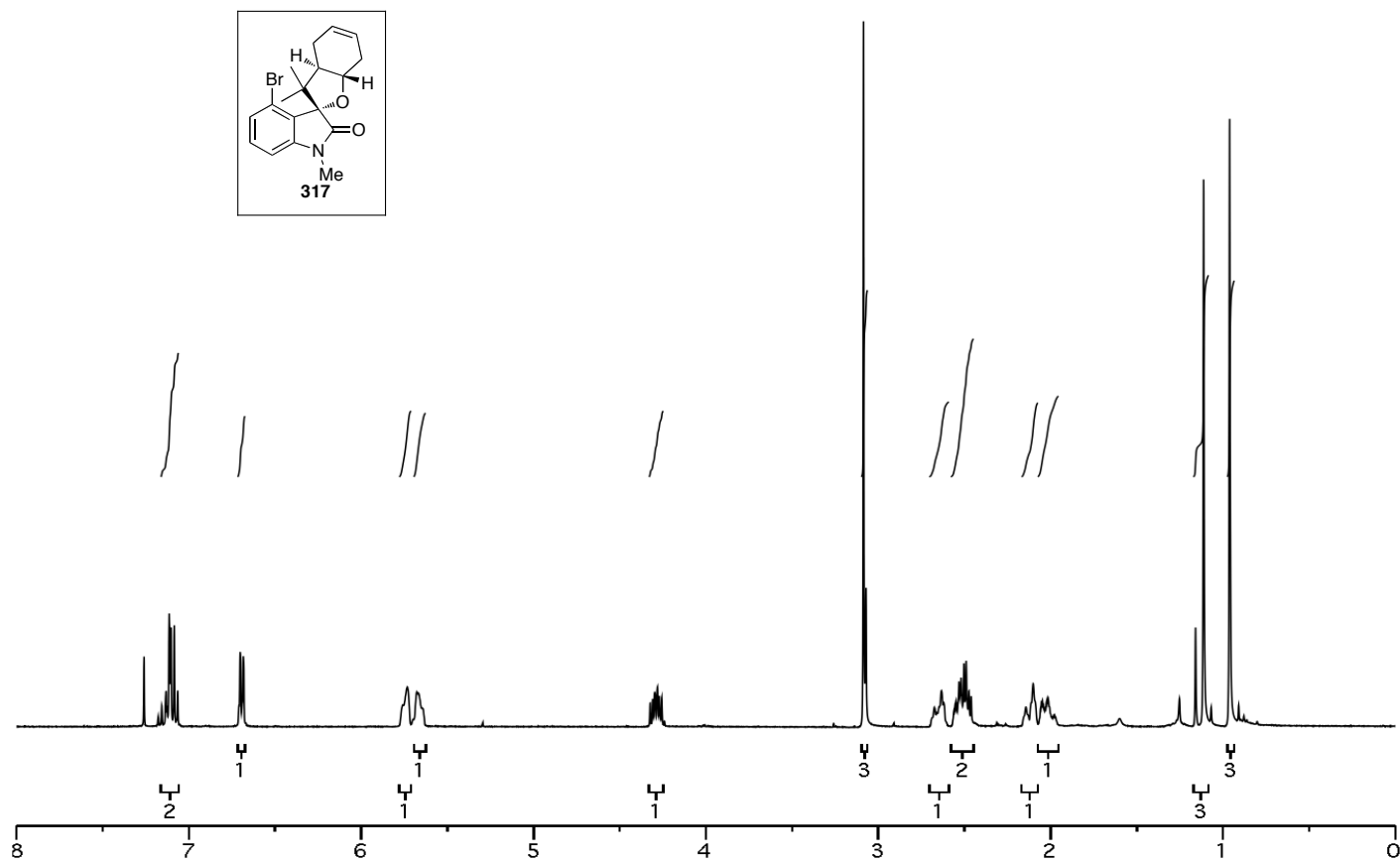


Figure A.2.16 ^1H NMR (400 MHz, CDCl_3) of compound 317.

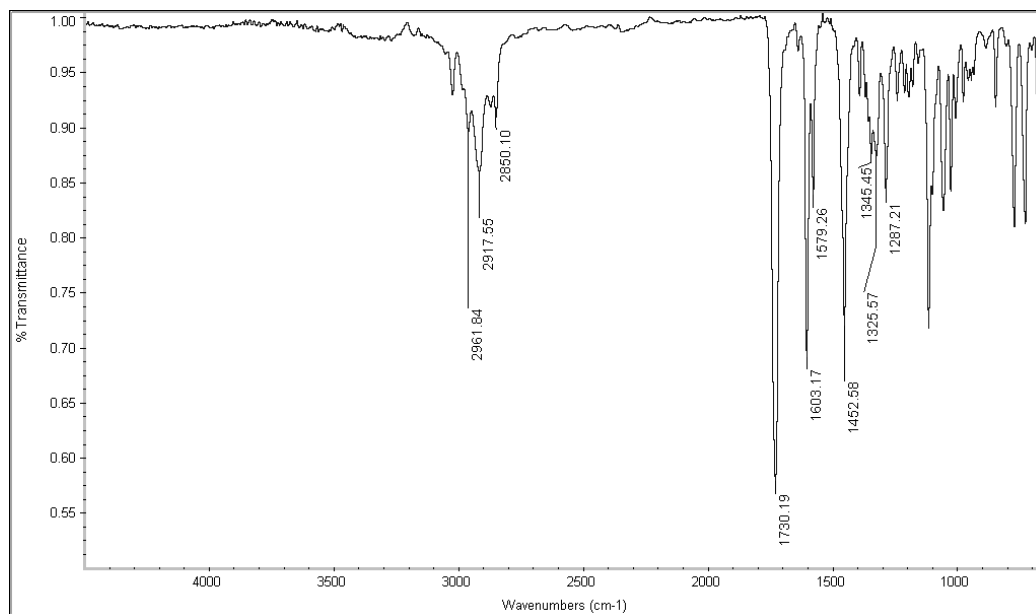


Figure A.2.17 Infrared Spectrum (thin film/NaCl) of compound **317**.

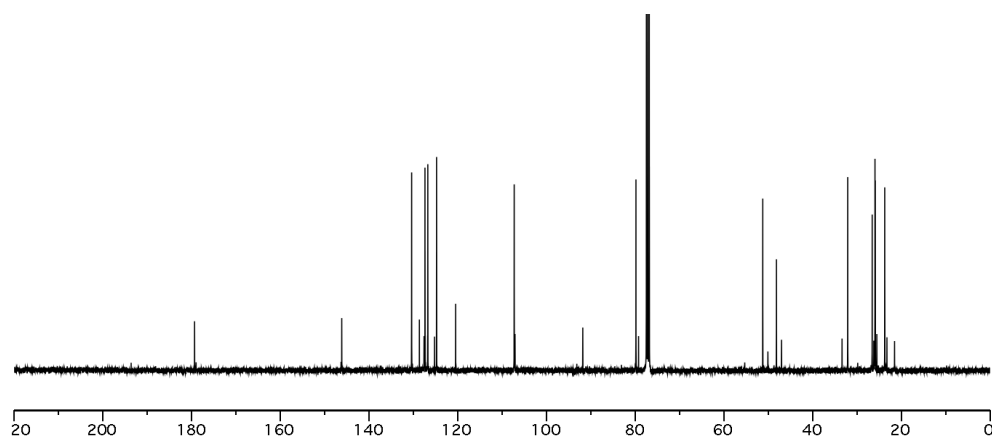


Figure A.2.18 ¹³C NMR (100 MHz, CDCl₃) of compound **317**.

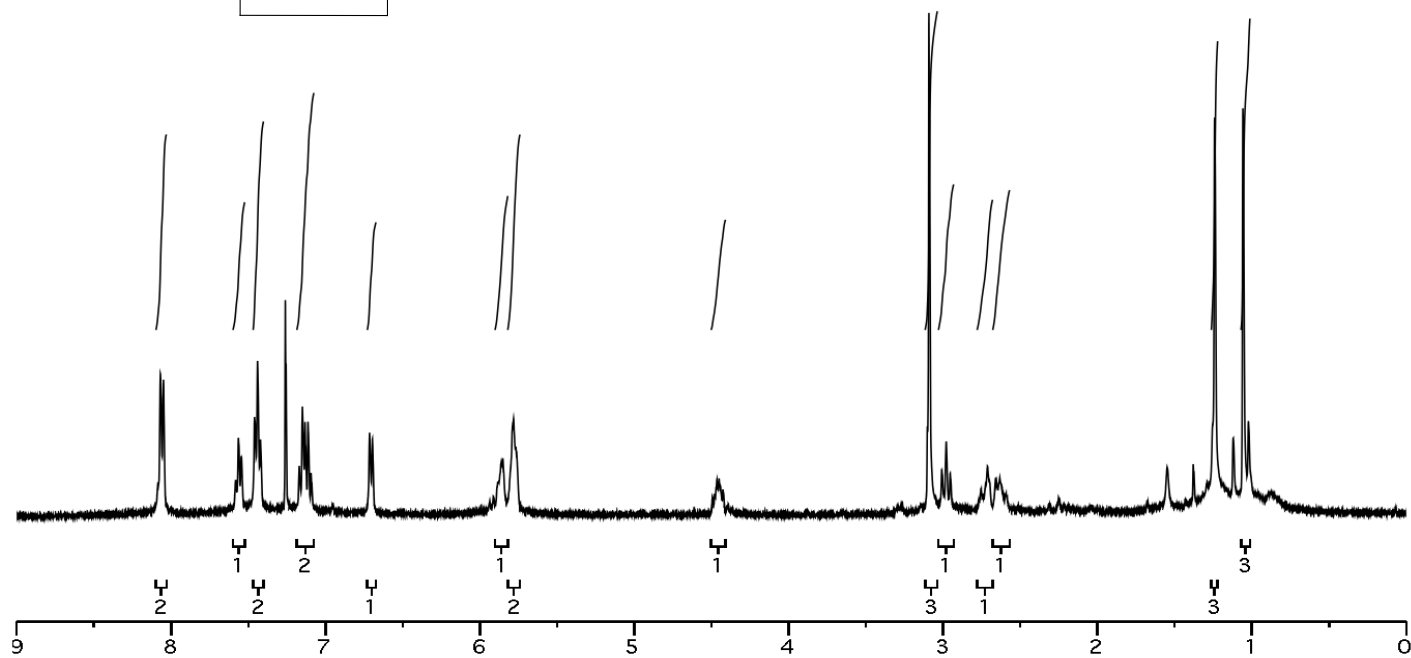
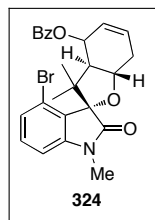


Figure A.2.19 ^1H NMR (400 MHz, CDCl_3) of compound 324.

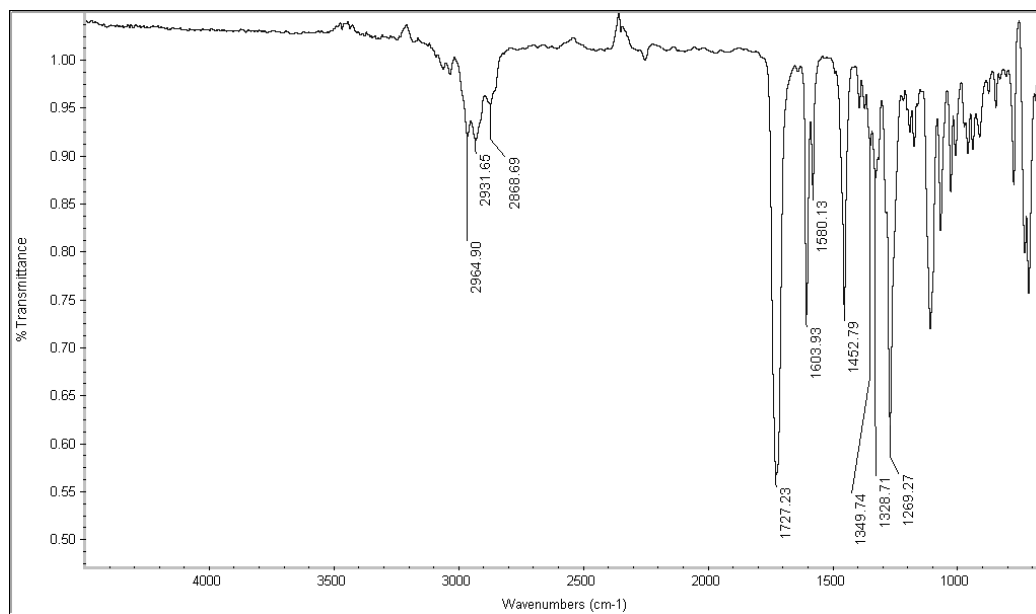


Figure A.2.20 Infrared Spectrum (thin film/NaCl) of compound **324**.

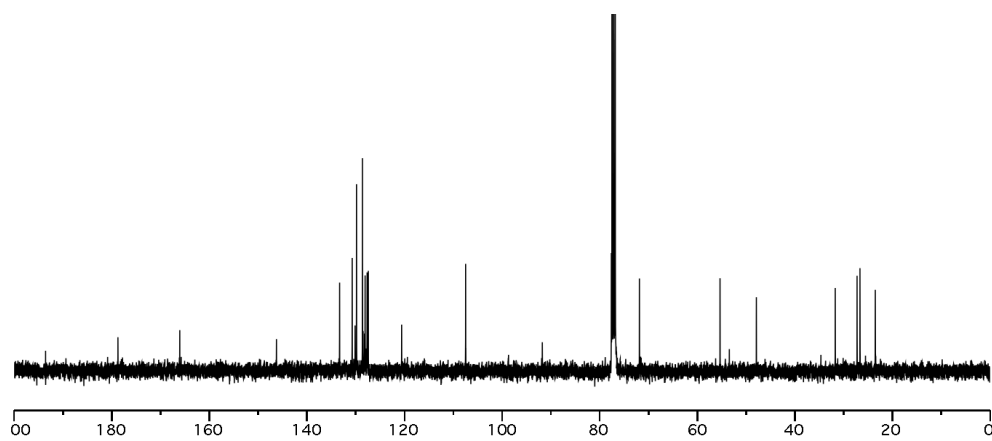


Figure A.2.21 ¹³C NMR (100 MHz, CDCl₃) of compound **324**.

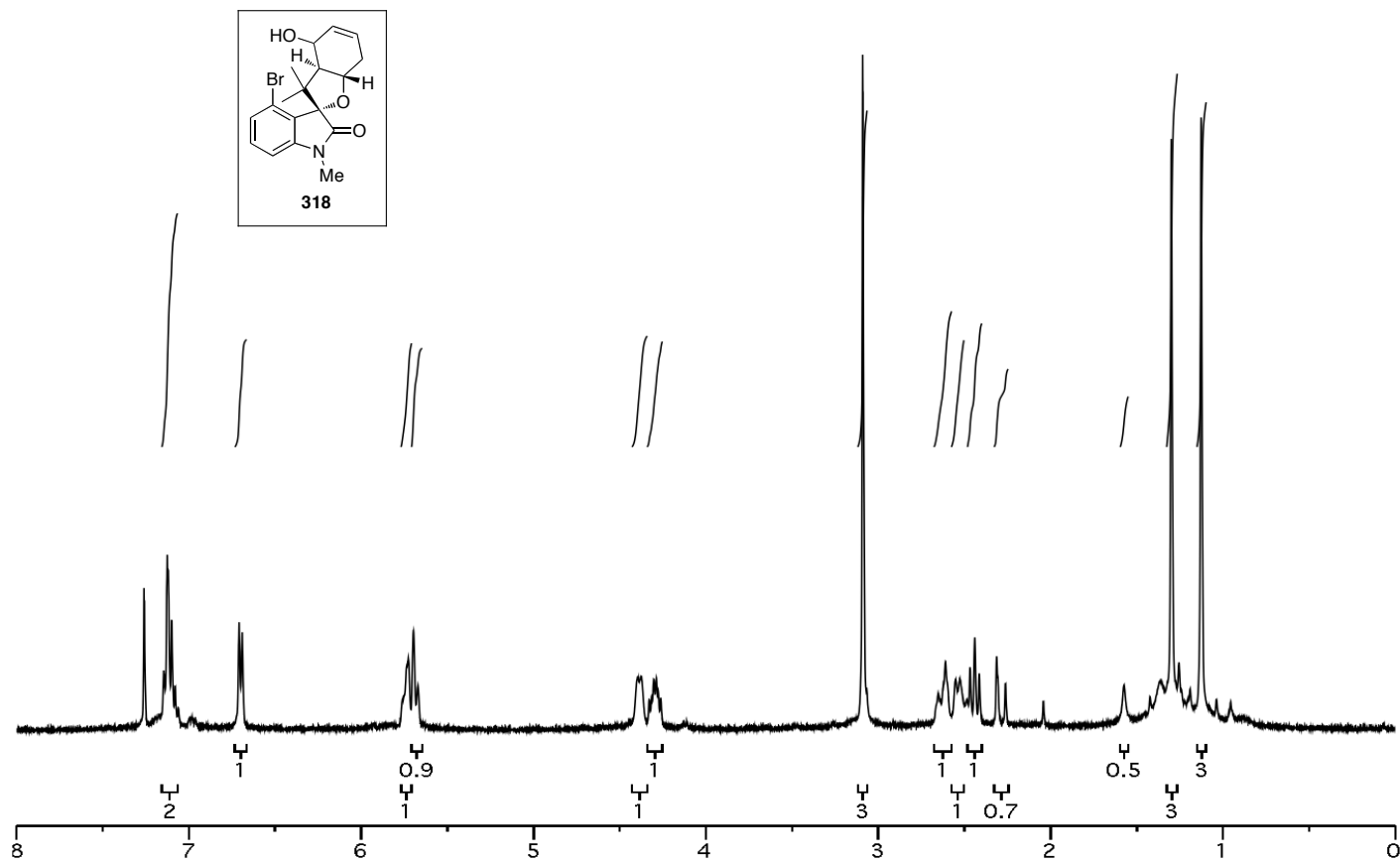


Figure A.2.22 ^1H NMR (400 MHz, CDCl_3) of compound **318**.

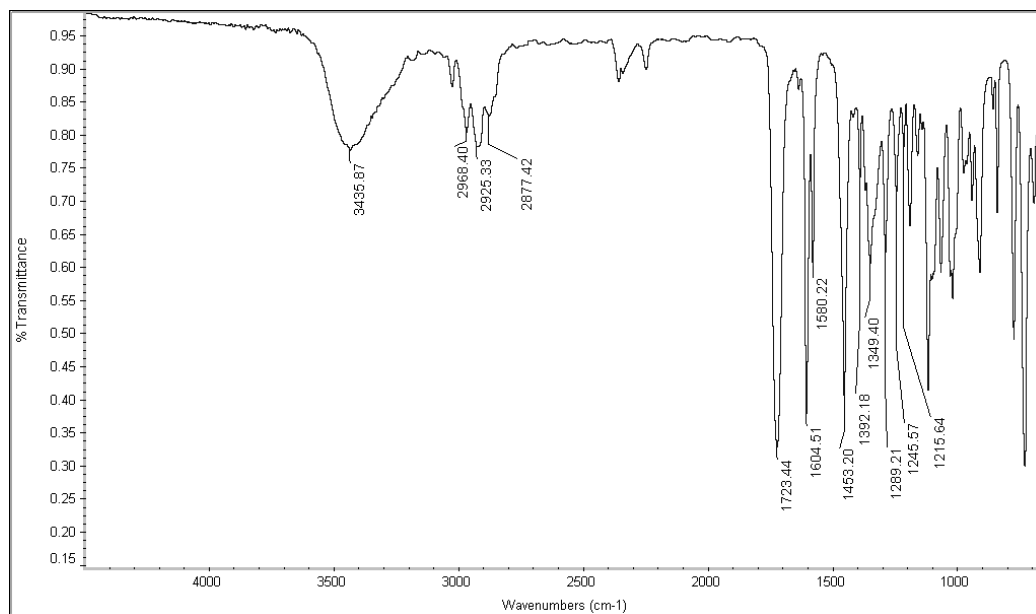


Figure A.2.23 Infrared Spectrum (thin film/NaCl) of compound **318**.

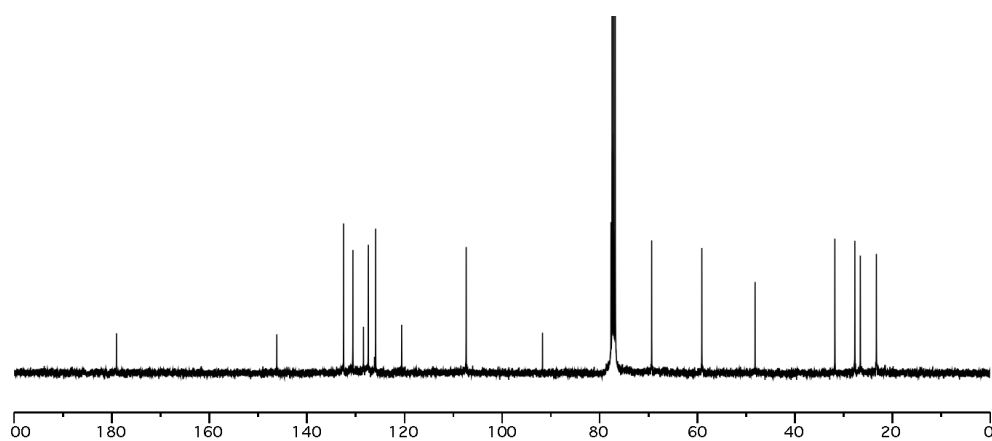


Figure A.2.24 ¹³C NMR (100 MHz, CDCl₃) of compound **318**.

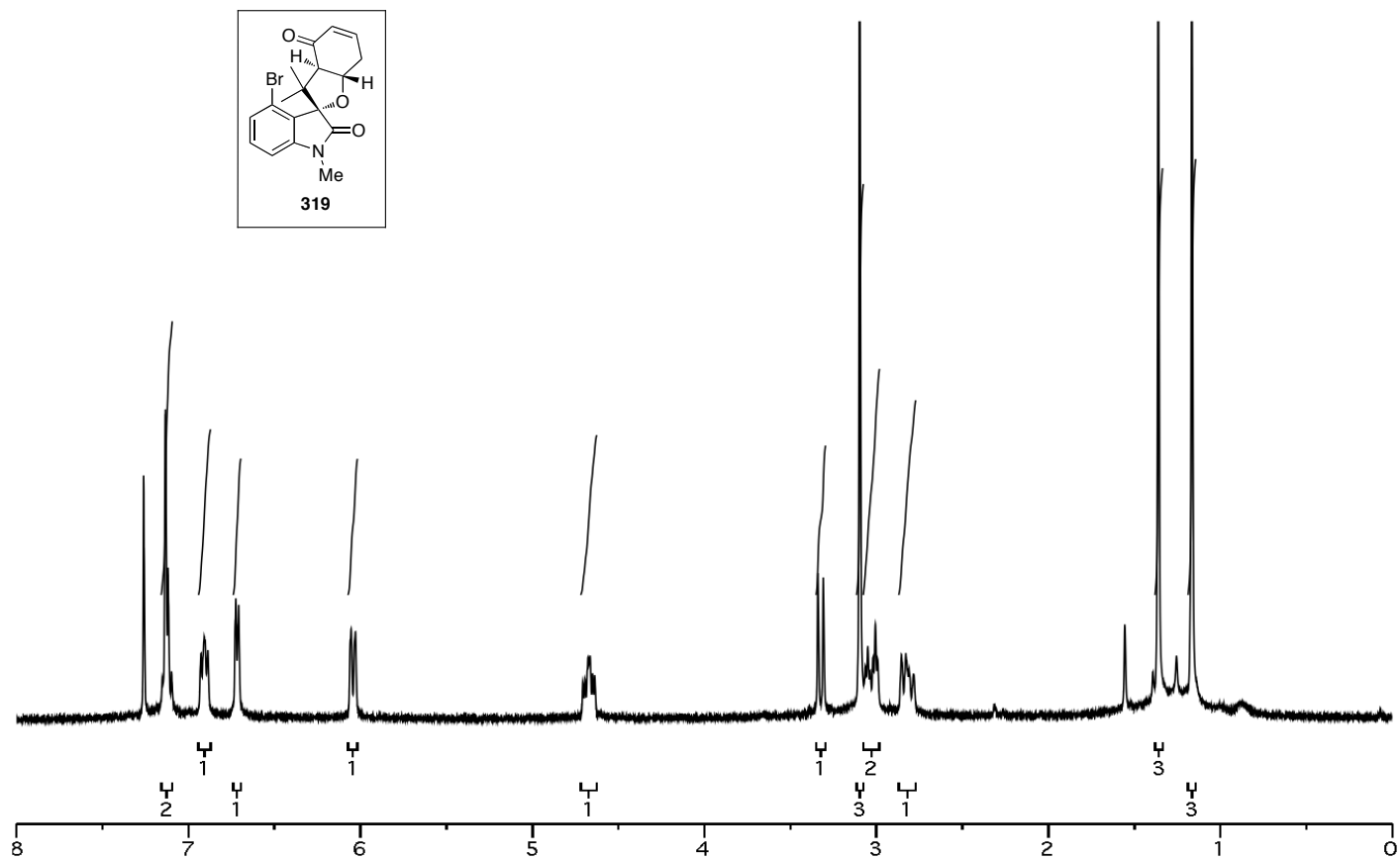


Figure A.2.25 ^1H NMR (400 MHz, CDCl_3) of compound 319.

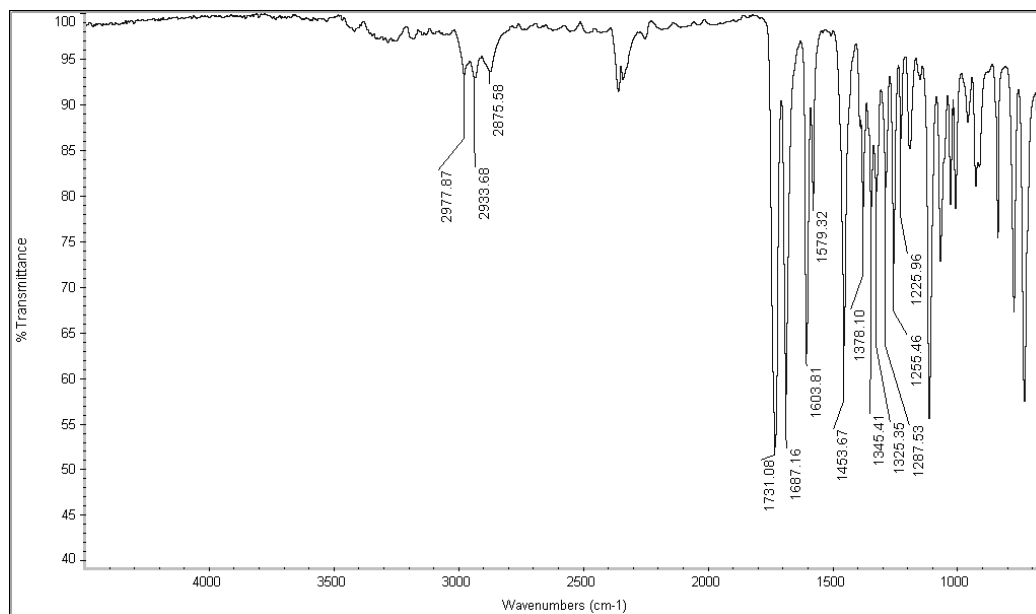


Figure A.2.26 Infrared Spectrum (thin film/NaCl) of compound **319**.

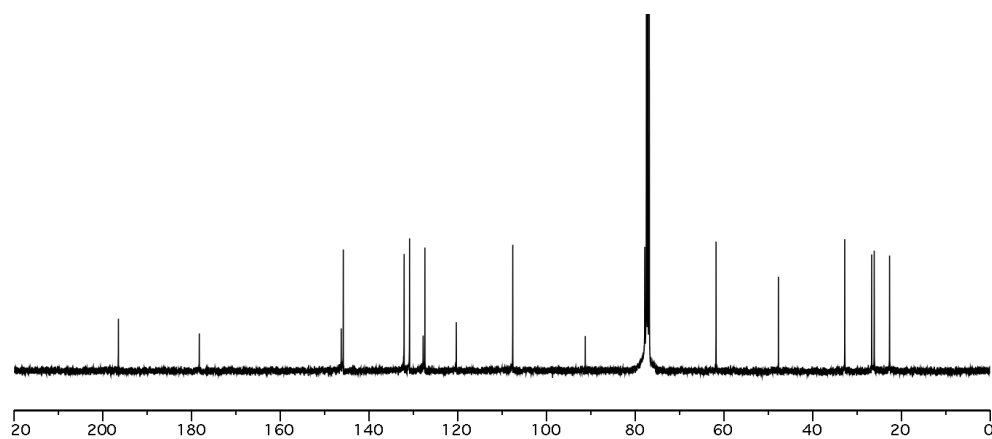


Figure A.2.27 ¹³C NMR (100 MHz, CDCl₃) of compound **319**.

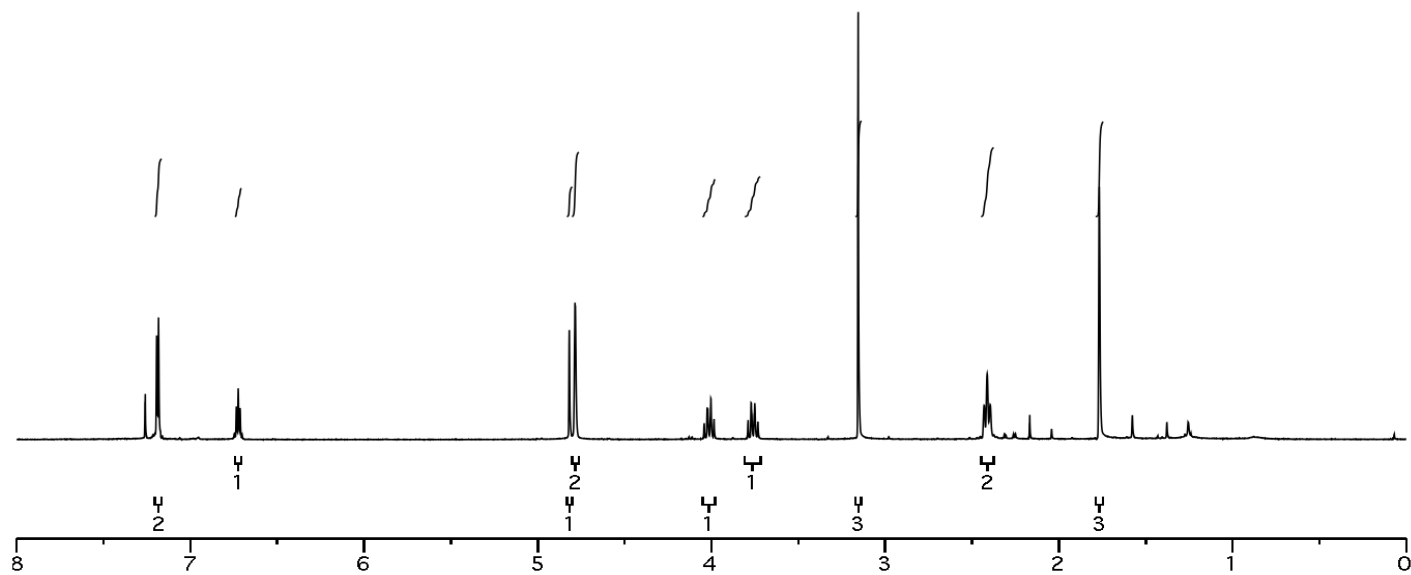
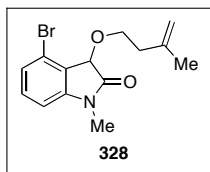


Figure A.2.28 ^1H NMR (400 MHz, CDCl_3) of compound 328.

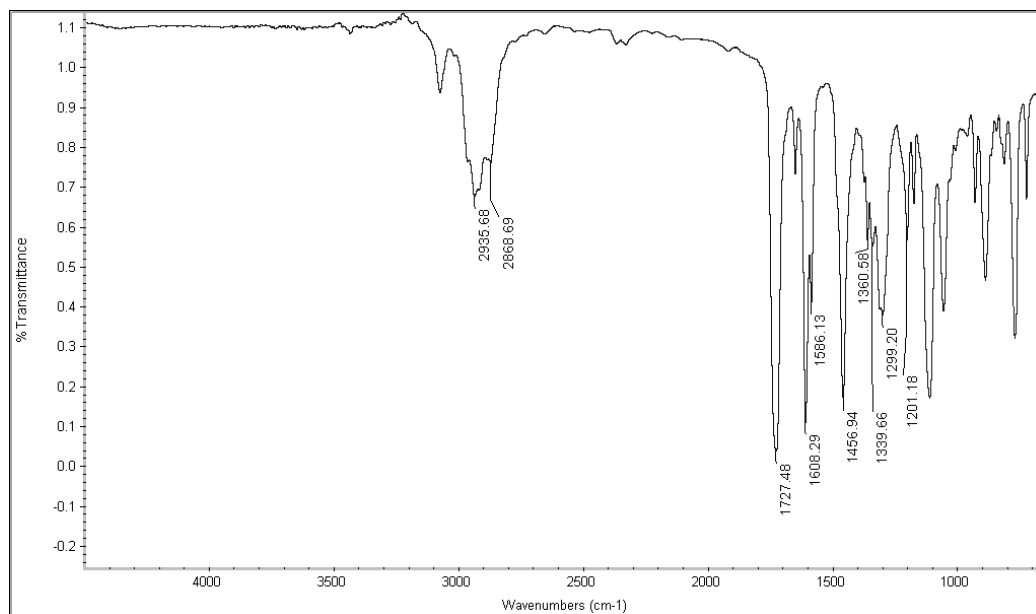


Figure A.2.29 Infrared Spectrum (thin film/NaCl) of compound **328**.

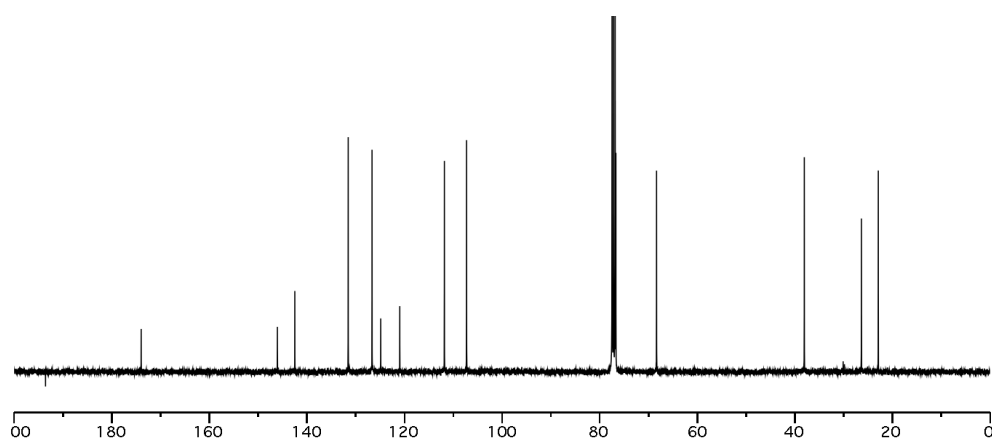


Figure A.2.30 ¹³C NMR (100 MHz, CDCl₃) of compound **328**.

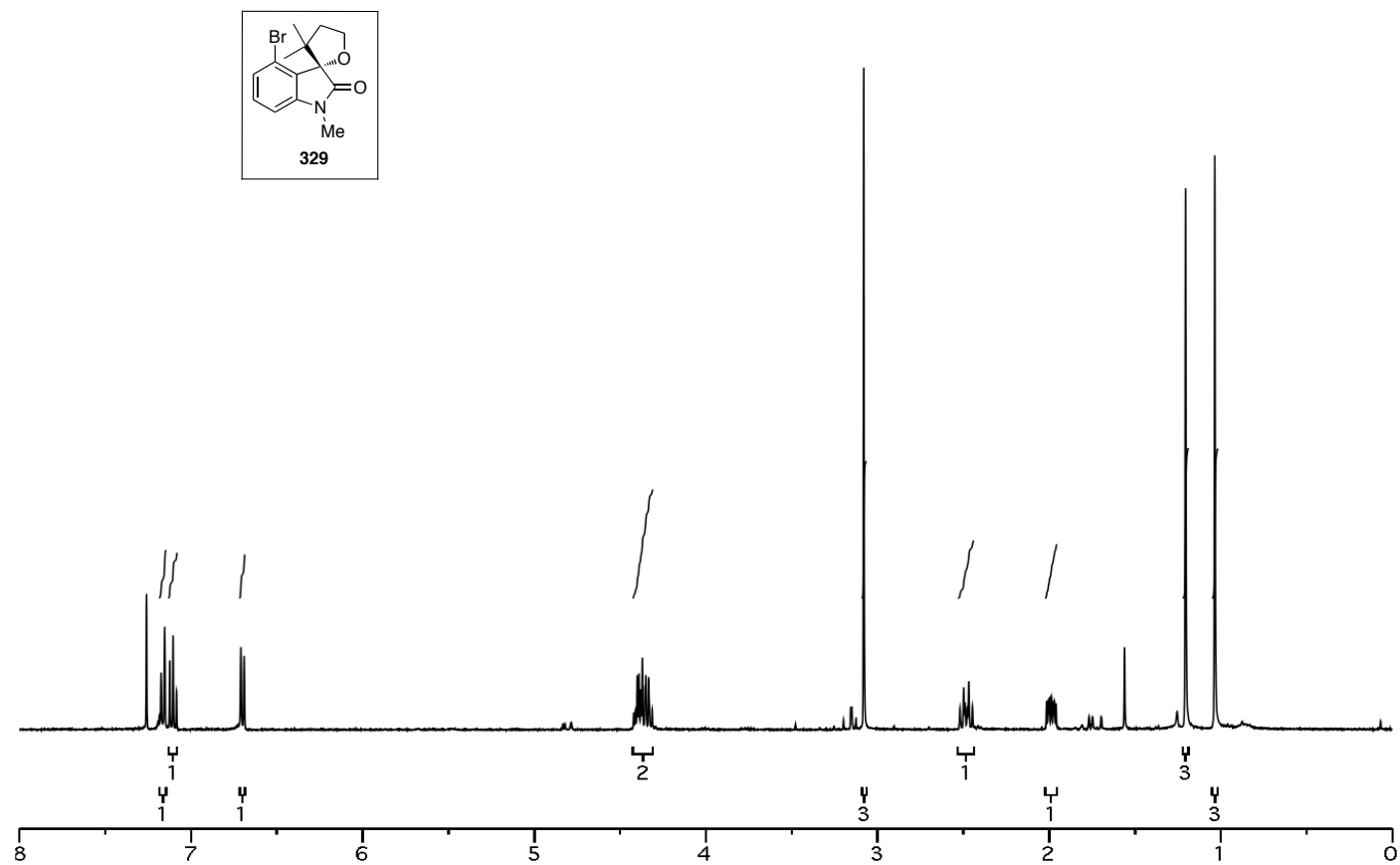


Figure A.2.31 ^1H NMR (400 MHz, CDCl_3) of compound **329**.

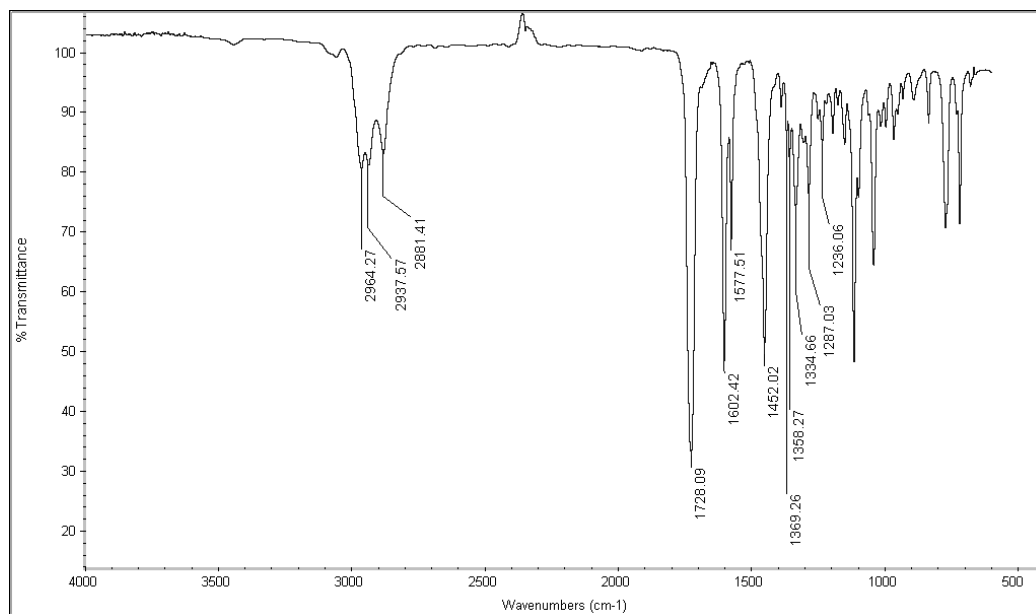


Figure A.2.32 Infrared Spectrum (thin film/NaCl) of compound **329**.

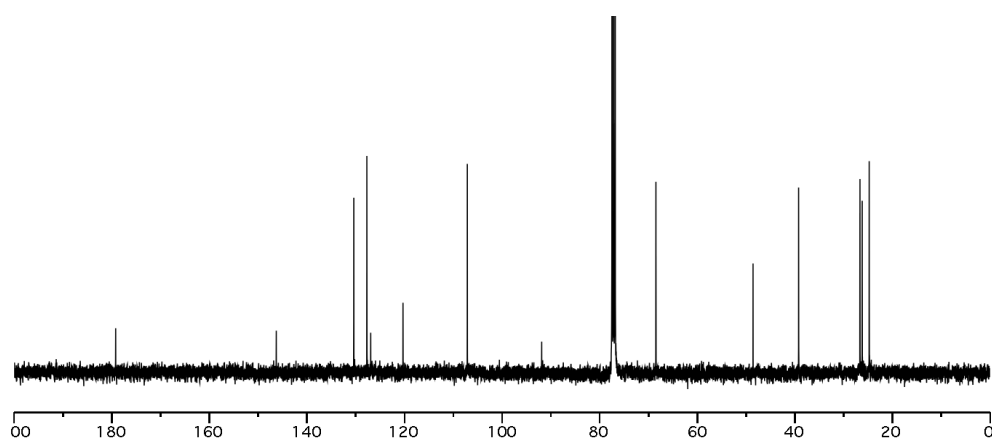


Figure A.2.33 ¹³C NMR (100 MHz, CDCl₃) of compound **329**.

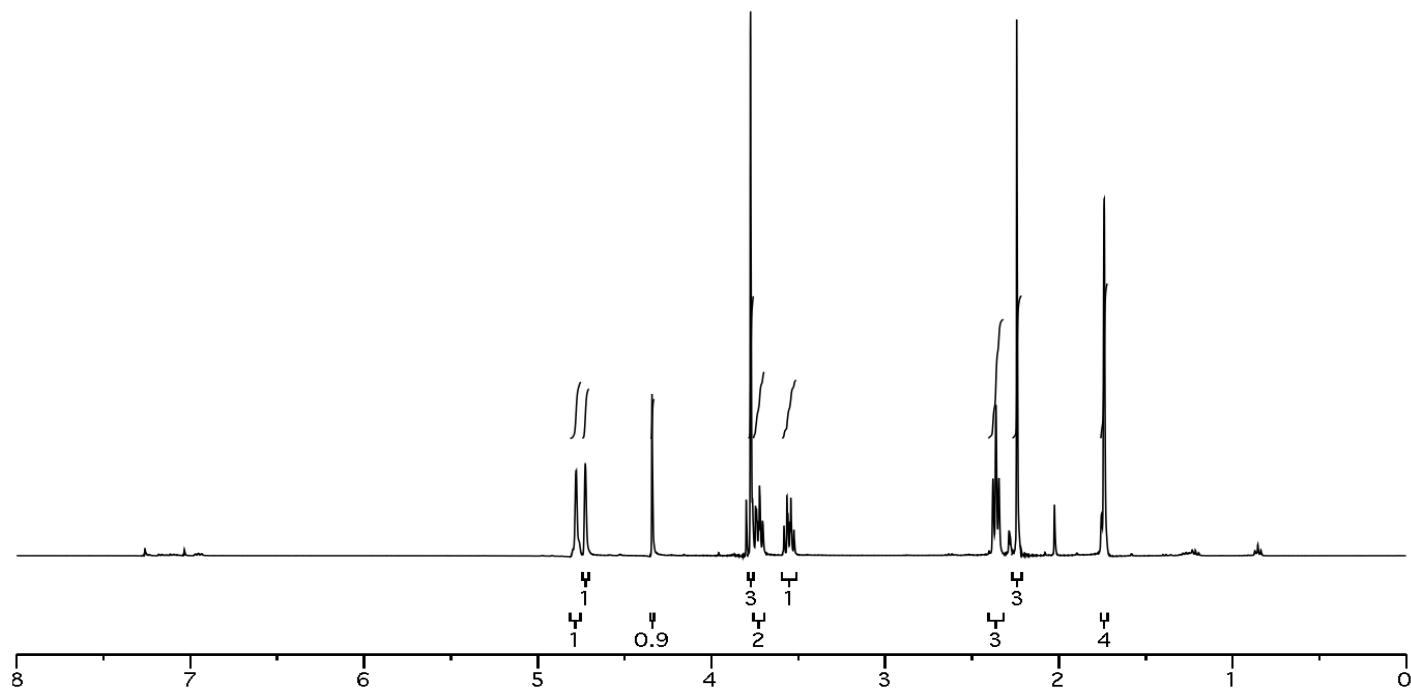
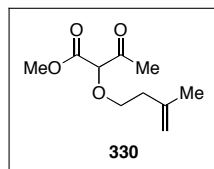


Figure A.2.34 ^1H NMR (400 MHz, CDCl_3) of compound **330**.

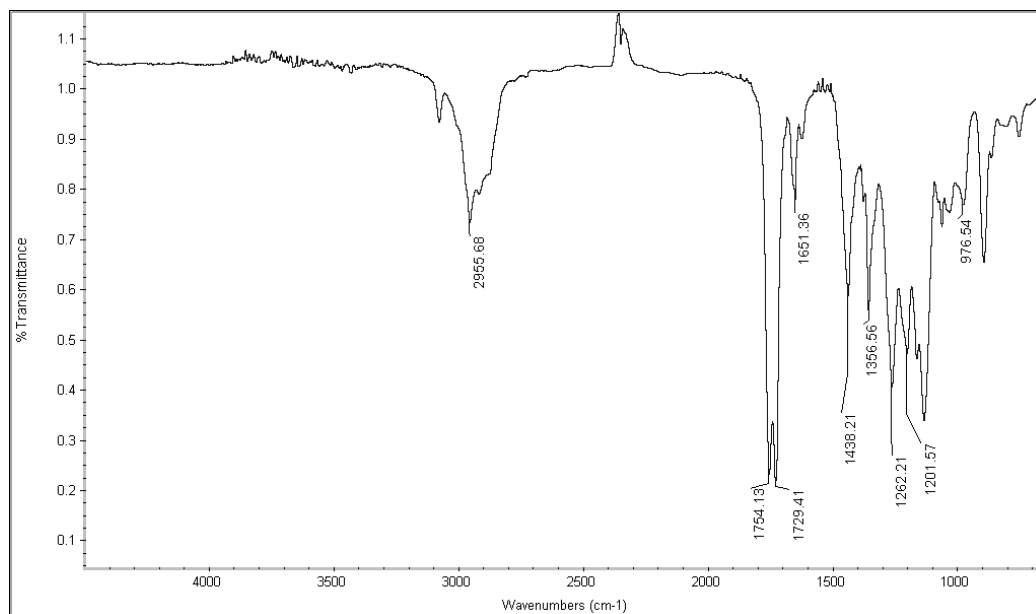


Figure A.2.35 Infrared Spectrum (thin film/NaCl) of compound **330**.

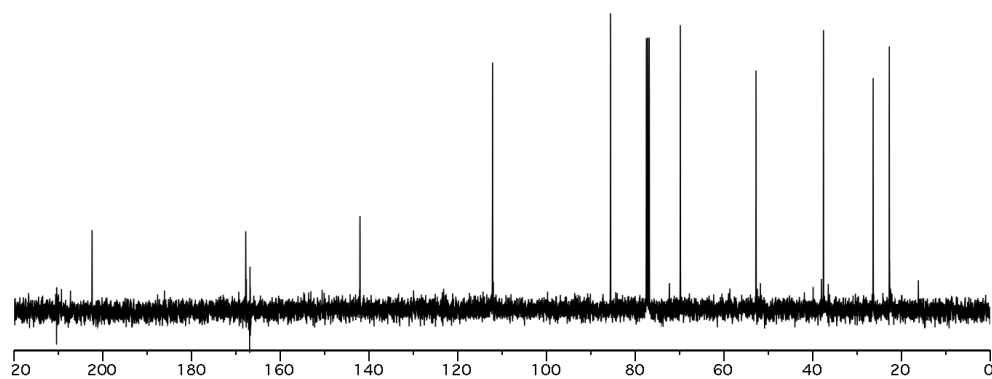


Figure A.2.36 ¹³C NMR (100 MHz, CDCl₃) of compound **330**.

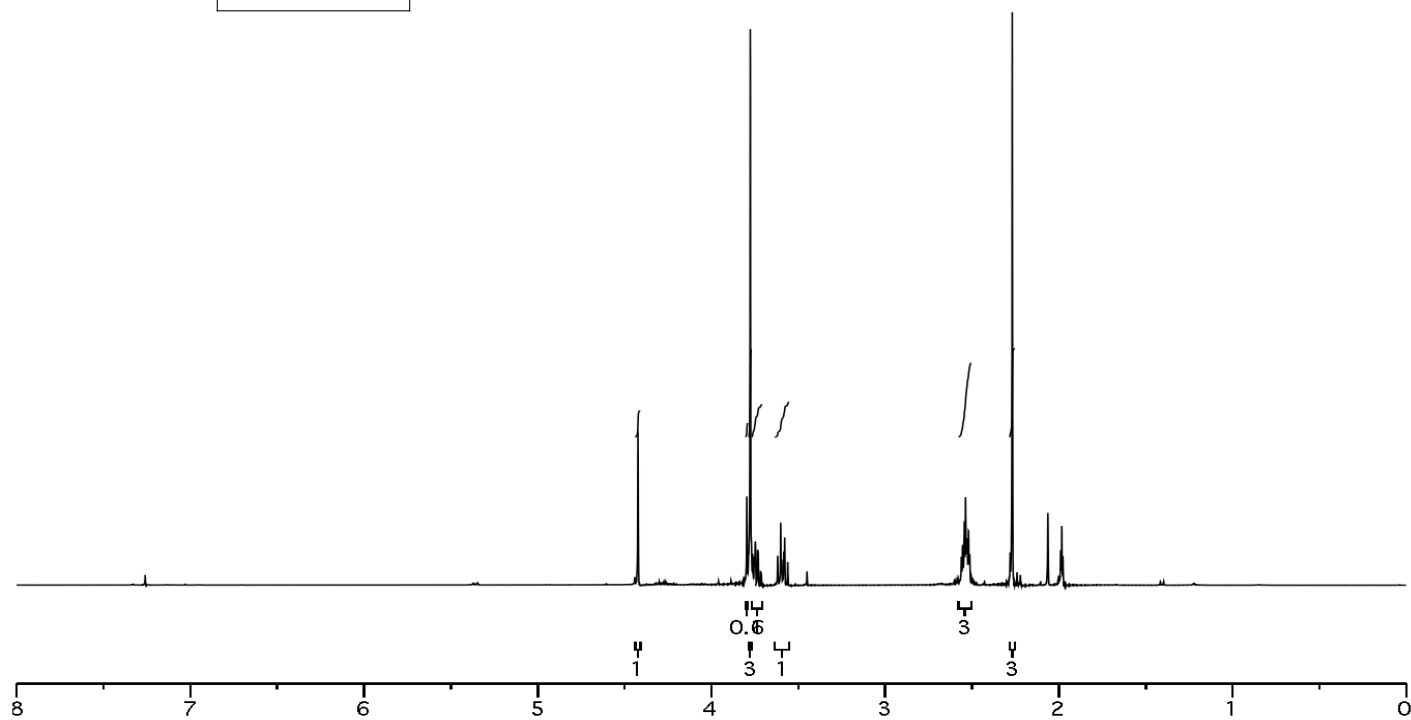
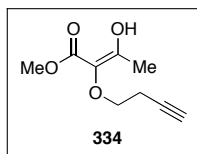


Figure A.2.37 ^1H NMR (400 MHz, CDCl_3) of compound **334**.

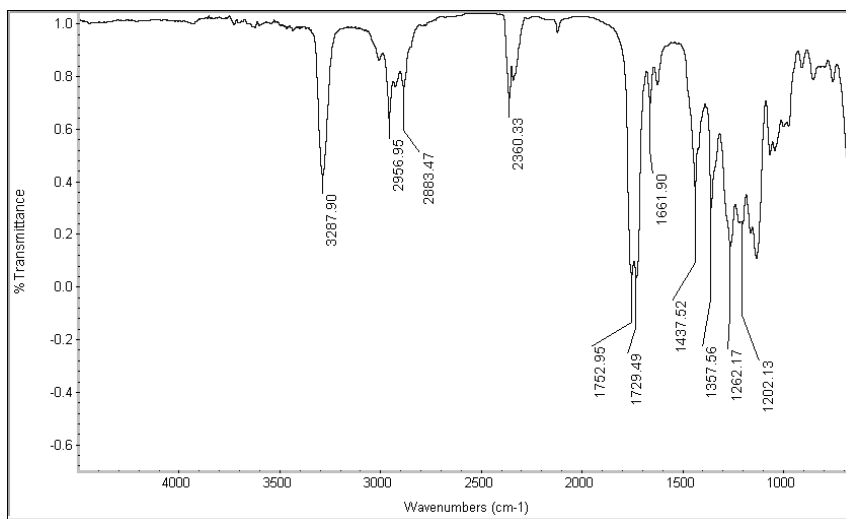


Figure A.2.38 Infrared Spectrum (thin film/NaCl) of compound **334**.

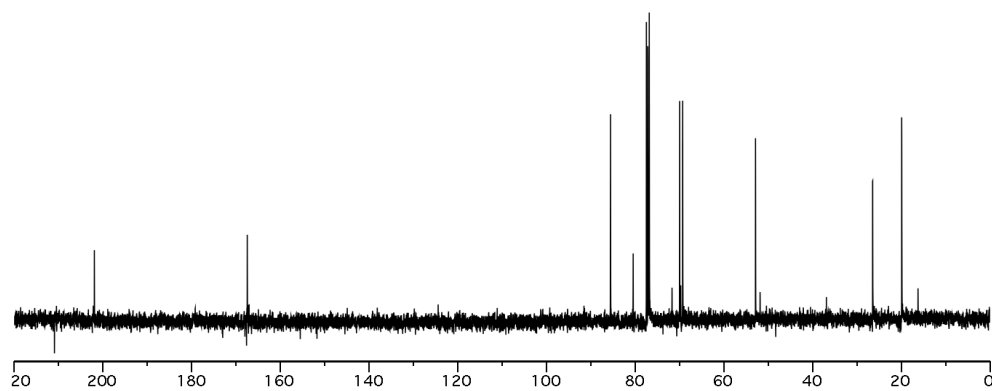


Figure A.2.39 ^{13}C NMR (100 MHz, CDCl_3) of compound **334**.

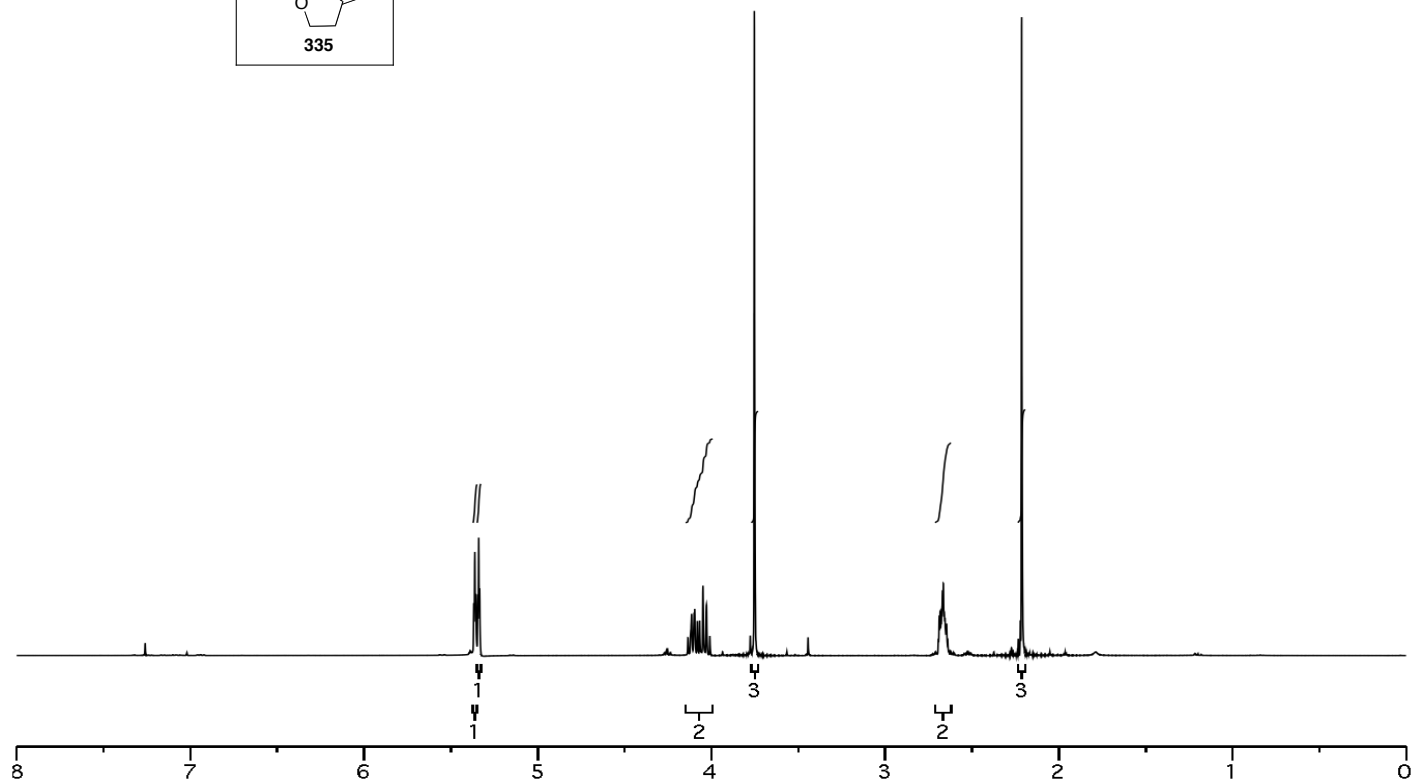
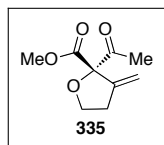


Figure A.2.40 ^1H NMR (400 MHz, CDCl_3) of compound **335**.

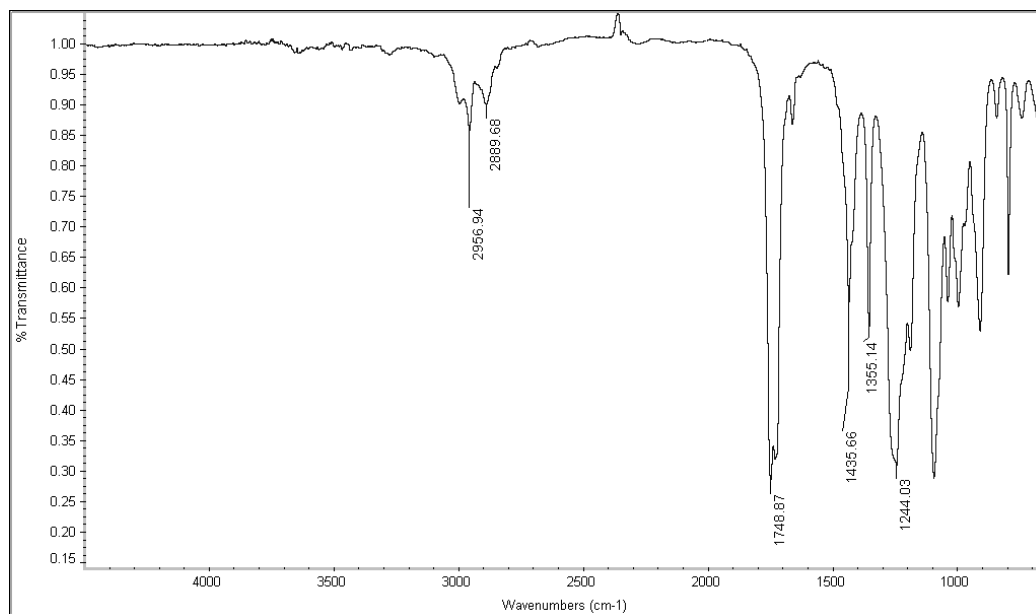


Figure A.2.41 Infrared Spectrum (thin film/NaCl) of compound **335**.

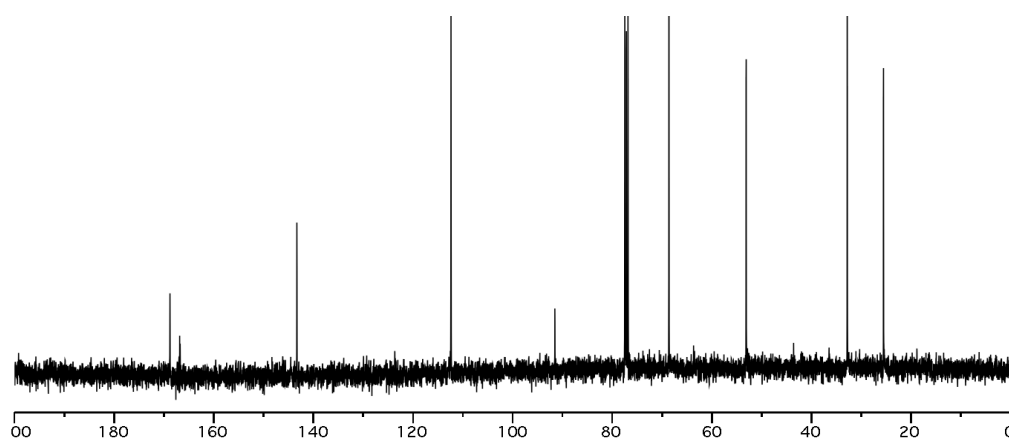


Figure A.2.42 ¹³C NMR (100 MHz, CDCl₃) of compound **335**.

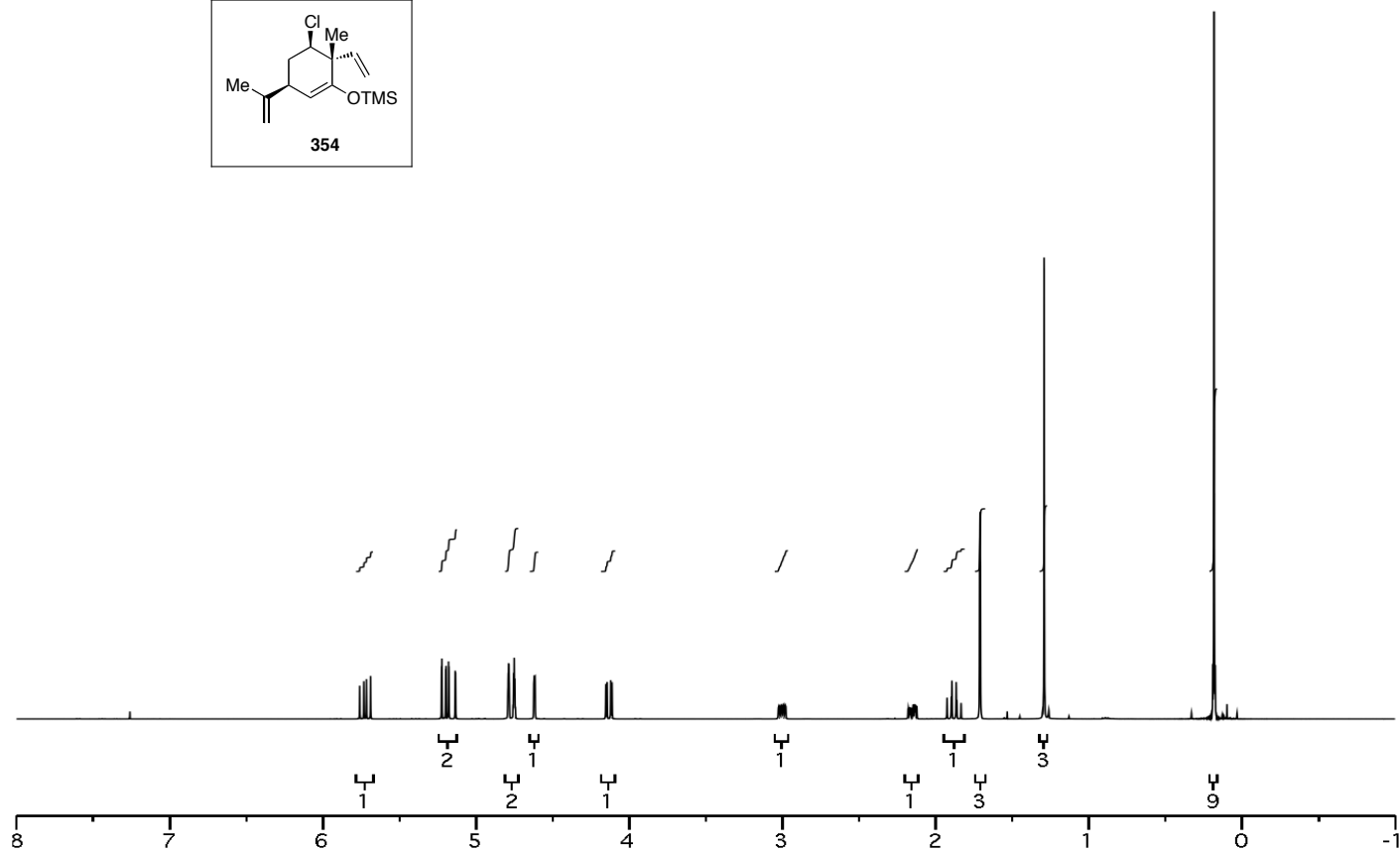
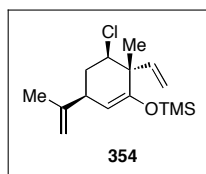


Figure A.2.43 ¹H NMR (400 MHz, CDCl₃) of compound **354**.

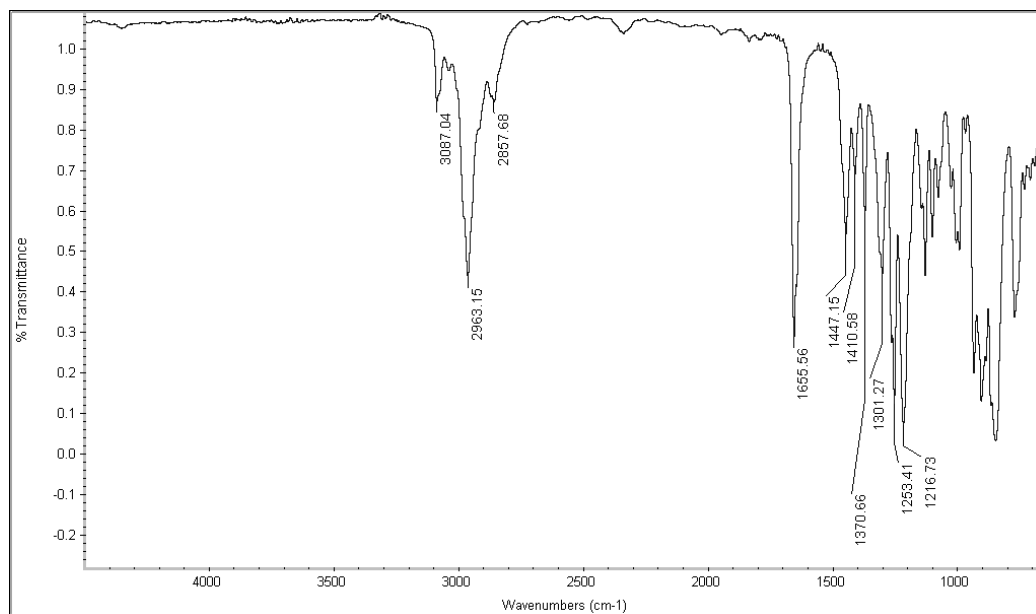


Figure A.2.44 Infrared Spectrum (thin film/NaCl) of compound **354**.

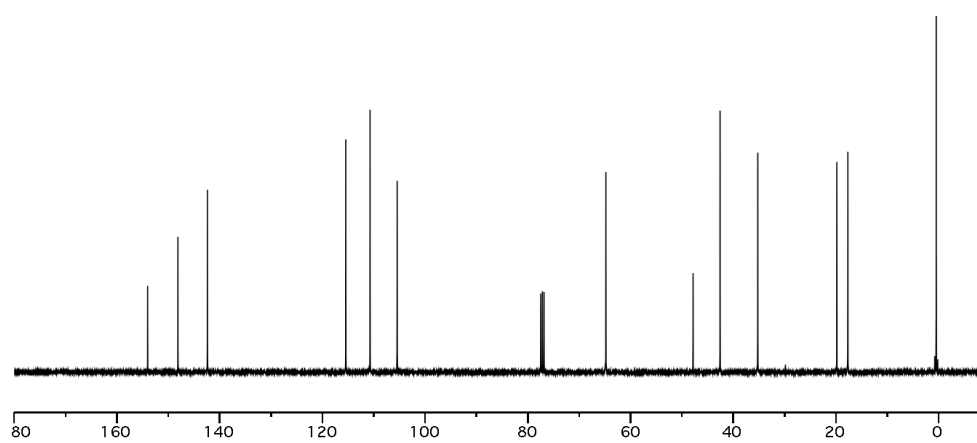


Figure A.2.45 ¹³C NMR (100 MHz, CDCl₃) of compound **354**.

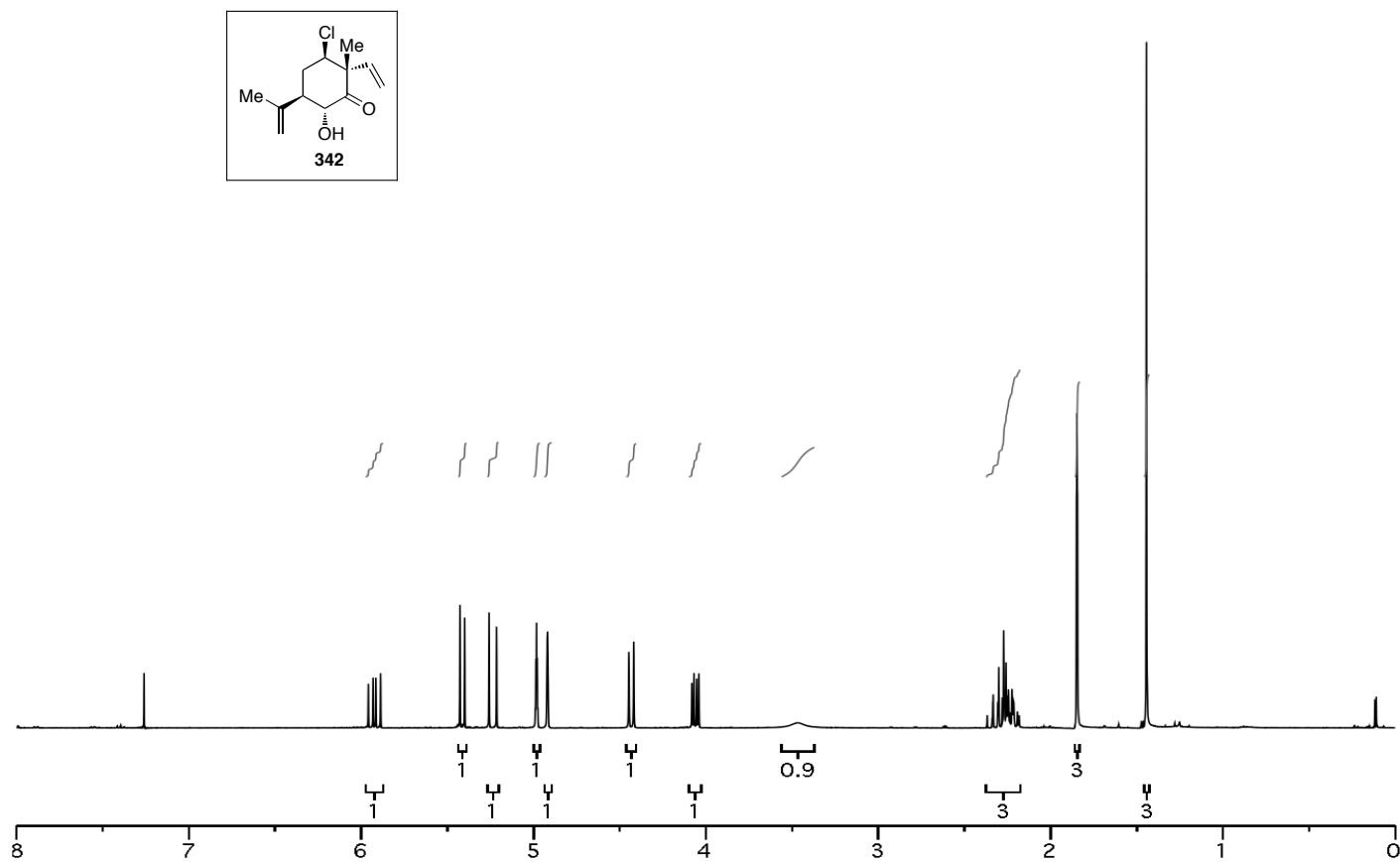


Figure A.2.46 ^1H NMR (400 MHz, CDCl_3) of compound **342**.

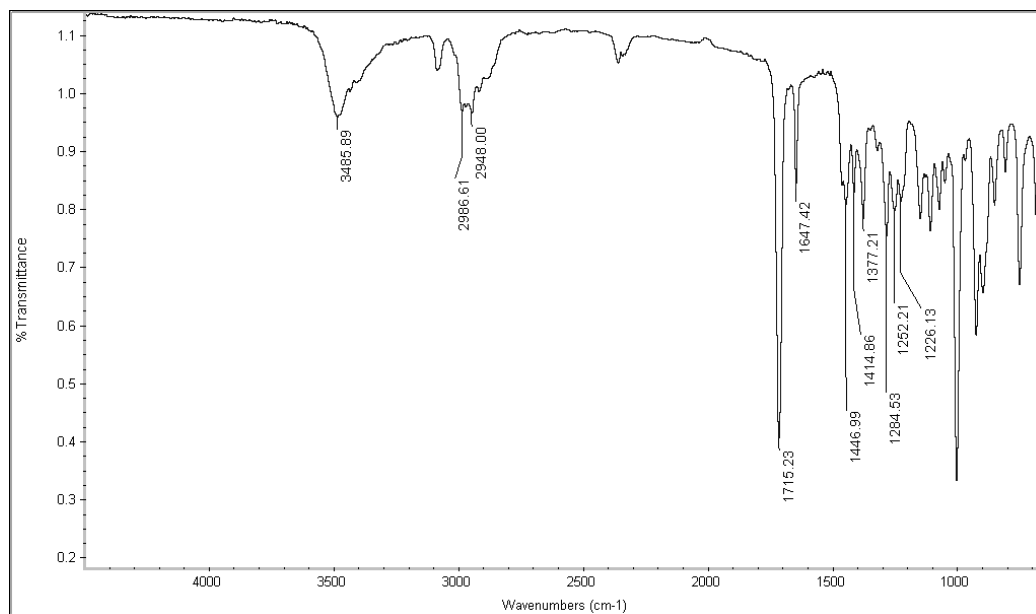


Figure A.2.47 Infrared Spectrum (thin film/NaCl) of compound **342**.

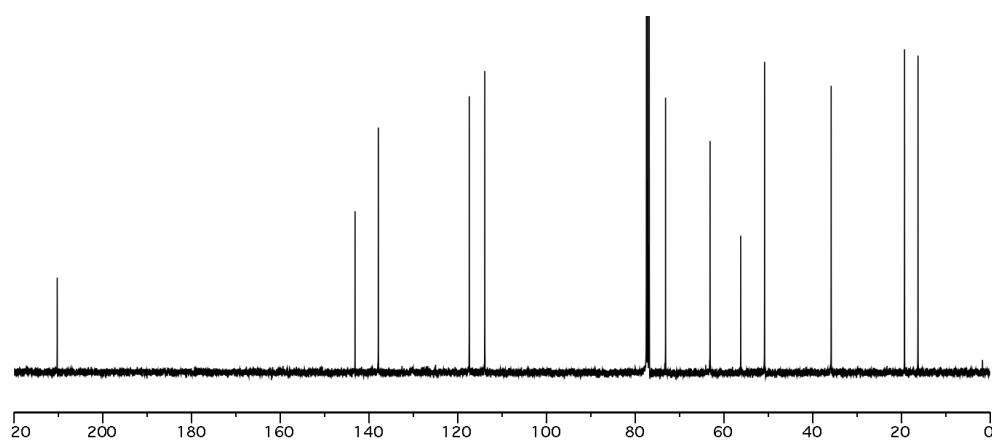
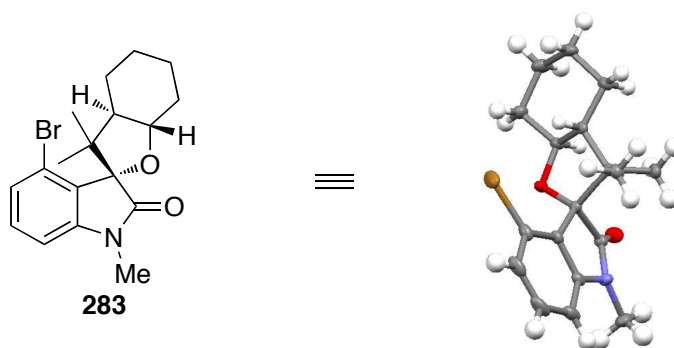


Figure A.2.48 ¹³C NMR (100 MHz, CDCl₃) of compound **342**.

**APPENDIX THREE: X-RAY CRYSTALLOGRAPHY
REPORTS RELEVANT
TO CHAPTER THREE**

X-Ray Crystallography Report For Spirocycle 283



A. Crystal data and structure refinement.

Identification code	wood11r_0m
Empirical formula	C ₁₈ H ₂₃ Br N O ₂
Formula weight	365.28
Temperature	120(2) K
Wavelength	0.71073 Å
Crystal system	Monoclinic
Space group	P 21/n
Unit cell dimensions	a = 10.9317(3) Å a = 90°. b = 7.5922(2) Å b = 95.204(2)°. c = 20.0056(6) Å g = 90°.
Volume	1653.53(8) Å ³
Z	4
Density (calculated)	1.467 Mg/m ³
Absorption coefficient	2.493 mm ⁻¹
F(000)	756
Crystal size	0.44 x 0.18 x 0.13 mm ³
Theta range for data collection	2.04 to 33.19°.
Index ranges	-9<=h<=16, -11<=k<=10, -25<=l<=30
Reflections collected	23412
Independent reflections	6308 [R(int) = 0.0306]
Completeness to theta = 33.19°	99.5 %
Absorption correction	Semi-empirical from equivalents
Max. and min. transmission	0.7392 and 0.4033
Refinement method	Full-matrix least-squares on F ²

Data / restraints / parameters	6308 / 0 / 199
Goodness-of-fit on F^2	1.031
Final R indices [$I > 2\sigma(I)$]	R1 = 0.0437, wR2 = 0.1159
R indices (all data)	R1 = 0.0699, wR2 = 0.1271
Largest diff. peak and hole	1.084 and -1.079 e.Å ⁻³

B. Atomic coordinates (x 10⁴) and equivalent isotropic displacement parameters (Å²x10³). U(eq) is defined as one third of the trace of the orthogonalized U^{ij} tensor.

atom	x	y	z	U(eq)
Br(1)	6313(1)	7302(1)	422(1)	32(1)
N(1)	4529(1)	8216(2)	1658(1)	10(1)
O(1)	4295(2)	7143(2)	3038(1)	27(1)
O(2)	6235(2)	6076(2)	2948(1)	31(1)
C(1)	6390(2)	6425(2)	1820(1)	17(1)
C(2)	7056(2)	6573(3)	1267(1)	23(1)
C(3)	8322(2)	6234(3)	1327(1)	31(1)
C(4)	8908(2)	5748(3)	1938(1)	33(1)
C(5)	8274(2)	5627(3)	2510(1)	27(1)
C(6)	7033(2)	5997(2)	2438(1)	19(1)
C(7)	6646(2)	6132(3)	3662(1)	28(1)
C(8)	5099(2)	6664(3)	2701(1)	18(1)
C(9)	5044(2)	6612(2)	1925(1)	15(1)
C(10)	4184(2)	5028(2)	1624(1)	16(1)
C(11)	3333(2)	6047(3)	1103(1)	16(1)
C(12)	2043(2)	5386(3)	885(1)	21(1)
C(13)	1445(2)	6713(3)	380(1)	27(1)
C(14)	1444(2)	8592(3)	658(1)	30(1)
C(15)	2738(2)	9220(3)	926(1)	24(1)
C(16)	3272(2)	7853(3)	1418(1)	18(1)
C(17)	4904(2)	3579(3)	1301(1)	22(1)
C(18)	3464(2)	4157(3)	2159(1)	24(1)

C. Bond lengths [Å] and angles [°].

Br(1)-C(2)	1.891(2)
N(1)-C(9)	1.424(2)
N(1)-C(16)	1.440(2)
O(1)-C(8)	1.211(2)
O(2)-C(8)	1.369(3)
O(2)-C(6)	1.403(3)
O(2)-C(7)	1.459(2)
C(1)-C(2)	1.383(3)
C(1)-C(6)	1.403(3)
C(1)-C(9)	1.511(3)
C(2)-C(3)	1.402(3)
C(3)-C(4)	1.378(4)
C(4)-C(5)	1.392(4)
C(5)-C(6)	1.380(3)
C(8)-C(9)	1.550(3)
C(9)-C(10)	1.609(3)
C(10)-C(17)	1.530(3)
C(10)-C(18)	1.534(3)
C(10)-C(11)	1.542(3)
C(11)-C(16)	1.513(3)
C(11)-C(12)	1.523(3)
C(12)-C(13)	1.531(3)
C(13)-C(14)	1.531(4)
C(14)-C(15)	1.542(3)
C(15)-C(16)	1.510(3)
C(9)-N(1)-C(16)	107.14(14)
C(8)-O(2)-C(6)	110.80(16)
C(8)-O(2)-C(7)	122.15(18)
C(6)-O(2)-C(7)	123.88(18)
C(2)-C(1)-C(6)	117.76(18)
C(2)-C(1)-C(9)	133.79(18)
C(6)-C(1)-C(9)	108.46(16)
C(1)-C(2)-C(3)	120.2(2)
C(1)-C(2)-Br(1)	121.66(16)

C(3)-C(2)-Br(1)	118.07(17)
C(4)-C(3)-C(2)	120.1(2)
C(3)-C(4)-C(5)	121.3(2)
C(6)-C(5)-C(4)	117.3(2)
C(5)-C(6)-C(1)	123.2(2)
C(5)-C(6)-O(2)	127.11(19)
C(1)-C(6)-O(2)	109.64(16)
O(1)-C(8)-O(2)	125.30(18)
O(1)-C(8)-C(9)	126.98(18)
O(2)-C(8)-C(9)	107.72(16)
N(1)-C(9)-C(1)	112.71(15)
N(1)-C(9)-C(8)	109.33(15)
C(1)-C(9)-C(8)	101.02(15)
N(1)-C(9)-C(10)	107.54(14)
C(1)-C(9)-C(10)	114.91(15)
C(8)-C(9)-C(10)	111.19(15)
C(17)-C(10)-C(18)	107.54(16)
C(17)-C(10)-C(11)	112.15(16)
C(18)-C(10)-C(11)	111.79(16)
C(17)-C(10)-C(9)	112.96(15)
C(18)-C(10)-C(9)	112.38(15)
C(11)-C(10)-C(9)	100.02(14)
C(16)-C(11)-C(12)	110.10(16)
C(16)-C(11)-C(10)	102.69(15)
C(12)-C(11)-C(10)	121.00(16)
C(11)-C(12)-C(13)	107.50(17)
C(12)-C(13)-C(14)	112.79(17)
C(13)-C(14)-C(15)	112.57(18)
C(16)-C(15)-C(14)	107.60(18)
N(1)-C(16)-C(15)	112.79(17)
N(1)-C(16)-C(11)	103.66(15)
C(15)-C(16)-C(11)	112.39(16)

D. Anisotropic displacement parameters ($\text{\AA}^2 \times 10^3$). The anisotropic displacement factor exponent takes the form: $-2p^2 [h^2 a^*2U^{11} + \dots + 2 h k a^* b^* U^{12}]$

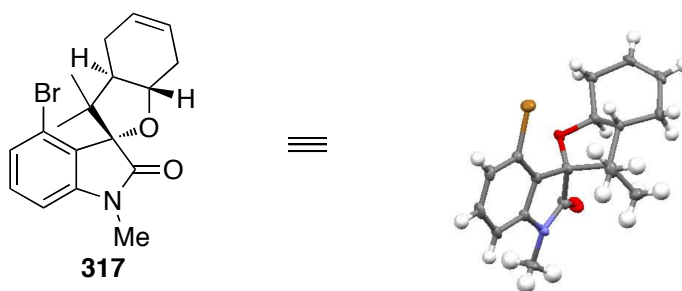
	U ¹¹	U ²²	U ³³	U ²³	U ¹³	U ¹²
Br(1)	38(1)	41(1)	20(1)	-1(1)	11(1)	-13(1)
N(1)	9(1)	7(1)	14(1)	0(1)	-4(1)	-2(1)
O(1)	23(1)	37(1)	20(1)	-5(1)	5(1)	1(1)
O(2)	33(1)	31(1)	28(1)	1(1)	-3(1)	1(1)
C(1)	15(1)	15(1)	22(1)	-2(1)	4(1)	-1(1)
C(2)	23(1)	20(1)	26(1)	-5(1)	9(1)	-6(1)
C(3)	22(1)	28(1)	47(1)	-12(1)	16(1)	-6(1)
C(4)	15(1)	23(1)	61(2)	-10(1)	6(1)	-1(1)
C(5)	18(1)	16(1)	45(1)	-4(1)	-6(1)	1(1)
C(6)	17(1)	12(1)	26(1)	-3(1)	0(1)	-1(1)
C(7)	35(1)	29(1)	19(1)	1(1)	-8(1)	-1(1)
C(8)	19(1)	20(1)	16(1)	-1(1)	1(1)	-1(1)
C(9)	15(1)	16(1)	15(1)	0(1)	1(1)	0(1)
C(10)	16(1)	15(1)	17(1)	0(1)	2(1)	-2(1)
C(11)	16(1)	18(1)	15(1)	0(1)	3(1)	-2(1)
C(12)	17(1)	26(1)	20(1)	-3(1)	1(1)	-4(1)
C(13)	20(1)	34(1)	24(1)	-3(1)	-5(1)	-1(1)
C(14)	25(1)	31(1)	31(1)	-2(1)	-8(1)	5(1)
C(15)	23(1)	23(1)	26(1)	2(1)	-4(1)	2(1)
C(16)	15(1)	19(1)	19(1)	-2(1)	-1(1)	-1(1)
C(17)	22(1)	17(1)	27(1)	-3(1)	2(1)	0(1)
C(18)	25(1)	25(1)	20(1)	5(1)	3(1)	-8(1)

E. Hydrogen coordinates ($\times 10^4$) and isotropic displacement parameters ($\text{\AA}^2 \times 10^3$).

	x	y	z	U(eq)
H(1A)	4898	9213	1644	12
H(3A)	8766	6337	954	38
H(4A)	9744	5496	1970	39

H(5A)	8671	5309	2923	32
H(7A)	5945	6181	3918	42
H(7B)	7146	7157	3756	42
H(7C)	7117	5095	3783	42
H(11A)	3767	6171	698	20
H(12A)	1568	5292	1270	25
H(12B)	2080	4233	679	25
H(13A)	605	6353	252	32
H(13B)	1883	6701	-21	32
H(14A)	908	8642	1018	35
H(14B)	1117	9385	306	35
H(15A)	3253	9349	559	29
H(15B)	2688	10351	1148	29
H(16A)	2773	7792	1800	21
H(17A)	4349	2670	1131	33
H(17B)	5503	3089	1630	33
H(17C)	5312	4068	938	33
H(18A)	2967	3223	1958	35
H(18B)	2947	5018	2344	35
H(18C)	4029	3687	2509	35

X-Ray Crystallography Report For Spirocycle 317



A. Crystal data and structure refinement.

Identification code	wood19	
Empirical formula	C ₁₈ H ₂₀ Br N O ₂	
Formula weight	362.26	
Temperature	120(2) K	
Wavelength	0.71073 Å	
Crystal system	Monoclinic	
Space group	P 2 ₁ /n	
Unit cell dimensions	a = 8.7457(4) Å	a = 90°.
	b = 31.5015(13) Å	b = 90.712(3)°.
	c = 11.5396(6) Å	g = 90°.
Volume	3178.9(3) Å ³	
Z	8	
Density (calculated)	1.514 Mg/m ³	
Absorption coefficient	2.593 mm ⁻¹	
F(000)	1488	
Crystal size	0.28 x 0.19 x 0.06 mm ³	
Theta range for data collection	1.88 to 30.75°.	
Index ranges	-12 ≤ h ≤ 12, -40 ≤ k ≤ 45, -16 ≤ l ≤ 16	
Reflections collected	67280	
Independent reflections	9819 [R(int) = 0.0532]	
Completeness to theta = 30.75°	98.9 %	
Absorption correction	Semi-empirical from equivalents	
Max. and min. transmission	0.8684 and 0.5347	
Refinement method	Full-matrix least-squares on F ²	
Data / restraints / parameters	9819 / 0 / 403	

Goodness-of-fit on F^2	1.041
Final R indices [$I > 2\sigma(I)$]	$R1 = 0.0482$, $wR2 = 0.1248$
R indices (all data)	$R1 = 0.0819$, $wR2 = 0.1491$
Largest diff. peak and hole	2.237 and $-0.988 \text{ e.}\text{\AA}^{-3}$

B. Atomic coordinates ($\times 10^4$) and equivalent isotropic displacement parameters ($\text{\AA}^2 \times 10^3$). $U(\text{eq})$ is defined as one third of the trace of the orthogonalized U^i_j tensor.

	x	y	z	$U(\text{eq})$
Br(1)	3627(1)	5208(1)	3705(1)	26(1)
Br(2)	4041(1)	2187(1)	8537(1)	26(1)
C(1)	2300(3)	4821(1)	4458(3)	19(1)
C(2)	2213(4)	4842(1)	5664(3)	24(1)
C(3)	1208(4)	4580(1)	6248(3)	24(1)
C(4)	241(4)	4304(1)	5648(3)	22(1)
C(5)	341(3)	4297(1)	4457(2)	17(1)
C(6)	1396(3)	4543(1)	3833(2)	17(1)
C(7)	1237(3)	4424(1)	2565(2)	16(1)
C(8)	-308(3)	4189(1)	2557(2)	18(1)
C(9)	-2058(4)	3882(1)	4018(3)	22(1)
C(10)	2571(3)	4124(1)	2082(3)	18(1)
C(11)	3911(4)	4075(1)	2925(3)	32(1)
C(12)	2022(5)	3686(1)	1738(5)	50(1)
C(13)	3100(5)	4403(1)	1048(3)	38(1)
C(14)	1830(5)	4673(1)	753(3)	41(1)
C(15)	2187(4)	5034(1)	-19(3)	28(1)
C(16)	3240(4)	4885(1)	-953(3)	34(1)
C(17)	4001(5)	4525(1)	-929(3)	37(1)
C(18)	3947(5)	4211(1)	54(3)	34(1)
C(19)	4983(4)	2643(1)	9346(3)	20(1)
C(20)	5020(4)	2635(1)	10547(3)	24(1)
C(21)	5803(4)	2951(1)	11153(3)	26(1)
C(22)	6594(4)	3272(1)	10579(3)	22(1)

C(23)	6528(3)	3269(1)	9381(3)	18(1)
C(24)	5699(3)	2969(1)	8743(2)	17(1)
C(25)	5862(3)	3061(1)	7463(2)	17(1)
C(26)	7187(4)	3391(1)	7501(3)	22(1)
C(27)	8541(4)	3828(1)	8972(3)	31(1)
C(28)	4369(4)	3250(1)	6812(2)	18(1)
C(29)	2975(4)	3278(1)	7583(3)	28(1)
C(30)	4662(4)	3694(1)	6311(3)	29(1)
C(31)	4149(4)	2909(1)	5862(2)	19(1)
C(32)	5714(4)	2732(1)	5689(3)	20(1)
C(33)	5671(4)	2310(1)	5073(3)	20(1)
C(34)	4697(4)	2362(1)	3995(3)	23(1)
C(35)	3721(4)	2680(1)	3832(3)	24(1)
C(36)	3426(4)	3030(1)	4708(3)	24(1)
N(1)	-632(3)	4080(1)	3678(2)	18(1)
N(2)	7318(3)	3536(1)	8620(2)	21(1)
O(1)	-1110(3)	4108(1)	1715(2)	26(1)
O(2)	1131(3)	4784(1)	1817(2)	19(1)
O(3)	7992(3)	3496(1)	6715(2)	31(1)
O(4)	6352(2)	2699(1)	6838(2)	18(1)

C. Bond lengths [Å] and angles [°].

Br(1)-C(1)	1.901(3)
Br(2)-C(19)	1.897(3)
C(1)-C(6)	1.377(4)
C(1)-C(2)	1.396(4)
C(2)-C(3)	1.387(5)
C(3)-C(4)	1.390(4)
C(4)-C(5)	1.378(4)
C(5)-C(6)	1.408(4)
C(5)-N(1)	1.408(4)
C(6)-C(7)	1.516(4)
C(7)-O(2)	1.428(3)
C(7)-C(8)	1.540(4)
C(7)-C(10)	1.607(4)

C(8)-O(1)	1.218(4)
C(8)-N(1)	1.372(4)
C(9)-N(1)	1.452(4)
C(10)-C(12)	1.512(5)
C(10)-C(11)	1.522(4)
C(10)-C(13)	1.557(4)
C(13)-C(14)	1.435(5)
C(13)-C(18)	1.501(5)
C(14)-O(2)	1.422(4)
C(14)-C(15)	1.480(5)
C(15)-C(16)	1.501(5)
C(16)-C(17)	1.317(6)
C(17)-C(18)	1.507(5)
C(19)-C(20)	1.386(4)
C(19)-C(24)	1.393(4)
C(20)-C(21)	1.393(5)
C(21)-C(22)	1.396(5)
C(22)-C(23)	1.383(4)
C(23)-C(24)	1.396(4)
C(23)-N(2)	1.405(4)
C(24)-C(25)	1.513(4)
C(25)-O(4)	1.419(3)
C(25)-C(26)	1.556(4)
C(25)-C(28)	1.612(4)
C(26)-O(3)	1.202(4)
C(26)-N(2)	1.374(4)
C(27)-N(2)	1.464(4)
C(28)-C(29)	1.521(4)
C(28)-C(30)	1.536(4)
C(28)-C(31)	1.545(4)
C(31)-C(32)	1.494(4)
C(31)-C(36)	1.516(4)
C(32)-O(4)	1.436(4)
C(32)-C(33)	1.507(4)
C(33)-C(34)	1.508(4)
C(34)-C(35)	1.327(5)

C(35)-C(36)	1.522(5)
C(6)-C(1)-C(2)	120.9(3)
C(6)-C(1)-Br(1)	121.2(2)
C(2)-C(1)-Br(1)	117.8(2)
C(3)-C(2)-C(1)	119.9(3)
C(2)-C(3)-C(4)	121.0(3)
C(5)-C(4)-C(3)	117.5(3)
C(4)-C(5)-C(6)	123.4(3)
C(4)-C(5)-N(1)	126.8(3)
C(6)-C(5)-N(1)	109.6(2)
C(1)-C(6)-C(5)	117.2(3)
C(1)-C(6)-C(7)	135.0(3)
C(5)-C(6)-C(7)	107.8(2)
O(2)-C(7)-C(6)	113.1(2)
O(2)-C(7)-C(8)	109.2(2)
C(6)-C(7)-C(8)	101.2(2)
O(2)-C(7)-C(10)	107.4(2)
C(6)-C(7)-C(10)	114.9(2)
C(8)-C(7)-C(10)	110.8(2)
O(1)-C(8)-N(1)	125.1(3)
O(1)-C(8)-C(7)	127.0(3)
N(1)-C(8)-C(7)	107.9(2)
C(12)-C(10)-C(11)	108.3(3)
C(12)-C(10)-C(13)	114.2(3)
C(11)-C(10)-C(13)	108.3(3)
C(12)-C(10)-C(7)	113.4(3)
C(11)-C(10)-C(7)	113.3(2)
C(13)-C(10)-C(7)	99.1(2)
C(14)-C(13)-C(18)	116.4(3)
C(14)-C(13)-C(10)	106.2(3)
C(18)-C(13)-C(10)	120.7(3)
O(2)-C(14)-C(13)	106.3(3)
O(2)-C(14)-C(15)	115.2(3)
C(13)-C(14)-C(15)	115.4(4)
C(14)-C(15)-C(16)	109.2(3)
C(17)-C(16)-C(15)	124.6(3)

C(16)-C(17)-C(18)	124.1(3)
C(13)-C(18)-C(17)	109.3(3)
C(20)-C(19)-C(24)	120.6(3)
C(20)-C(19)-Br(2)	118.8(2)
C(24)-C(19)-Br(2)	120.5(2)
C(19)-C(20)-C(21)	119.6(3)
C(20)-C(21)-C(22)	121.5(3)
C(23)-C(22)-C(21)	117.0(3)
C(22)-C(23)-C(24)	123.1(3)
C(22)-C(23)-N(2)	127.3(3)
C(24)-C(23)-N(2)	109.4(2)
C(19)-C(24)-C(23)	118.0(3)
C(19)-C(24)-C(25)	132.6(3)
C(23)-C(24)-C(25)	109.3(2)
O(4)-C(25)-C(24)	112.0(2)
O(4)-C(25)-C(26)	108.8(2)
C(24)-C(25)-C(26)	100.4(2)
O(4)-C(25)-C(28)	107.9(2)
C(24)-C(25)-C(28)	116.1(2)
C(26)-C(25)-C(28)	111.4(2)
O(3)-C(26)-N(2)	125.0(3)
O(3)-C(26)-C(25)	127.3(3)
N(2)-C(26)-C(25)	107.6(2)
C(29)-C(28)-C(30)	107.8(3)
C(29)-C(28)-C(31)	111.2(3)
C(30)-C(28)-C(31)	112.7(2)
C(29)-C(28)-C(25)	113.6(2)
C(30)-C(28)-C(25)	111.9(3)
C(31)-C(28)-C(25)	99.6(2)
C(32)-C(31)-C(36)	110.4(3)
C(32)-C(31)-C(28)	104.4(2)
C(36)-C(31)-C(28)	119.7(2)
O(4)-C(32)-C(31)	104.4(2)
O(4)-C(32)-C(33)	112.2(2)
C(31)-C(32)-C(33)	112.0(3)
C(32)-C(33)-C(34)	107.7(2)

C(35)-C(34)-C(33)	123.7(3)
C(34)-C(35)-C(36)	124.5(3)
C(31)-C(36)-C(35)	109.2(3)
C(8)-N(1)-C(5)	110.5(2)
C(8)-N(1)-C(9)	123.4(3)
C(5)-N(1)-C(9)	123.4(2)
C(26)-N(2)-C(23)	110.6(2)
C(26)-N(2)-C(27)	121.5(3)
C(23)-N(2)-C(27)	124.5(3)
C(14)-O(2)-C(7)	107.5(2)
C(25)-O(4)-C(32)	107.1(2)

D. Anisotropic displacement parameters ($\text{\AA}^2 \times 10^3$). The anisotropic displacement factor exponent takes the form: $-2p^2 [h^2 a^* U_{11} + \dots + 2hka^* b^* U_{12}$

	U ₁₁	U ₂₂	U ₃₃	U ₂₃	U ₁₃	U ₁₂
Br(1)	25(1)	24(1)	30(1)	-1(1)	6(1)	-9(1)
Br(2)	26(1)	23(1)	29(1)	1(1)	4(1)	-7(1)
C(1)	16(1)	21(1)	20(1)	1(1)	1(1)	-2(1)
C(2)	22(2)	30(2)	20(2)	-7(1)	-2(1)	-3(1)
C(3)	23(2)	37(2)	11(1)	-2(1)	2(1)	0(1)
C(4)	19(2)	29(2)	17(2)	4(1)	2(1)	0(1)
C(5)	16(1)	20(1)	14(1)	1(1)	-1(1)	-1(1)
C(6)	17(1)	19(1)	14(1)	1(1)	0(1)	1(1)
C(7)	18(1)	16(1)	12(1)	4(1)	1(1)	0(1)
C(8)	18(2)	23(1)	13(1)	2(1)	0(1)	0(1)
C(9)	21(2)	24(1)	21(2)	2(1)	2(1)	-6(1)
C(10)	19(2)	18(1)	18(1)	1(1)	2(1)	2(1)
C(11)	28(2)	35(2)	32(2)	-6(1)	-7(2)	12(1)
C(12)	33(2)	29(2)	88(4)	-24(2)	4(2)	0(2)
C(13)	47(2)	45(2)	24(2)	14(2)	15(2)	23(2)
C(14)	63(3)	33(2)	27(2)	10(1)	24(2)	13(2)
C(15)	21(2)	40(2)	22(2)	16(1)	-1(1)	0(1)

C(16)	30(2)	59(2)	12(2)	9(2)	0(1)	-15(2)
C(17)	42(2)	54(2)	16(2)	-8(2)	12(2)	-17(2)
C(18)	40(2)	33(2)	30(2)	-10(1)	18(2)	-4(2)
C(19)	19(2)	21(1)	19(1)	0(1)	-1(1)	0(1)
C(20)	23(2)	32(2)	18(2)	8(1)	2(1)	3(1)
C(21)	28(2)	40(2)	10(1)	2(1)	0(1)	5(1)
C(22)	24(2)	28(2)	14(1)	-4(1)	-4(1)	5(1)
C(23)	20(2)	21(1)	14(1)	-1(1)	0(1)	2(1)
C(24)	18(2)	21(1)	13(1)	-2(1)	2(1)	2(1)
C(25)	18(2)	23(1)	11(1)	-2(1)	0(1)	-4(1)
C(26)	24(2)	27(2)	16(1)	3(1)	-1(1)	-6(1)
C(27)	37(2)	29(2)	26(2)	-5(1)	-6(2)	-14(1)
C(28)	21(2)	19(1)	14(1)	0(1)	0(1)	-1(1)
C(29)	24(2)	38(2)	23(2)	2(1)	2(1)	6(1)
C(30)	35(2)	20(1)	30(2)	1(1)	-2(2)	-1(1)
C(31)	23(2)	22(1)	13(1)	2(1)	-3(1)	-1(1)
C(32)	23(2)	23(1)	12(1)	0(1)	-1(1)	-4(1)
C(33)	21(2)	23(1)	14(1)	-4(1)	1(1)	-2(1)
C(34)	27(2)	29(2)	12(1)	-6(1)	1(1)	-10(1)
C(35)	26(2)	34(2)	12(1)	2(1)	-5(1)	-11(1)
C(36)	29(2)	24(2)	17(2)	4(1)	-7(1)	-1(1)
N(1)	16(1)	24(1)	14(1)	2(1)	1(1)	-5(1)
N(2)	24(1)	24(1)	14(1)	-1(1)	-2(1)	-8(1)
O(1)	24(1)	37(1)	17(1)	0(1)	-5(1)	-6(1)
O(2)	24(1)	18(1)	14(1)	6(1)	6(1)	5(1)
O(3)	28(1)	40(1)	24(1)	6(1)	3(1)	-17(1)
O(4)	21(1)	23(1)	10(1)	-2(1)	-2(1)	2(1)

E. Hydrogen coordinates ($\times 10^4$) and isotropic displacement parameters ($\text{\AA}^2 \times 10^3$).

	x	y	z	U(eq)
H(2)	2828	5032	6075	29
H(3)	1180	4588	7053	29

H(4)	-447	4132	6035	26
H(9A)	-2748	4097	4290	33
H(9B)	-1860	3681	4626	33
H(9C)	-2508	3740	3364	33
H(11A)	3568	3940	3620	48
H(11B)	4322	4350	3110	48
H(11C)	4690	3904	2575	48
H(12A)	2869	3523	1462	75
H(12B)	1260	3710	1135	75
H(12C)	1588	3548	2398	75
H(13)	3846	4598	1401	46
H(14)	1092	4495	331	49
H(15A)	2671	5259	425	33
H(15B)	1251	5144	-363	33
H(16)	3363	5060	-1594	40
H(17)	4611	4460	-1559	45
H(18A)	3435	3953	-200	41
H(18B)	4978	4137	300	41
H(20)	4525	2419	10945	29
H(21)	5798	2949	11959	31
H(22)	7142	3478	10985	27
H(27A)	9470	3672	9098	46
H(27B)	8262	3970	9675	46
H(27C)	8693	4035	8373	46
H(29A)	2115	3379	7137	42
H(29B)	3181	3472	8209	42
H(29C)	2749	3002	7891	42
H(30A)	3756	3793	5920	43
H(30B)	5488	3680	5772	43
H(30C)	4927	3886	6928	43
H(31)	3523	2682	6192	23
H(32)	6320	2933	5238	24
H(33A)	5238	2094	5572	23
H(33B)	6697	2223	4869	23
H(34)	4786	2160	3412	27
H(35)	3179	2688	3133	29

H(36A)	3861	3295	4437	28
H(36B)	2334	3070	4797	28

APPENDIX FOUR: NOTEBOOK CROSS-REFERENCES

NOTEBOOK CROSS-REFERENCE

The following notebook cross-reference has been included to facilitate access to the original spectroscopic data obtained for the compounds presented in this thesis. Unless otherwise labeled, each compound is labeled corresponding to the notebook, page number, and compound within the reaction (for example, DBFIV-141-1 represents notebook DBFIV, page 141, and compound 1). All spectroscopic data obtained for the compounds presented in this thesis are archived in characterization folders with hard copies. All spectral data is stored electronically on the Wood Group external hard drive.

Compounds Appearing in Chapter Two

Compound	Folder	¹ H NMR	¹³ C NMR	IR
203	DBF-diketone-trisubolefin	DBF-diketone-trisubolefin	DBF-diketone-trisubolefin	DBF-diketone-trisubolefin
204	DBFIV-141-1	DBFIV-141-1.400.h1	DBFIV-141-1	DBFIV-141-1.400.c13
208	DBFIV-143-1	DBFIV-143-1.400.h1	DBFIV-143-1.400.c13	DBFIV-143-1
344	DBFIV-143-2	DBFIV-143-2.400.h1	DBFIV-143-2.400.c13	DBFIV-143-2
210 and 345	DBFIV-146-2	DBFIV-146-1.400.h1	DBFIV-146-1.400.c13	DBFIV-146-2
212	DBFIII-222-1	DBFIII-222-1	DBFIII-222-1.c13	DBFIII-222-1
213	DBFIII-224-2	DBFIII-224-2	DBFIII-224-2	DBFIII-224-2
214	DBFIII-225-3	DBFIII-225-3	DBFIII-225-3.13C.400	DBFIII-225-3
216	DBFIII-228-3	DBFIII-228-3	DBFIII-245-1.13C.400	DBFIII-228-3
223	DBFIII-221-1	DBFIII-221-1	DBFIII-221-2.13C.400	DBFIII-221-1
218	DBFIII-226-2	DBFIII-226-2.1H.400	DBFIII-226-2.c13.12.30.09	
226	DBFIV-125-1	DBFIV-125-1.300.h1	DBFIV-125-1.300.c13	DBFIV-125-1
227	DBFIV-127-4	DBFIV-127-4.400.h1	DBFIV-127-4.400.c13	DBFIV-127-4
229	DBFIII-240-1	DBFIII-240-1.1H.400	AK-1-151	
240a	DBFIV-BOE1	DBFIV-BOE1-h1	DBFIV-BOE1.c13.300	DBFIV-BOE1
240b	DBFIV-BOE2	DBFIV-BOE2.300.h1	DBFIV-BOE2.400.c13	DBFIV-BOE2

241	DBFIV-129-2	DBFIV-129-2.400.h1	DBFIV-129-2.400.c13	DBFIV-129-2
242	DBFIV-133-2	DBFIV-133-2.300.h1	DBFIV-133-2.300.c13	DBFIV-133-2
247	DBFIV-172-3	DBFIV-172-3-PROTON_001	DBFIV-172-3-CARBON_001	DBFIV-172-3
251	DBFIV-138-1	DBFIV-132-1 PROTON_001	DBFIV-132-1 CARBON_001	DBFIV-138-1
252	DBFIV-156-2	DBFIV-156-2.400.h1	DBFIV-156-2.400.c13	DBFIV-156-2
254	DBFIV-139-1	DBFIV-139-1.300.h1.CD3CN	DBFIV-139-1.300.400.c13	DBFIV-139-1
253	DBFIV-139-2	DBFIV-139-2.300.h1.CD3CN	DBFIV-139-2.400.c13	DBFIV-139-2
255a	DBFIV-144-1	DBFIV-144-1.400.h1a	DBFIV-144-1.c13.400	DBFIV-144-1
255b	DBFIV-144-2	DBFIV-144-2.400.h1	DBFIV-144-2.400.c13.b	DBFIV-144-2
256a	DBFIV-145-1	DBFIV-145-1.400.h1	DBFIV-145-1.400.c13	DBFIV-145-1
256b	DBFIV-159-1	DBFIV-159-1.400.h1	DBFIV-159-1.400.c13	DBFIV-159-1
259	DBFIV-163-4	DBFIV-163-4 PROTON_001	DBFIV-163-4 CARBON_001	DBFIV-163-4

Compounds Appearing in Chapter Two

Compound	Folder	¹ H NMR	¹³ C NMR	IR
269	DBFIV-147-1	DBFIV-147-1.300.h1	DBFIV-147-1.300.c13	DBFIV-147-1
270	DBFIV-148-1	DBFIV-148-1.400.h1b	DBFIV-148-1.400.c13	DBFIV-148-1
271	DBFIV-diazoisatin	DBFIV-diazoisatin.400.h1	DBFIV-diazoisatin.400.c13	DBFIV-diazoisatin
283	DBFIV-153-1	DBFIV-153-1.400.h1	DBFIV-153-1.400.c13	DBFIV-153-1
323	DBFIV-158-1	DBFIV-158-2_PROTON_001	DBFIV-158-1.300.c13	DBFIV-158-1
317	DBFIV-174-1	DBFIV-174-1_400_PROTON	DBFIV-174-1_400_CARBON	DBFIV-174-1
324	DBFIV-181-3	DBFIV-181-3-2_PROTON	DBFIV-181-3_PROTON	DBFIV-181-3
318	DBFIV-183-2	DBFIV-183-2 PROTON_001	DBFIV-183-2 CARBON_001	DBFIV-183-2
319	DBFIV-184-2	DBFIV-184-	DBFIV-184-	DBFIV-184-2

		2_PROTON_001	2_CARBON_001	
328	DBFIV-178-2	DBFIV-178- 2_PROTON_001	DBFIV-178- 2_CARBON_001	DBFIV-178-2
329	DBFIV-192-2	DBFIV-192- 2a CARBON	DBFIV-192- 2A PROTON	DBFIV-192-2
330	DBFIV-91-2	DBFIV-91- 2.400.h1	DBFIV-91- 2.400.c13	DBFIV-91-2
334	DBFIV-86-1	DBFIV-86- 1.400.h1	DBFIV-86- 1.400.c13	DBFIV-86-1
335	DBFIV-87-1	DBFIV-87- 1.400.h1	DBFIV-87- 1.400.c13	DBFIV-87-1
354	DBFIV-164-2	DBFIV-164- 2_PROTON_001	DBFIV-164- 2_CARBON_001	DBFIV-164-2
342	DBFIV-167-2	DBFIV-167- 2_PROTON_001	DBFIV-167- 2_CARBON_001	DBFIV-167-2

BIBLIOGRAPHY

- Aldaz, H.; Rice, L. M.; Stearns, T.; Agard, D. A. "Insight into Microtubule Nucleation from the Crystal Structure of Human γ -Tubulin" *Nature* **2005**, *435*, 523–527.
- Ambudkar, S. V.; Dey, S.; Hrycyna, C. A.; Ramachandra, M.; Pastan, I.; Gottesman, M. M. "Biochemical, Cellular, and Pharmacological Aspects of the Multidrug Transporter" *Annu. Rev. Pharmacol. Toxicol.* **1999**, *39*, 361–398.
- Avendaño, C.; Menéndez, J. C. "Inhibitors of Multidrug Resistance to Antitumor Agents (MDR)" **2002**, *9*, 159–193.
- Avendaño, C.; Menéndez, J. C. "Synthetic Studies on *N*-Methylwelwitindolinone C Isothiocyanate (Welwistatin) and Related Substructures" *Curr. Org. Synth.* **2004**, *1*, 65–82.
- Balme, G.; Bouyssi, D; Faure, R.; Gore, J.; Van Hemelryck, B. "Formation de cyclopentanes a partir de malonates δ -ethyleniques par un processus catalytique en palladium(0) stereochemie et mecanisme" *Tetrahedron* **1992**, *48*, 3891–3902.
- Baran, P. S.; Richter, J. M. "Enantioselective Total Syntheses of Welwitindolinone A and Fischerindoles I and G" *J. Am. Chem. Soc.* **2005**, *127*, 15394–15396.
- Baran, P.S.; Maimone, T.J.; Richter, J.M. "Total synthesis of marine natural products without using protecting groups" *Nature* **2007**, *446*, 404–408.
- Baudoux, J.; Blake, A. J.; Simpkins, N. S. "Rapid Access to the Welwitindolinone Alkaloid Skeleton by Cyclization of Indolcarboxaldehyde Substituted Cyclohexanones" *Org. Lett.* **2005**, *7*, 4087–4089.

- Bellamy, W. T. "P-glycoproteins and Multidrug Resistance" *Annu. Rev. Pharmacol. Toxicol.* **1996**, *36*, 161–183.
- Boaventura, M. A.; Drouin, J.; Conia, J. M. "Doubly Catalyzed Cyclization of ϵ -Acetylenic Carbonyl Compounds" *Synthesis*, **1983**, 801–804.
- Boger, D. L.; Cassidy, K. C.; Nakahara, S. "Total Synthesis of Streptonigrone" *J. Am. Chem. Soc.* **1993**, *115*, 10733–10741.
- Boissel, V.; Simpkins, N. S.; Bhalay, G. "Singlet oxygen conversion of indoles into α,β -unsaturated oxindoles in model compounds related to the welwitindolinone alkaloids" *Tetrahedron Lett.* **2009**, *50*, 3283–3286.
- Bouyssi, D.; Montiero, N.; Balme, G. "Intramolecular carbocupration reaction of unactivated alkynes bearing a stabilized nucleophile: Application to the synthesis of iridoid monoterpenes" *Tetrahedron Lett.* **1999**, *40*, 1297–1300.
- Brailsford, J. A.; Lauchli, R.; Shea, K. J. "Synthesis of the Bicyclic Welwitindolinone Core via an Alkylation/Cyclization Cascade Reaction" *Org. Lett.* **2009**, *11*, 5330–5333.
- Brunel, J. M.; Billottet, L.; Letourneux, Y. "New Efficient and Totally Stereoselective Copper Allylic Benzoyloxylation of Sterol Derivatives" *Tetrahedron: Asymm.* **2005**, *16*, 3036–3041.
- Cava, M. P.; Litle, R. L.; Napier, D. R. "Condensed Cyclobutane Aromatic Systems. V. The Synthesis of Some α -Diazoindanones: Ring Contraction in the Indane Series" *J. Am. Chem. Soc.* **1958**, *80*, 2257–2263.

- Chatterjee, A. K.; Choi, T. L.; Sanders, D. P.; Grubbs, R. H. "A General Model for Selectivity in Olefin Cross Metathesis" *J. Am. Chem. Soc.* **2003**, *125*, 11360-11370.
- Checchi, P. M.; Nettles, J. H.; Zhou, J.; Snyder, J. P.; Joshi, H. C. "Microtubule-Interacting Drugs for Cancer Treatment" *Trends Pharmacol. Sci.* **2003**, *24*, 361-365.
- Chun, Y. S.; Ko, Y. O.; Shin, H.; Lee, S. "Tandem Blaise-Alkenylation with Unactivated Alkynes: One-Pot Synthesis of α -Vinylated β -Enaminoesters from Nitriles" *Org. Lett.* **2009**, *11*, 3414-3417.
- Conia, J. M.; Le Perche, P. "The Thermal Cyclisation of Unsaturated Carbonyl Compounds" *Synthesis*, **1975**, 1-19.
- Conia, J. M.; Leyendecker, F.; Dubois-Faget, C. "Le comportement thermique des cetonnes ethyleniques aliphatiques en fonction du nombre de carbonnes separant les deux centres insatures, et celui cis-alcoyl-2 acylcyclanes en fonction de la taille du cycle" *Tetrahedron Lett.* **1966**, *7*, 129-133.
- Corkey, B. K.; Toste, F. D. "Catalytic Enantioselective Conia-Ene Reaction" *J. Am. Chem. Soc.* **2005**, *127*, 17168-17169.
- Cruciani, P.; Aubert, C.; Malacria, M. "Studies on diastereoselectivity of the cobalt(I) catalyzed cycloisomerization of substituted α -acetylenic β -ketoester" *Tetrahedron Lett.* **1994**, *35*, 6677-6680.
- Cruciani, P.; Stammler, R.; Aubert, C.; Malacria, M. "New Cobalt-Catalyzed Cycloisomerization of ϵ -Acetylenic β -Keto Esters. Application to a Powerful Cyclization Reactions Cascade" *J. Org. Chem.* **1996**, *61*, 2699-2708.

- Deng, H.; Konopelski, J. P. "Aryllead(II) Reagents in Synthesis: Formation of the C11 Quaternary Center of *N*-Methylwelwitindolinone C Isothiocyanate" *Org. Lett.* **2001**, *3*, 3001–3004.
- Dess, D. B.; Martin, J. C. "A useful 12-I-5 triacetoxyperiodinane (the Dess-Martin periodinane) for the selective oxidation of primary or secondary alcohols and a variety of related 12-I-5 species" *J. Am. Chem. Soc.* **1991**, *113*, 7277-7287.
- Driver, T. G.; Franz, A. K.; Woerpal, K. A. "Diastereoselective Silacyclopropanations of Functionalized Chiral Alkenes" *J. Am. Chem. Soc.* **2002**, *124*, 6524–6525.
- Falb, E.; Bechor, Y.; Nudelman, A.; Hassner, A.; Albeck, A.; Gottlieb, H. E. "IOOC Route to Substituted Chiral Pyrrolidines. Potential Glycosidase Inhibitors" *J. Org. Chem.* **1999**, *64*, 498-506.
- Fukuyama, T.; Chen, X. "Stereocontrolled Synthesis of (–)-Hapalindole G" *J. Am. Chem. Soc.* **1994**, *116*, 3125–3126.
- Funk, R. L.; Horcher, L. H. M.; Daggett, J. U.; Hansen, M. M. "Facile bridged bicycloalkane synthesis via intramolecular nitron-olefin cycloaddition" *J. Org. Chem.* **1983**, *48*, 2632-2634.
- Gao, Q.; Zheng, B.; Li, J.; Yang, D. "Ni(II)-Catalyzed Conia-Ene Reaction of 1,3-Dicarbonyl Compounds with Alkynes" *Org. Lett.* **2005**, *7*, 2185–2188.
- Grandjean-Forestier, F.; Stenger, C.; Robert, J.; Verdier, M.; Ratinaud, M.-H. "The P-glycoprotein 170: Just a Multidrug Resistance Protein of a Protean Molecule?" In *ABC Transporters and Multidrug Resistance*; Boumendjel, A.; Boutonnat, J.; Robert, J.; John Wiley and Sons, Inc.: Hoboken, 2009; 17–46.

- Greshock, T. J.; Funk, R. L. "An Approach to the Total Synthesis of Welwistatin" *Org. Lett.* **2006**, *8*, 2643–2645.
- Grieco, P. A.; Masaki, Y.; Boxler, D. "Sesterterpenes. I. Stereospecific total synthesis of moenocinol" *J. Am. Chem. Soc.* **1975**, *97*, 1597-1599.
- Grieco, P. A.; Noguez, J. A.; Masaki, Y. "Total synthesis of deoxyvernolepin" *Tetrahedron Lett.* **1975**, *16*, 4213-4216.
- Heidebrecht, R. W.; Gullledge, B.; Martin, S. F. "Approaches to *N*-Methylwelwitindolinone C Isothiocyanate: Facile Synthesis of the Tetracyclic Core" *Org. Lett.* **2010**, *12*, 2492–2495.
- Hoffmann, H. M. R. "Ene reaction" *Angew. Chem., Int. Ed. Engl.* **1969**, *8*, 556–577.
- Huisgen, R. "1,3-Dipolar Cycloadditions. Past and Future" *Angew. Chem., Int. Ed.* **1963**, *2*, 565-598.
- Itoh, Y.; Tsuji, H.; Yamagata, K.; Endo, K.; Tanaka, I.; Nakamura, M.; Nakamura, E. "Efficient Formation of Ring Structures Utilizing Multisite Activation by Indium Catalysis" *J. Am. Chem. Soc.* **2008**, *130*, 17161–17167.
- Jimenez, J. I.; Huber, U.; Moore, R. E.; Patterson, G. M. L. "Oxidized Welwitindolinones from Terrestrial *Fischerella* spp." *J. Nat. Prod.* **1999**, *62*, 569–572.
- Jung, M. E.; Slowinski, F. "Rhodium-Catalyzed Decomposition of Indole-Substituted α -Diazo- β -keto Esters: Three Different Reactions Based on Indole Oxidation State" *Tetrahedron Lett.* **2001**, *42*, 6835–6838.
- Kabat, M. M.; Garofalo, L. M.; Daniewski, A. R.; Hutchings, S. D.; Liu, W.; Okabe, M.; Radinov, R.; Zhou, Y. F. "Efficient Synthesis of 1α -Fluoro A-Ring Phosphine

Oxide, a Useful Building Block for Vitamin D Analogues, from (*S*)-Carvone via a Highly Selective Palladium-Catalyzed Isomerization of Dieneoxide to Dieneol” *J. Org. Chem.* **2001**, *66*, 6141-6150.

Katagiri, N.; Okada, M.; Morishita, Y.; Kaneko, C. “Synthesis of chiral spiro 3-oxazolin-5-one 3-oxides (chiral nitrones) *via* a nitrosoketene intermediate and their asymmetric 1,3-dipolar cycloaddition reactions leading to the EPC synthesis of modified amino acids” *Tetrahedron* **1997**, *53*, 5725-5746.

Kawatsura, M.; Hartwig, J. F. “Simple, Highly Active Palladium Catalysts for Ketone and Malonate Arylation: Dissecting the Importance of Chelation and Steric Hindrance” *J. Am. Chem. Soc.* **1999**, *121*, 1473–1478.

Kennedy-Smith, J. J.; Staben, S. T.; Toste, F. D. “Gold(I)-Catalyzed Conia-Ene Reaction of β -Ketoesters with Alkynes” *J. Am. Chem. Soc.* **2004**, *126*, 4526–4527.

Kharasch, M. S.; Sosnovsky, G.; Yang, N. C. “Reactions of *t*-Butyl Perester. I. The Reaction of Peresters with Olefins” *J. Am. Chem. Soc.* **1959**, *81*, 5819–5824.

Kitagawa, O.; Suzuki, T.; Inoue, T.; Watanabe, Y.; Taguchi, T. “Carbocyclization Reaction of Active Methine Compounds with Unactivated Alkenyl or Alkynyl Groups Mediated by $\text{TiCl}_4\text{-Et}_3\text{N}$ ” *J. Org. Chem.* **1998**, *63*, 9470–9475.

Konopelski, J. P.; Deng, H.; Schiemann, K.; Keane, J. M.; Olmstead, M. M. “Stereoselective Conjugate Addition Directed by an Enantiomerically Pure Ketal. Preparation of the Cyclohexanone Fragment of *N*-Methylwelwitindolinone C Isothiocyanate.” *Synlett*, **1998**, 1105–1107.

Kuninobu, Y.; Kawata, A.; Takai, K. “Rhenium-Catalyzed Insertion of Terminal Acetylenes into a C–H Bond of Active Methylene Compounds” *Org. Lett.* **2005**, *7*, 4823–4825.

- Lauchli, R.; Shea, K. J. "A Synthesis of the Welwistatin Core" *Org. Lett.* **2006**, *8*, 5287–5289.
- Lebel, N. A.; Banucci, "Intramolecular nitron-allene cycloadditions" *E. J. Am. Chem. Soc.* **1970**, *92*, 5278.
- Lebel, N. A.; Post, M. E.; Hwang, D. "Oxidation of isoxazolidines with peroxy acids. Nitrones and N-hydroxy-1,3-tetrahydrooxazines" *J. Org. Chem.* **1979**, *44*, 1819–1823.
- Lebold, T. P.; Leduc, A. B.; Kerr, M. A. "Zn(II)-Catalyzed Synthesis of Piperidines from Propargyl Amines and Cyclopropanes" *Org. Lett.* **2009**, *11*, 3770–3772.
- López-Alvarado, P.; García-Granda, S.; Álvarez-Rúa, C.; Avendaño, C. "Controlled Generation of Three Contiguous Stereocentres in the Michael Addition of 1-Pyrrolidinocyclohexene to (*E*)-(1-Methyl-2-oxoindolin-3-ylidene)acetophenone" *Eur. J. Org. Chem.* **2002**, 1702–1707.
- Lu, C.-D.; Liu, H.; Chen, Z.-Y.; Hu, W.-H.; Mi, A.-Q. "Three-Component Reaction of Aryl Diazoacetates, Alcohols, and Aldehydes (or Imines): Evidence of Alcoholic Oxonium Ylide Intermediates" *Org. Lett.* **2005**, *7*, 83–86
- MacKay, J. A.; Bishop, R. L.; Rawal, V. H. "Rapid Synthesis of the *N*-Methylwelwitindolinone Skeleton" *Org. Lett.* **2005**, *7*, 3421–3424.
- Mandelkow, E.; Mandelkow, E.-M. "Microtubule Structure" *Curr. Opin. Struct. Biol.* **1994**, *4*, 171–179.

- Matsubara, S.; Okazoe, T.; Oshima, K.; Takai, K.; Nozaki, H. "Isomerization of Allylic Alcohols Catalyzed by Vanadium or Molybdenum Complexes" *Bull. Chem. Soc. Jpn.* **1985**, *58*, 844–849.
- McDonald, F. E.; Olson, T. C. "Group VI metal-promoted *endo*-carbocyclizations via alkyne-derived metal vinylidene carbenes" *Tetrahedron Lett.* **1997**, *38*, 7691–7692.
- Menéndez, J. C. "Chemistry of the Welwitindolinones" *Top. Heterocycl. Chem.* **2007**, *11*, 63–101.
- Moniz, G. A.; Wood, J. L. "Catalyst-Based Control of [2,3]- and [3,3]-Rearrangement in α -Diazoketone-Derived Propargyloxy Enols" *J. Am. Chem. Soc.* **2001**, *123*, 5095–5097.
- Moniz, G. A.; Wood, J. L. "Rhodium Carbonoid-Initiated Claisen Rearrangement: Scope and Mechanistic Observations" *Org. Lett.* **1999**, *1*, 371–374.
- Moreno-Dorado, F. J.; Guerra, F. M.; Manzano, F. L.; Aladro, F. J.; Jorge, Z. D.; Massanet, G. M. "CeCl₃/NaClO: a safe and efficient reagent for the allylic chlorination of terminal olefins" *Tetrahedron Lett.* **2003**, *44*, 6691–6693.
- Morjani, H.; Madoulet, C. "Reversal Agents for P-glycoprotein-Mediated Multidrug Resistance" In *ABC Transporters and Multidrug Resistance*; Boumendjel, A.; Boutonnet, J.; Robert, J.; John Wiley and Sons, Inc.: Hoboken, 2009; 241–259.
- Murray, R. W. S., M. "Synthesis of Epoxides Using Dimethyldioxirane: *trans*-Stilbene Oxide" *Org. Synth.* **1998**, *9*, 288.

- Muthusamy, S.; Gunanathan, C. "Rh₂(OAc)₄-Catalyzed Regioselective Intermolecular C–H Insertion Reactions: Novel Synthesis of 2-Pyrrol-3'-yloxindoles" *Synlett*, **2002**, *11*, 1783–1786.
- Nicolaou, K. C.; Koide, K. "Synthetic studies on maduropeptin chromophore 1. Construction of the aryl ether and attempted synthesis of the [7.3.0] bicyclic system" *Tetrahedron Lett.* **1997**, *38*, 3667-3670.
- Nicolaou, K. C.; Zhang, H.; Ortiz, A.; Dagneau, P. "Total Synthesis of the Originally Assigned Structure of Vannusal B" *Angew. Chem., Int. Ed.* **2008**, *47*, 8605-8610.
- Obrecht, R.; Herrmann, R.; Ugi, I. "Isocyanide Synthesis with Phosphoryl Chloride and Diisopropylamine" *Synthesis* **1985**, 400-402.
- OOI, N. S.; Wilson, D. A. *Journal of Chemical Research-S* **1980**, 366-367.
- Overman, L. E. "Mercury(II)- and Palladium(II)-Catalyzed [3,3]-Sigmatropic Rearrangements" *Angew. Chem., Int. Ed.* **1984**, *23*, 579-586.
- Overman, L. E.; Campbell, C. B.; Knoll, F. M. "Mild procedures for interconverting allylic oxygen functionality. Cyclization-induced [3,3] sigmatropic rearrangement of allylic carbamates" *J. Am. Chem. Soc.* **1978**, *100*, 4822-4834.
- Padwa, A. "Intramolecular 1,3-Dipolar Cycloaddition Reactions" *Angew. Chem., Int. Ed.* **1976**, *15*, 123-136.
- Padwa, A.; Hornbuckle, S. F. "Ylide Formation from the Reaction of Carbenes and Carbenoids with Heteroatom Lone Pairs" *Chem. Rev.* **1991**, *91*, 263–309.
- Palmisano, G.; Danieli, B.; Lesma, G.; Trupiano, F.; Pilati, T. "Oxidation of .beta.-anilinoacrylate alkaloids vincadifformine and tabersonine by Fremy's salt. A

- mechanistic insight into the rearrangement of Aspidosperma to Hunteria eburnea alkaloids” *J. Org. Chem.* **1988**, *53*, 1056-1064.
- Pangborn, A. B.; Giardello, M. A.; Grubbs, R. H.; Rosen, R. K.; Timmers, F. J. “Safe and Convenient Procedure for Solvent Purification” *Organometallics* **1996**, *15*, 1518–1520.
- Paterson, I.; Yeung, K.-S.; Ward, R. A.; Smith, J. D.; Cumming, J. G.; Lambole, S. “The Total Synthesis of Swinholide A. Part 4: Synthesis of Swinholide A and Isoswinholide A from the Protected Monomeric Seco Acid, Pre-Swinholide A.” *Tetrahedron* **1995**, *51*, 9467–9486.
- Pérez-Tomás, R. “Multidrug Resistance: Retrospect and Prospects in Anti-Cancer Drug Treatment” *Curr. Med. Chem.* **2006**, *13*, 1859–1876.
- Perlman, N.; Albeck, A. “Efficient and Stereospecific Synthesis of (Z)-Hex-3-Enedioic Acid, A Key Intermediate for Gly-Gly *Cis* Olefin Isostere” *Synth. Commun.* **2000**, *30*, 4443–4449.
- Porcheddu, A.; Giacomelli, G.; Salaris, M. “Microwave-Assisted Synthesis of Isonitriles: A General Simple Methodology” *J. Org. Chem.* **2005**, *70*, 2361-2363.
- Rajkovic, M.; Lorenc, L.; Petrovic, I.; Milovanovic, A.; Mihailovic, M. L. “Oxidative hydrolysis and acid-catalyzed rearrangement of steroidal isoxazolidines” *Tetrahedron Lett.* **1991**, *32*, 7605-7608.
- Ready, J. M.; Reisman, S. E.; Hirata, M.; Weiss, M. M.; Tamaki, K.; Ovaska, T. V.; Wood, J. L. “A Mild and Efficient Synthesis of Oxindoles: Progress Towards the Synthesis of Welwitindolinone A Isonitrile” *Angew. Chem., Int. Ed.* **2004**, *43*, 1270–1272.

- Reisman, S. E.; Ready, J. M.; Hasuoka, A.; Smith, C. J.; Wood, J. L. "Total Synthesis of (\pm)-Welwitindolinone A Isonitrile" *J. Am. Chem. Soc.* **2006**, *128*, 1448–1449.
- Reisman, S. E.; Ready, J. M.; Weiss, M. M.; Hasuoka, A.; Hirata, M.; Tamaki, K.; Ovaska, T. V.; Smith, C. J.; Wood, J. L. "Evolution of a Synthetic Strategy: Total Synthesis of (\pm)-Welwitindolinone A Isonitrile" *J. Am. Chem. Soc.* **2008**, *130*, 2087–2100.
- Renaud, J. L.; Aubert, C.; Malacria, M. "Cobalt-mediated cycloisomerization of δ -substituted -acetylenic β -ketoesters construction of angular triquinane by a sequence ene/Pauson-Khand reactions" *Tetrahedron* **1999**, *55*, 5113–5128.
- Richter, J. M.; Ishihara, Y.; Masuda, T.; Whitefield, B. W.; Llamas, T.; Pohjakallio, A.; Baran, P. S. "Enantiospecific Total Synthesis of the Hapalindoles, Fischerindoles, and Welwitindolinones *via* a Redox Economic Approach" *J. Am. Chem. Soc.* **2008**, *130*, 17938–17954.
- Sevastya.Tk; Volodars.Lb. *Zh. Org. Khim.* **1971**, *7*, 1974.
- Sheps, J.; Ling, V. "Introduction: What is Multidrug Resistance?" In *ABC Transporters and Multidrug Resistance*; Boumendjel, A.; Boutonnat, J.; Robert, J.; John Wiley and Sons, Inc.: Hoboken, 2009; 1–13.
- Smith, C. D.; Zilfou, J. T.; Stratmann, K.; Patterson, G. M. L.; Moore, R. E. "Welwitindolinone Analogues that Reverse P-Glycoprotein-Mediated Multiple Drug Resistance" *Mol.Pharmacol.* **1995**, *47*, 241–247.
- Still, W. C.; Kahn, M.; Mitra, A. "Rapid chromatographic technique for preparative separations with moderate resolution" *J. Org. Chem.* **1978**, *43*, 2923–2925.

- Storm, D. L.; Spencer, T. A. "Furan Synthesis by 1,4-Addition of Carboethoxycarbene to α -Methoxymethylene Ketones" *Tetrahedron Lett.* **1967**, *8*, 1865–1867.
- Stratmann, K.; Burgoyne, D. L.; Moore, R. E.; Patterson, G. M. L. "Hapalysin, a Cyanobacteria Cyclic Depsipeptide with Multidrug-Resistance Reversing Activity" *J. Org. Chem.* **1994**, *59*, 7219–7226.
- Stratmann, K.; Moore, R. E.; Bonjouklian, R.; Deeter, J. B.; Patterson, G. M. L.; Shaffer, S.; Smith, C. D.; Smitka, T. A. "Welwitindolinones, Unusual Alkaloids from the Blue-Green Algae *Hapalosiphon welwitschii* and *Westiella intricate*. Relationship to Fischerindoles and Hapalindoles" *J. Am. Chem. Soc.* **1994**, *116*, 9935–9942.
- Suzuki, M.; Oda, Y.; Noyori, R. "Palladium(0) catalyzed reaction of 1,3-diene epoxides. A useful method for the site-specific oxygenation of 1,3-dienes" *J. Am. Chem. Soc.* **1979**, *101*, 1623-1625.
- Takahashi, K.; Midori, M.; Kawano, K.; Ishihara, J.; Hatakeyama, S. "Entry to Heterocycles Based on Indium-Catalyzed Conia-Ene Reactions: Asymmetric Synthesis of (–)-Salinosporamide A" *Angew. Chem. Int. Ed.* **2008**, *47*, 6244–6246.
- Tian, X.; Hutters, A. D.; Douglas, C. J.; Garg, N. K. "Concise Synthesis of the Bicyclic Scaffold of *N*-methylwelwitindolinone C Isothiocyanate via an Indolyne Cyclization" *Org. Lett.* **2009**, *11*, 2349–2351.
- Trost, B. M.; McDougall, P. J. "Access to a Welwitindolinone Core Using Sequential Cycloadditions" *Org. Lett.* **2009**, *11*, 3782–3785.
- Tsukamoto, Y.; Sato, K.; Kinoto, T.; Yanai, T. "13 β -Hydroxylation of Milbemycins by Selenium Dioxide" *Bull. Chem. Soc. Jpn.* **1992**, *65*, 3300–3307.

- Uemura, e. a. *Nippon Kagaku Zasshi* **1966**, *87*, 986.
- Wade, R. H. “On and Around Microtubules: An Overview” *Mol. Biotechnol.* **2009**, *43*, 177–191.
- Wang, B. M.; Song, Z. L.; Fan, C. A.; Tu, Y. Q.; Chen, W. M. “Halogen Cation Induced Stereoselective Semipinacol-type Rearrangement of Allylic Alcohols: A Highly Efficient Approach to α -Quaternary β -Haloketo Compounds” *Synlett* **2003**, 1497-1499.
- Wood, J. L.; Holubec, A. A.; Stoltz, B. M.; Weiss, M. M.; Dixon, J. A.; Doan, B. D.; Shamji, M. F.; Chen, J. M.; Heffron, T. P. “Application of Reactive Enols in Synthesis: A Versatile, Efficient, and Stereoselective Construction of the Welwitindolinone Carbon Skeleton” *J. Am. Chem. Soc.* **1999**, *121*, 6326–6327.
- Wood, J. L.; Moniz, G. A. “Rhodium Carbenoid-Initiated Claisen Rearrangement: Scope and Mechanistic Observations” *Org. Lett.* **1999**, *1*, 371-374.
- Wood, J. L.; Moniz, G. A.; Pflum, D. A.; Stoltz, B. M.; Holubec, A. A.; Dietrich, H. J. “Development of a Rhodium Carbenoid-Initiated Claisen Rearrangement for the Enantioselective Synthesis of α -Hydroxy Carbonyl Compounds” *J. Am. Chem. Soc.* **1999**, *121*, 1748-1749.
- Yan, J. B.; Herndon, J. W. “Stereoselective Preparation of Vitamin D Precursors Using the Intramolecular Coupling of Alkynes and Cyclopropylcarbene–Chromium Complexes: A Formal Total Synthesis of (\pm)-Vitamin D₃” *J. Org. Chem.* **1998**, *63*, 2325-2331.

Zamora, J. M.; Pearce, H. L.; Beck, W. T. "Physical-Chemical Properties Shared by Compounds that Modulate Multidrug Resistance in Human Leukemic Cells" *Mol. Pharmacol.* **1988**, *33*, 454–462.

Zhang, X. Q.; Smith, C. D. "Microtubule Effects of Welsistatin, a Cyanobacterial Indolinone that Circumvents Multiple Drug Resistance" *Mol. Pharmacol.* **1996**, *49*, 288–294.

Zoretic, P. A.; Wang, M.; Zhang, Y.; Shen, Z. "Total Synthesis of *d,l*-Isospongiadiol: An Intramolecular Radical Cascade Approach to Furanoditerpenes" *J. Org. Chem.* **1996**, *61*, 1806–1813.

About the Author

David Blandy Freeman was born in Palm Springs, California on November 18th, 1982 to Barbara Jane and Dennis Lyle Freeman. Two and half years prior, Dave's older brother Philip Morgan Freeman was born and began the process of introducing Dennis and Barbie to parenthood. Phil and Dave were inseparable from the start wreaking havoc on their parents with games such as "bury mom's treasure (i.e. wedding ring)" and "cover the house in peanut butter." David's passion for fort building, climbing, and dismantling of household appliances kept his parents busy until he was old enough for preschool.

Dennis and Barbie enrolled David in preschool at Desert Sunshine in Palm Springs, California. Preschool and kindergarten gave Dave's parents some respite and allowed David to build life-long friendships with his fellow classmates. Upon completion of preschool, David attended St. Theresa's Catholic School in Palm Springs, California for his elementary education. During this time the Freeman family moved to Rancho Mirage, California. The daily commute to St. Theresa's developed David's affection for oldies music and exposed him to more lasting friendships.

It was in his elementary school years when David began to take interest in science. His parents, realizing David's interest and curiosity, supplied him with chemistry sets and science books of all types. In David's earlier years he was too impatient for reading and decided to spend the majority of his time outside attempting to use the chemistry set to manufacture explosives. His other hobbies included baseball, hockey, and shooting.

David attended Palm Desert High School, Palm Desert California in 1997 where his interest in several areas blossomed. David played baseball and wrestled until his senior year where his position as Associated Student Body President consumed most of his extracurricular time. David's interest in chemistry was further expanded after taking Diane "Mac" MacMillan's AP Chemistry course. Her enthusiasm for the subject inspired David and he spent the following semester aiding in laboratory setup for other classes.

After graduating from high school in 2001, David attended the University of California, Santa Barbara in Santa Barbara, California. During his first year at the university, David explored a variety of subjects including linguistics and film studies, but none drew his interest like chemistry. In the fall of 2002, David took his first organic chemistry class with Prof. Robert Neuman. Because of his enjoyment in the subject, Prof. Neuman suggested to David to conduct undergraduate research with a research professor. His suggestion led David to Prof. Thomas R. R. Pettus. At first request, Prof. Pettus rejected David from conducting research in his laboratory. However, after repeated visits and requests, Prof. Pettus finally agreed. It was David's undergraduate research experience in Prof. Pettus' lab that inspired him to pursue a career in organic chemistry.

Upon completion of his undergraduate degree in chemistry, David proceeded to Colorado State University for graduate school. There he met Prof. John Wood and eventually joined his group. David was given the opportunity to work on the challenging total synthesis of *N*-methylwelwitindolinone C isothiocyanate. It was this project that led him to discover an extension of the group's O-H insertion/Claisen rearrangement

chemistry: the O–H insertion/Conia-ene cyclization. Upon completion of his Ph.D., David will begin postdoctoral studies with Prof. Corey Stephenson at Boston University.